

GEOLOGICA ULTRAIECTINA

Mededelingen van de  
Faculteit Geowetenschappen  
Universiteit Utrecht

No. 271

**Bio- and Petroleum Geochemistry of Mud Volcanoes in the  
Sorokin Trough (NE Black Sea) and in the Gulf of Cadiz  
(NE Atlantic): From Fluid Sources to Microbial Methane  
Oxidation and Carbonate Formation**

Alina N. Stadnitskaia

Bio- and Petroleum Geochemistry of Mud Volcanoes in the Sorokin Trough (NE Black Sea) and in the Gulf of Cadiz (NE Atlantic): From Fluid Sources to Microbial Methane Oxidation and Carbonate Formation

Biogeochemie en Petroleum Geochemie van Moddervulkanen in de Sorokin Trog (noordoostelijke Zwarte Zee) en in de Golf van Cadiz (noordoostelijke Atlantische Oceaan): Over de Oorsprong van uit de Aardkorst Ontsnappende Modder en Koolwaterstofgas, Microbiële Oxidatie van Methaan en Carbonaatvorming

(met een samenvatting in het Nederlands)

Биохимия и Нефтяная Геохимия Грязевых Вулканов из Прогиба Сорокина (Северо-Восточная Часть Черного моря) и из Залива Кадис (Северо-Восточная Атлантика): Источники Глубинных Флюидов, Микробиальное Окисление Метана и Формирования Аутигенных Карбонатов

(С резюме на русском языке)

## Proefschrift

ter verkrijging van de graad van doctor  
aan de Universiteit Utrecht  
op gezag van de rector magnificus, prof.dr. W.H. Gispen,  
ingevolge het besluit van het college voor promoties  
in het openbaar te verdedigen  
op maandag 22 januari 2007 des middags te 2.30 uur

door

Alina Nikolaievna Stadnitskaia

geboren op 18 juli 1974, te Moskou, Rusland

Promotores: Prof. Dr. Ir. J.S. Sinninghe Damsté  
Prof. Dr. T.C.E. van Weering  
Prof. Dr. M.K. Ivanov

These studies were supported by a fellowship of the President of the Russian Federation, by a grant from the Huygens Programme of the Netherlands Organization for International Cooperation in Higher Education (Nuffic), and by the cooperative NWO/РФФИ Dutch-Russian project between the Royal Netherlands Institute for Sea Research (NIOZ, the Netherlands) and the UNESCO/Moscow State University Centre for Marine Geology and Geophysics (Russia) entitled “Evolution and Ecology of Cold Seep Structures in the Gulf of Cadiz”.

## MUD VOLCANO

Leagues beneath the grey-green surface  
rumbles Neptune's seething mound.  
Oozing molten muck and seeping gas it reigns,  
dark and forbidding, unbidden.  
It's pressured rage spewing forth a vaporous plume  
into the unsuspecting world above.  
It's summit wears a frozen crystal lattice crown;  
White, ice-like, unearthly.

Ice and fire entombed by earth and water.

A towering monument encircled by ghostly moat  
it reeks of primal violence, fractured crusts;  
The stuff of legend gurgling from its core -  
The heat of forgotten eons rising to the ocean floor.  
And on its surface roils the wormed monster,  
guarding the sacred fire from prying eyes.  
Like twisted roots the vermicular horde writhes  
across  
the mud;  
White, worm-like, unearthly.

Life forms sucking the residue of decay.

Original version by Sherrod Sturrock.  
*Geo-Marine Letters* 19: 169-170 (1999).

To Vera N. and Irina G. Stadnitskaia



ISBN 90-5744-133-0

<b>Summary</b>		1
<b>Samenvatting</b>		3
<b>Резюме</b>		5
<b>Chapter 1.</b>	General introduction	7
 <b>Part I. The Sorokin Trough, NE Black Sea</b>		
<b>Chapter 2.</b>	Sources of hydrocarbon gases in mud volcanoes from the Sorokin Trough, NE Black Sea, based on molecular and carbon isotopic compositions. To be submitted to <i>Marine and Petroleum Geology</i>	29
<b>Chapter 3.</b>	Lipid biomarkers in sediments of mud volcanoes from the Sorokin Trough, NE Black Sea: Probable source strata for the erupted material. Accepted by <i>Organic Geochemistry</i> (2006).	51
<b>Chapter 4.</b>	Biomarker and 16S rDNA evidence for anaerobic oxidation of methane and related carbonate precipitation in deep-sea mud volcanoes of the Sorokin Trough, Black Sea. Published in <i>Marine Geology</i> , 217, 67-96 (2005).	73
<b>Chapter 5.</b>	Novel archaeal macrocyclic diether core membrane lipids in a methane-derived carbonate crust from a mud volcano in the Sorokin Trough, NE Black Sea. Published in <i>Archaea</i> , 1, 165-173 (2003).	109

<b>Part II.</b>	<b>The Gulf of Cadiz, NE Atlantic</b>	
<b>Chapter 6.</b>	Molecular and carbon isotopic variability of hydrocarbon gases from mud volcanoes in the Gulf of Cadiz, NE Atlantic. Published in <i>Marine and Petroleum Geology</i> , 23, 281-296 (2006).	123
<b>Chapter 7.</b>	Application of lipid biomarkers to detect sources of organic matter in mud volcano deposits and post-eruptional methanotrophic processes in the Gulf of Cadiz, NE Atlantic. To be submitted to the Special Issue of the TTR Programme in <i>Marine and Petroleum Geology</i> .	149
<b>Chapter 8.</b>	Carbonate formation by anaerobic oxidation of methane in the Gulf of Cadiz. (NE Atlantic). In preparation.	171
<b>Chapter 9.</b>	Synthesis.	193
<b>Appendix</b>	Colour figures	199
<b>References</b>		203
<b>Acknowledgements</b>		225
<b>Curriculum Vitae</b>		227

## Summary

---

The Sorokin Trough (NE Black Sea) and the Gulf of Cadiz (NE Atlantic) are both mud volcano (MV) provinces characterized by the presence of gas hydrates, methane-related carbonates, and chemosynthetic biota but possess differences in geological history, tectonics, composition of sedimentary cover, and water column conditions. This thesis compares the geological and biogeochemical processes taking place within these MV provinces. It attempted to elucidate the deep-fluid dynamics in both areas, to identify possible sources for ascending hydrocarbon gases, and to assess the source-strata for the erupted sediments. The environmental impact of expelled methane-rich fluids on the development of microbial communities involved in the anaerobic oxidation of methane (AOM), a process inducing carbonate precipitation, was also investigated.

A significant contribution of non-microbial, mature hydrocarbons in the migrated fluid was apparent from the composition and the stable carbon isotope signatures of the gases. Comparison of the hydrocarbon gas and biomarker data revealed that the formation of the MV fluid starts with the discharge of over-pressurized hydrocarbons and is followed by dynamic entrainment of the surround sediments on its way up. The biomarker composition of the mud breccia matrix in the Sorokin Trough indicated different depths of de-fluidization related to the position of fracture zones or diapiric folds in the subsurface. The biomarker composition of various MVs from the Gulf of Cadiz designated similar source strata for the erupted material.

The study of living microbial mats and related carbonates from the Sorokin Trough and an ancient methane-related carbonate crust from the Gulf of Cadiz revealed a substantial contribution of microbes involved in AOM to the microbial community and the dominant role of AOM in processes of carbonate formation. The lipid biomarker and 16S rRNA gene sequence data showed that AOM signals appear to be strongest within carbonates and are considerably weaker in the surrounding sediments, indicating that local oversaturation of pore waters with bicarbonate, (formed by AOM) induced carbonate precipitation. The data also revealed changes in the archaeal community structure during carbonate crust formation in the Gulf of Cadiz, which are interpreted as resulting from changes in the conditions (e.g. methane flux) during the crusts' accretion.

## Summary

---

Despite the presence of an anoxic water column in the Sorokin Trough and oxygenated waters in the Gulf of Cadiz, the lipid biomarker and 16S rDNA sequence data demonstrated AOM to be the dominant biogeochemical process for methane oxidation in both areas. The distribution of anaerobic methanotrophs is directly linked to the intensity of methane flux and to fluid chemistry. However, in comparison with the Sorokin Trough, the AOM signal in the Gulf of Cadiz is muted. This probably indicates the absence of active fluid transport in the Gulf although the ubiquitous presence of outcropping methane-related carbonates signifies episodes of fluid discharge in the past. Reduced AOM in the Gulf of Cadiz is likely the result of “fluid-flux-starvation” environments established after a period of MV eruptions followed by a consumption of allochthonous methane and other organic and inorganic constituents. In contrast, fluid inflow in the Sorokin Trough is still going on, resulting in development of chemosynthetic microbial communities and in carbonate precipitation.

## Samenvatting

---

De Sorokin Trog (noordoostelijke Zwarte Zee) en de Golf van Cadiz (noordoostelijke Atlantische Oceaan) zijn gebieden die gekarakteriseerd worden door het voorkomen van moddervulkanen op de zeebodem en daaraan gerelateerde gashydraten, carbonaatkorsten en chemosynthetische biota. Beide gebieden hebben echter een contrasterende geologische geschiedenis, tektoniek, sedimentsamenstelling en waterkolomcondities. In dit proefschrift worden de geologische en biogeochemische processen die gepaard gaan met de eruptie van moddervulkanen voor deze twee verschillende gebieden onderzocht en vergeleken. Zowel de oorsprong van de koolwaterstofgassen die met de modder mee omhoog komen als de oorsprong van de modder zelf is onderzocht. Daarnaast werd de invloed van uit de moddervulkaan ontsnappend methaan op de samenstelling van specifieke microbiële levensgemeenschappen bestudeerd. Deze microben zijn actief in de anaërobe oxidatie van methaan, een proces dat de vorming van carbonaatkorsten op de bodem van de oceaan bevordert.

De samenstelling van de gassen en hun stabiele koolstofisotoopsamenstelling in de naar boven komende vloeistoffen duiden op een substantiële bijdrage van niet-biogene, thermisch rijpe koolwaterstoffen. Deze bevinding, in relatie tot de thermische maturatiegraad van biomarkers in de uitgestoten en afgezette modderbreccia, gaf aan dat de modderstromen waarschijnlijk ontstaan door een “ontsnapping” van koolwaterstoffen uit een laag in de diepe aardkorst, die vervolgens op haar pad naar boven ondieper gelegen sedimenten mee naar boven neemt. De biomarker samenstelling van modderbreccia's van moddervulkanen in de Sorokin Trog liet zien dat deze bestaan uit verschillende lagen van verschillende oorsprong terwijl modderbreccia's van moddervulkanen in de Golf van Cadiz juist een vrij uniforme samenstelling hadden, hetgeen suggereert dat deze modderstromen afkomstig zijn van eenzelfde laag in de aardkorst.

De studie van levende microbiële matten en daaraan gerelateerde carbonaten in de Sorokin Trog en van een door methaanoxidatie gevormde, fossiele carbonaatkorst van de Golf van Cadiz toonde aan dat een belangrijk bestandsdeel van de microbiële levensgemeenschappen gevormd wordt door actief bij de anaërobe oxidatie van methaan betrokken microben. De biomarker samenstelling en de detectie van specifieke 16S rDNA

## Samenvatting

---

sequenties lieten zien dat het signaal van anaërobe methaanoxidatie veel sterker aanwezig is in de carbonaten dan in de omringende sedimenten. Carbonaatforming wordt dus blijkbaar geïnduceerd door de anaërobe methaanoxidatie, waarschijnlijk doordat er lokaal een oververzadiging aan bicarbonaat in het poriewater ontstaat. In de carbonaatkorst uit de Golf van Cadiz werd bovendien een zonering in de archaeale levensgemeenschappen aangetroffen, hetgeen te verklaren is door veranderende omstandigheden (bijv. in de methaanflux) tijdens het aangroeien van de korst.

Ondanks het grote verschil in het zuurstofgehalte van het bodemwater, anoxisch in de Sorokin Trog en oxisch in de Golf van Cadiz, laten de biomarker en 16S rDNA data zien dat in beide gebieden anaërobe oxidatie van methaan het belangrijkste proces is voor oxidatie van het weglekkende methaan. De samenstelling van de microbiële levensgemeenschap is direct gerelateerd aan de grootte van de methaanflux en waarschijnlijk ook aan de chemische samenstelling van de modderstroom. In vergelijking met de Sorokin Trog is de intensiteit van het signaal van anaërobe methaanoxidatie laag. Dit komt waarschijnlijk doordat er in de Golf van Cadiz op dit moment geen actief transport van modderstromen plaats vindt. Het grootste gedeelte van het ontsnapte methaan is reeds geconsumeerd. Daarentegen is de Sorokin Trog nog steeds een actief gebied, hetgeen resulteert in levende microbiële levensgemeenschappen en actieve precipitatie van carbonaat.

Прогиб Сорокина (СВ Черного моря) и залив Кадис (СВ Атлантика) являются грязевулканическими провинциями, характеризующимися присутствием газовых гидратов, карбонатов, возникших в результате окисления метана, и хемосинтетических организмов. Однако, эти провинции отличаются между собой геологической историей, тектоникой, составом осадочного чехла и условиями водной среды бассейнов. В настоящей диссертации проведено сравнение геологических и биохимических процессов, имеющих место в этих грязевулканических провинциях. Сделана попытка пролить свет на глубинную флюидодинамику в обоих районах, определить возможные источники мигрирующих углеводородных газов и изверженных осадков (обломков пород). Также было изучено воздействие обогащенных метаном флюидов на развитие микробного сообщества, вовлеченного в анаэробное окисление метана (АОМ), и процессы, стимулирующие осаждение карбонатов.

Существенный вклад зрелых (немикробных) углеводородов стал очевидным исходя из анализа состава и изотопии углерода газов. Сравнение биомаркеров и данных по углеводородным газам показало, что образование грязевулканических флюидов начинается с высвобождения углеводородов в зонах аномальных давлений. Этот процесс сопровождается мобилизацией окружающих осадков и вовлечением их в движение вверх по разрезу, что подтверждается различной степенью термальной преобразованности вещества. Состав биомаркеров матрикса грязевулканических брекчий в прогибе Сорокина указывает на различные глубины дефлюидизации, которые связаны с положением разломных зон или диапировых складок в разрезе. Состав биомаркеров из различных грязевых вулканов залива Кадис позволили выявить отложения являющиеся источниками изверженного на поверхность материала.

Изучение современных микробных матов и осаждающихся аутигенных карбонатов в прогибе Сорокина, а также связанных с метаном древних карбонатных кор в заливе Кадис указывает на существенную роль микробов, вовлеченных в АОМ, и на роль АОМ в формировании карбонатных кор. Липидные биомаркеры и 16S rRNA генетические последовательности микроорганизмов показали, что влияние АОМ проявляется гораздо сильнее внутри карбонатов и значительно слабее в окружающих осадках, указывая на то, что локальное перенасыщение поровых вод бикарбонатом является продуктом АОМ, которое вызывает осаждение карбонатов. Результаты исследований также показали изменения в структуре сообщества архей в процессе формирования карбонатов в заливе Кадис. Эти вариации связаны с изменениями условий среды (например, с активизацией метановых источников) во время роста карбонатной коры.

Не смотря на сероводородное заражение воды в прогибе Сорокина и окислительные обстановки в придонных водах залива Кадис, липидные биомаркеры и



## Резюме

---

16S rDNA последовательности демонстрируют, что АОМ является доминирующим биогеохимическим процессом при окислении метана в обоих районах.

Распространение анаэробных метанотрофов напрямую связано с интенсивностью метановых сипов и также, вероятно, с химическим составом флюидов. Однако, по сравнению с прогибом Сорокина АОМ в заливе Кадис практически не фиксируется (невозможно установить). Это, вероятно, указывает на отсутствие активной флюидной разгрузки в заливе в настоящее время, хотя повсеместное присутствие метано-производных карбонатов однозначно свидетельствует об эпизодах флюидной разгрузки в прошлом. Редуцированное (сокращенное) АОМ в заливе Кадис по всей вероятности является результатом обстановок «флюидного голода», возникших после периода активных извержений грязевых вулканов и последующего потребления (усвоения) аллохтонного метана и других органических и неорганических соединений (компонентов). В противоположность этому, в прогибе Сорокина существует современный флюидный поток, который питает живущее ныне хемосинтетическое сообщество и приводит к активному осаждению карбонатов.

### 1. General Introduction

#### 1.1. Cold seeps at the sea floor: an overview

Recent geological exploration of the ocean floor has led to the discovery of numerous fields of submarine fluid discharge with seep emissions, in contrast to the longer known hydrothermal vents, with the same temperature as the surrounding seawater. These vents were called “cold-seeps” or “seepages” and these terms include everything from a small-scale gas bubbling at the seabed (Hovland and Judd, 1988) to a catastrophic burst of geofluids [hydrocarbon gas (predominantly methane), hydrogen sulfide, carbon dioxide, petroleum products, pore waters and mud] from the subsurface (Ivanov et al., 1998; e.g. Figure 1). These vents are concentrated along continental margins and induce the development of vigorous and complex cold-seep systems at and below the seafloor surface.

Cold-seepage at the sea floor is often the result of upward fluid discharge from the subsurface. This migration of fluids through zones of weakness, i.e. fault system, cracks, and fissures, affects sea-floor morphology. It results in formation of (i) pockmarks, i.e. negative topographic features formed due to seepage (Hovland and Judd, 1988), (ii) large fissure eruptions of sediments from the subsurface (Figure 2; Ivanov et al., 1998), and (iii) mud volcanoes (MVs).

##### *1.1.1. Historical background*

MVs and gas/oil seepages are known from immemorial times. The Fire Temple, alternatively known as a Atashgah Temple, the Zarathustra Temple or the Temple of the Fire Worshippers is a shrine devoted to Zoroastrianism, one of the first religions in the World (1400-1200 BC). The temple is located close to Baku (Azerbaijan) and was built at a place with “eternal” fires that was considered as a sacred. These fires resulted from natural gas seepages, which are still common in this area. The MVs in the Black Sea (or Pontus Euxene) were known to the Ancient Greeks, and were mentioned in the “Odyssey”, Homer's epic from Greek mythology, where Homer mentioned MVs from the Kerch strait as the entrance to the Kingdom of Pluto. Marco Polo, who passed through Azerbaijan in the 13<sup>th</sup> century, wrote, "On the confines toward Georgine there is a fountain from which oil springs in great abundance, inasmuch as a hundred shiploads might be taken from it at one time. This oil is not good to use with food, but it is good to burn, and is also used to anoint camels that have the mange. People come from vast distances to fetch it, for in all countries round there is no other oil".

Voskoboynikov and Gur'ev (1832) were one of the first scientists who described MVs during the geological survey of the Taman peninsula (Ukraine). The specific term “mud

volcano” was introduced by Gelmersen (1886) and is a literal translation of the German word “mudevulkan”, used by G.V. Abich when he described MVs on the Kerch and Taman peninsulas in 1873. The first mud or “dirt” volcanoes were discovered in areas with intensive volcanic activity in Iceland, Sicily and Flegrey Fields (Kholodov, 2002). Layell, (1850) and Neumayr (1899) interpreted these phenomena as endogenic processes and classified them in the group of “normal” lava-volcanoes. Later, Kalitskii (1910, 1914), Veber and Kalitskii (1911), Golubyatnikov, (1923), and Gubkin (1913, 1937) demonstrated that development of these structures is strongly related to the distribution of petroleum provinces and not related to the lava-volcanoes. Concurrently, Arkhangel’skii (1925) highlighted the importance of tectonic processes (i.e. diapirism, faulting) in the formation and development of MVs.

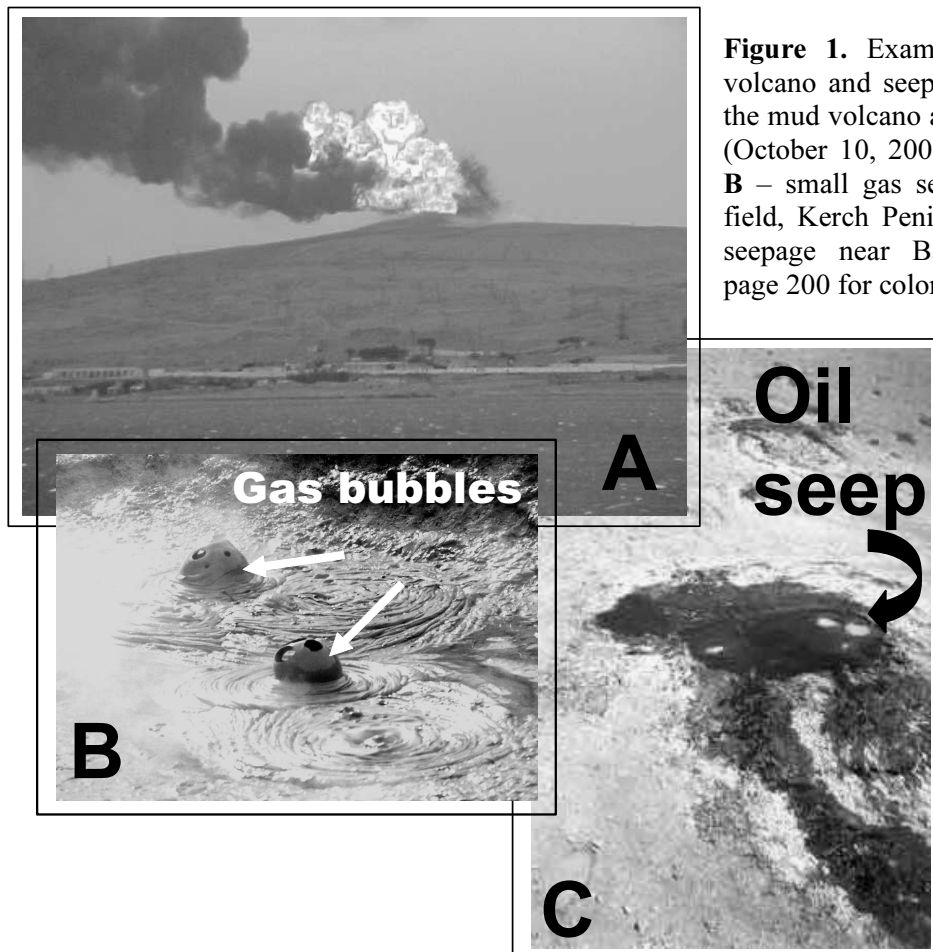


**Figure 1.** Examples of on-land mud volcano and seepages. **A** – Eruption of the mud volcano at Lokbatan, near Baku (October 10, 2001; Photo: Phil Hardy); **B** – small gas seepage (Bulganak MV field, Kerch Peninsular); **C** – small oil seepage near Baku, Azerbaijan. See page 200 for color figure.

### 1.1.2. Formation of mud volcanoes

MVs are low-temperature representatives of seepage-related geomorphological features and the most remarkable indication of fluid venting (Ivanov et al., 1998). They are like magmatic volcanoes in the sense that their eruptions are powerful, sometimes

accompanied with flames of up to hundreds of meters. However, instead of lava, MVs expel a complex mixture of products including hydrocarbon gases (e.g. methane and wet hydrocarbons), hydrogen sulfide, carbon dioxide, petroleum, pore waters and mud. Hydrocarbon gases and petroleum often represent one of the main constituents of the erupted material and this explains the vigorous flames during the eruptions of MVs on the continent (Figure 1).

MVs are often topographic elevations and are expressed as dome-like structures, reaching several kilometres in diameter and hundreds meters in height caused by catastrophic explosion of fluids at the sea floor (Figure 2; Ivanov et al., 1998 and references therein). Simultaneously, MVs can also be represented by a depression of a few kilometres in diameter as caldera-like developments. This type of MV has resulted from the collapse of the ground following explosive eruptions of large volumes of erupted sedimentary gas/water saturated material (Woodside et al., 1997). At continental margins, MVs and seeps can significantly alter the topography and induce continental slope instability. At relatively shallow water depths, MVs sometimes form islands and banks.

MVs develop as a result of strong lateral or vertical compressions of the earth crust, which allow deep-lying sediments to move upward and be transported to the sea floor. Through the feeder channel (Figure 2) of a MV, large volumes of clastic material, saturated with gas and other fluids, are transported in a mixture of clay-silt fluidized matrix and deposited on the seafloor (Ivanov et al., 1998). This emitted sedimentary material is called “argille scaliuse”, “diapiric mélange”, or more frequently “mud breccia” (Cita, et al., 1981; Akhmanov, 1996). It is a complex mixture of a matrix and rock fragments, mechanically grasped by the powerful upward transport of fluids (Akhmanov, 1996; Akhmanov and Woodside, 1998). These fragments of rocks represent sediments deposited millions of years ago and buried in the subsurface, which are brought to the seafloor due to the activity of the MV. Both mud breccia rock clasts and matrix contain important information regarding the composition and genesis of sediments in the subsurface, and maturity, and hydrocarbon potential of the area (Akhmanov, 1998; Kozlova, 2003; Ovsanikov et al., 2003). Accordingly, MVs can be considered as “free bore-holes”, providing us material from great depths below the seafloor surface, originating from up to 20 km sedimentary depth (Kholodov, 2002; Shnyukov et al., 2005), where drilling is not yet possible.

### *1.1.3. Distribution and occurrence of mud volcano provinces*

MVs are most common in areas of recent tectonic activity, i.e. within mobile tectonic belts of Alpine-Himalayas, Pacific and Central-Asia, and with a thick sedimentary cover (5-20 km). For instance, the South Caspian Basin is known for a dense distribution of MVs. The

sedimentary sequence in this area possesses up to 1 km of Quaternary sediments, the base of Cenozoic sediments is located at ca. 14 km depths and Palaeozoic-Mesozoic sediments lie at depths of 19-20 km (Kholodov, 1990). The intensive investigations of off-shore MVs and fluid venting areas in general were started at the end of seventies. Lebedev (1978) and later Kholodov (1983, 1990, 1991) demonstrated the connection of submarine MVs from the Caspian Sea with petroleum-bearing deposits and regional tectonics. At the end of eighties - the beginning of nineties, a series of research cruises to the Black Sea revealed the existence of deep sea MV provinces (Ivanov et al., 1989; Ivanov and Limonov, 1996; Ivanov, 1999). This was a time of increased scientific interest in underwater cold-venting and associated phenomena. Numerous field studies in the last couple of decades have revealed that locations where subsurface fluids are discharged spontaneously are distributed worldwide. Such areas are now known to be a widespread feature on active continental margins, e.g. the Makran accretionary prism (White, 1982; von Rad et al., 1996), Barbados (Le Pichon et al., 1990; Lallemand et al., 1995), Aleutian subduction zone (Wallman et al., 1997; Suess et al., 1998), the Cascadia margin (Han and Suess, 1989; Cragg et al., 1996), the Nankai Trough (Kawahta and Fujokor, 1986; Taira et al., 1992), Chili (Banes et al., 1993; Sellanes, et al., 2004), Indonesia (van Weering et al., 1989; Karig, 1986), Peru (Kvenvolden and Kastner, 1990), Eastern Mediterranean (Cita et al., 1994, Ivanov and Limonov, 1995; Ivanov et al., 1996; Limonov, 1996), North California (Brooks et al., 1991), the Gulf of Cadiz (Kenyon et al., 2000, 2001, 2002, 2003; Gardner, 2001; Pinheiro et al., 2003), the Anaximander sea-mountains (Woodside, et al., 1998; Zitter et al., 2005), on passive continental margins, e.g. Black Sea (Ivanov et al., 1989; Ginsburg et al., 1990; Ivanov et al., 1996, 1998; Michaelis et al., 2002), Vøring Plato (Bugge et al., 1988; Bouriak et al., 1999), the Nile deep-sea Fan (Masclé et al., 2001; Lonke et al., 2002), the Gulf of Mexico (Roberts, 1990; Aharon et al., 1997), Blake Outer Ridge (Galimov et al., 1983; Paull et al., 1993, 1996), and the Norwegian margin of the Barents Sea (Vogt, et al., 1997; Lein et al., 1998; Niemann et al., 2005). Thus, present-day marine research has led to the discovery of fluid venting areas and mud volcano provinces all over the globe.

#### *1.1.4. Mud volcanoes: the connection with subsurface hydrocarbon reservoirs.*

Comprehensive investigations of numerous mud volcanic/seepage provinces have provided overwhelming evidence for the role of hydrocarbon gases in their formation. This explains why these fluid seepages are also called “gas seeps” or “methane seeps”. MVs and seeps in general are direct indicators of hydrocarbon migration and provide a view of the hydrocarbon potential of the deeper sediments (Gubkin, 1937; Kalinko, 1964; McCrossan et al., 1971; Jones and Drozd, 1979; Mousseau and Williams, 1979; Drozd et al., 1981; Richers

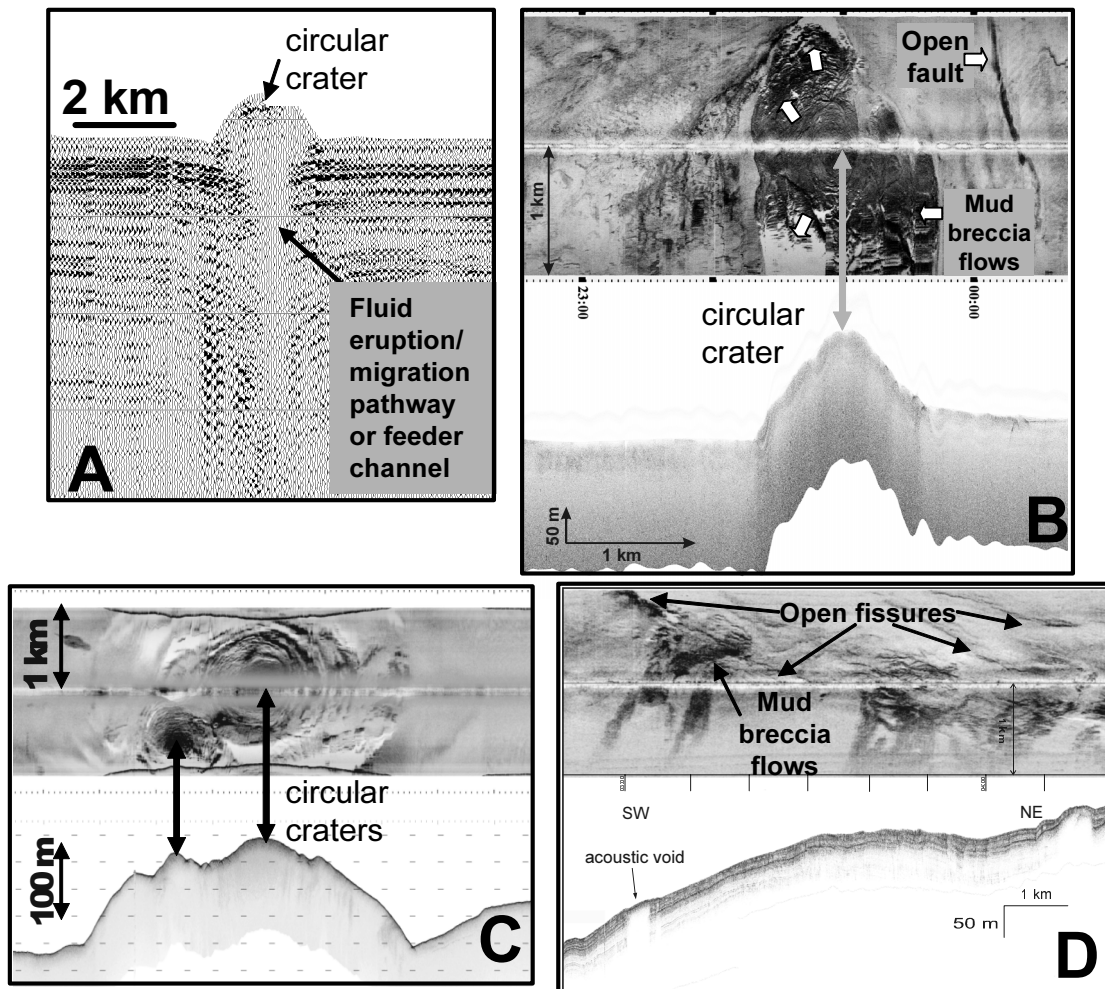


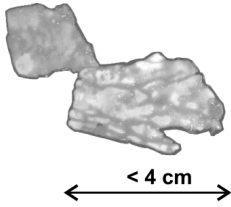
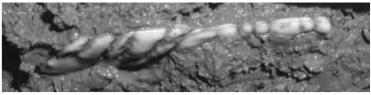
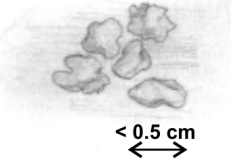
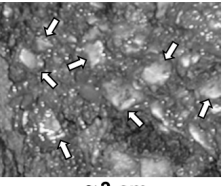
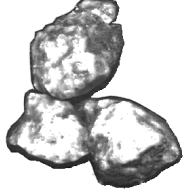
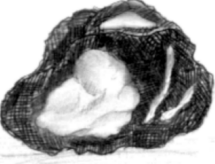
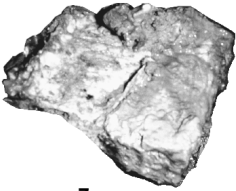
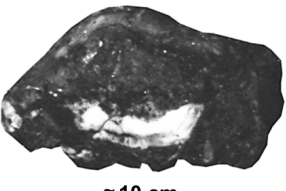
**Figure 2.** Examples of deep-sea mud volcanoes. **(A)** Fragment of seismic line across the Kovalevsky MV, Central Black Sea (after Kenyon et al., 2002); **(B)** Fragment of 30 kHz sidescan sonar sonograph and subbottom profiler record across the Kazakov MV, Sorokin Trough, NE Black Sea (after Kenyon et al., 2002); **(C)** Fragment of OREtech deep-towed sidescan sonar across the Yuma MV from the Gulf of Cadiz (NE Atlantic; after Pinheiro et al., 2003); **(D)** Fragment of MAK-1 deep-towed sidescan sonar across the Odessa MV from the Sorokin Trough showing fissure eruption of mud breccia (NE Black Sea; after Ivanov et al., 1998, 1999). See <http://ioc.unesco.org/ttr/>.

et al., 1982, 1986; Jones and Drozd, 1983; Richers, 1984; Rakhmanov, 1987; Guliev and Feizullayev, 1997; Ivanov et al., 1998; Kholodov, 2002). The connection between seepage and hydrocarbon reservoirs in the deep subsurface was advocated by Link (1952) who stated that "oil and gas seeps gave the first clues to most oil-producing regions. Many great oil fields are the direct result of seepage drilling". MVs and gas venting areas commonly occur in petroliferous regions (Guliev and Feizullayev, 1997), and, as a rule, the hydrocarbon gases emitted are often thermogenic (i.e. formed by cracking of organic matter in the subsurface resulting from increase in temperature and pressure upon subsurface burial) in nature. The presence of a seep thus indicates the subsurface presence of a mature source of gas, the existence of migration pathways as well as the absence of a proper seal. An alternative origin of methane is microbial decomposition of organic matter under anoxic conditions, i.e. methanogenesis (microbial or biogenic gas) (see 1.2.1). Biogenic and thermal methane can be readily discriminated by their  $^{13}\text{C}$  content (Sackett, 1978; Stahl et al., 1979; Rice and Claypool, 1981). In fluid venting areas and MVs, gaseous compounds may be present in dissolved form, as a gas phase, and as a solid phase (in hydrate form), depending on gas composition, temperature, and pressure.

#### *1.1.5. Phenomena associated with cold-seepage*

MVs and seepage in general induce the development of complex cold-seep systems/ecosystems at and below the seafloor surface. Continuous upward migration of hydrocarbon-rich fluids may result in the development of submarine gas hydrate accumulations in the subsurface, hosting considerable quantities of methane (Ginsburg and Soloviev, 1997; Soloviev and Ginsburg, 1997; Ivanov et al., 1998; Bouriak and Akmetjanov, 1998). Gas hydrates are an ice-like crystalline solid composed of a mixture of water and natural gas, frequently methane. They are stable under the specific pressure and temperature conditions (Kvenvolden, 1993; Henriot and Mienert, 1998 and references therein), filling the pore spaces of sediments (Table 1).

When migrating up fluids reach the seafloor, they provoke the development of a marked biological activity manifested in the appearance of persistent chemosynthetic colonization of benthic organisms such as mollusks, methane-related tube worms, microbial mats, and a diversity of microbes fuelled by hydrocarbon gases (especially methane), sulphide and other reduced elements transported by fluids (Hovland and Judd, 1988; Sibuet et al., 1988; Corselli and Basso, 1996; Olu et al., 1996, 1997; Sibuet and Olu, 1998). Migrating fluids contain organic and inorganic components offering sources of carbon and energy and other essential nutrients for diverse microbial chemosynthetic communities. This encompasses utilization of migrated components, especially methane. Figure 3 schematically

GAS HYDRATE	IN SEDIMENT	MORPHOLOGY
 <p data-bbox="288 696 464 734">&lt; 4 cm</p>	 <p data-bbox="639 658 719 685">≈ 5 cm</p>	<p data-bbox="903 468 1377 707">Flat, irregular shaped tabular fragments up to 4 cm across. Some of these edifices observe myriad “crack-like” features on the upper and the lower surfaces, dividing hydrate into number of small “segments” oriented in the same direction. Within sediments this type of gas hydrates forms layers and/or lenses.</p> <p data-bbox="903 741 1310 768">MVs: Odessa, Collapsed Structure II</p>
 <p data-bbox="336 983 416 1010">&lt; 0.5 cm</p>	 <p data-bbox="639 1016 719 1043">≈ 3 cm</p>	<p data-bbox="903 799 1377 983">Commonly observed “ice-drop-like” sub-rounded aggregates not exceeding 0.5 cm in diameter. Within hosting sediments this type ether forms “patched accumulations”, separated inclusions or they surround bigger clasts of gas hydrates.</p> <p data-bbox="903 1016 1286 1077">MVs: Odessa, Kazakov, Collapsed Structure II</p>
 <p data-bbox="320 1308 400 1335">&lt; 3 cm</p>	 <p data-bbox="655 1301 735 1328">≈ 5 cm</p>	<p data-bbox="903 1111 1377 1261">Flat, Isomeric sub-rounded clasts up to 3 cm across. The surface is crooked with occasional cracks. Some aggregates after been sliced observed “pores” inside the hydrate aggregate.</p> <p data-bbox="903 1294 1302 1321">MVs: Odessa, Collapsed Structure II</p>
 <p data-bbox="288 1588 368 1615">≈ 7 cm</p>	 <p data-bbox="624 1588 703 1615">≈ 10 cm</p>	<p data-bbox="903 1435 1377 1552">Massive tabular aggregates up to 7 cm in size. Lateral sizes are noticed by appearance of visible crystals growing perpendicular to the surface of the hydrate.</p> <p data-bbox="903 1585 1038 1612">MV: Odessa</p>

**Table 1.** Morphology of gas hydrates found in the Sorokin Trough, NE Black Sea.



summarises methane turnover in marine sediments. The dominant methane sink in the marine settings is microbial anaerobic oxidation of methane (AOM) performed by a consortium of methanogenic archaea and sulfate reducing bacteria (Boetius, et al., 2000; Michelis et al., 2002, Orphan et al., 2001). This process subsequently results in mineral transformations and precipitation of different authigenic minerals, e.g. carbonates, sulfides, gypsum, etc.

Thus, fluids expelled from MVs and from other venting related structures not only portray the products of generation and migration from deep-subsurface, but also fuel microbial processes and create the basis for life of the diverse chemosynthetic ecosystems at the seafloor and subsurface.

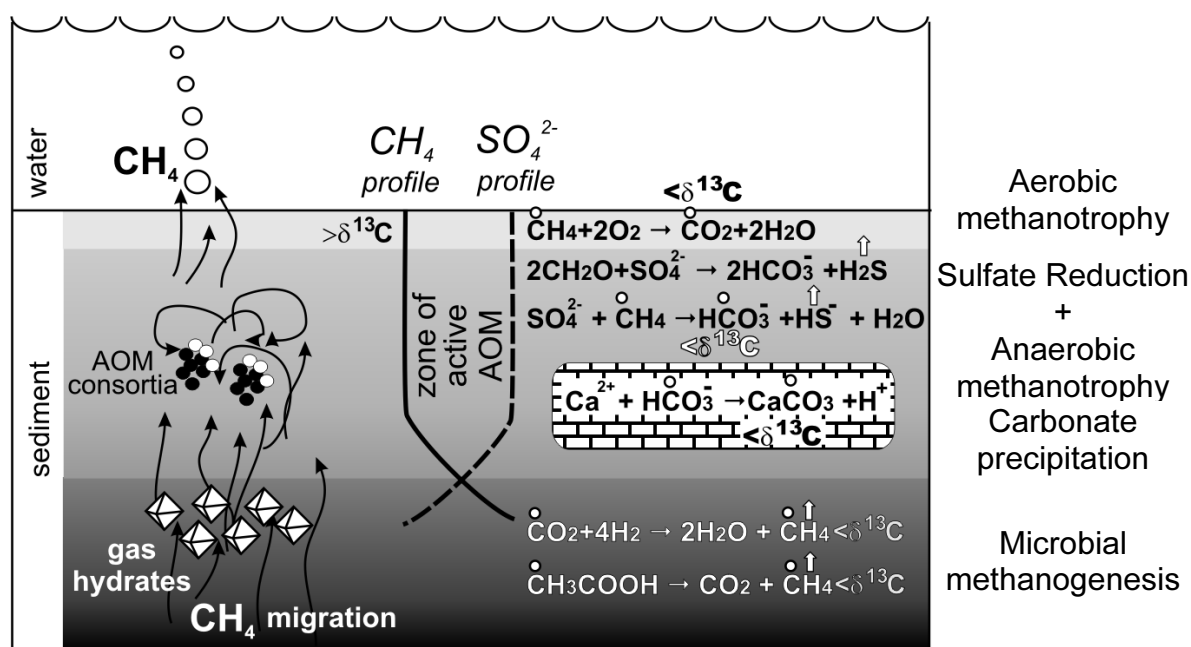


Figure 3. Schematic sketch of the marine methane cycle.

Fluid escape zones are also known for mineral formation under the influence of microbiological activity (Figure 3). Oxidation of methane results in production of bicarbonate ions which leads to oversaturation of pore waters and ultimately in the formation of carbonate minerals. The occurrence of neofomed diagenetic carbonates is a widespread phenomenon in modern cold-seep settings (Ritger et al., 1987; Roberts and Aharon, 1994; Von Rad et al., 1996; Peckmann et al., 1999a, 1999b, 2001; Aloisi et al., 2000, 2002; Michaelis et al., 2002; Cambell et al., 2002; Peckmann and Thiel, 2004). Such seep deposits were also described in Cenozoic strata (Cambell and Bottjer, 1993; Kauffman et al., 1996; Campbell et al., 2002), in Palaeozoic deposits (Campbell and Bottjer, 1995; Peckmann et al., 1999a, 2001a), and the oldest seep deposits are Middle Devonian in age (Peckmann et al., 1999b).

These modern and ancient seep carbonates display different morphologies, mineralogy, and stable carbon and oxygen isotopic compositions (Hovland et al., 1987; Roberts and Aharon, 1994; Peckmann et al., 1999a, 1999b, 2001, 2002; Stakes et al., 1999; Aloisi et al., 2000, 2002) and occur in the form of crusts, concretions, pavements, chimneys, varying in sizes from few millimetres precipitants to several meters high chimneys and tenths of meters extended carbonate pavements. Chemical analyses showed that these carbonates are depleted in  $^{13}\text{C}$  which led to the suggestion that carbon in such carbonates is, at least in part, derived from methane (Peckmann et al., 1999a, 1999b, 2001, 2002; Stakes et al., 1999; Aloisi et al., 2000, 2002). Gauter, (1985) and Paull et al. (1992) showed that aerobic oxidation of organic matter is of minor importance for the carbonate formation whereas sulfate reduction process is believed to be one of the important processes accountable for the precipitation of these carbonates. Baker and Kastner (1981) revealed that dissolved sulfate reduces dolomite formation, which lead to the assumption of its precipitation within the methanogenic zone (Gauter, 1985; Stakes, 1999). It was suggested that the precipitation of authigenic methane-derived bicarbonate is the result of increased alkalinity created by AOM (Ritger et al., 1987; Paull et al., 1992; Von Rad et al., 1996; Thiel et al., 1999), i.e. AOM serves as a source of inorganic carbon for the formation of carbonate cement, concretions, crusts, and other carbonate build-ups. However, only the recent discovery of tower-like microbialites, formed by methane-filled calcifying spheres constructed by living microbial mats at sites of active methane discharge in the Black Sea (Michaelis, et al., 2002; Reitner, et al., 2005), directly proved that microbial consortia performing AOM indeed induce carbonate precipitation in methane-seepage environments.

### **1.2. Key microbial processes for cold seeps**

#### *1.2.1 Methanogenesis*

Microbial methanogenesis is considered to be an important source of methane in the world oceans. In marine sediments, methane is the only hydrocarbon gas generated in relatively high quantities (Tissot and Welte, 1978). Methanogens, which belong to the Domain of the Archaea, fall in the phylogenetic groups of *Methanobacteriales*, *Methanococcales*, *Methanomicrobiales*, *Methanosarcinales*, and *Methanopyrales* within the kingdom of Euryarchaeota (Madigan et al., 2000).

Microbial methane formation is controlled by physiological and ecological factors. Methanogenic archaea are obligate anaerobes and cannot cope with even traces of oxygen. They are ubiquitous in anoxic environments where degradation of organic matter at redox levels of  $<-200$  mV takes place (Madigan et al., 2000). Methanogens can form methane using

H<sub>2</sub>/CO<sub>2</sub> (1), acetate (2), formate (3), methanol (4), methylamines (5) and CO (6) as the substrates (Daniels et al., 1984; Zehnder, 1988). H<sub>2</sub>/CO<sub>2</sub> and acetate are the most widely used substrates (Balch et al., 1979; Schlegel, 1985; Claypool and Kaplan, 1974; Whiticar et al., 1986; Borowski, et al., 1999). H<sub>2</sub> and acetate can be also exploited by sulfate reducing bacteria (SRB; Zehnder, 1988) and other bacteria. Methane, formed by methanogens *via* CO<sub>2</sub> reduction, has the lowest values in δ<sup>13</sup>C (-60 to -110‰) relative to the methane formed by the acetate fermentation (-50 to -65‰) (Whiticar et al., 1986). Archaea performing methanogenesis by the CO<sub>2</sub> reduction pathway are generally outcompeted by SRB (Lovley et al., 1982). Methanogenesis due to acetate fermentation is limited by substrate competition between the methanogens and SRB (Schönheit et al., 1982). Thus, methane is only formed in distinct biochemical environments, which are commonly located below the sulfate-reduction zone in marine sediments.

### *1.2.2 Anaerobic oxidation of methane*

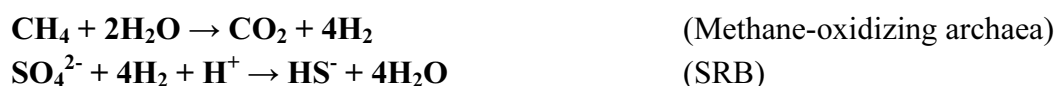
Methane belongs to the greenhouse gases since it has an ability to trap and re-emit infrared radiation and its global warming potential is over 20 times larger than an equivalent amount of carbon dioxide. Recent biogeochemical studies of gas-saturated and gas hydrate-bearing sediments were aimed to elucidate controls of methane production and consumption under anoxic conditions. More than 90% of the methane produced in marine settings is consumed anaerobically with sulfate (SO<sub>4</sub><sup>2-</sup>) as electron acceptor. Thus, AOM is one of the processes that control the atmospheric concentrations of methane and is considered as one of the important methane sinks in marine environments (Hinrichs and Boetius, 2002 and references therein). AOM is a widespread microbial process, and it apparently occurs at a range of scales from a small, few cm-thick zone in normal pelagic sediments, to large areas associated with the escape of methane from accumulations at depth. Although AOM is geochemically well documented, no organism that can consume methane anaerobically has as yet been isolated.

The occurrence of AOM was firstly suggested by Martens and Berner (1974) who noticed in anoxic marine sediments that the concentration of methane decreased in the sulfate reduction zone and concluded that methane is likely oxidized with sulfate as an electron acceptor (Martens and Berner, 1974). Barnes and Goldberg (1976) suggested that sulfate could play a role as a terminal electron acceptor according to reaction:



This is a net reaction and intermediate biochemical reactions are still unknown. Alternative mechanisms for AOM were suggested by Valentine and Reeburg (2000 and reference therein) and by Hinrichs and Boetius (2002 and reference therein).

Consumption of methane at the base of the sulphate reduction zone typically results in a characteristic concave-up methane concentration profile as observed in many marine sediments (Figure 3). Hoehler et al. (1994) proposed a putative consortium of methanogens with SRB that perform AOM through the process of “reverse methanogenesis”. Hydrogen syntrophy was suggested as one of the possible pathways that form the basis for this putative consortium. It was hypothesized that the use of hydrogen as an electron donor by the SRB results in a low partial pressure of hydrogen, thereby creating thermodynamically favourable conditions for methanogenic archaea to act as methane-oxidizers (Reeburg, 1976; Zender and Brock, 1979; Alperin and Reeburg, 1985; Hoehler et al., 1994; Hoehler and Alperin, 1996) according to the following reactions:



Direct proof for the co-existence of Archaea and SRB, i.e. AOM-consortia, was obtained by molecular ecological studies using fluorescence in situ hybridization (FISH) (Boetius et al., 2000; Michaelis et al., 2002), secondary ion mass spectrometry (SIMS) analyses of individual cell aggregates (Orphan et al., 2001a,b; Michaelis et al., 2002) and molecular phylogeny (Boetius et al., 2000; Orphan et al., 2001a, 2001b; Nauhaus et al., 2002; Teske et al., 2002; Michaelis et al., 2002) and biogeochemical studies using structural and stable carbon isotopic compositional information of lipids (e.g. Elvert et al., 1999, 2000; Thiel et al., 1999, 2001; Hinrichs et al., 1999, 2000a; 2000b; Pancost et al., 2000, 2001a, 2001b; Bian et al., 2001). Archaeal membrane lipids show distinct structures which contain in principal ether-linked (bi)phytanyl side-chains in contrast to the ester-bound fatty acids biosynthesized by Bacteria (Figure 4). These differences are often used as chemotaxonomical markers for the Archaeal and Bacterial domains and their specific groups. Direct evidence for anaerobic methanotrophy was provided by compound-specific carbon isotopic studies of archaeal lipids such as crocetane (**I**; Figure 5), pentamethylcosane (**II**), archaeol (**III**), hydroxyarchaeols (**IV**, **V**), and glycerol tetraethers (**VI**, **VII**, **VIII**, **IX**). The significantly <sup>13</sup>C-depleted archaeal lipids in the MVs and cold venting settings proved that archaea use methane-derived carbon as carbon source (Hinrichs et al., 1999; Elvert et al., 2000; Hinrichs et al., 2000b; Pancost et al., 2000; Thiel et al., 1999, 2001; Pancost et al., 2001a, 2001b; Aloisi et al., 2002; Teske et al., 2002; Zhang et al., 2002, 2003; Schouten et al., 2003). The

presence of specific  $^{13}\text{C}$ -depleted lipids possibly associated with SRB (X-XIV; Pancost et al., 2000, 2001b) and from the *Desulfosarcina/Desulfococcus* species (XV; Elvert et al., 2003) marked a close metabolic association between SRB and methanotrophic archaea.

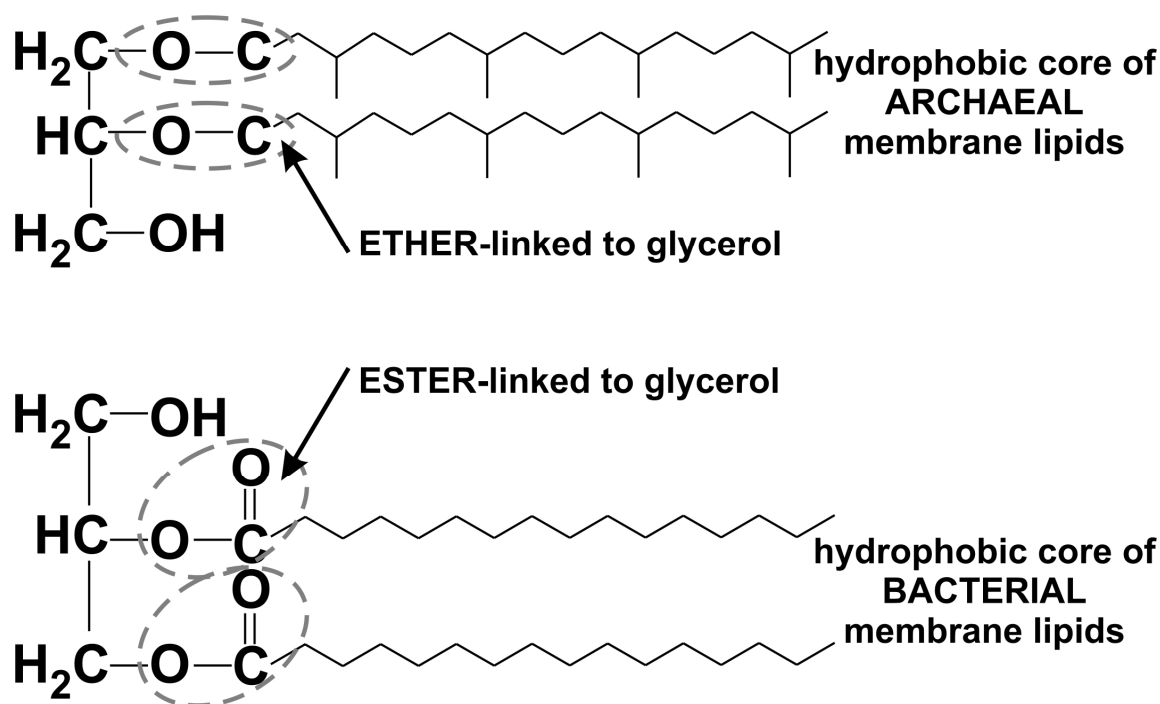


**Figure 4.** Distinct features of archaeal and bacterial core membrane lipids.

Phylogenetic analyses of ribosomal RNA (rRNA) gene sequences have revealed three distinct lineages among the *Euryarchaeota* capable of anaerobic methanotrophy (Figure 6). Archaea belonging to the ANaerobic MEthanotrophs (ANME) ANME-1 cluster do not contain any cultured relatives (Hinrichs et al., 1999; Orphan et al., 2002; Knittel et al., 2005). The ANME-2 archaeal cluster affiliated to the cultured members of the methanogenic *Methanosarcinales* (Boetius et al., 2000; Orphan et al., 2001a, 2001b; Knittel et al., 2005). The ANME-3 archaeal cluster is closer related to cultivated genera *Methanococoides* spp. than ANME-1 and ANME-2 (Knittel et al., 2005).

Various studies have also revealed a large variety in distribution and composition of archaea/SRB microbial biomass in gas-venting settings (Boetius et al., 2000; Orphan, 2001a; Pancost et al., 2001a; Michaelis, 2002). For example, SRB affiliated with members of the genera *Desulfosarcina* and *Desulfococcus* have been found in association with archaeal cells belonging to the ANME-1 and ANME-2 groups, representing in both cases putative methanotrophic consortia (Boetius et al., 2000; Orphan et al., 2001a, 2001b; Michaelis et al., 2002). An independent *Methanosarcinales*-related ANME-2 lineage composed of bacteria-



free archaeal cells has also been reported (Orphan, 2001a). The ANME-3 archaea are found to occur as single cells and in association with SRB of *Desulfobulbus* relatives (Lösekann, in prep.).

### **1.3. Scope and framework of the thesis**

#### *1.3.1 Research questions and goals*

The general view on MVs and cold seeps is that the fluids escaping from the subsurface contain methane and more complex organic compounds (wet gas, petroleum) that derive from accumulations of hydrocarbons in the deep subsurface at depths where microbial activity is lacking. In case of MVs, the fluid flow from the subsurface also contains a mixture of sediments and rock clasts. An important question is how deep the source strata for the erupted material are and whether the erupted sediments and hydrocarbons originated from the same sedimentary facies or not?

AOM is the microbiological key-process in cold seep systems (Boetius et al., 2000; Michaelis et al., 2002; Hinrichs and Boetius, 2002 and references therein), although the regulation of methane turnover in marine sediments is still not entirely understood. AOM prevents to a large extent the release of methane into the water column and atmosphere. AOM-related carbonates serve as barriers for the upcoming methane. Accordingly, how much methane can be converted into carbonates due to AOM? Is it possible to reconstruct palaeo-seepage environments and related changes in AOM-communities during the development of a carbonate in geological time? Are the archaeal/bacterial populations in carbonates and sediments constant over time or do they vary and how is the AOM consortium distributed with sedimentary depth?

The current thesis is devoted to expand our knowledge of the evolution and ecology of gas seepage structures. It includes studies of fluid origin, microbial methane cycle, and related carbonate formation. This is the first attempt of in-depth comparison of two principally different MV areas in the Sorokin Trough (NE Black Sea) and in the Gulf of Cadiz (in the NE Atlantic), using integrated geo-, bio-, and ecological approaches on processes associated with seepages from the seafloor. The aims of the applied biogeochemical program were focused on two different topics. The first was directed towards organic/petroleum geochemical perspectives and the goal of this part included identification of source/nature and maturity properties of up-going fluid *via* study of hydrocarbon gas mixtures (molecular and carbon stable isotope compositions of C<sub>1</sub> through C<sub>5</sub> hydrocarbons) and organic matter (lipid biomarker distribution) from gas saturated sediments and mud volcano deposits. We aimed to determine whether erupted gases and sediments initially belong to the same sedimentary strata

or not. These can give a clue to the possible location of roots of MVs and thus to the primary source of the erupted fluids. The second topic of the biogeochemical program aimed to study *in situ* diagenetic alterations associated with migrated hydrocarbon gas, especially methane, *via* the study of the methane cycle and related carbonate formation. The key factors determining the biogeochemical pathways and microbial mutual benefits in the various seepage environments are still largely unknown. This part of study includes detailed state-of-the-art biomarker analyses in combination with phylogenetic characterization of microbes potentially involved in the AOM and carbonate-shaping ecosystems. We compared molecular signatures (lipid biomarkers and 16S rRNA gene sequences) from MV deposits and methane-related carbonates collected from both MV areas aimed at describing the microbial processes in different cold seep systems and related carbonate formation.

The two areas were selected because of their fundamentally contrasting natural environments. The Sorokin Trough is located in the Black Sea, a unique, restricted deep-water basin with a stratified and almost stagnant water column, marked by hydrogen sulphide production and consequent strict anoxic environments starting at a depth of 100-150 m below the sea level. Gas seepage is the dominant methane source in the water column of the Black Sea (Reeburgh, et al., 1991; Luth et al., 1999) and AOM in the water column utilizes about 99 % of the  $2.9 \times 10^{11}$  mol of methane discharged annually from the seepages and MVs (Reeburgh et al., 1991; Wakeham et al., 2004). In contrast, the Gulf of Cadiz possesses oxygenated bottom waters and is characterized by active hydrodynamics, which are controlled by the exchange of water masses through the Gibraltar Strait. This water exchange corresponds to a mean surface inflow of the turbulent, cool-water mass of Atlantic Inflow Water on the surface and a denser, highly saline and warm outflow of water masses from the Mediterranean near the bottom (Ambar and Howe, 1979).

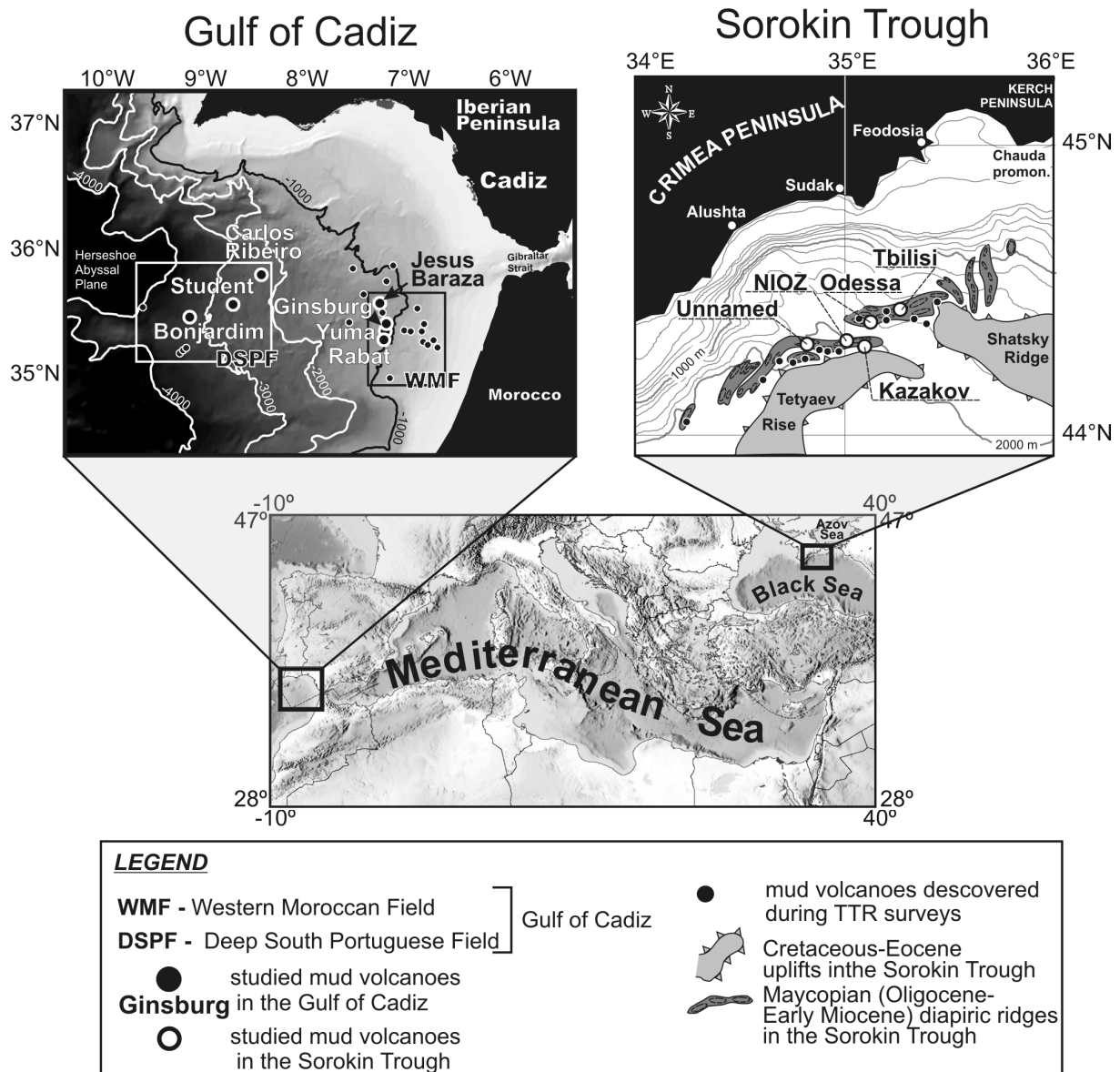
### 1.3.2. Research areas

Figure 7 shows the location of the two studied fluid venting provinces and MVs discussed in this thesis. The existence of both fluid venting areas was discovered and extensively investigated during several international multidisciplinary marine expeditions of the Training-Through-Research (TTR) programme carried out by the UNESCO-MSU Research and Training Center for Marine Geology and Geophysics between 1996 and 2001 (Woodside et al., 1997; Ivanov et al., 1998, 1999; Bouriak and Akhmetjanov, 1998; Gardner, 2001; Pinheiro et al., 2003; Kenyon et al., 2000, 2001, 2002, 2003, 2005). During these expeditions, a rich sample collection for the research described in this thesis was obtained.

Both study areas are characterized by the presence of MVs with extensive flows of gas saturated mud breccias, by the occurrence of the same features associated with fluid-venting



i.e. gas hydrates and methane-related carbonates, and by existence of chemosynthetic biota. Both areas have a relatively thick sedimentary cover, but a different geotectonical history and



**Figure 7.** Location of the studied MV provinces.

modern ecological environments. The presence of anoxic (in the Sorokin Trough) and oxygenated (in the Gulf of Cadiz) bottom waters will affect sedimentary conditions and likely affects methane turnover pathways, the location of the AOM zone, and the metabolic

interactions between microbial communities dominating these habitats and subsequent diagenetic mineral transformations in the subsurface.

Both areas are characterized by different fluid venting activity and modes of MV eruptions. This affects the intensity and constancy of methane fluxes. The Sorokin Trough is known by ubiquitous and presently active fluid venting. Various indications of subsurface gas presence and its upward transport were detected in the seismic records (for a comprehensive review on the geology, tectonics, and fluid venting associates in the Sorokin Trough, see Ivanov et al., 1998). Gas hydrates of different shapes and morphologies were frequently recovered from mud breccias and gas saturated sediments (Table 1; Woodside et al., 1997; Ivanov et al., 1998; Bouriak and Akhmetzhanov, 1998; Kenyon et al., 2002; Mazzini et al., 2004). Methane-related carbonates with microbial mats were also regularly found within MV deposits (Woodside et al., 1997; Ivanov et al., 1998; Kenyon et al., 2002; Mazzini et al., 2004). In contrast, no indications of the subsurface accumulations of hydrocarbons were until present detected during geophysical surveys in the Gulf of Cadiz although gas hydrates were frequently recovered from several MVs in the Gulf (see Pinheiro et al., 2003 and references therein). However, the presence of “graveyards” of carbonate chimneys, crusts and pavements in the Gulf of Cadiz testify of fluid (methane) release from the subsurface in the past (Díaz-del-Río et al., 2003).

### *1.3.3. Framework of the thesis*

This thesis provide a multifaceted view on how processes and products of seep activity may portray distinct eruptive dynamics of MVs, reveal possible sources of emitted gases and sediments and how these gases, especially methane, interplay with benthic ecosystems at and beneath the seafloor. To achieve this, a wide variety of geochemical, biogeochemical and molecular ecological techniques was used in combination with geological and sedimentological studies. The experimental techniques applied include a combination of methods for the qualitative, quantitative, and compound specific carbon isotope analysis for lipid biomarkers and hydrocarbon gases, molecular ecology using 16S rRNA gene sequence analysis and mineralogy together with stable carbon and oxygen isotope analysis of carbonates.

This thesis is subdivided into two parts. **Part I** comprises a multidisciplinary set of biogeochemical studies applied to MVs in the Sorokin Trough (NE Black Sea), and **Part II** describes the same suite of studies applied to MVs in the Gulf of Cadiz (NE Atlantic).

**Part I “The Sorokin Trough, NE Black Sea”** consists of **Chapters 2 to 5**.

**Chapter 2** describes hydrocarbon gas data from the Sorokin Trough (NE Black Sea), and shows that gas mixtures from all studied mud volcanoes and gas hydrates can be

interpreted as a consequence of oil cracking and/or biodegradation in the deep subsurface. Despite the first evidence for different maturity properties, the wet gas components in all mud volcanoes and gas hydrates are related to each other. Gases from mud volcanoes associated with up-doming diapiric structures, possess a mixture of mature and possibly secondary microbial methane with wet gases from the same sources.

**Chapter 3** shows through detailed biomarker analyses different mud breccia sources for MVs in the Sorokin Trough, which are directly linked to the location of the fracture zones or diapiric folds formed due to tectonic compression in the area. It is also demonstrated that lipid biomarkers can be used to recognize different mud eruption episodes.

**Chapter 4** describes a study of methanotrophic microbial mats associated with authigenic carbonates in the deep Black Sea and mud breccia. Concentrations and  $\delta^{13}\text{C}$  values of methane and specific archaeal and bacterial lipids, supplemented by archaeal and bacterial 16S rRNA gene sequences analysis, are reported. Using the data it is shown that AOM-mediated carbonate formation started within the sediment, below the sediment/water interface, corresponding to the intervals with high AOM rates, i.e. where methane and sulphate are abundant. Since Black Sea waters are anoxic, the carbonate growth direction is suggested to follow the pathways of migrated methane (that is, mainly laterally or/and upwards). Further, the lipid biomarker study integrated with a survey of 16S rRNA gene sequences revealed a distinct difference in archaeal assemblage between the microbial mats/carbonate crusts and the mud breccias. Nevertheless, AOM in these settings was predominantly performed by archaea affiliated with the so-called ANME-1 group.

As a follow-up study **Chapter 5** describes the finding of two novel macrocyclic diphytanyl glycerol diethers (DGDs), containing one or two cyclopentane rings in the same carbonates and describes in detail principal differences in membrane lipid structures of Archaea and Bacteria. Structurally similar compounds were previously identified in the deep-sea hydrothermal vent methanogen *Methanococcus jannaschii* (Comita et al., 1984) and in this chapter, we show that these macrocyclic DGDs are not restricted to thermophilic methanogens and could relate either to unknown methanogenic archaea or to other microbes involved in AOM and carbonate shaping in cold-venting habitats.

**Part II “The Gulf of Cadiz, NE Atlantic”** includes **Chapters** from **6** to **8**.

**Chapter 6** provides evidence for the presence of two groups of hydrocarbon gases in the Gulf of Cadiz. Both types of gases are relatively mature, allochthonous to the erupted mud breccia and are represented by a complex of redeposited, secondary migrated, mixed, and microbially altered hydrocarbon gas mixtures. The hydrocarbon gas data indicate the absence of strong upward gas transport and active biological processes within ca. 50-100 cm bsf. This

indicates that at present at the studied locations of the Gulf of Cadiz hydrocarbon gas does not escape into the overlying water column.

In **Chapter 7**, lipid biomarker data are presented which allow the comparison of mud breccia matrixes of three MVs in the Gulf of Cadiz. It reveals strong compositional resemblance as well as similar thermal maturity properties of the organic matter. This is evidence that the primary source for the erupted material in all studied MVs from the Gulf is derived from similar litho-stratigraphic units. This chapter also discusses the microbial processes related to the methane cycle as evident from specific biomarker lipids and their stable carbon isotopic compositions. Biomarkers for *in-situ* AOM processes were detected but occur in relatively low amounts, suggesting that AOM rates after eruption of MVs and formation of the mud breccia flows at sea floor ceased rapidly.

In **Chapter 8**, different horizons of a carbonate crust from the Gulf of Cadiz were studied in detail to elucidate microbial diversity during the development of the crust within the local methane-seepage habitat. A combined lipid biomarker and 16S rRNA gene sequence analysis revealed a two-step development of the crust in habitats with varying pore fluid compositions and methane flux environments. These changes likely affected the AOM community structures, which were represented by ANME-1 and ANME-2 archaeal groups, showing dominance of one group of archaea over another along the crust.

**Chapter 9 (Synthesis)** compares briefly the fluid venting phenomena in the Gulf of Cadiz and in the Sorokin Trough. Based on the data presented in chapters 2-8, possible geotectonic and environmental factors both in the present and in the geological past are described. These have drastically influenced MV activity in both areas and, as a response, microbial fabrics and carbonate-shaping ecosystems in general.



The Sorokin Trough,  
NE Black Sea



### **SOURCES OF HYDROCARBON GASES IN MUD VOLCANOES FROM THE SOROKIN TROUGH, NE BLACK SEA, BASED ON MOLECULAR AND CARBON ISOTOPIC COMPOSITIONS.**

A. Stadnitskaia<sup>a,b</sup>, M.K. Ivanov<sup>b</sup>, E.N. Poludetkina<sup>b</sup>, R. Kreulen<sup>d</sup>  
and T.C.E. van Weering<sup>a,c</sup>

<sup>a</sup>*Royal Netherlands Institute for Sea Research (NIOZ), P.O. Box 59, 1790 AB Den Burg, Texel, The Netherlands.*

<sup>b</sup>*Geological Faculty, UNESCO-MSU Centre for Marine Geosciences, Moscow State University, Vorobjevy Gory, Moscow 119899, Russian Federation.*

<sup>c</sup>*Department of Paleoclimatology and Geomorphology, Free University of Amsterdam, de Boelelaan 1085, 1081 HV Amsterdam, The Netherlands.*

<sup>d</sup>*ISOLAB, 1e Tieflaarsestraat 23, 4182 PC Neerijnen, The Netherlands.*

To be submitted to *Marine and Petroleum Geology*

#### **Abstract**

Molecular and stable carbon isotope properties of the hydrocarbon gas (methane through pentanes) reveal their origin and/or source of and their subsurface microbial alteration. This is defined in seven sediment cores collected from five mud volcanoes (MVs) in the Sorokin Trough (NE Black Sea). The data obtained show that hydrocarbon gases from all studied mud volcanoes and gas hydrates can be characterized and defined as a consequence of oil cracking and/or biodegradation in the deep subsurface. Despite the first evidence for different maturity properties, the wet gas components in all mud volcanoes and gas hydrates are related to each other. Gases from mud volcanoes associated with up-doming diapiric structures, possess a mixture of mature and probably secondary microbial methanes with wet gases from the same source. Probably, the most mature, and unaltered gas in the mud breccia from the Kazakov MV represents the original gas properties of the hydrocarbons trapped in the deep subsurface of the Sorokin Trough. Analysis of the hydrocarbon gas data, complemented with maturity characteristics of organic matter from the Maycopian rock clast and mud breccia matrix implies that the original source of gases likely is located below the Maycopian Shale Formation.



## **1. Introduction**

Mud volcanoes (MVs) are documented world wide in both on- and offshore locations. They reflect the presence of hydrocarbon reservoirs in the deep subsurface. Gas and oil seepage are related phenomena. The roots of MVs can reach down 20 km sediment depth (Shnyukov et al., 2005), thus providing key information on the geological history of the area and on the possible hydrocarbon potential (Ivanov et al., 1998; Ivanov, 2003). Comprehensive investigations of numerous on- and off-shore mud volcano provinces have revealed the overwhelming input of hydrocarbon gases (HCGs) in their formation. Eruptions are often manifest in a catastrophic emission of fluids consisting of HCGs (especially methane), hydrogen sulfide, carbon dioxide, petroleum products, water, and a complex mixture of sediments, so called “mud breccia” (Ivanov et al., 1998; Akhmanov, 1996; Akhmanov et al., 1998; Ivanov, 2003).

The Black Sea region is well known for the presence of fluid-related structures in shallow to deep-water environments (Ivanov et al., 1989, 1992, 1998; Ginsburg et al., 1990; Konyukhov et al., 1990; Kruglyakova et al., 1993; Limonov et al., 1994; Shnyukov et al., 1995; Woodside et al., 1997; Peckmann et al., 2001; Thiel et al., 2001; Michaelis et al., 2002; Kenyon et al., 2002; Blinova et al., 2003; Bohrmann et al., 2003; Cifci et al., 2002; Ergun et al., 2002), and there is an active debate about the possible sources of emitted fluids/HCGs. An extensive overview about fluid fluxes and mud volcanism in the Sorokin Trough was completed by Ivanov et al. (1998). Mazzini et al. (2004) partially introduced HCG data from the Sorokin Trough in the context of formation of methane-related carbonates. Here, we combined all data on molecular and stable carbon compositions of HCG from pelagic sediments, mud breccias and gas hydrates collected during Training-Through-Research (TTR) expeditions, in 1996 (ANAXIPROBE/TTR-6) and in 2001 (TTR-11) in the north-eastern part of the Black Sea, within the Sorokin Trough (Figure 1). The data-set obtained during ANAXIPROBE/TTR-6 expedition in 1996 resulted in the recognition of sixteen new MVs (Ivanov et al., 1998). Re-visiting the Sorokin Trough during the first part of the TTR-11 cruise in 2001 aimed at a detailed investigation of previously discovered structures for features associated with cold-seep phenomena. In this paper, we report on the molecular and stable carbon isotope properties of methane through pentanes, that were defined to reveal the origin/source of HCG and its eventual subsurface microbial alteration, in seven sediment cores collected from five MVs in the Sorokin Trough (Figure 1 and Figure 2). All locations are related to sites characterized by various acoustic anomalies associated with hydrocarbon migration/accumulation (Ivanov et al., 1998; Bouriak and Akhmetzhanov, 1998; Kenyon et al., 2002). The MVs are located relatively close to each other and are characterized by a suite of distinct features, such as variable modes of mud eruptions and venting activity, which are

reflected in the mound morphology, in the occurrence of various fluid venting associates, such as gas hydrates, methane-related carbonates with microbial mats (Ivanov et al., 1998; Mazzini et al., 2004; Stadnitskaia et al., 2005), or in lithological characteristics of the erupted material (Figure 2).

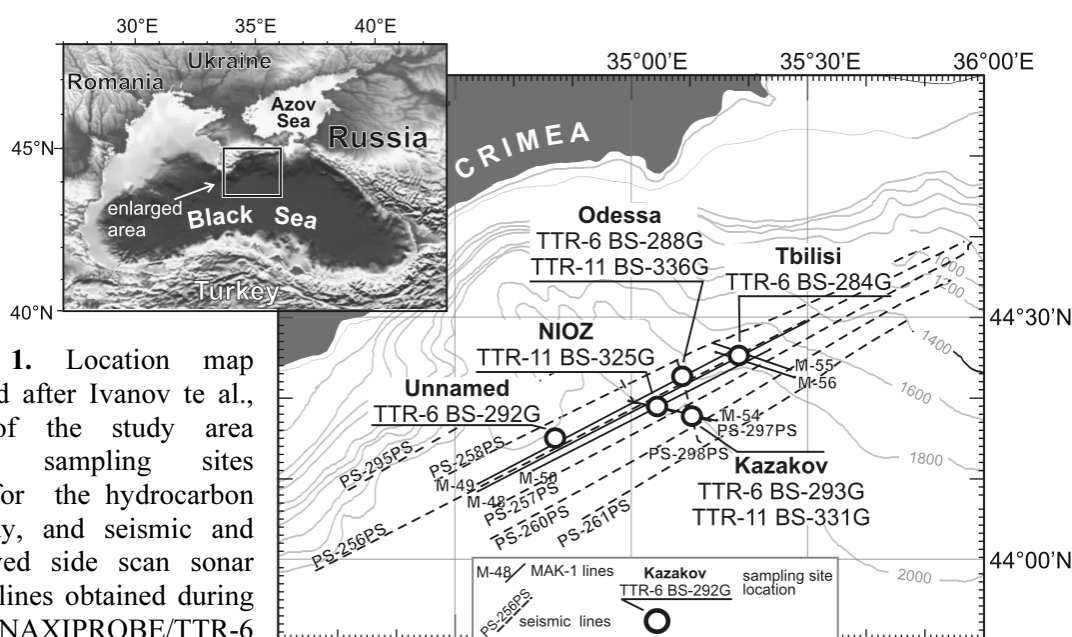


**Figure 1.** Location map (modified after Ivanov et al., 1998) of the study area showing sampling sites chosen for the hydrocarbon gas study, and seismic and deep-towed side scan sonar MAK-1 lines obtained during the ANAXIPROBE/TTR-6 (1996) and TTR-11 (2001) cruises.

## 2. Geological and tectonic background

The Sorokin Trough is situated south-east of the Crimea peninsula, and forms one of the largest depressions in the Eastern Black Sea. The Trough extends from the Chaudian promontory on the Kerch Peninsula to Yalta, has a length of about 150 km and is 45-50 km wide (Tugalesov et al., 1985). The Trough is orientated from SW to NE in water depths of 600-2100 m (Figure 1). To the south-east it is bounded by Cretaceous-Eocene Tetyaev and Shatsky uplifts (Belousov et al., 1988). It gradually narrows to the NE (Belousov, et al., 1988). The Sorokin Trough is considered to have formed the Crimean Alpine foredeep established during Maykopian (Oligocene-Early Miocene) time, which is known as a period of abrupt tectonic changes associated with culmination of the Alpine-Himalayan orogeny.

The depocentre of the Sorokin Trough contained up to 2-3 km Paleocene-Eocene sediments (Belousov, et al., 1988), and up to 5-6 km Oligocene-Early Miocene Maykopian Shale, the Maykopian Shale Formation (MSF), which forms numerous diapiric structures (Tugalesov, et al., 1985). The total thickness of the overlying Middle Miocene-Pliocene sediments is rarely over 1 km, while Quaternary sediments attain up to 2-3 km in thickness, mainly due to accumulations in the paleo-Don/paleo-Kuban Pleistocene composite fan

(Tugolesov et al., 1985; Woodside et al.,; Ivanov et al., 1998; Bouriak and Akhmetzhanov, 1998). The thickness of the Quaternary sediments is controlled by the underlying complex of mud-diapiric systems (Limonov et al., 1997), which originate from the protrusion of plastic, fluid-saturated Maycopian Shales (Woodside et al., 1997).

Maycopian diapiric folds among of the most spectacular structural characteristics of the Sorokin Trough's sediment fill (Limonov et al., 1997; Ivanov et al, 1998). The MSF is the regional source rock in basins from the Carpathians in the western Black Sea region, through the Crimea and the Caucasus Mountains, to the South Caspian Basin in the east. Besides, the MSF also locally includes reservoirs with significant oil and gas accumulations. In the Sorokin Trough, Maycopian diapirs are intensively faulted (Limonov et al., 1997; Ivanov et al, 1998). In some cases, faults continue into the Quaternary sediments or reach the seafloor and occur as large parallel NW-SE orientated fissures (Woodside et al., 1997; Limonov et al., 1997, Ivanov et al., 1998; Bouriak and Akhmetzhanov, 1998).

Most MVs are situated on the flanks of the Maycopian diapiric ridges (Ivanov et al., 1998). Seismic and acoustic records obtain during the TTR-6 (1996) and TTR-11 (2001) expeditions in the Sorokin Trough show various signs of the presence of gas. On a number of seismic sections and acoustic lines acoustically transparent zones, which indicate fluid migration pathways, were detected (Ivanov et al., 1998; Bouriak and Akhmetzhanov, 1998, Kenyon et al., 2002). Secondary accumulations of hydrocarbons are reflected by numerous acoustic anomalies, which have been traced at the flanks of diapirs and between deep fault systems in Pliocene-Quaternary sediments (Bouriak and Akhmetzhanov, 1998; Kenyon et al., 2002).

### **3. Sampling, material and methods**

All sediments collected during the ANAXIPROBE/TTR-6 and TTR-11 cruises were obtained using a 6 m long gravity corer (ca. 1500 kg) with an internal diameter of 14.7 cm (Kenyon et al., 2000, 2001). In total, 25 sediment cores showed gas saturation and ten out of these contained gas hydrates (Ivanov et al., 1998; Mazzini et al., 2004).

Presence of gas was also frequently noted in freshly recovered mud breccia and hemipelagic sediments. This is reflected in the formation of gas forced gaps induced by substantial sediment expansion. Subsampling for HCG analysis was subsequently performed taking into consideration the lithology of the recovered sediments. The degassing was accomplished according to the Head-space technique (Bolshakov and Egorov, 1987). To reduce intensive degassing, especially from mud breccias with gas hydrates, subsampling of such sediments was carried out in a cold-room with a constant temperature of -15 to -20°C.

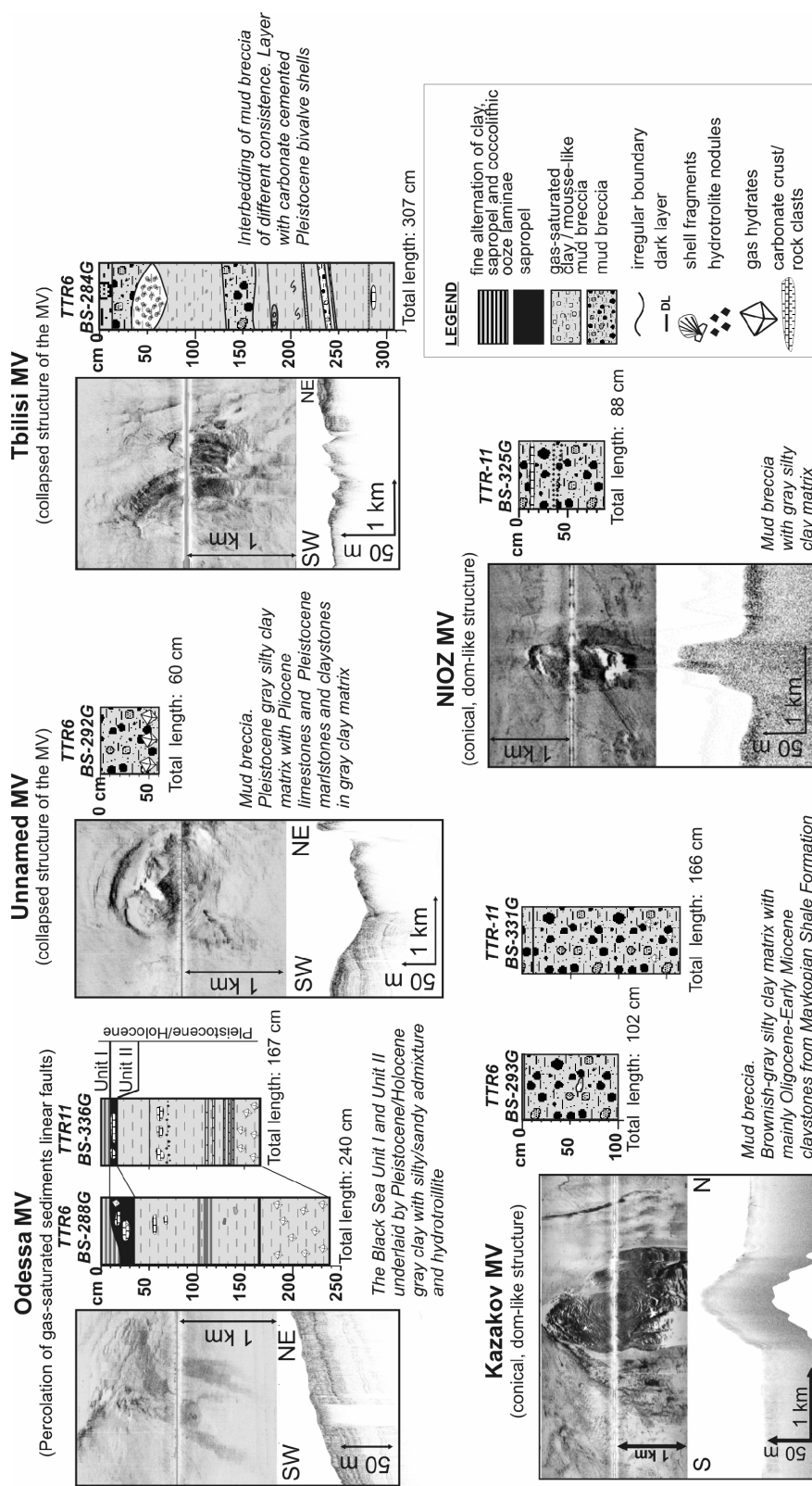


**Figure 2.** Fragments of MAK-1 sonographs and sub-bottom profiler record obtained during ANAXIPROBE/TTR-6 and TTR-11 cruises, imaging mud volcanoes and sampled sedimentary cores with schematic lithology (modified after Ivanov et al., 1998 and Bouriak and Akhmetzhanov, 1998).

Gases from gas hydrates were then obtained by spontaneous degassing in salt-saturated water solution (Mazurenko et al., 2002).

The molecular composition of HCG in the C<sub>1</sub> through C<sub>6</sub> range, including alkenes (ethene, propene and butene) and alkanes with isomeric molecular structure (*i*C<sub>4</sub>, *i*C<sub>5</sub> and  $\Sigma$ *i*C<sub>6</sub>) were determined in the laboratory using a gas chromatograph (GC) equipped with an on-column injector and a flame ionization detector. Gas components were separated on a 3 m packed column with activated Al<sub>2</sub>O<sub>3</sub> as a stationary phase. The samples were injected at 40°C and this temperature was held for 10 min. Then the GC oven temperature was raised to 70°C at a rate of 1°C/min. The temperature was then held constant for 20 min.

Consideration must be given to the fact that part of the gases may have been lost on deck due to active degassing of the recovered sediments during sectioning and cutting of the cores. Thus, we do not direct our attention on the general concentration level, although concentrations of HCG are still high even with a partial loss. Taking into account that the “head-space” technique is a qualitative rather than a quantitative method, the absolute concentration (expressed as ml/l of wet sediment) values are used here only to indicate the trends of the HCG distribution profiles and to reveal *in situ* microbial alteration of migrated gaseous constituents, e.g. AOM and C<sub>2+</sub> consumption. The later should be reflected in the molecular and stable carbon isotope properties of the HCG mixture.

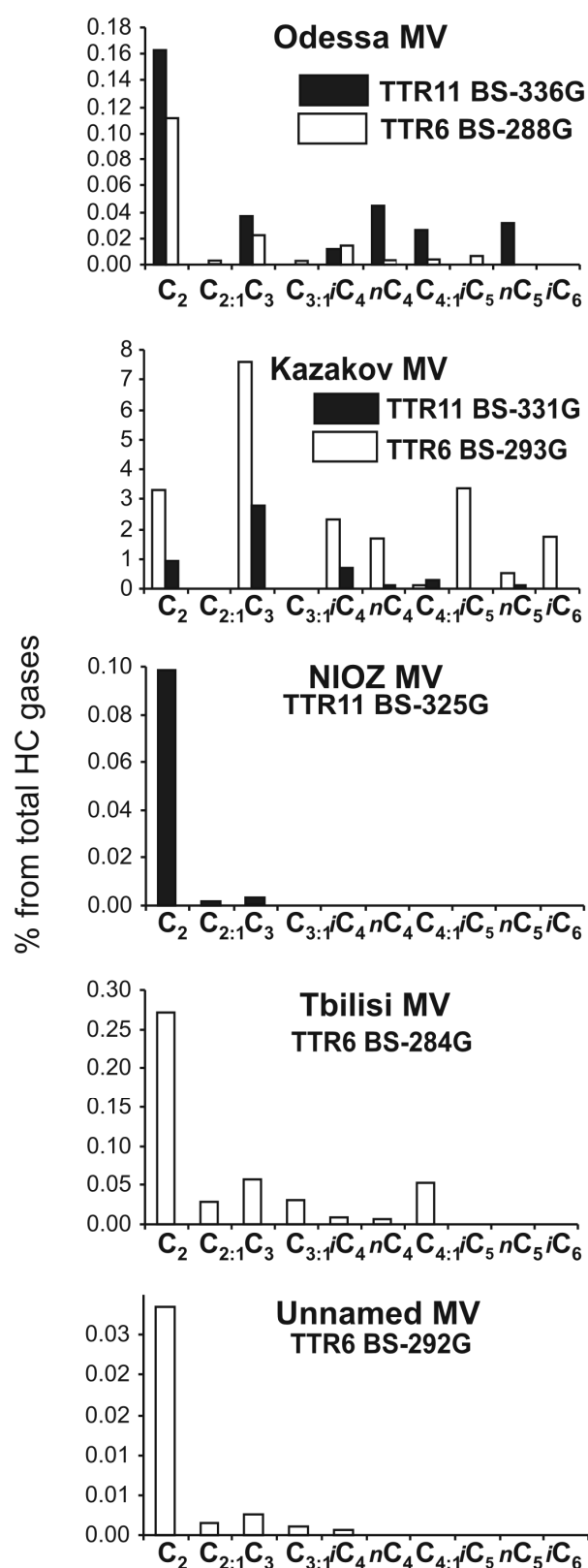
The carbon isotope ratios from C<sub>1</sub> to C<sub>5</sub> including *i*C<sub>4</sub> and *i*C<sub>5</sub> HCGs were measured on a Finnigan Delta S mass spectrometer with a HP 5890 GC and a GC-combustion interface. Methane was separated on a 5 Å molecular sieve plot column using either split- or split-less injection, depending on the concentrations. Alkanes C<sub>2</sub>-C<sub>5</sub> were cryogenically enriched (trough trapping in liquid nitrogen) and separated on a poraplot-Q column. The carbon stable isotope concentrations are expressed in the  $\delta$ -notation (‰) relative to Vienna Pee Dee Belemnite (VPDB) standard. The overall precision for the stable carbon isotope measurements by parallel definitions was ca. 0.3 ‰ for C<sub>1</sub> and C<sub>2+</sub>.

## 4. Results

### 4.1. Molecular and stable carbon isotope properties of HCG

#### 4.1.1. Sediments

The natural gases from the five MVs in the Sorokin Trough (Figure 1) show different molecular compositions. Methane is the dominant alkane of all HCGs. Its concentration varies from 0.02 to 170 ml/l and its content ranges from 47.9 to 99.9 % relative to the total HCGs (Table 1). The lowest abundances of methane were detected in the topmost sedimentary intervals, where AOM processes are active (Stadnitskaia et al., 2005).



The richest assortment and the highest concentrations of wet gas components, including ethane (C<sub>2</sub>), propane (C<sub>3</sub>), *iso*-butane (*i*C<sub>4</sub>), normal butane (*n*C<sub>4</sub>), *iso*-pentane (*i*C<sub>5</sub>), normal pentane (*n*C<sub>5</sub>), and *iso*-hexanes (*i*C<sub>6</sub>), was detected in mud breccias from the Kazakov MV (Figure 3). In contrast, mud breccias from the NIOZ MV showed only the presence of C<sub>2+</sub> gases till C<sub>3</sub>. Although C<sub>2+</sub> contents did not exceed 0.3 % from the total HCGs, sediments from the Odessa MV contained a suite of methane homologues to C<sub>5</sub> including *i*C<sub>4</sub> and *i*C<sub>5</sub>, and mud breccias from the Tbilisi and Unnamed MVs were represented by a set of alkanes from C<sub>2</sub> through C<sub>4</sub> (Figure 3).

Except for the Kazakov MV, where C<sub>3</sub> is the main methane homologue, all other MVs displayed C<sub>2</sub> as the dominant constituent among the detected wet gas components (Figure 3). The prevalence of C<sub>3</sub> in the Kazakov MV is reflected in the low (0.8-1.1) ethane/propane ratio. Simultaneously, the Tbilisi and Odessa MVs show ethane/propane ratios of ca. 7.2 -7.8. In the NIOZ MV, this ratio is on average ca. 72.2 and in the Unnamed MVs, the ratio is about 1.3 (Table 1).

**Figure 3.** Molecular composition and relative abundance of wet gas components. Abundances represent an average percentage of each methane homologue relative to the amount of total wet gas components. Filled bars indicate data from the TTR-11 (2001) cruise and dashed bars refer to data from the ANAXIPROBE/TTR-6 (1996) cruise.

**Table 1.** Molecular composition and molecular ratios of hydrocarbon gases.

*Izobilis MV*  
TTR6 BS-284G

depth, cm b.s.f.	TOC, wt %	% from total identified HC gas	concentration, ml/wet sediment		concentration $\times 10^{-4}$ ml/wet sediment						molecular ratios																			
			methane		ethane		propane		propene		iso-butane		n-butane		butene		C <sub>1</sub> /C <sub>2</sub>		C <sub>2</sub> /C <sub>3</sub>		C <sub>1</sub> /C <sub>2</sub> +		C <sub>1</sub> /(C <sub>2</sub> +C <sub>3</sub> )		C <sub>n</sub> H <sub>2n+2</sub> /C <sub>n</sub> H <sub>2n</sub>		Gas Wetness			
0	0.8	99.75	1.4	20.4	8.9	3.5	3.8	n.d.*	n.d.	n.d.	n.d.	706.1	5.8	-	601.5	392.9	1.9	0.17												
23	1.1	98.77	0.9	102.1	3.5	6.8	3.8	n.d.	n.d.	n.d.	n.d.	91.2	15.0	-	85.5	80.1	14.8	1.16												
35	0.6	99.90	14.2	132.8	traces	7.7	3.2	n.d.	n.d.	n.d.	n.d.	1066.7	17.3	-	1008.4	979.6	34.0	0.10												
64	0.9	99.96	56.1	218.9	3.8	10.0	traces	n.d.	n.d.	n.d.	n.d.	2560.6	21.8	-	2448.5	2402.0	51.7	0.04												
84	0.9	99.97	37.8	86.1	5.9	11.5	7.1	n.d.	n.d.	n.d.	n.d.	4383.6	7.5	-	3867.1	3413.3	7.5	0.03												
100	1.2	99.95	24.2	95.0	3.8	11.8	7.1	n.d.	n.d.	n.d.	n.d.	2552.8	8.1	-	2270.7	2060.2	9.8	0.04												
118	1.1	99.95	26.0	109.4	8.0	10.6	6.2	n.d.	n.d.	n.d.	n.d.	2372.0	10.3	-	2162.2	1934.1	8.5	0.05												
131	1.6	99.72	13.0	276.1	11.8	56.6	15.6	n.d.	n.d.	n.d.	n.d.	470.1	4.9	-	390.1	360.4	12.1	0.26												
152	1.3	99.49	6.2	202.7	10.0	46.9	15.0	5.3	2.1	33.9	305.7	4.3	2.6	248.2	196.1	4.4	0.41													
170	0.8	99.57	6.2	82.6	10.0	23.6	11.8	3.2	4.1	130.4	750.0	3.5	0.8	583.3	233.1	0.7	0.18													
187	0.9	99.76	6.8	89.7	11.8	25.7	6.2	3.5	4.1	22.7	756.6	3.5	0.9	588.2	414.4	3.0	0.18													
203	2.4	99.33	6.2	262.0	19.8	92.9	24.5	2.1	n.d.	18.0	236.5	2.8	-	174.6	147.8	5.7	0.57													
230	2.0	97.39	1.2	139.8	27.7	42.8	33.0	13.0	10.9	56.3	86.5	3.3	1.2	66.2	37.4	1.8	1.68													
255	1.0	99.75	7.4	120.1	8.0	21.5	10.9	3.0	3.2	16.8	614.3	5.6	0.9	520.8	401.9	4.1	0.20													
275	2.0	99.85	13.6	154.3	8.0	28.0	8.0	2.7	3.5	n.d.	879.5	5.5	0.8	744.3	663.8	11.8	0.14													

*Odessa MV*  
TTR6 BS-288G

depth, cm b.s.f.	TOC, wt %	% from total identified HC gas	concentration, ml/wet sediment		concentration $\times 10^{-4}$ ml/wet sediment												molecular ratios															
			methane		ethane		ethene		propane		propene		iso-butane		n-butane		butene		C <sub>1</sub> /C <sub>2</sub>		C <sub>2</sub> /C <sub>3</sub>		iso-C <sub>4</sub> /n-C <sub>4</sub>		C <sub>1</sub> /(C <sub>2</sub> +C <sub>3</sub> )		C <sub>1</sub> /C <sub>2</sub> +		C <sub>n</sub> H <sub>2n+2</sub> /C <sub>n</sub> H <sub>2n</sub>		Gas wetness	
0	1.6	99.52	11.6	387.2	15.5	108.0	0.6	28.2	10.2	15.5	n.d.	n.d.	300.4	3.6	2.8	234.9	205.8	16.9	0.46													
16	1.7	99.75	44.7	572.4	n.d.*	239.1	1.7	98.5	29.0	23.8	176.7	780.1	2.4	3.4	550.3	391.3	43.8	0.25														
37	1.8	99.65	35.1	392.9	n.d.	136.8	1.3	519.3	15.5	11.0	154.8	892.8	2.9	33.6	662.2	284.8	99.7	0.35														
53	0.4	99.86	23.5	258.1	n.d.	28.8	27.6	4.0	0.8	12.7	n.d.	911.9	8.9	5.0	820.3	708.8	7.2	0.12														
63	0.3	99.92	16.5	106.6	n.d.	17.1	1.5	1.6	1.0	n.d.	n.d.	1547.6	6.2	1.6	1334.0	1290.6	84.2	0.08														
85	0.3	99.88	43.6	488.3	n.d.	27.3	1.8	2.9	1.8	n.d.	n.d.	893.2	17.9	1.6	845.8	835.2	281.9	0.12														
100	0.5	99.82	9.5	137.5	4.8	19.4	1.3	1.4	1.0	6.6	n.d.	687.9	7.1	1.3	602.9	550.0	12.6	0.17														
115	0.3	99.86	15.2	182.4	n.d.	16.4	2.2	2.2	1.4	0.8	6.3	834.9	11.1	1.6	766.1	719.3	69.6	0.14														
119	0.3	99.88	23.2	235.7	n.d.	20.3	1.5	1.8	1.4	9.3	n.d.	983.8	11.6	1.3	905.8	888.6	23.9	0.11														
136	0.6	99.80	14.5	232.8	12.6	24.7	3.9	1.8	1.4	8.5	n.d.	624.4	9.4	1.3	564.5	508.7	10.4	0.18														
148	0.7	99.88	21.1	218.9	n.d.	20.9	1.5	1.8	1.2	7.8	n.d.	964.7	10.5	1.6	880.7	837.5	26.0	0.11														
158	0.6	99.90	23.2	196.4	n.d.	20.7	1.7	1.0	1.4	7.8	n.d.	1181.0	9.5	0.8	1068.6	1012.6	22.9	0.09														
170	0.5	99.87	26.0	308.7	n.d.	14.5	0.9	0.7	0.6	8.1	n.d.	841.1	21.2	1.2	803.3	778.5	36.1	0.12														
177	0.4	99.87	21.5	216.1	7.4	30.0	2.4	9.9	2.4	6.5	n.d.	993.1	7.2	4.1	872.0	781.2	15.9	0.12														
192	0.4	99.91	20.5	95.4	10.3	46.7	2.7	26.0	4.5	n.d.	n.d.	2152.4	2.0	5.8	1444.8	1107.0	13.4	0.08														
213	0.4	99.86	34.2	280.6	12.8	67.7	2.8	44.7	10.2	11.9	42.2	1217.1	4.1	4.4	980.5	722.3	16.2	0.13														
220	0.5	99.91	38.0	171.1	8.5	68.4	1.8	61.0	2.2	10.0	29.8	2218.5	2.5	27.8	1584.8	1075.5	16.3	0.09														
235	0.4	99.88	22.5	117.8	8.3	57.6	3.1	34.3	4.8	9.2	35.9	1909.9	2.0	7.1	1282.9	830.1	12.1	0.11														

Table 1. Continuation.

Odeasa MV  
TIR11 BS-336G

depth, cm b.s.f.	TOC, wt %	% from total identified HC gas	concentration, $mll$ / wet sediment		molecular ratios													
			methane		Σpentanes (iso-pentane+n-pentane)													
				ethane	ethene	propane	propene	iso-butane	n-butane	butene	Σpentanes (iso-pentane+n-pentane)	C <sub>1</sub> /C <sub>2</sub>	C <sub>2</sub> /C <sub>3</sub>	iso-C <sub>4</sub> /n-C <sub>4</sub>	C <sub>1</sub> /(C <sub>2</sub> +C <sub>3</sub> )	C <sub>1</sub> /C <sub>2</sub> +C <sub>1</sub>	C <sub>1</sub> /C <sub>2</sub> +C <sub>1</sub> H <sub>2</sub> m <sub>2</sub> /C <sub>1</sub> H <sub>2</sub> n	Gas wetness
0	-	99.28	3.0	165.2	traces	4.5	n.d.	2.9	15.5	3.9	26.0	182.0	37.0	0.2	177.2	137.8	52.3	0.62
9	-	99.88	46.4	397.6	0.9	44.0	n.d.	7.7	27.2	7.2	78.0	1168.3	9.0	0.3	1051.8	825.8	68.4	0.10
13	0.4	99.91	110.0	827.3	0.9	63.8	n.d.	1.9	6.5	10.3	72.8	1329.3	13.0	0.3	1234.1	1118.2	86.8	0.08
19	-	99.95	43.6	126.5	1.7	21.9	n.d.	1.0	7.8	15.4	31.2	3447.9	5.8	0.1	2938.6	2123.1	11.0	0.04
23	0.4	99.95	43.7	108.9	0.9	30.6	n.d.	1.0	7.8	17.8	70.2	4014.4	3.6	0.1	3133.2	1843.7	11.7	0.03
27	-	99.81	26.2	268.9	0.4	54.9	n.d.	14.4	56.9	34.1	67.6	972.7	4.9	0.3	807.9	526.1	13.4	0.15
31	-	99.83	27.3	374.2	0.5	26.8	n.d.	1.0	5.2	7.4	57.2	730.2	14.0	0.2	681.4	578.7	59.3	0.15
35	-	99.83	23.9	304.0	1.3	23.0	n.d.	1.0	5.2	14.0	62.4	786.3	13.2	0.2	731.1	582.0	25.9	0.14
39	0.5	99.14	19.1	499.9	0.9	287.1	n.d.	93.8	362.2	301.5	114.3	382.6	1.7	0.3	243.0	115.2	4.5	0.65
47	-	99.36	16.0	204.7	1.3	140.2	n.d.	66.7	334.0	233.0	54.6	781.3	1.5	0.2	463.6	154.6	3.4	0.46
55	0.5	99.94	167.4	317.2	1.7	170.8	n.d.	44.0	238.5	229.9	67.6	5279.2	1.9	0.2	3431.7	1565.4	3.6	0.05
65	-	99.40	14.3	406.3	1.7	75.3	n.d.	44.0	168.1	76.8	88.3	3530.0	5.4	0.3	297.8	166.7	10.0	0.48
70	0.6	99.29	9.6	374.2	1.3	92.0	n.d.	22.7	105.4	10.9	72.8	2556.0	4.1	0.2	205.1	140.8	54.9	0.62
80	-	99.79	22.3	347.9	1.7	38.3	n.d.	1.3	6.5	11.4	67.6	640.1	9.1	0.2	576.6	469.1	35.2	0.18
95	0.6	99.72	16.7	249.9	1.5	60.0	n.d.	13.4	49.1	27.9	70.2	666.8	4.2	0.3	537.8	353.1	15.1	0.22
135	-	99.72	18.7	296.7	0.9	71.5	n.d.	10.5	47.9	35.6	57.2	630.7	4.2	0.2	508.3	359.8	13.3	0.23
155	0.5	99.73	27.0	409.2	n.d.	100.8	n.d.	22.0	69.8	49.7	72.8	659.2	4.1	0.3	528.9	372.5	13.6	0.22
167	1.0	99.80	38.9	496.9	0.9	183.7	n.d.	74.6	7.8	traces	traces	783.4	2.7	9.6	571.9	509.6	889.0	0.20

Kazakov MV  
TIR-6 BS-293G

depth, cm b.s.f.	TOC, wt %	% from total identified HC gas	concentration, $mll$ / wet sediment		molecular ratios														
			methane		Σpentanes (iso-pentane+n-pentane)														
				ethane	ethene	propane	propene	iso-butane	n-butane	butene	Σpentanes (iso-pentane+n-pentane)	C <sub>1</sub> /C <sub>2</sub>	C <sub>2</sub> /C <sub>3</sub>	iso-C <sub>4</sub> /n-C <sub>4</sub>	C <sub>1</sub> /(C <sub>2</sub> +C <sub>3</sub> )	C <sub>1</sub> /C <sub>2</sub> +C <sub>1</sub> H <sub>2</sub> m <sub>2</sub> /C <sub>1</sub> H <sub>2</sub> n	Gas wetness		
0	1.6	92.19	0.7	387.3	2.1	168.3	5.6	21.8	15.0	0.0	0.0	0.0	18.3	2.3	1.5	12.7	11.8	77.4	7.7
23	1.5	86.93	3.5	3874.2	n.d.*	1244.3	4.7	106.8	9.4	36.9	0.0	0.0	9.1	3.1	11.3	6.9	6.7	125.9	13.0
39	1.4	47.97	2.2	466.4	n.d.	10367.5	8.0	2978.6	2211.9	268.7	5094.7	2186.8	46.6	0.0	1.3	2.0	0.9	84.2	51.7
55	1.5	93.42	66.4	1750.5	n.d.	15551.2	5.6	6395.0	4599.1	42.5	12763.8	5623.6	379.2	0.1	1.4	38.4	14.2	970.8	6.6
79	1.6	75.94	19.2	1277.1	n.d.	19085.3	10.3	9239.4	6789.1	53.7	16517.3	7791.2	150.2	0.1	1.4	9.4	3.2	948.2	24.0



Table 1. Continuation.

Kazakov/MV  
TTR-11 BS-331G

depth, cm b.s.f.	TOC wt %	% from total identified HC gas	methane		concentration $n \times 10^{-4}$ ml/l wet sediment							molecular ratios								
			concentration, ml/l wet sediment	ethane	ethene	propane	propene	iso- butane	n-butane	butene	$\Sigma$ pentanes (iso- pentane+n- pentane)	$\Sigma$ iso- hexanes	$C_1/C_2$	$C_2/C_3$	iso- $C_4/n-C_4$	$C_1/(C_2+C_3)$	$C_1/C_{2+}$	$C_{1+}H_{2+2}/C_{1+}H_{2n}$	Gas wetness	
0	1.7	96.05	3.0	841.9	20.6	228.4	0.0	61.2	1.1	52.8	29.9	0.0	0.0	35.7	3.7	57.4	28.1	24.3	15.8	3.7
5	1.4	96.26	2.7	692.8	10.3	216.3	0.0	31.6	1.2	55.9	26.0	0.0	0.0	38.4	3.2	26.3	29.3	25.8	14.8	3.5
11	1.3	97.77	7.5	1169.3	13.7	245.0	0.0	114.8	9.1	139.7	18.7	0.0	0.0	64.3	4.8	12.7	53.1	43.9	10.1	2.0
21	1.2	96.75	30.1	1765.6	13.7	5839.0	0.0	1515.9	93.9	834.2	28.6	0.0	0.0	170.2	0.3	16.1	39.5	29.8	10.9	3.0
25	1.0	92.00	8.3	1227.7	n.d.	4685.7	0.0	895.3	40.6	208.5	81.1	0.0	0.0	67.9	0.3	24.5	14.1	11.5	33.6	7.8
29	1.2	95.67	15.2	877.0	n.d.	4409.9	0.0	1095.9	70.4	333.7	79.0	0.0	0.0	172.9	0.2	15.6	28.7	22.1	19.6	4.1
33	1.2	93.85	21.9	1177.0	13.7	9718.0	0.0	2449.9	185.9	620.8	45.9	0.0	0.0	249.2	0.1	13.0	20.6	15.3	21.6	5.9
41	1.2	94.22	26.6	1870.8	13.7	9718.0	0.0	2694.9	204.9	1365.8	45.4	0.0	0.0	142.4	0.2	13.2	23.0	16.3	10.8	5.3
45	1.2	95.52	17.1	2467.2	n.d.	2327.4	0.0	1760.9	138.7	1149.6	173.3	0.0	0.0	69.2	1.1	12.7	35.6	21.3	6.0	3.9
61	1.1	93.51	21.2	1613.6	n.d.	9064.7	0.0	2174.3	192.1	1280.2	358.6	0.0	0.0	131.2	0.2	11.3	19.8	14.4	10.5	6.0
71	1.2	93.81	17.8	1373.9	n.d.	7063.9	0.0	1730.3	356.4	896.3	300.4	0.0	0.0	129.3	0.2	4.9	21.0	15.2	12.1	5.7
81	1.1	92.50	15.0	1333.0	n.d.	7145.6	0.0	1837.4	1676.2	0.0	194.4	0.0	0.0	112.7	0.2	1.1	17.7	12.3	-	7.5
91	1.2	95.19	18.4	795.1	n.d.	6574.0	0.0	1125.4	393.8	305.2	123.9	0.0	0.0	231.9	0.1	2.9	25.0	19.8	28.5	4.7
101	1.2	94.81	21.2	1531.8	2.7	7349.8	0.0	1454.6	149.4	795.4	300.4	0.0	0.0	138.2	0.2	9.7	23.8	18.3	13.5	4.8
111	1.2	98.62	47.8	1601.9	n.d.	3062.4	0.0	1133.1	138.7	496.7	276.5	0.0	0.0	298.5	0.5	276.5	102.5	71.3	12.5	1.3
121	1.4	97.83	51.9	1473.3	n.d.	7513.1	0.0	1347.5	157.9	756.6	265.0	0.0	0.0	352.3	0.2	8.5	57.8	45.1	14.2	2.0
131	1.3	94.76	14.8	795.1	n.d.	4593.6	0.0	1944.6	106.7	439.8	318.0	0.0	0.0	186.4	0.2	18.2	27.5	18.1	17.6	5.0
141	1.2	94.08	17.1	1110.8	n.d.	7227.3	0.0	1255.6	149.4	727.9	265.0	0.0	0.0	153.7	0.2	8.4	20.5	15.9	13.7	5.5
165	1.2	93.15	17.9	1099.1	n.d.	8983.0	0.0	1837.4	352.2	610.5	274.4	0.0	0.0	162.8	0.1	5.2	17.7	13.6	20.6	6.6

MOZ/MV  
TTR-11 BS-325G

depth, cm b.s.f.	TOC wt %	% from total identified HC gas	methane		concentration $n \times 10^{-4}$ ml/l wet sediment							molecular ratios									
			concentration, ml/l wet sediment	ethane	ethene	propane	propene	iso- butane	n-butane	butene	$\Sigma$ pentanes (iso- pentane+n- pentane)	$\Sigma$ iso- hexanes	$C_1/C_2$	$C_2/C_3$	iso- $C_4/n-C_4$	$C_1/(C_2+C_3)$	$C_1/C_{2+}$	$C_{1+}H_{2+2}/C_{1+}H_{2n}$	Gas wetness		
0	0.6	99.95	43.7	228.0	n.d.*	2.9	1917.1	79.4	1893.3	1478.4	10.5	1349.8	0.0	0.0	35.7	3.7	57.4	28.1	24.3	15.8	3.7
9	-	99.92	3.0	20.1	2.6	1.9	1478.4	10.5	1349.8	1478.4	10.5	1349.8	0.0	0.0	35.7	3.7	57.4	28.1	24.3	15.8	3.7
13	0.5	99.93	33.5	226.5	n.d.	2.9	1458.5	79.9	1440.4	1458.5	79.9	1440.4	0.0	0.0	35.7	3.7	57.4	28.1	24.3	15.8	3.7
17	-	99.84	51.9	312.8	n.d.	3.8	1659.6	81.7	1639.5	1659.6	81.7	1639.5	0.0	0.0	35.7	3.7	57.4	28.1	24.3	15.8	3.7
21	0.6	99.93	27.3	201.7	n.d.	2.6	1364.5	79.0	1337.6	1364.5	79.0	1337.6	0.0	0.0	35.7	3.7	57.4	28.1	24.3	15.8	3.7
25	-	99.91	32.8	281.4	n.d.	4.1	1165.2	67.8	1148.3	1165.2	67.8	1148.3	0.0	0.0	35.7	3.7	57.4	28.1	24.3	15.8	3.7
29	-	99.93	13.7	97.9	n.d.	1.0	1398.4	102.3	1384.9	1398.4	102.3	1384.9	0.0	0.0	35.7	3.7	57.4	28.1	24.3	15.8	3.7
37	-	99.96	36.9	144.7	n.d.	4.1	2548.9	34.9	2477.9	2548.9	34.9	2477.9	0.0	0.0	35.7	3.7	57.4	28.1	24.3	15.8	3.7
41	0.6	99.87	3.1	102.3	traces	2.2	307.1	45.8	300.5	307.1	45.8	300.5	0.0	0.0	35.7	3.7	57.4	28.1	24.3	15.8	3.7
44	0.6	99.81	9.6	181.2	n.d.	3.2	527.6	56.8	516.5	527.6	56.8	516.5	0.0	0.0	35.7	3.7	57.4	28.1	24.3	15.8	3.7
49	-	99.96	37.2	149.1	n.d.	4.1	2496.9	35.9	2429.3	2496.9	35.9	2429.3	0.0	0.0	35.7	3.7	57.4	28.1	24.3	15.8	3.7
53	-	99.84	6.5	103.8	n.d.	traces	625.3	162.7	621.4	625.3	162.7	621.4	0.0	0.0	35.7	3.7	57.4	28.1	24.3	15.8	3.7
57	-	99.96	30.7	108.5	n.d.	1.9	2832.1	56.7	2783.0	2832.1	56.7	2783.0	0.0	0.0	35.7	3.7	57.4	28.1	24.3	15.8	3.7
65	0.6	99.80	10.6	206.0	n.d.	1.9	506.5	109.2	501.9	506.5	109.2	501.9	0.0	0.0	35.7	3.7	57.4	28.1	24.3	15.8	3.7
80	-	99.88	17.1	197.3	n.d.	1.9	865.4	103.1	857.1	865.4	103.1	857.1	0.0	0.0	35.7	3.7	57.4	28.1	24.3	15.8	3.7
88	0.6	99.95	28.7	126.1	1.3	2.6	2275.6	49.4	2230.4	2275.6	49.4	2230.4	0.0	0.0	35.7	3.7	57.4	28.1	24.3	15.8	3.7

**Table 1.** Continuation.

**Unnamed MV**  
**TTR-6 BS-292G**

depth, cm b.s.f.	TOC, wt %	% from total identified HC gas	concentration, m//l wet sediment	concentration $n \times 10^{-4}$ m//l wet sediment					molecular ratios				
				methane	ethane	ethene	propane	propene	iso- butane	$C_1/C_2$	$C_2/C_3$	$C_1/(C_2+C_3)$	$C_1/C_{2+}$
0	0.7	99.97	37.2	82.6	3.8	8.3	1.5	2.1	4500.0	10.0	4090.9	3783.8	17.5
27	0.6	99.96	31.0	110.9	5.0	9.7	4.7	2.7	2792.6	11.4	2567.2	2328.2	12.7
49	0.8	99.96	46.3	164.9	n.d.*	9.7	2.4	2.1	2808.6	16.9	2652.0	2586.5	74.9
57	0.7	99.97	19.2	39.5	5.9	5.6	3.8	1.5	4850.7	7.1	4248.4	3403.1	4.8

n.d.\* - not determined

Unsaturated HCGs, such as ethene ( $C_{2:1}$ ), propene ( $C_{3:1}$ ), and butenes ( $C_{4:1}$ ), were detected at all sampling locations (Table 1). Overall concentrations of unsaturated HCGs were relatively low; the dominance of  $C_2$  over  $C_{2:1}$  and  $C_3$  over  $C_{3:1}$  is clear. Conversely, the concentrations of  $C_{4:1}$  is often higher than  $nC_4$  and its distribution trend is often not concurrent with other hydrocarbons (Table 1).

Table 2 shows  $\delta^{13}C$  data for three cores, from the Odessa, Kazakov, and NIOZ MVs. These locations were selected for a detailed study of the  $C_1$ - $C_5$  stable carbon isotope variations along the sedimentary successions. Ranges of stable carbon isotope compositions for the  $C_1$ - $C_5$  hydrocarbons and the mean isotopic separation between ethane-methane and propane-ethane pairs are listed in Table 2. The  $\delta^{13}C$  of  $C_1$  and  $C_2$  values of the Kazakov MV showed 10 to 20 ‰ heavier values compared with the  $C_1$  and  $C_2$  from the Odessa and NIOZ MVs. The  $\delta^{13}C$  values of  $C_3$  in the Odessa MV appear to be remarkably enriched (Table 2). In the Kazakov MV,  $nC_4$  and  $iC_4$  show the same  $\delta^{13}C$  characteristics. Down-core the  $\delta^{13}C$  values of  $C_1$ - $C_5$  alkanes remain the same. Only  $nC_5$  showed marginal changes in its  $\delta^{13}C$  values along the mud breccia (Table 2).

#### 4.1.2. Gas hydrates

Table 3 shows the molecular and isotope properties of HCG from the gas hydrates. Four gas hydrates show relatively similar molecular compositions of the  $C_{2+}$  components. Three gas hydrates from the Odessa MV have similar  $\delta^{13}C$  values of  $C_1$ , whereas the gas hydrate from the Unnamed MV displays more  $^{13}C$ -enriched methane (Table 3). The  $\delta^{13}C$  values of  $C_2$  from both the gas hydrate and the sediments from the Odessa MV (TTR-11 BS-336G), were also identical (Table 2 and Table 3). The  $\delta^{13}C$  signature of  $C_3$  and  $iC_5$  in the gas hydrate from the Odessa MV (TTR-11 BS-336G) is the same as found in the mud breccia from the Kazakov MV. The  $\delta^{13}C$  values of  $nC_4$  and  $iC_4$  gases in the gas hydrate display the

same  $\delta^{13}\text{C}$  values as the  $\text{C}_5$  HCGs in the mud breccia from the Kazakov MV (Table 2 and Table 3).

## 5. Discussion

### 5.1. Methane

Primary thermogenic methane has  $\delta^{13}\text{C}$  values of  $-55\text{‰}$  (Sackett, 1978), and becomes heavier with increasing thermal maturity (Rice and Claypool, 1981). In the Kazakov MV, the  $\delta^{13}\text{C}_1$  values of ca.  $-56\text{‰}$  are characteristic for all samples, indicating relatively mature properties of the methane. In contrast, the  $\delta^{13}\text{C}$  of  $\text{C}_1$  in gas hydrates (Table 3) and sediments from the Odessa MV, in the gas hydrate from the Unnamed MV, and

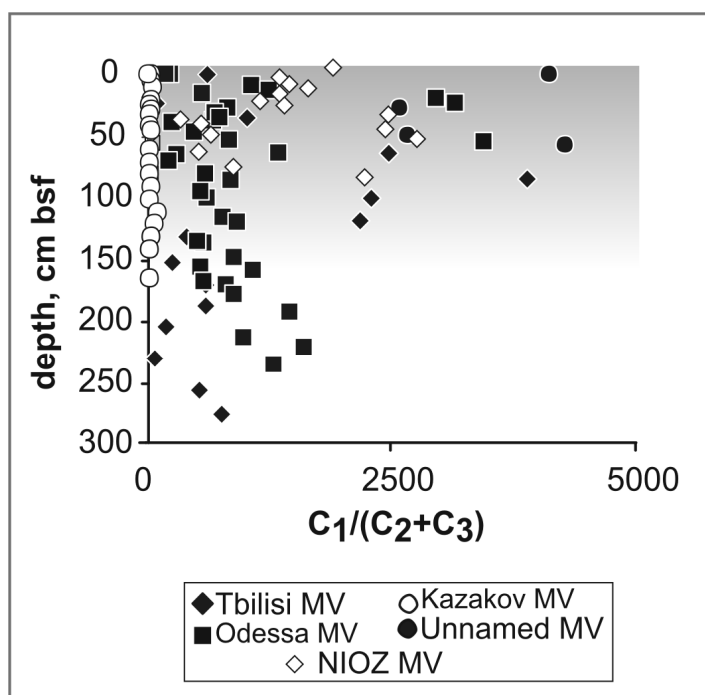


**Figure 4.** Bernard parameter as a function of depth showing compositional variations of the HCGs induced by microbial interactions in the uppermost part of sedimentary column (grey area).

in the mud breccia from the NIOZ MVs (Table 2) show average values of  $-65\text{‰}$ ,  $-60\text{‰}$ ,  $-68\text{‰}$  and  $-63\text{‰}$ , respectively, indicating a microbial origin of methane (Rice and Claypool, 1981). In the Odessa and NIOZ MVs, the uppermost sediments show inequable  $\delta^{13}\text{C}_1$  values, ranging from  $3\text{‰}$  to  $7\text{‰}$ , respectively (Table 2). Since both locations are characterized by the presence of AOM-mediating-microbial mats and associated development of authigenic carbonate crusts (Mazzini et al., 2004; Stadnitskaia et al., 2005), the changes in stable carbon isotope ratios most likely are the consequence of active microbial processes, including of AOM (Stadnitskaia et al., 2005).

Accordingly, the stable carbon isotope data indicate the presence of two types of methane: (i) relatively mature methane in the Kazakov MV and (ii) microbial/immature methane in the Odessa and NIOZ MVs.

### 5.2. Wet gas components

Figure 3 and Table 1 show significant differences in the presence of  $\text{C}_{2+}$  compounds among the studied MVs. Despite the generally “dry” gas characteristics of the HCGs, in all sampling locations, the concentration of each wet gas constituent is relatively high. Figure 4

demonstrates the Bernard parameter,  $C_1/(C_2+C_3)$ , for gas data as a function of depth. Almost all locations studied show  $C_1/(C_2+C_3)$  ratio's above 1000, indicating gas mixtures of microbial origin (Bernard et al., 1976). The highest scatter of  $C_1/(C_2+C_3)$  values, which results from microbial activity, is observed in the uppermost ca. 100 cm of almost all MVs (Figure 4). Only mud breccias from the Kazakov MV are characterized by a pronounced wet gas signal, as reflected in ratio  $C_1/(C_2+C_3)$  values below 50. This indicates that HCG from this MV results from thermogenic gases related to petroleum (Bernard et al., 1976). The low values of the ethane/propane ratio in the Kazakov MV also indicate that the gas derived from a petroleum source rather than from non-associated or biogenic natural gas. In contrast, ethane/propane ratios from other MVs show a wide range of values (Table 1). Such a high variability of values likely results from secondary processes, such as migration, microbial alteration or a combination of these.

Despite the different suites of  $C_{2+}$  components in the MVs and gas hydrates, the

interval cm b.s.f.	$\delta^{13}C$							Isotope separation	
	methane	ethane	propane	<i>iso</i> -butane	<i>n</i> -butane	<i>iso</i> -pentane	<i>n</i> -pentane	$\delta^{13}C$ ( $C_2-C_1$ )	$\delta^{13}C$ ( $C_3-C_2$ )
<b><u>Kazakov MV: TTR11 BS-331G</u></b>									
20-25	-55	-42	-33	-30	-30	-28	-29	14	9
40-45	-55	-42	-33	-30	-31	-28	-29	14	9
79-84	-56	-42	-34	-31	-31	-28	-28	14	8
99-101	-56	-42	-34	-31	-31	-28	-29	14	9
140-142	-56	-42	-34	-31	-31	-28	-29	14	8
160-166	-56	-42	-34	-31	-31	-28	-30	14	8
Average	-56	-42	-34	-31	-31	-28	-29	14	8
<b><u>Odessa MV: TTR11 BS-336G</u></b>									
0-17	-70	-51	-18	n.d.	n.d.	n.d.	n.d.	19	33
20-27	-68	-50	n.d.*	n.d.	n.d.	n.d.	n.d.	17	-
30-37	-68	-51	-17	n.d.	n.d.	n.d.	n.d.	17	34
50-55	-67	-51	-22	n.d.	n.d.	n.d.	n.d.	16	29
69-78	-70	-32	n.d.	n.d.	n.d.	n.d.	n.d.	39	-
123-138	-67	-51	-22	n.d.	n.d.	n.d.	n.d.	16	29
148-158	-67	-46	-22	n.d.	n.d.	n.d.	n.d.	21	24
Average	-68	-47	-20					21	30
<b><u>NIOZ MV: TTR11 BS-325G</u></b>									
0-4	-66	-49	n.d.	n.d.	n.d.	n.d.	n.d.	17	-
8-11	-67	-44	n.d.	n.d.	n.d.	n.d.	n.d.	23	-
22-27	-61	-50	n.d.	n.d.	n.d.	n.d.	n.d.	11	-
52-57	-60	-46	n.d.	n.d.	n.d.	n.d.	n.d.	14	-
87-88	-60	-49	n.d.	n.d.	n.d.	n.d.	n.d.	11	-
Average	-63	-47						15	

n.d.\* - not defined

**Table 2.** Stable carbon isotope composition of hydrocarbon gases, ‰  $\delta^{13}C$  vs VPDB standart.

presence of high molecular weight *n*-alkanes in gas mixtures, especially the C<sub>4</sub>-C<sub>6</sub> constituents, signifies an input of thermogenic hydrocarbons from deep sources (Cline and Holms, 1977; Sandstorm et al., 1983; Hunt, 1995; Pepper and Corvi, 1995). The absence of

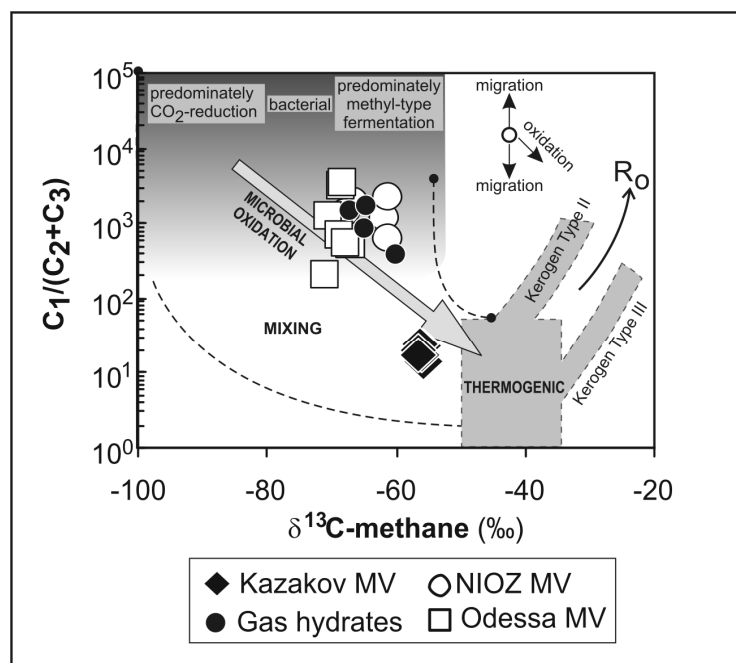


**Figure 5.** Bernard diagram to outline gas types (after Whiticar, 1994).

correlation with the TOC content is an additional argument for an allochthonous nature of the C<sub>2+</sub> gases to the erupted and redeposited MV deposits.

In addition to diagnostic chemical-compositional gas ratios (Table 1), the Bernard diagram (Figure 5; Bernard et al., 1978; Faber and Stahl, 1984) designates two hypothetical gas types. Hydrocarbon gases from the Kazakov MV fall within the mixing range, close to the “thermogenic gas” area, with a general trend to originate from deeper reservoirs. In contrast, HCGs from the rest of the MVs

and gas hydrates show less mature, microbial signatures indicating shallow reservoirs (Figure 5). Furthermore, the smaller isotopic separation between the ethane-methane and propane-ethane pairs suggests in general higher maturities for the HCGs in the mud breccia from the Kazakov MV. However, the two genetic types of the HCGs identified, have to be considered with great care, since post-genetic processes such as chemical and microbial alteration, mixing and/or physical migration may radically modify the original molecular and stable carbon isotope signatures of a gas mixture (Galimov, 1967; Lebedev and Syngayevski, 1971; Prinzhofer and Pernaton, 1997; Prinzhofer and Battani, 2003).

### 5.3. Secondary processes

#### 5.3.1. Biodegradation

##### 5.3.1.1. Saturated HCGs

The dryness of HCGs may partially result from subsurface biodegradation processes, which can provoke supplementary loss of C<sub>3</sub>-C<sub>6</sub> components (Heritier et al., 1979, Larter and Primio, 2005). Our data show that all sampling locations are characterized by the presence of

$C_2$  through  $C_5$  ( $C_6$ ) HCGs with methane contents of almost 100 % (Table 1). Recent studies of gas and oil biodegradation processes demonstrate increasing evidence that dry-gas fields developed from the microbial degradation of oil (Dimitrakopoulos and Muehlenbachs, 1987; Pallasser, 2000; Larter and Primio, 2005). During the utilization of *n*-alkanes,  $C_3$ , *n* $C_4$  and *n* $C_5$  are preferentially removed while the *iso*-alkanes show considerably reduced degrees of removal (Connan and Coustau, 1984; James and Burns, 1984; Larter, 1993). This is reflected in high  $iC_4/nC_4$  ratios (Pallasser, 2000; Larter and Primio, 2005). Figure 6 indicates that biodegradation processes resulted in the drying of the HCGs, and in elevated  $C_2/C_3$  and  $iC_4/nC_4$  ratios. Although the highest  $C_2/C_3$  and  $iC_4/nC_4$  values are attributed to the uppermost sediment intervals, Table 1 shows that these ratios remain generally high throughout the sedimentary column. At the same time, all MVs are characterized by anomalously light  $\delta^{13}C$  values of ethane (Table 2). All together, this suggests that the HCGs from each studied location represent products of subsurface oil biodegradation. This is consistent with the results of lipid biomarker studies of sediments from the same sampling locations (Stadnitskaia et al., in press), which so far suggest the presence of oil and various stages of its microbial alteration.

Simultaneously, the presence of  $^{13}C$ -enriched propane (James and Burnes, 1984) together with  $^{13}C$ -depleted methane (Pallasser, 2003) in sediments from the Odessa MV (Table 2) provides evidence for microbial gas modification in the subsurface. This implies

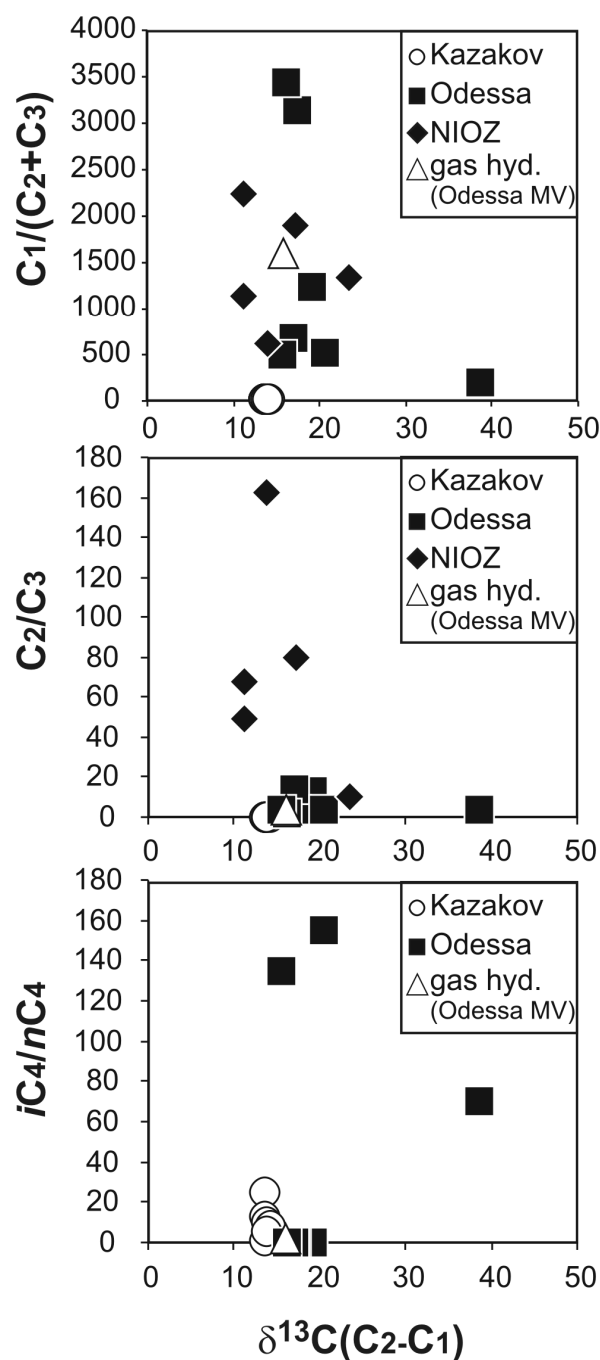


**Figure 6.** The relationship of gas ratios to ethane-methane carbon isotope separations.

that HCG initially derived from oil biodegradation, was further microbially altered before it reached the surface sediments.

Previous study of the same MVs revealed recent active microbial processes in the uppermost ca. 30 cm (Stadnitskaia et al., 2005). In all MVs this interval is characterized by the highest  $C_2/C_3$  and  $iC_4/nC_4$  values (Table 2) and by changes in the  $\delta^{13}C$  composition of  $C_1$ - $C_4$  components (Table 2), which indicates *in-situ*

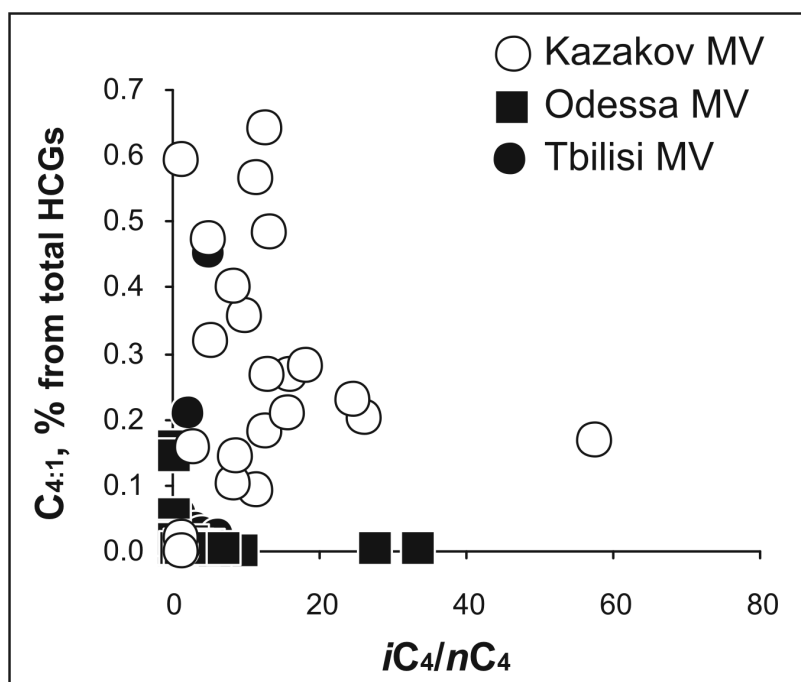


Figure 7. The relationship between  $C_4$  hydrocarbon gases.

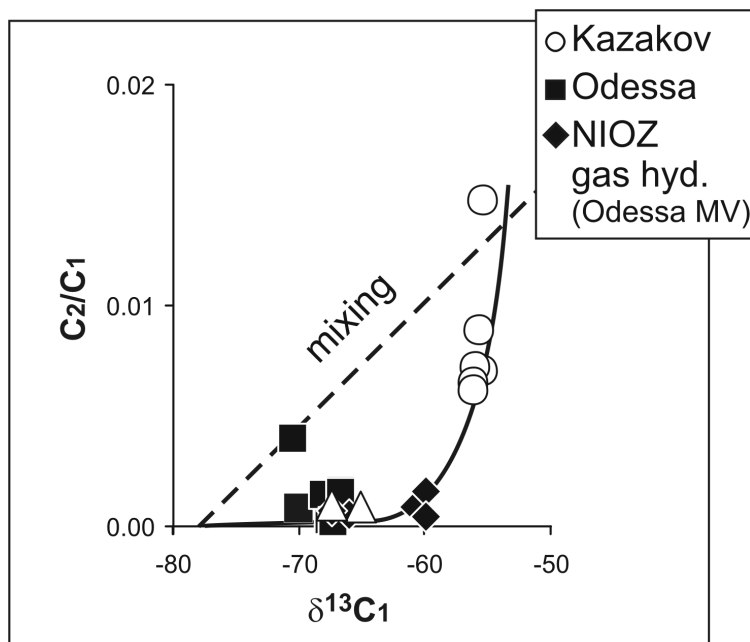


Figure 8. Mixing diagram  $C_2/C_1$  vs  $\delta^{13}C$  of methane.

microbial alteration/consumption of already biologically modified and upward migrated HCGs in the topmost sediments. Furthermore, this suggests that microbial utilization of  $C_{2+}$  components is taking place together with active methanotrophy (Stadnitskaia et al., 2005, 2006).

### 5.3.1.2. Unsaturated HCGs

Marine organisms produce both ethene and propene, and these hydrocarbons are not present in thermogenic gases (Hunt, 1974). The distribution profiles of  $C_nH_{2n-2}$  in the all

locations are dominantly not coherent with “consumption signatures” of  $C_1$  and  $C_{2+}$  HCGs as was noticed in the cold-venting sediments from the Gulf of Cadiz (Stadnitskaia et al., 2006).

In almost all studied locations, these hydrocarbons appear throughout the whole sedimentary successions, which is indicative of their allochthonous nature rather than for *in-situ* biosynthesis (Table 1). Overall, C<sub>2</sub> and C<sub>3</sub> are predominant over C<sub>2:1</sub> and C<sub>3:1</sub>, respectively, indicating the mature characteristics of the gas mixtures. Still, these hydrocarbons in the sediments can be indicative of either microbial activity or other non-thermal subsurface processes (Hunt, 1975).

In contrast, concentrations of butenes often exceed concentrations of C<sub>4</sub> alkanes (Table 1). The biological source for butenes is unknown. Hence, their high concentrations possibly are the result of cracking of early petroleum products rather than a product of deep subsurface microbial degradation. This view is supported by the fact that the highest C<sub>4:1</sub> content is related to the HCGs from the Kazakov MV; these are characterized by the most mature chemical properties compared with all other MVs (Figure 7).

### 5.3.2. Mixing and migration

Mixing of gases of different origins is a common phenomenon (Whiticar, 1994). Nevertheless, our data show the absence of an expected linear relation between the C<sub>2</sub>/C<sub>1</sub> ratio values and the δ<sup>13</sup>C signatures of the methane (Figure 8). Instead, a “curved trend”, which is incompatible with a scenario of mixing between a thermogenic and microbial end-members, is clearly displayed. Such a distribution was previously reported by Prinzhofer and Battani, (2003) for gases from the North Sea field, and was interpreted as resulting from chemical and isotopic fractionation during leakage of a thermogenic fluid accumulated in a reservoir located below.

On the other hand, fields of primary gases are delineated by the <sup>13</sup>C differences of co-genetic methane-ethane pairs (Schoell, 1983), where in a thermogenic C<sub>1</sub>-C<sub>2</sub> pair, ethane is enriched between 5 ‰ and 10 ‰ in <sup>13</sup>C (Whiticar, 1994). In the sediments and gas hydrates

hydrocarbon gas	Odessa mud volcano						Unnamed MV	
	TTR-6 BS-288G		TTR-6 BS-288G		TTR-11 BS-336G		TTR-6 BS-292G	
	molecular composition, mole %	δ <sup>13</sup> C, ‰ VPDB	molecular composition, mole %	δ <sup>13</sup> C, ‰ VPDB	molecular composition, mole %	δ <sup>13</sup> C, ‰ VPDB	molecular composition, mole %	δ <sup>13</sup> C, ‰ VPDB
methane	99.87	-65	99.93	-65	99.93	-67	99.7	-60
ethane	0.09	–	0.04	–	0.05	-51	0.18	–
propane	0.03	–	0.02	–	0.02	-34	0.09	–
<i>iso</i> -butane	0.01	–	traces	–	0.01	-29	traces	–
<i>n</i> -butane	traces	–	trases	–	traces	-28	0.01	–
<i>iso</i> -pentane	n.d.	–	n.d.*	–	traces	-28	n.d.	–
<i>n</i> -pentane	n.d.	–	n.d.	–	n.d.	–	traces	–
<i>n</i> -hexane	n.d.	–	n.d.	–	n.d.	–	traces	–

\* n.d. - not defined

**Table 3.** Molecular and carbon isotopic composition of hydrocarbon gases from gas hydrates.



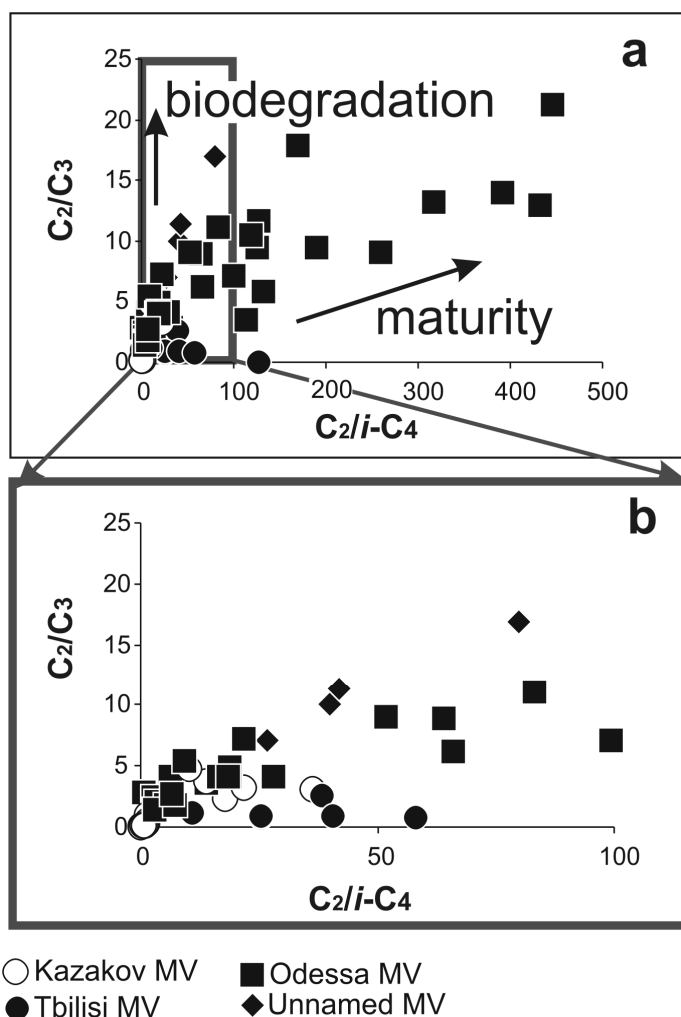


**Figure 9.** Diagram distinguishing maturity trend from a biodegradation trend (after Prinzhofer and Battani, 2003).

intensity of fluid transport. Several migration experiments, where gas migration occurs by diffusion through saturated or not with water a slice of shale or sandstone, Prinzhofer and Battani, (2003) demonstrated a purely microbial  $\delta^{13}C$  signature for methane and a  $\delta^{13}C$  signature corresponding to mixing, while the initial gas is actually of a thermogenic origin. With regard to the molecular composition of  $C_{2+}$  HCGs, Coleman et al., (1977) showed that migrated gases may be completely stripped of  $C_{2+}$  hydrocarbons. In fact, depletion in wet gas components dominantly occurs due to shallow gas migration (Schoell, 1983). Gas leakage through less permeable, less consolidated and fluidized sediment pathways result in segregation of  $C_{2+}$  HCGs (Schoell, 1983) or in retrograde condensation of  $C_5$  hydrocarbons in reservoirs of lower pressure (Silverman, 1971). Accordingly, the dry characteristics of the

from the Odessa MV and in the mud breccias from the NIOZ MV,  $\delta^{13}C$  ( $C_2-C_1$ ) separation values are in general  $< 15 \text{ ‰}$ , indicating the absence of a co-genetic origin of the methane and ethane (Silverman, 1971). The  $\delta^{13}C$  ( $C_2-C_1$ ) and the  $\delta^{13}C$  ( $C_3-C_2$ ) values in the gas hydrate from the Odessa MV, (16 ‰ and 17.2 ‰, respectively), are clearly different from those in the surrounding sediments (Table 2). Simultaneously, the smallest  $\delta^{13}C$  ( $C_2-C_1$ ) separation values (ca. 14 ‰) are attributed to the mud breccia from the Kazakov MV, implying a minimum admixture of none co-genetic gas during migration.

In addition to the biodegradation processes as discussed in the previous section, the observed differences in the molecular and stable carbon isotope compositions also may partly result from a combination of adsorption/desorption processes during gas migration from various sediment depths, as well as may reflect the

HCGs and the compositionally instable suite of the C<sub>2+</sub> compounds from the Unnamed, Tbilisi, NIOZ, and Odessa MVs may partially result from shallow migration. Such type of fluid transport is anticipated since numerous signs indicating the presence of gas in the sediments in the Sorokin Trough at ~ 250-300 m below the seafloor surface were observed during numerous geophysical surveys in the area (Ivanov et al., 1998; Bouriak and Akhmetzhanov, 1998; Krastel et al., 2003).

On the contrary, deep-migrated HCGs would increase the gas wetness (Schoell, 1983). The wet characteristics and the stable isotope properties of HCG from the Kazakov MV thus point toward greater depths for gas migration compared to the other MVs. Besides, the constant and not significantly altered  $\delta^{13}\text{C}$  composition of C<sub>1</sub>-C<sub>5</sub> HCGs suggests recent activity of the MV and, accordingly, rapid fluid transport from the depths below.

### *5.4. Source evaluation*

The original gas source as well as the level of maturity is imprinted in the  $\delta^{13}\text{C}$  signatures of C<sub>2</sub>-C<sub>4</sub> (C<sub>5</sub>) constituents (James, 1990). Microbial alteration and mixing processes can significantly change initial source/maturity signatures, making recognition of these both parameters difficult. As was outlined above, all HCGs result mostly from oil cracking and/or biodegradation processes. The extent of alteration of these gases and oils, which were initially derived from the same reservoir, subsequently migrated further, mixed and biodegraded, do not parallel each other. No direct relationship between the extent of microbial alteration and mixing in all studied HCGs, although all gases exhibit effects of both processes. The gas from the Kazakov MV is the least altered and the most mature, and may thus still exhibit source fingerprints. Only in this HCG the  $\delta^{13}\text{C}$  values of the wet gas components almost follows the regular progression of their carbon isotope compositions (James, 1990). The  $\delta^{13}\text{C}$  signatures of methane from the Kazakov MV do not indicate deep-formed methane from overmature zones below zones of oil generation (Table 2). However, the  $\delta^{13}\text{C}$  values of initial methane formed from cracking reactions in petroleum range from -50 ‰ to -60 ‰ (Schoell, 1983). In the Kazakov MV, the carbon isotope composition of C<sub>1</sub>-C<sub>5</sub>, however, is identical from sample to sample in the sedimentary column (Table 2). Such similarities of the individual wet gas components and maturity properties suggest that these HCGs all came from the same source.

By contrast, the  $\delta^{13}\text{C}$  signatures of methane in gas hydrates from the Unnamed MV, in gas hydrates and sediments from the Odessa MV, and in the mud breccia from the NIOZ MV contain light  $\delta^{13}\text{C}_1$  compositions and appear to be composed of predominantly microbial methane mixed with minor amounts of mature gas. This may imply that methane from all mentioned MVs might have been characterized as derived from different sources and with

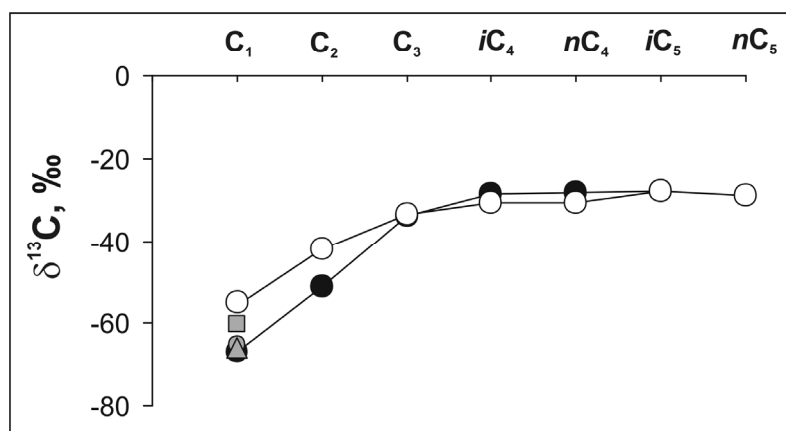


**Figure 10.** Isotope type curve for a gas hydrate sample collected from the Odessa MV (black circles) and average  $\delta^{13}\text{C}$  values of  $\text{C}_1$ - $\text{C}_5$  HCGs from the Kazakov (white circles) MV. Grey geometrical figures indicate  $\delta^{13}\text{C}$  of  $\text{C}_1$  from other gas hydrates collected from the Odessa and Unnamed MVs during the TTR-6 in 1996.

different maturity compared to the methane from the Kazakov MV.

Alternatively, methanogenesis and oil biodegradation are linked processes (Pallasser, 2000) and consequently the presence of “dry” natural gas in these MVs with  $^{13}\text{C}_1$ -depleted signatures is attributed to the presence of “secondary microbial gas”.

However, the gas hydrate from the Odessa MV shows stable carbon isotope values of  $\text{C}_1$ - $\text{C}_5$  alkanes similar to the  $\delta^{13}\text{C}$  values of  $\text{C}_1$  and  $\text{C}_2$  from the

Odessa MV and to the  $\delta^{13}\text{C}$  values of  $\text{C}_3$  and  $i\text{C}_5$  from the Kazakov MV. The  $\delta^{13}\text{C}$  values of  $\text{C}_2$  from all locations are exceptionally light, which additionally supports the idea that HCGs originated from early cracking products of petroleum, known to be depleted of heavy isotopes (Schoell, 1983). Figure 9 shows that HCGs from all locations studied dominantly fall into the maturity field, reflecting a more rapid decrease of  $i\text{C}_4$  proportions relative to  $\text{C}_3$  proportions (Prinzhofer and Battani, 2003). Biodegradation may also be defined in the sediments from the Odessa MV (Figure 9a), as during this processes  $\text{C}_3$  is more efficiently altered than  $i\text{C}_4$  (James and Burnes, 1984; Prinzhofer and Battani, 2003). The latter is consistent with the  $\delta^{13}\text{C}$  values of the  $\text{C}_3$  component, clearly indicating its microbial consumption (Table 2).

Concurrently, the  $\delta^{13}\text{C}$  of  $\text{C}_1$  in the gas hydrates and sediments from the Odessa MV, gas hydrates from the Unnamed MV and mud breccia from the NIOZ MV resemble each other (Figure 10). The depleted  $\delta^{13}\text{C}$  signatures of the methane from gas hydrates and all studied MVs (except the Kazakov MV) together with the “dry” gas characteristics of the HCGs are rather the effect of physical and/or mechanical secondary processes, such as shallow gas migration and its partial dilution with immature methane. In this case, the isotope composition of the higher molecular weight components remains unaffected by non-biological processes.

Accordingly, on the basis of analysis of the wet-gas component and the molecular and stable carbon isotope compositions, the origin of HCGs from all studied MVs and gas hydrates can be defined as a consequence of oil cracking and/or biodegradation in the deep

subsurface. Except at the Kazakov MV, a complex suite of post-depositional processes has changed the original properties of the gas mixtures. This is evidence for shallow, mainly dispersed fluid transport of already redeposited HCGs, supplemented by microbial alteration processes in the subsurface. In contrast, the composition of HCG in the mud breccia from the Kazakov MV evidently provides evidence for rapid and focused fluid transfer from the deep subsurface towards the seafloor.

Containment of overpressured fluids is most effectively accomplished in compressional tectonic regimes (Sibson and Scott, 1998), in our case thus assuming the presence of overpressured sediments or fluids below or within the Maycopian Shales. Numerous acoustic anomalies in sub-bottom sediments reflecting shallow accumulations of hydrocarbons were ascribed to the presence of Maycopian diapir-bodies, which served either as a source for these fluids or as a secondary trap for migrated and re-deposited hydrocarbons (Ivanov et al., 1998; Bouriak and Akhmetzhanov, 1998; Kenyon et al., 2002). The presence of material from the MSF in the mud breccia from the Kazakov MV (Ivanov et al., 1998) does indicate that fluids percolated through the MSF. These could form a potential source for HCGs. However, the presence of MSF material in the mud breccias (Ivanov et al., 1998; Kozlova et al., 2003) does not necessarily identify the Maycopian sequence as the only possible unit from which the initial fluid was generated. Previous studies of the Maycopian mud breccia rock clasts (Kozlova, 2003) and mud breccia matrixes (Stadnitskaia et al., in press) revealed generally immature properties of the organic matter. This is not consistent with the chemical and stable carbon isotope characteristics of the studied HCGs, especially from the Kazakov MV. Considerable quantities of non-microbial thermogenic methane are not generated until the temperature is higher than 100 °C (Frank et al., 1974); C<sub>2</sub>-C<sub>4</sub> gaseous compounds are formed primarily between 70 and 150 °C (Hunt, 1995). In general, the gas generation window is situated within the temperature intervals of ca. 105-155 to 175-220 °C (Pepper and Corvi, 1995), which indicates that the original source of HCGs is located deeper than the source strata for the erupted sedimentary material, e.g. can be found below the MSF.

Accordingly, all gases, except those from the Kazakov MV, are mixtures of differently originated/altered methanes and their mature wet gas components, and have a common origin. The similarity of the  $\delta^{13}\text{C}$  properties of HCGs in the gas hydrates from the Odessa MV and from the Kazakov MV, supports this suggestion. Our data show that wet gas components in all MVs are related to each other and that HCGs from the Kazakov MV most probably represent the original gas properties of hydrocarbons trapped in the deep subsurface of the Sorokin Trough.

## **6. Conclusions**

Hydrocarbon gas from mud breccias and associated gas hydrates collected from five MVs in the Sorokin Trough have been studied to reveal their sources and to identify the post-depositional processes affecting their molecular and stable carbon isotope properties.

HCGs from all studied MVs and gas hydrates can be defined as the result of oil cracking and/or biodegradation in the deep subsurface. The “dry” characteristics of the HCGs and the compositional variations in C<sub>2+</sub> from the Unnamed, Tbilisi, NIOZ, and Odessa MVs appear to result partially from (i) by a chemical and isotopic fractionation during fluid leakage from redeposited accumulations during shallow migration; (ii) “secondary microbial gas” resulted from oil biodegradation; (iii) a combination of both. No direct relationship appears to exist between the extent of microbial alteration and mixing/migration in all studied HCGs, although all gases exhibit the effects of both.

The resemblance of stable carbon isotope properties in HCGs from the gas hydrate in the Odessa MV and the mud breccia from the Kazakov MV, and the light  $\delta^{13}\text{C}$  values of ethanes in all MVs indicate that wet gas components have a common origin. The gas data indicate that the original source of the gases likely is located below the MSF. Accordingly, gases from MVs related to up-doming diapiric structures (e.g. the Odessa and the NIOZ MVs) represent a mixture of mature and likely secondary microbial methanes. Wet gas components in all MVs are likely related to each other; the HCGs from the Kazakov MV probably represent the original gas properties of the hydrocarbons trapped in the deep subsurface of the Sorokin Trough.

### LIPID BIOMARKERS IN SEDIMENTS OF MUD VOLCANOES FROM THE SOROKIN TROUGH, NE BLACK SEA: PROBABLE SOURCE STRATA FOR THE ERUPTED MATERIAL

A. Stadnitskaia <sup>a,b</sup>, V. Blinova <sup>b</sup>, M.K. Ivanov <sup>b</sup>, M. Baas <sup>a</sup>,  
E. C. Hopmans <sup>a</sup>, T.C.E. van Weering <sup>a,c</sup> and J.S. Sinninghe Damsté <sup>a</sup>

<sup>a</sup>Royal Netherlands Institute for Sea Research (NIOZ), P.O. Box 59, 1790 AB Den Burg, Texel, The Netherlands.

<sup>b</sup>Geological Faculty, UNESCO-MSU Centre for Marine Geosciences, Moscow State University, Vorobjevy Gory, Moscow 119899, Russian Federation.

<sup>c</sup>Department of Paleoclimatology and Geomorphology, Free University of Amsterdam, de Boelelaan 1085, 1081 HV Amsterdam, The Netherlands.

Organic Geochemistry: In Press

#### Abstract

Mud volcanoes (MVs) are formed by expulsion due to lateral or vertical compression of overpressured fluids in the subsurface. Their sediments are characterized by a specific lithology called mud breccia, which is composed of inorganic and organic matter sourced from different sedimentary units and transported from the subsurface to the seafloor. Biomarker lipid distributions were determined in sediment cores collected from the Kazakov, NIOZ and Odessa MVs in the Sorokin Trough, north-eastern Black Sea. This revealed different mud breccia sources that are directly linked to the location of the fracture zones or diapiric folds formed by tectonic compression. The Kazakov MV shows biomarker characteristics of relatively mature organic matter, which is likely related to the Maycopian Shale Formation. The NIOZ and Odessa MVs contain immature organic matter derived from much shallower sediments overpressed by rising Maycopian diapirs. In the mud breccia from the NIOZ MV, biomarkers clearly recorded two different mud eruption episodes reflected in distinct distributions from unrelated sedimentary facies. Hence, this study shows that although the organic matter of a mud breccia is sourced from a complex mixture of lithofacies, the collective biomarker signal reveals specific signatures of those sedimentary sections that contributed most to the migrated fluid.

## **1. Introduction**

Cold-seepage at the sea floor is often the result of upward fluid passage in the subsurface. This migration of fluids through zones of weakness, fault system, cracks, and fissures also affects sea-floor morphology. It results in the formation of (i) pockmarks, i.e. negative topographic features formed due to seepage (Hovland and Judd, 1988), (ii) large fissure eruptions of sediments from the subsurface (Ivanov et al., 1998), and (iii) mud volcanoes (MVs), i.e. mounds or negative collapsed structures caused by catastrophic explosion of fluids at the seafloor (Ivanov et al., 1998). Mud volcanoes are thus a clear indication of fluid venting. The term fluid, as used here, implies a complex mixture of products including hydrocarbon gases (e.g. methane and C<sub>2+</sub> hydrocarbons), hydrogen sulfide, carbon dioxide, petroleum, pore waters and mud. The emitted mud, so called mud breccia (Akhmanov, 1996), is one of the major constituents of the migrated fluid. It is a complex mixture of a fine-grained matrix of clays and terrigenous material (silt or/and sand) plus rock fragments that have been mechanically entrained by the powerful upward transport of fluids (Akhmanov, 1996, Akhmanov and Woodside, 1998). Mud breccia forms at a subsurface depth where overpressured rocks are situated (more than 10 km sedimentary depth; Shnyukov et al., 2005), and its composition provides key insight into the geological history of the area and information about the source strata, e.g. on their hydrocarbon potential.

On the basis of comprehensive geophysical surveys carried out during the TTR-6 (1996) and the TTR-11 (2001) cruises, a considerable number of MVs were discovered in the Sorokin Trough (Ivanov et al., 1996; Woodside et al., 1997; Ivanov et al., 1998; Bouriak and Akhmetzhnov, 1998; Kenyon et al., 2002). During the 11<sup>th</sup> Training Trough Research (TTR-11; 2001) cruise of the Russian R/V Professor Logachev, the Kazakov, NIOZ and Odessa MVs were investigated in detail (Kenyon et al., 2002; Mazzini et al., 2004; Stadnitskaia et al., 2005). The results of integrated lipid biomarker and 16S rRNA gene studies of four methane-derived carbonates with microbial mats and mud breccias from the NIOZ, Odessa and Kazakov MVs showed that anaerobic oxidation of methane (AOM) plays a crucial role in carbonate formation (Stadnitskaia et al., 2005). Hydrocarbon gas analysis from mud breccias, gas saturated sediments, and gas hydrates collected from these MVs revealed deep sources for the ejected fluids (Stadnitskaia, unpublished data). The source of fluids in the Sorokin Trough, and in the Black Sea in general, is the subject of on-going study. Here, we report for the first time a detailed biomarker study of the mud breccia matrix from the Kazakov, NIOZ and Odessa MVs (Figure 1). This study has revealed probable sources for the erupted material from an examination of lipid biomarkers used as fossil molecular fingerprints for sediments that were mechanically entrained by the migrating fluid. Differences in biomarker compositions and distributions were expected due to the distinctive lithological characteristics

of the mud breccias and age difference of mud breccia clasts (Ivanov et al., 1998; Kozlova, 2003).

## 2. Geological setting

The Sorokin Trough is located in the north-eastern part of the Black Sea, on the continental slope of the south-eastern margin of the Crimea Peninsula at water depths of 600 to 2100 m. It extends for about 150 km and has a width of 50-60 km, and is bordered by the Cretaceous-Eocene uplifts: Shatsky Ridge and Tetyaev Rise (Fig. 1). The trough is considered to be the Crimean Alpine foredeep formed during the Maycopian (Oligocene-Early Miocene). It is one of the largest depressions in the eastern Black Sea, which is well known for active cold-seepage, in particular mud volcanism (Ivanov et al., 1998; Shnyukov et al., 2005).

The existence of active fluid venting provinces in the Sorokin Trough was discovered during expeditions of the Russian Training-Through-Research (TTR) programme (Woodside et al., 1997; Bouriak and Akhmetjanov, 1998; Ivanov et al., 1998; Kenyon et al., 2002). These studies revealed that mud volcanism is mainly related to diapiric folds of the Maycopian Shale Formation (MSF) comprising Oligocene-Early Miocene marine shales and representing regional source rocks in basins from the Carpathians to the west of the Black Sea region, through the Crimea and the Caucasus Mountains, to the South Caspian Basin at the east.

The MSF consists of grey and dark-brown clays, with siderite concretions, layers/lenses of silt and glauconite sands. Generally, these clays are enriched in total organic carbon (TOC). Based on data from the Terek-Caspian Petroleum System (Middle Caspian Basin, Russia; Ulmishek, 2001), the lower Maycopian clays and marlstones are commonly

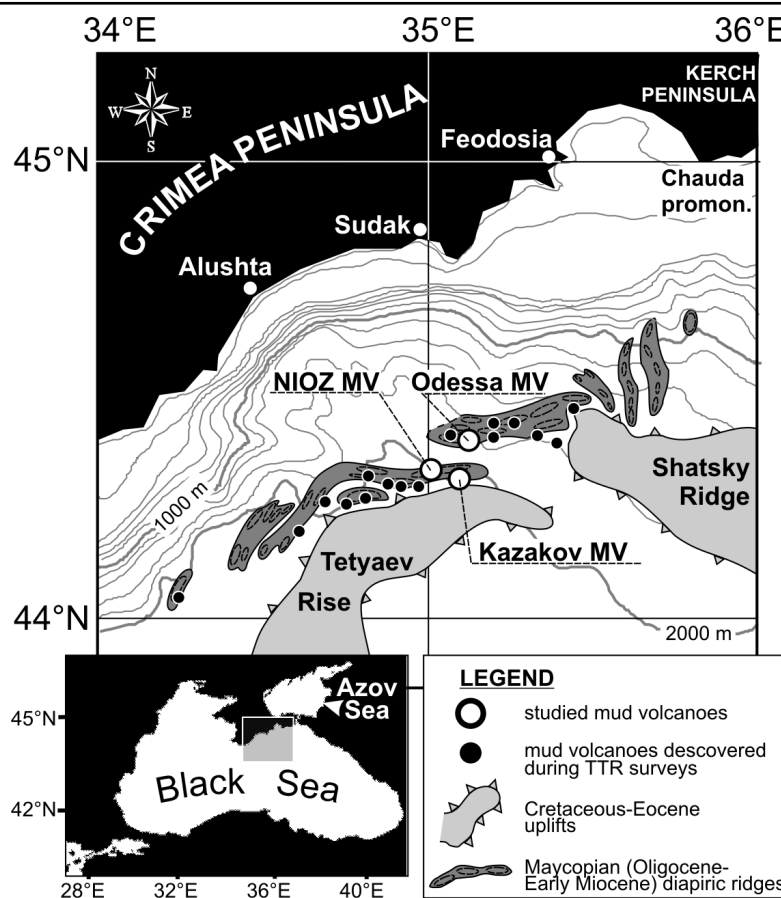


**Figure 1.** Location of mud volcanoes and diapir ridges in the Sorokin Trough (modified after Woodside et al., 1997).



characterised by high total TOC contents (up to 4.4%) and contain predominantly type II kerogen. Towards the uppermost part of the formation, TOC decreases to 12 % and organic matter contains a higher proportion of terrigenous constituents. The thickness of Maycopian sediments in the Sorokin Trough is about 5 km (Tugolesov et al., 1985). The Middle-Upper Miocene complex overlying the MSF has a terrigenous composition and a thickness from hundreds of meters on the Shatsky Ridge to 3 km at the Guriy foredeep (Nikishin et al., 2003). The Pliocene-Quaternary unit consists mostly of clays (Tugolesov et al., 1985) and in the Sorokin Trough, the Quaternary sediments reach a thickness of 2 km, increasing progressively to 3 km toward palaeo-Don/palaeo-Kuban Pleistocene fan in the northeast (Tugolesov et al., 1985).

Most MVs in the area are situated on the flanks of the Maycopian diapiric ridges (Ivanov et al., 1998; Krastel et al., 2003). Percolation of gas-saturated sediments was also detected from pock-mark-like depressions and through linear faults oriented roughly along the continental slope (Ivanov et al., 1998).

Three of the MVs in the Sorokin Trough, i.e., the NIOZ (44°19'N; 35°04'E, water depth of ca. 2020 m), the Odessa (44°23'N; 35°09'E, water depth of ca. 1830 m) and the Kazakov (44°18'N; 35°11'E, water depth of ca. 1920 m), were selected for this study (Fig. 1). These MVs are characterized by different modes of mud eruption and venting activity. The Kazakov MV is the largest MV in the Sorokin Trough. It is a 140 m high by 1.8 km wide conical-shaped mound. Based on seismic records obtained during the TTR-11 cruise, the Kazakov MV has deep roots, which are not visible in the seismic section. The feeder channel of the MV has a width of 2 km (Kenyon et al., 2002), indicating a deep source for the migrated fluid and likely vigorous eruptions. The NIOZ MV is a smaller, conical feature, 70 m high and 1.2 km wide. The NIOZ MV has a 1.2 km wide feeder channel masked by the acoustically homogenous MSF diapir from which the MV arises (Kenyon et al., 2002). Rise of the diapir was possibly a trigger for mud outbreaks. The feeder channel of the NIOZ MV is also relatively wide, indicating powerful eruptions, although the depths of erupted material are supposed to be shallower than for the Kazakov MV. In the area between both MVs a NE-SW trending fault was observed on the subbottom profiler line (Kenyon et al., 2002).

Compared to the Kazakov and the NIOZ MVs, the nature and the mode of mud eruption in the Odessa MV are fundamentally different (Ivanov et al., 1998). Instead of vigorous emissions, mud flows out from an open fault situated at the top of a diapiric ridge (Woodside et al., 1997, Ivanov et al., 1998; Kenyon et al., 2002). These outflows of mud from the subsurface force the overlying hemipelagic sediments to slide or slump down the slope leading to extensive flows of fluidized sediments. Widespread sediment movement, outcrops of possibly recent (Pleistocene clays with hydrotrilite) sediments, sliding and slumping bodies, all resulting from intensive fluid discharge, are common features of this part of the

Sorokin Trough (Ivanov et al., 1998). All sedimentary cores from the Odessa MV and adjacent mud flows from the system of parallel faults, recovered the Black Sea Units I and II (Degens and Ross, 1972) and Pleistocene/Holocene clays showing evidence of slumping activity (Kenyon et al., 2002).

### 3. Material and methods

#### 3.1. Sample collection

Bottom sampling was performed according to standard TTR-procedures (Ivanov et al., 1992). All samples were taken using a 6 m long, 1500 kg gravity corer with an internal diameter of 14.7 cm (Kenyon et al., 2002). Following removal of the core from the plastic liner, the lithology was described and then sediments were sub-sampled for TOC measurements and for the biomarker lipid study. Recovered sediments were then stored at -20°C.

#### 3.2. Total organic carbon content

The measurement of TOC content was accomplished on a Fisons Instruments NCS-1500 Elemental Analyzer using flash combustion at 1013°C. Standard deviations of duplicate measurements were ca. 0.3 %.

#### 3.3. Biomarker lipid analysis

Ca. 20-50 g of each sample was freeze-dried, crushed in an agate mortar to a fine powder, and extracted with an automatic Accelerated Solvent Extractor (ASE 200/DIONEX) using a solvent mixture dichloromethane (DCM):methanol (MeOH) (9:1, v/v) at 1000 psi and 100°C. Elemental sulfur was removed from the total extract by elution through a small pipette filled with activated copper. An aliquot of the total extract was chromatographically separated into apolar and polar fractions using a column with activated (2 h at 150°C) Al<sub>2</sub>O<sub>3</sub> as stationary phase. Apolar compounds were eluted using hexane:DCM (9:1, v/v), and polar compounds, including glycerol ether core membrane lipids, were obtained with MeOH:DCM (1:1, v/v) as eluent. Fatty acids were methylated by heating at 60°C for 5 min in BF<sub>3</sub>-MeOH complex (in excess MeOH, ca.12 wt.% BF<sub>3</sub>), and alcohols were transformed into trimethylsilyl ether derivatives by adding 25 µl of pyridine and 25 µl of BSTFA and heating at 60°C for 20 min. A known amount of 2,3-dimethyl-5-(1,1-dideuterohexadecyl)-thiophene (C<sub>22</sub>H<sub>38</sub>SD<sub>2</sub>) was added to each fraction as an internal standard. In order to remove saturated normal hydrocarbons and to enrich branched/cyclic compounds, the apolar fraction was filtered over silicalite using cyclohexane as an eluent.

Gas chromatography (GC) was performed using a Hewlett Packard 6890 gas chromatograph equipped with an on-column injector and a flame ionization detector. A fused silica capillary column (CPSil5 25 m x 0.32mm,  $d_f = 0.12 \mu\text{m}$ ) with helium as a carrier gas was used. The samples were injected at 70 °C. The GC oven temperature was subsequently raised to 130 °C at a rate of 20 °C  $\text{min}^{-1}$ , and then to 320 °C at 4 °C  $\text{min}^{-1}$ . The temperature was then held constant for 15 min.

All fractions were analyzed by gas chromatography-mass spectrometry (GC-MS) for compound identification. GC-MS was conducted using a Hewlett Packard 5890 gas chromatograph interfaced to a VG Autospec Ultima Q mass spectrometer operated at 70 eV with a mass range of  $m/z$  50–800 and a cycle time of 1.8 s (resolution 1000). The gas chromatograph was equipped with a fused silica capillary column (CPSil 5 25 m x 0.32 mm,  $d_f = 0.12 \mu\text{m}$ ) and helium as carrier gas. The temperature program used for GC-MS was the same as for GC. The structural designation of lipids was evaluated by the comparison their mass spectral fragmentation patterns and pseudo-Kovats retention indices with reported data.

median interval, (cm b.s.f.)	TOC (wt %)	Lithology <sup>a</sup>	Age <sup>b</sup>
<b>Kazakov MV (TTR11 BS331G)</b>			
0	1.7	Mud breccia: olive grey, water saturated, structureless and homogeneous. Strong sulfide smell.	
2	1.4		
4	1.4		
6	1.4		
8	1.2		
10	1.3		
11	1.3		
12	1.1		
14	1.1		
16	1.0		
18	1.1	Mud breccia: similar to the upper interval, but less water saturated. Strong sulfide smell. Gas hydrates were present.	Oligocene-Low Miocene; Maycopian Shale Formation
20	1.2		
24	0.6		
30	1.2		
34	1.2		
36	1.2		
42	1.2		
55	1.1		
85	1.2		
120	1.1		
Average	1.2		
<b>NIOZ MV (TTR11 BS325G)</b>			
0	0.6	Mud breccia: grey clay with high silty admixture and small clasts of dark grey clay up to 0.5 cm in size. Structureless, water saturated. Young mud breccia flow.	not identified
6	0.5		
17	0.6	Mud breccia: similar to the overlaid mud breccia interval, grey stiff massive with darker layers of hydrotrillite. Strong sulfide smell.	
44	0.6		
62	0.6		
87	0.6		
Average	0.6		
<b>Odessa MV (TTR11 BS336G)</b>			
15	0.4	Clay and silt; grey, homogeneous, structureless with thin silty layers.	Holocene
25	0.4		
38	0.5		
50	0.5		
69	0.6	Clay; structureless with silty admixture varying along the interval. Hydrotrillite content increases toward the bottom. Strong sulfide smell. Gas hydrates were present.	Pleistocene
97	0.6		
115	0.5		
148	0.5		
160	1.0		
Average	0.5		

<sup>a</sup> - Kenyon et al., 2002

<sup>b</sup> - Ivanov et al., 1998

**Table 1.** TOC contents and lithological characteristics of examined samples.

To determine the distribution and composition of intact glycerol dialkyl glycerol tetraethers (GDGTs), samples were analyzed using a high performance liquid chromatography–mass spectrometry (HPLC–MS) method for their direct analysis (Hopmans et al., 2000). GDGTs were analyzed using an Agilent 1100 series / 1100 MSD series instrument, with auto-injection system and HP-Chemstation software. An Alltech Prevail Cyano column (150 mm x 2.1 mm, 3  $\mu\text{m}$ ) was used with hexane:propanol (99:1, 13 v) as a mobile phase. For the first 5 min, the flow rate of the eluent was 0.2 ml min<sup>-1</sup>. In the following 45 min the flow rate was used with a linear gradient to 1.8 % propanol. MS-analysis and quantification of both isoprenoidal and branched GDGTs followed methods reported in Wijers et al. (2006, in press).

### 4. Results

#### 4.1. Sedimentary lithologies and bulk parameters

Figure 1 shows the location of studied MVs and Figure 2 shows lithologies of the MV deposits. The recovered sediments were gas-saturated and were characterized by a strong smell of hydrogen sulfide.

Core TTR-11 BS-331G was collected from the crater of the Kazakov MV. The core recovered 166 cm of gas-saturated mud breccia (Kenyon et al., 2002; Stadnitskaia et al., 2005), with no pelagic sediments on top and with drop-sized gas hydrates at the base (Figure 2a). A variety of rock clasts were found within the mud breccia matrix. Previous investigations revealed that the age of the rock clasts in the Kazakov mud volcano is mainly Oligocene-Early Miocene, i.e. they are derived from the MSF (Ivanov et al., 1998). This type of mud breccia is characteristic of MVs from the Kerch Peninsula and from the Central Black Sea (Ivanov et al., 1998).

Core TTR-11 BS-325G (Figure 2b), taken from the crater of the NIOZ MV, retrieved 88 cm of mud breccia with rock clasts of different lithologies in a silty-clayey matrix (Kenyon et al., 2002). At the level of 1213 cm, a carbonate crust layer with microbial mats was present (Stadnitskaia et al., 2005). The crust was overlain by an hydrotroilite (colloidal hydrous ferrous mono-sulfide) interval, which gave the interval a black color.

Core TTR-11 BS-336G, taken from the Odessa MV, recovered 167 cm of sediments composed of pelagic Black Sea Unit I and II sediments (Degens and Ross, 1972) and clays of Pleistocene/Holocene age (Figure 2c). A carbonate crust with pink microbial mats was situated at the boundary between the clay interval and the Unit II sediments (Stadnitskaia et al., 2005). Hydrotroilite content increased down core, resulting in a changing sediment color towards dark grey. Unfortunately, no sediment samples of the Holocene Unit I and Unit II

were obtained for the lipid study. Therefore, the lipid data for this sampling location is presented only for the underlying Pleistocene/Holocene clay interval (Figure 2c).

Bulk parameters and lithological description for these sedimentary sections are summarized in Table 1. Overall, TOC values were relatively low. In the NIOZ and Odessa MVs, TOC content was ca. 0.5 wt % (Table 1). Mud breccias of the Kazakov MV were characterized by slightly higher TOC values (ca. 1.2 wt %).

#### 4.2. Compositional variations and sources of selected biomarker groups

The distributions of lipid biomarkers in the mud breccia matrix from the Kazakov and NIOZ MVs, and in the Pleistocene/Holocene clays from the Odessa MV were distinct. Figure 2 shows concentration profiles of selected biomarker lipids in the cores obtained from these MVs. Figure 3 shows the typical carbon number distributions of *n*-alkanes, straight-chain fatty acids, and alcohols for the three MVs.

In general, lipid extracts comprised a complex mixture of (i) components indigenous to the erupted mud breccia with an admixture of petroleum-derived compounds and (ii) a variety of *in situ* formed archaeal and bacterial lipids, abundantly present in the uppermost intervals of the studied sediments (Stadnitskaia et al., 2005). The biomarker distribution in the authigenic carbonates found within the mud breccia has been discussed previously (Stadnitskaia et al., 2005).

##### 4.2.1. *n*-Alkanes

Series of *n*-alkanes ranged in carbon number from C<sub>19</sub> to C<sub>36</sub> (Figure 3). C<sub>23</sub>-C<sub>33</sub> *n*-alkanes were the most dominant homologues in the Kazakov MV, showing an odd-over-even carbon-number predominance with a maximum at C<sub>29</sub> or C<sub>31</sub>. Mud breccias from the NIOZ MV and sediments from the Odessa MV showed smoother *n*-alkane distributions, with *n*-C<sub>25</sub> as the dominant member (Figure 3). The Carbon Preference Index (CPI; Bray and Evans,

interval, cm b.s.f.	<i>n</i> -alkanes		FAME
	CPI (C <sub>25</sub> - C <sub>34</sub> )	CPI (C <sub>23</sub> -C <sub>30</sub> )	CPI (C <sub>22</sub> -C <sub>30</sub> )
<b>Kazakov MV (TTR11 BS331G)</b>			
0-10	2.6	2.1	5.7
10-20	2.9	2.1	5.0
30-40	2.4	2.2	4.7
40-50	2.6	2.1	4.3
50-60	2.8	2.2	5.2
79-91	2.4	2.2	4.9
119-120	2.2	2.0	4.5
160-166	2.5	2.0	4.2
Average	2.6	2.6	4.8
<b>NIOZ MV (TTR11 BS325G)</b>			
0-4	1.2	1.1	8.2
4-10	1.3	1.1	9.2
16-22	1.9	1.1	11.2
24-25	2.7	1.4	9.1
44-46	2.3	1.8	6.9
62-67	4.5	1.5	8.1
84-88	1.6	2.9	6.5
Average	2.2	1.6	8.0
<b>Odessa MV (TTR11 BS336G)</b>			
15-25	1.2	1.1	6.0
25-35	1.3	1.1	5.9
38-48	1.3	1.1	7.4
50-58	1.2	1.2	5.1
68-78	1.6	1.1	4.5
97-105	1.2	1.3	4.6
115-125	1.2	1.1	2.0
148-153	1.1	1.1	3.4
Average	1.3	1.1	4.9
n/a - not applicable			

**Table 2.** Values of CPI calculated for the *n*-alkanes and straight-chain fatty acids.

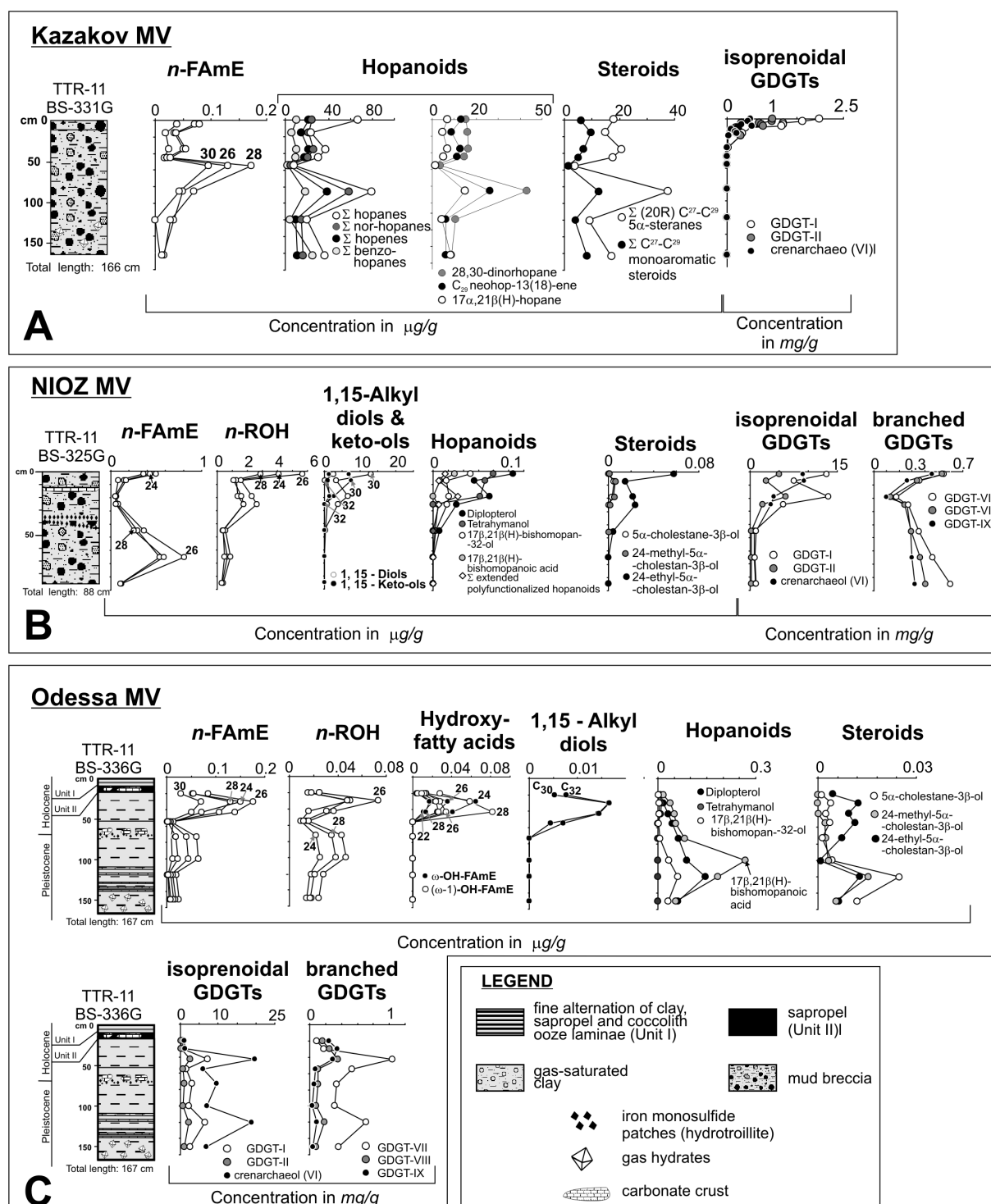


**Figure 2.** Concentration profiles with depth of selected biomarkers: A - Kazakov MV; B - NIOZ MV; C - Odessa MV. Numbers next to the curves indicate the total number of carbon atoms. The top 20 cm of the isoprenoidal GDGT profile data for the Kazakov and NIOZ MVs are from Stadnitskaia et al. (2005). For GDGT structures see Figure 5.

1961) for C<sub>25</sub>-C<sub>34</sub> *n*-alkanes from the Kazakov, NIOZ and Odessa MVs were on average 2.6, 2.1, and 1.2, respectively (Table 2).

#### 4.2.2. Fatty acids and *n*-alcohols

Fatty acids were the dominant compound class in the sediments from the Odessa MV (up to 50 cm), whereas *n*-alcohols represented important constituents in the mud breccia from the NIOZ MV. In the mud breccia from the Kazakov MV, *n*-alcohols were present in low concentrations, whereas fatty acids occurred in similar quantities as in the Odessa MV. Even-carbon-numbered compounds were dominant in the distributions of both compound classes in all studied MVs (Figure 3).

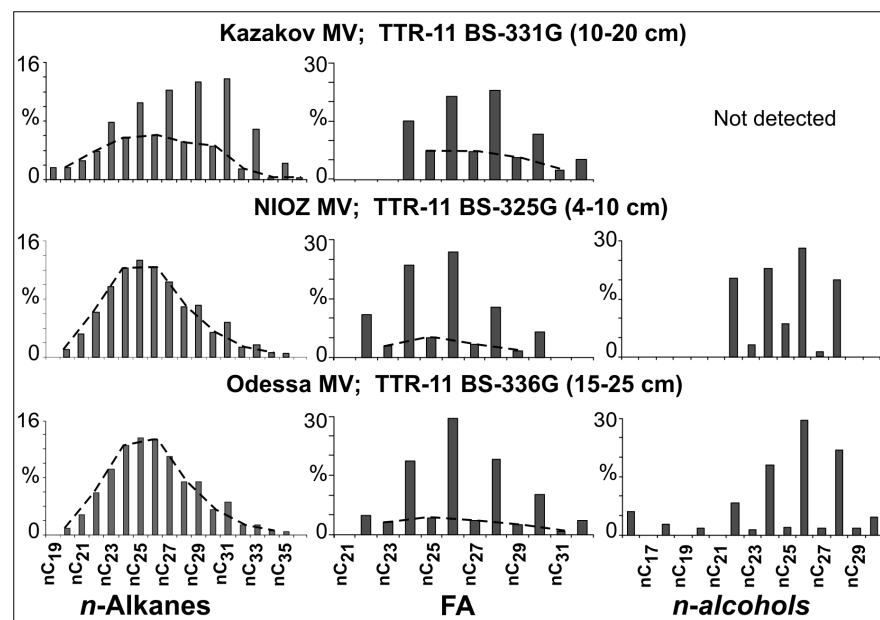


**Figure 3.** Typical carbon number distributions of the *n*-alkanes, the straight-chain fatty acids and the *n*-alcohols in the three MVs. The distributions are expressed as the percentage of the total sum normalized on 100%. The dashed contour outlines the compound distributions with an even (in case of the *n*-alkanes) or odd (in case of the straight-chain fatty acids) number of carbon atoms.

and Odessa MVs *n*-alcohols occurred in the carbon number range C<sub>22</sub> to C<sub>28</sub> and C<sub>16</sub> to C<sub>32</sub>, respectively (Figure 3). Both MVs showed C<sub>26</sub> as the dominant compound and a strong even-over-odd carbon number predominance (Figures. 2 and 3). The strong even-over-odd carbon number predominance for fatty acids in the mud breccia from the Kazakov MV and for both compound classes in the mud breccia from the NIOZ and Pleistocene/Holocene clays from the Odessa MVs (Figures. 2 and 3) marks their origin from higher plant epicuticular waxes (Eglington and Hamilton, 1967; Kolattukudy, 1980).

In all mud breccias, long-chain *n*-fatty acids ranged in carbon number from C<sub>22</sub> to C<sub>32</sub>. Short-chain fatty acids, including C<sub>16</sub> and C<sub>18</sub>, were either not observed or present at low concentrations. The distribution of fatty acids differs between the Kazakov and the NIOZ/Odessa MVs (Figure 3). In the NIOZ

#### 4.2.3. Alkyl diols and keto-ols

Straight-chain saturated C<sub>23</sub> and C<sub>25</sub> 1,2-diols, with an as yet unknown biological origin, and C<sub>30</sub> and C<sub>32</sub> 1,15-diols, derived from the class of Eustigmatophyceae microalgae (Volkman et al., 1992, 1998, 1999; Gelin et al., 1997; Versteegh et al., 1997; Méjanelle et al., 2003), were detected in the uppermost 45 cm of the mud breccia from the NIOZ and Odessa MVs (Figure 2). In the mud breccia from the Kazakov MV these compounds were not found. C<sub>30</sub> and C<sub>32</sub> alkyl keto-ols, previously observed in sediments (for a review see Versteegh et al., 1997) and water column (e.g. Wakeham et al., 2002) were detected only in the mud breccia from the NIOZ MV (Figure 2). These may be a post-depositional oxidation product of the mid-chain diols (Volkman et al., 1992; Ferreira et al., 2001). Overall, the 1,15-isomers dominated the diol distributions. The C<sub>25</sub> 1,2-diol was detected as the major diol-member only in the topmost interval (Figure 2). In the sediments from the Odessa MV, C<sub>30</sub> and C<sub>32</sub> mid-chain diols occurred within the uppermost 70 cm (Figure 2). Keto-ols were not detected.

#### 4.2.4. Long-chain hydroxy fatty acids

In the sediments from the Odessa MV, even carbon numbered C<sub>22</sub>C<sub>28</sub>  $\omega$ - and C<sub>26</sub>C<sub>30</sub> ( $\omega$ -1)-hydroxy fatty acids were present in the uppermost 50 cm. In the mud breccia from the NIOZ MV they occurred in trace amounts, and in the Kazakov MV these lipids were not observed.  $\omega$ -Hydroxy fatty acids were predominant over the ( $\omega$ -1)-compounds with C<sub>24</sub> as the dominant member (Figure 3). In the sediments from the Odessa MV, concentration profiles of hydroxy fatty acids exhibited a similar concentration profile as the even-numbered straight-chain fatty acids and *n*-alcohols (Figure 3), suggesting a probable terrestrial origin.

#### 4.2.5. Pentacyclic triterpenoids

The distribution of pentacyclic triterpenoids is illustrated by *m/z* 191 mass chromatograms (Figure 4). Numbers refer to compounds listed in Table 3. The mud breccia from the Kazakov MV contained the most extensive series of pentacyclic triterpanes, which also formed a prevailing group of biomarkers in the total lipid fractions. Hopanes were the dominant constituents, followed by hopenes and benzohopanes. Homohopanes showed a notable predominance of the 22S- over the 22R-epimer. C<sub>30</sub>-C<sub>32</sub> hopanes with  $\beta\alpha$ - and  $\beta\beta$ -configurations were less abundant than their  $\alpha\beta$ -epimers (Figure 4). Norhopanes were present in all samples, including 17 $\alpha$  (H)-trisorhopane, 28,30-dinorhopane, and 17 $\beta$ ,21 $\alpha$  (H)-30-norhopane (Figure 4). 28,30-Dinorhopane and 17 $\alpha$ ,21 $\beta$ (H)-homohopane were prominent members among the pentacyclic triterpanes (Figure 4). All samples also contained unsaturated hopanoids, including C<sub>29</sub> and C<sub>30</sub> neohop-13(18)-enes, and (22R)- and (22S)-C<sub>31</sub> hop-17(21)-



enes. C<sub>32</sub> to C<sub>34</sub> benzohopanes were only found in this mud breccia. No polar hopanoids were detected in the mud breccia from the Kazakov MV.

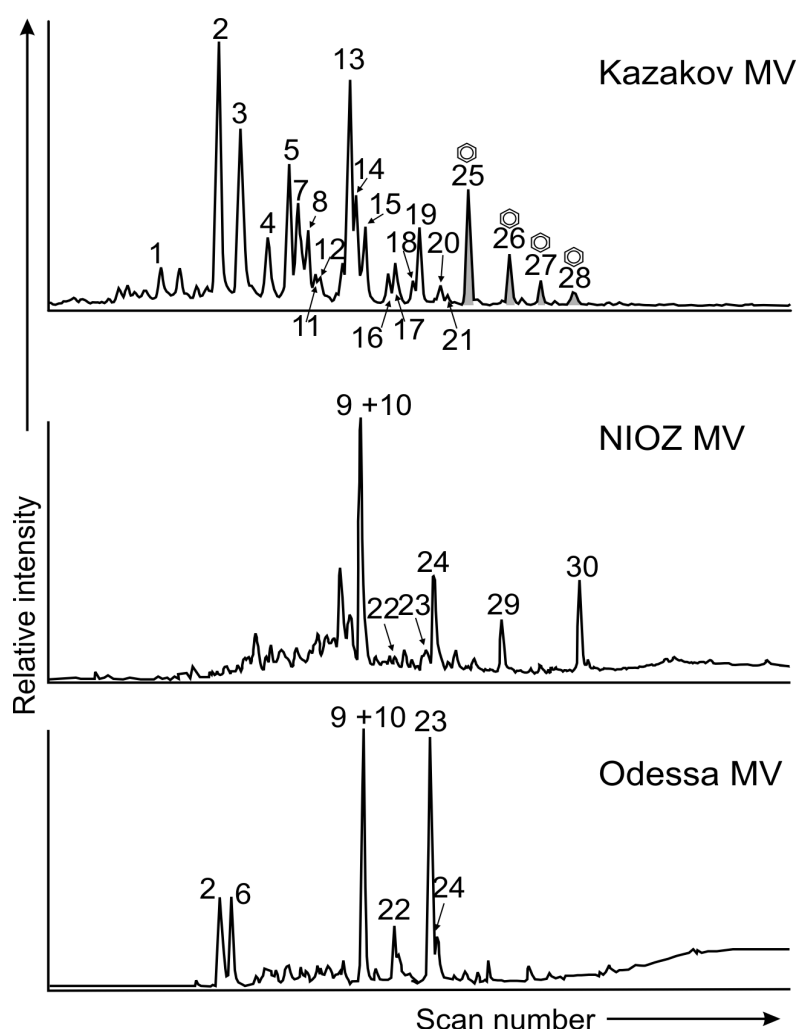


**Figure 4.** Typical *m/z* 191 mass chromatograms showing distributions of pentacyclic triterpenoids present in the mud breccias of the three studied MVs in the Sorokin Trough in the Black Sea. Numbers refer to compounds listed in Table 3.

Hopanoids characterize a biomarker group derived almost exclusively from prokaryotic sources (Ourisson et al., 1979), and they are ubiquitous in sediments (Rohmer et al., 1984). Tetrahymanol is a characteristic lipid in bacterivorous ciliates such as marine scuticociliates, which feed mainly on bacteria, or the freshwater ciliate *Tetrahymena* (Mallory et al., 1963; Thompson and Nozawa, 1972; Harvey and McManus, 1991). 28,30-Dinorhopane is often prominent in sediments deposited in anoxic environments (Grantham et al., 1979; Katz and Elrod, 1983; Peters et al., 2005). This hopanoid is also detected in many crude oils

In contrast, functionalized triterpenoids such as diplopterol (17 $\beta$ 21 $\beta$ (H)-hopan-22-ol) and the non-hopanoid tetrahymanol (gammaceran-3 $\beta$ -ol; ten Haven, et al., 1989) were dominant in the mud breccia from the NIOZ MV and sediments from the Odessa MV (Figure 4; Stadnitskaia et al., 2005). Both mud breccias contained 17 $\beta$ 21 $\beta$ (H)-bishomohopan-32-ol (Stadnitskaia et al., 2005) and  $\alpha\beta$ - and  $\beta\beta$ -epimers of bishomohopanoic acid (Figure 4). The uppermost 45 cm of the mud breccia from the NIOZ MV showed the presence of two extended polyfunctionalized hopanoids (Figure 4; Table 3). The molecular ion of compound 29 was not detected, while compound 30 had an  $M^+$ =672 (Table 3).

(Seifert et al., 1978; Grantham et al., 1979; Schoell et al., 1992), and in Recent (Anders et al., 1978) and older sediments (Katz and Elrod, 1983; Schouten et al., 1997).

Peak number	Compound name	Carbon number
1	17 $\alpha$ (H) -trisorhopane	27
2	28,30-disorhopane	28
3	30-nor-neohop -13(18) - ene	29
4	17 $\beta$ , 21 $\alpha$ (H) - 30- norhopane	29
5	17 $\alpha$ , 21 $\beta$ (H) - hopane	30
6	Diploptene (hop - 22(29) - ene)	30
7	neohop - 13(18) - ene	30
8	17 $\beta$ , 21 $\alpha$ (H) - hopane	30
9	Tetrahymanol, gammaceran-3 $\beta$ -ol	30
10	Diplopterol (17 $\beta$ , 21 $\beta$ (H)-hopan-22-ol)	30
11	hop - 17(21) - ene 22S	31
12	hop - 17(21) - ene 22R	31
13	17 $\alpha$ , 21 $\beta$ (H) - homohopane 22S	31
14	17 $\alpha$ , 21 $\beta$ (H) - homohopane 22R	31
15	17 $\beta$ , 21 $\alpha$ (H) - homohopane	31
16	17 $\alpha$ , 21 $\beta$ (H) - bishomohopane 22S	32
17	17 $\alpha$ , 21 $\beta$ (H) - bishomohopane 22R	32
18	17 $\beta$ , 21 $\alpha$ (H) - bishomohopane	32
19	17 $\beta$ , 21 $\beta$ (H) - homohopane	31
20	17 $\alpha$ , 21 $\beta$ (H) - trishomohopane 22S	33
21	17 $\alpha$ , 21 $\beta$ (H) - trishomohopane 22R	33
22	17 $\alpha$ , 21 $\beta$ (H) - bishomohopanoic acid	32
23	17 $\beta$ , 21 $\beta$ (H) - bishomohopanoic acid	32
24	17 $\beta$ , 21 $\beta$ (H) - bishomohopan-32-ol	32
25	20,32-cyclo-17 $\alpha$ -bishomohopane-20,22,31-triene 22	32
26	20,32-cyclo-32-methyl-17 $\alpha$ -bishomohopane-20,22,31-triene 22	33
27	20,32-cyclo-32-ethyl-17 $\alpha$ -bishomohopane-20,22,31-triene 22S	34
28	20,32-cyclo-32-ethyl-17 $\alpha$ -bishomohopane-20,22,31-triene 22R	34
29	extended polyfunctionalized hopanoid M <sup>+</sup> - ?	35 ?
30	extended polyfunctionalized hopanoid M <sup>+</sup> = 672	35 ?

**Table 3.** Pentacyclic triterpanes identified in mud breccias and sediments.

#### 4.2.6. Steroids

The distribution of steroids was examined using mass chromatograms for  $m/z$  217, 231 and 253. Steroids were present in lower abundances than hopanoids. Mud breccia from the Kazakov MV contained the highest concentrations of steroids compared to the sediments from the NIOZ and Odessa MVs. Only mud breccia from the Kazakov MV contained (20R)-5 $\alpha$ ,14 $\alpha$ ,17 $\alpha$ (H) C<sub>27</sub>, C<sub>28</sub>, and C<sub>29</sub> regular steranes and C<sub>27</sub>-C<sub>29</sub> C-ring monoaromatic steroids.

The mud breccia from the NIOZ and the Pleistocene/Holocene clays from the Odessa MVs showed similar steroid compositions. Both were relatively poor in steroids, including only C<sub>27</sub>-, C<sub>28</sub>-, and C<sub>29</sub>-5 $\alpha$ -sterols with the latter as the dominant member. Sediments from the Odessa MV additionally contained C<sub>28</sub> 24-methyl-5 $\alpha$ -cholest-24(28)-en-3 $\beta$ -ol and C<sub>29</sub> 24-ethylcholestanol (5 $\alpha$ (H)-sitostanol).

#### 4.2.7. Isoprenoidal and branched Glycerol Dialkyl Glycerol Tetraethers

The distribution of glycerol dialkyl glycerol tetraethers (GDGTs) in the mud breccias of the different MVs is shown in Figure 5. Both isoprenoidal and branched GDGTs were identified in the NIOZ and Odessa MVs. By contrast, the Kazakov mud volcano deposits only contained isoprenoidal GDGTs. The distribution profiles of isoprenoidal GDGTs within the top 20 cm of the cores has been reported (Stadnitskaia et al., 2005) and revealed GDGTs

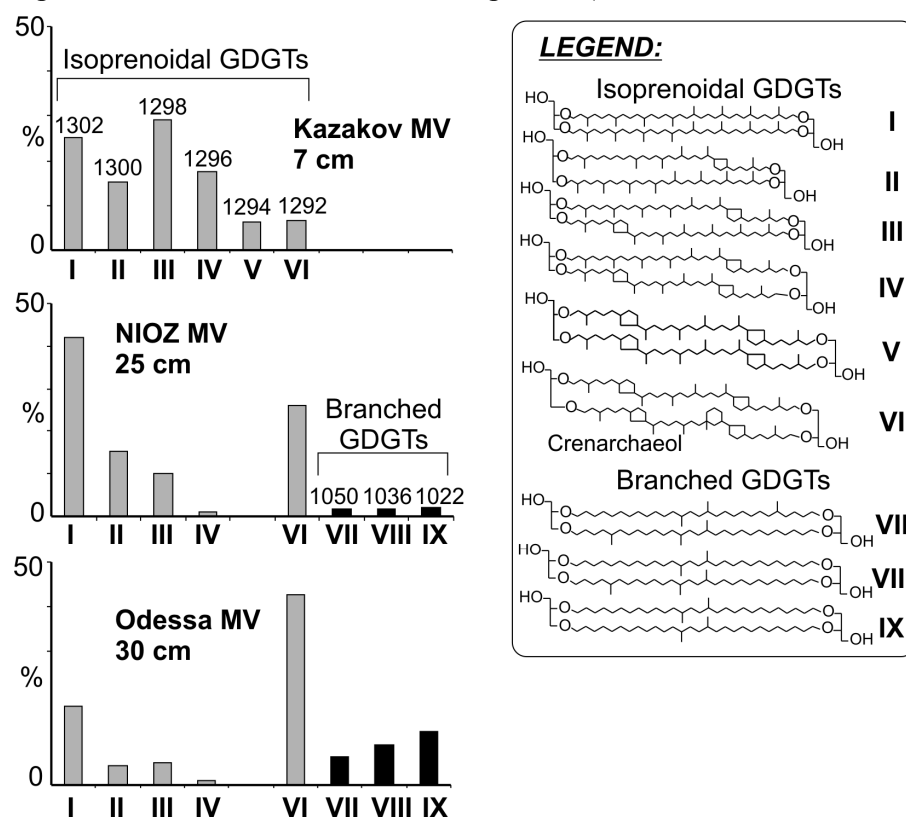


**Figure 5.** Typical distribution of GDGTs in the mud breccias of the three studied MVs in the Sorokin Trough in the Black Sea. The distributions are expressed as the percentage of the total sum normalized on 100%. The roman number under the each bar relates to the number of the compound structure represented in the Legend. Numbers such as "1050" indicated the dominant [M+H]<sup>+</sup> ion.

derived from archaea involved in the anaerobic oxidation of methane (AOM) (Stadnitskaia et al., 2005; see also Figure 2). In this paper, we extended the GDGT data in order to demonstrate the quantitative and qualitative changes of these compounds in the sedimentary sections. The appearance of these compounds below the 20 cm depth interval is not related to the AOM processes.

Isoprenoidal GDGTs are unique membrane lipids of ecologically diverse

archaea and can contain 0 to 8 cyclopentane rings (De Rosa et al., 1983, Langworthy, 1985,

De Rosa and Gambacorta, 1988). The presence of methanotrophic archaea performing AOM is indicated by the dominance of isoprenoidal GDGTs with 0-2 cyclopentane rings (Pancost et al., 2001; Aloisi et al., 2002; Stadnitskaia et al., 2005). Crenarchaeol is a marker of ubiquitous planktonic crenarchaeota (Hoefs et al., 1997; Schouten et al., 2000, 2001; Sinninghe Damsté et al., 2002a,b; Wakeham et al., 2003), which also biosynthesize other GDGTs having either no, or to a smaller extent 1–3, cyclopentane rings. Schouten et al. (2000) suggested that GDGTs were biosynthesized by organisms thriving predominantly in terrestrial environments. Recently, Weijers et al. (2006) showed that they were abundant in the anoxic parts of peat bogs and soils and suggested an origin from anaerobic bacteria based on the stereochemistry of the glycerol moiety. The occurrence of branched GDGTs is evidence for fluvial transport of terrestrial organic matter (Hopmans et al., 2004), which in our case is most likely related to activities of palaeo-rivers, such as palaeo-Don and palaeo-Kuban, transporting material from the Crimea and Caucasus mountains, adjacent valleys, and plateaus into the Black Sea.

### **5. Discussion**

Mud breccias represent a complex mixture of material from sedimentary units that were captured by vertically migrating fluid. Recovered mud breccia sections often show an alternation of lithologically different intervals representative of different mud flows. Recent studies of mud volcano deposits revealed that mud breccia rock-clasts possess valuable information on the composition and genesis of the deposits in the deep sedimentary succession, the sedimentary evolution of the area, its petroleum potential and information on potential source rocks (Akhmanov and Woodside, 1998; Ovsianikov et al., 2003; Kozlova et al., 2003, 2004). In contrast to the rock clasts, which are “direct” source indicators because each clast is derived from a specific sedimentary horizon, the mud breccia matrix represents an integrated signal from various sedimentary intervals. This also holds true for the organic matter including the biomarkers. Thus, depending on the sources of the mud, the biomarker distributions in one mud flow can differ from that of another mud flow, designating, therefore, different source strata for the erupted sediments. Often, mud breccias from neighboring MVs are lithologically distinctive, indicating their different origin. Since the roots of the MVs can originate from sediments more than 10 km deep (Shnukov et al., 2005), an assessment of the thermal maturity of the organic matter can be used to relate erupted mud breccias with deeper-lying horizons. We attempted to characterize source-strata for the erupted material from an evaluation of maturity properties and the composition of lipid biomarkers of individual mud breccia intervals.

## 5.1. Thermal maturity

Among the studied MVs, mud breccia from the Kazakov MV contains a suite of hopanes that can be used to examine the degree of thermal maturation from an examination of the degree of epimerization (Table 4). The 22S/(22S+22R) ratios for C<sub>31</sub>, C<sub>32</sub> and C<sub>33</sub>

**Table 4.** Maturity dependant hopane ratios.

interval, cm b.s.f.	Hopanes					
	C <sub>31</sub> 22S/(22S+22R)	C <sub>32</sub> 22S/(22S+22R)	C <sub>33</sub> 22S/(22S+22R)	C <sub>30</sub> $\beta\alpha/(\alpha\beta+\beta\alpha)$	C <sub>31</sub> $\beta\beta/(\beta\beta+\alpha\beta+\beta\alpha)$	C <sub>32</sub> $\beta\alpha/(\alpha\beta+\beta\alpha)$
0-10	0.19	0.46	0.65	0.29	0.05	0.21
10-20	0.68	0.47	0.67	0.29	0.18	0.21
30-40	0.67	0.40	0.75	0.34	0.13	0.20
40-50	0.67	0.40	0.70	0.36	0.16	0.19
50-60	0.74	0.41	0.56	0.32	0.14	0.20
79-91	0.68	0.44	0.66	0.32	0.13	0.22
119-120	0.73	0.48	0.57	0.28	0.13	0.20
160-166	0.78	0.47	0.51	0.29	0.08	0.15
Average	0.64	0.44	0.63	0.31	0.13	0.20

homohopanes show values of 0.64, 0.44, and 0.63, respectively (Table 4). These ratios are close to the thermodynamic equilibrium ratio (ca. 0.6; Seifert and Moldovan, 1980; van Duin et al., 1997), indicating a relatively mature state for the organic matter. The absence of both isoprenoidal and branched GDGTs in the mud breccia layers not affected by AOM (Figure 2) is in accordance with this maturity assessment; sediments with hopanoid ratios  $17\alpha,21\beta(H)$  [ $22S/(22S+22R)$ ]  $> 0.2$  and  $[\beta\beta/(\beta\beta+\alpha\beta+\beta\alpha)] < 0.2$  generally do not contain detectable amounts of GDGTs as revealed by artificial maturation experiments (Schouten et al., 2004). In addition, the general lack of polar lipids and the presence of steroid hydrocarbons is also evidence for a relatively high level of thermal maturity. The presence of small amounts of  $17\beta,21\beta(H)$ -homohopane and a  $\beta\beta/(\beta\beta+\alpha\beta+\beta\alpha)$  ratio for C<sub>31</sub>-homohopanes of ca. 0.13 throughout the interval (Table 4) may signify an admixture with immature sedimentary organic matter since  $17\beta,21\beta(H)$ -hopanes are usually not present when  $17\alpha,21\beta(H)$  hopane [ $22S/(22S+22R)$ ] ratios are close to the thermodynamic equilibrium value. An admixture with thermally immature components is also evident from the *n*-alkane distributions (Figure 3); the CPI values are relatively high (average 2.6; Table 2), which is somewhat unexpected and indicates an admixture with immature sediments containing high amounts of terrestrial *n*-alkanes. Consequently, the maturity parameters and lipid biomarker composition in the mud breccia matrix from the Kazakov MV suggests a mixture of (i) a moderately mature organic matter with (ii) immature constituents, typical for sediments that have not yet entered the oil window.

In contrast to the Kazakov MV, biomarker lipid compositions in the mud breccia from the NIOZ MV and Pleistocene/Holocene clays from the Odessa MV show in general

indications for relatively immature organic matter (Figures 2 and 5). The absence of hopanes and steranes and the presence of hopenes, extended polyfunctionalized hopanoids, hopanoic acids, hopanols, sterols, diols, keto-ols and both isoprenoidal and branched GDGTs all testify to the low degree of maturation of the organic matter. By contrast, the distribution of the *n*-alkanes (Figure 3), characterized by generally lower CPI values than observed for the Kazakov MV (Table 2), suggest more mature organic matter and can perhaps be explained by small amounts of petroleum in the emitted products. Again, this points to different sedimentary sources for the organic components contained in one mud breccia horizon from the NIOZ MV and in the Pleistocene/Holocene clays from the Odessa MV.

## *5.2. Origin of the organic matter from mud volcano deposits*

### *5.2.1. Kazakov MV*

Kazakov MV has the deepest roots of the three MVs investigated (see Geological Setting). This fits well with the biomarker data, showing variable, but generally, more mature organic matter characteristics in comparison with the mud breccia from the NIOZ MV and the sediments from the Odessa MV.

The mud breccia from the Kazakov MV does not contain a cover composed of pelagic sediments, indicating that it has been formed by a recent eruption event. The 166 cm of mud breccia sediments could represent one or several mud flows. Since the qualitative lipid composition (Figure 2) and investigated maturity parameters (Tables 2 and 4) remain the same in this mud breccia interval, the whole recovered mud breccia most likely represents a part of a single mud-flow event. Some variations in the concentrations are noted but these are most likely due to the inhomogeneity of the migrating fluid. This is in agreement with the finding that all sedimentary cores from the Kazakov MV showed lithologically similar mud breccias with very little or no hemipelagic coverage (Kenyon et al., 2002). Rock clasts from the Kazakov MV were mostly represented by various claystones from the MSF of Oligocene-Lower Miocene age (Ivanov et al., 1998; Kozlova et al., 2003). This implies that the organic matter in the mud breccia matrix from the Kazakov MV must also possess a signal from the MSF.

The development of the Sorokin Trough as well as other troughs in the Eastern Deep (Kerch-Taman, Indolo-Kuban, and Tuapse) took place during the Maycopian, as a result of tectonic subsidence of the eastern Black Sea basin (Tugalesov, 1985; Nikishin et al., 2003). The fast eustatic sea-level fall during the Upper Oligocene (Haq et al., 1987), and lowered base level of erosion resulted in a sharp activation of the palaeo-rivers at that time (Nedumov, 1994). This induced a substantial increase in the invasion of a large amount of terrigenous, mainly sandy material into the Maycopian basin (Nedumov, 1994). Table 1 shows that mud

breccia matrix from the Kazakov MV has an average TOC values of ca. 1.2 %, which is characteristic for the upper part of Maycopian Shales (Ulmishek, 2001), known to be deposited under an increased influx of terrestrial organic matter (Nedumov, 1994).

Pyrolysis data from the Maycopian mud breccia rock clasts showed a wide maturation range and a mixture of Type II and Type III kerogens (Kozlova, 2003). In the Sorokin Trough, these rocks are in most cases immature ( $T_{\max} = 415-435^{\circ}\text{C}$ ; Kozlova, 2003), although 25% of the rock samples was at the beginning of oil window ( $T_{\max} = 430-435^{\circ}\text{C}$ ; Kozlova, 2003). The presence of a thick sedimentary cover in the Sorokin Trough considerably reduces the heat flow. In addition, shales are known to have low heat conductivity which is probably the reason for a heat loss. A series of limited low ( $20-30 \text{ mW m}^{-2}$ ) heat flow anomalies were observed in zones of deep basement subduction in the offshore troughs, such as Sorokin and Tuapse (Kutas et al., 1998). However, in the eastern Black Sea, some local anomalies of high heat flow were distinguished (Kutas et al., 1998). Kutas et al. (1998) suggested that the amplitude of heat flow anomalies in the eastern basin slightly depends on the sediment thickness, testifying to lateral inhomogeneities in the thermal field and implying that sources of these anomalies are likely associated with young magmatic formations or fluid dynamics. This may explain why, despite the large thickness of the Maycopian and Pliocene-Quaternary deposits in the Sorokin Trough, the middle and upper parts of the Maycopian suite are relatively thermally immature. The presence of moderately mature organic matter with immature constituents is characteristic of the mud breccia matrix from the Kazakov MV. This allows us to attribute moderately mature biomarkers to the lower sections of the MSF. The dominance of 28,30-dinorhopane, generally considered as an indicator of anoxic depositional environments (Grantham et al., 1980; Katz and Elrod, 1983; Peters et al., 2005), could be also assigned to the lower parts of the Maycopian shales, which are thought to have accumulated in a deep anoxic marine basin (Ulmishek and Harrison, 1981; Kholodov and Nedumov, 1991; Popov and Stolyarov, 1997).

In summary, the biomarker composition and maturation properties of the mud breccia matrix indicate that the MSF is the largest contributing source for the mud breccia erupted from the Kazakov MV. Compared to the NIOZ and Odessa MVs, the deficit of immature biomarker signatures suggests a forceful mud eruption through the already formed conduit, perhaps predominantly from the lower parts of the MSF.

### *5.2.2. NIOZ MV*

Despite the fact that the NIOZ MV is located only several kilometers from the Kazakov MV, its development is quite different since it relates to a rising Maycopian diapir (Kenyon et al., 2002). This already indicates that the source of the erupted material is likely

much shallower than in case of the Kazakov MV. This is consistent with the presence of less-mature organic matter in the mud breccia from the NIOZ MV.

The mud breccia from the NIOZ MV is also characterized by the absence of a pelagic cover, indicating that it has been formed by a recent eruption event. However, qualitative and quantitative analyses of lipid composition revealed two principally different mud breccia layers. Based on the concentration profiles of *n*-alcohols, C<sub>30</sub> and C<sub>32</sub> mid-chain alkyl diols and keto-ols, hopanoids, steroids, and isoprenoidal GDGTs, the boundary between the two mud breccia intervals is located at ca. 45 cm below sea floor (Figure 2). At this level the concentration profiles of these components show a marked decrease or increase (Figure 2), indicating that the biomarker composition above and below this interval is so different that it unlikely to be explained by inhomogeneity of the mud breccia. This boundary is not apparent from the initial sedimentological description (Figure 2). This may indicate that the uppermost mud breccia interval consists of a mixture of sediments that were deposited in an environment characterized by a distinct algal productivity, the presence of hopanoid-producing bacteria, a palaeo-river freshwater discharge, and perhaps stratification of the water column. In contrast, the underlying mud breccia shows another source for the erupted material. Notably, the increase in concentration of terrestrial *n*-fatty acids and branched GDGTs within the second mud breccia unit points towards an enhanced terrestrial contribution to the organic matter, suggesting that the dominant source for this mud breccia unit is a terrigenous facies with a lower input of marine organic matter. These data suggest that as the fluid moved through the sedimentary units it acquired substantial terrestrial organic matter but hardly any of plankton and bacterial origin. Submarine river fan systems are known to be developed by the accumulation of terrestrial material carried during episodes of low sea level stand. Based on the lipid biomarker characteristics, it is difficult to ascribe the lower mud breccia interval to a specific stratigraphic unit. However, since the formation of the NIOZ MV is likely induced by the upward growth of the Maycopian diapir, which created overpressured sediments that consequently erupted at the seafloor surface, it is likely that erupted material at the seafloor could be derived from sediments, which are younger than the Maycopian deposits. It is known that the Middle-Upper Miocene complex overlying Maycopian sediments has a terrigenous origin (Nikishin et al., 2003). In addition, at the northeastern part of the Sorokin Trough, the slope is covered by Quaternary sediments of the palaeo-Don and palaeo-Kuban Rivers which are as thick as 2-2.5 km (Tugolesov et al., 1985). It follows that the lower mud breccia interval can possess a signal from terrigenous facies deposited due to paleo-river discharge. In fact, the closer the diapir reaches to the surface, the more recent would be the sediments that are extruded. Accordingly, the lowermost mud breccia interval from the NIOZ MV is likely to



be more related to the “older” terrigenous facies than the overlaying mud breccia interval, which possesses a biomarker signature of more recent, possibly Quaternary sediments.

### *5.2.3. Odessa MV*

The area where the Odessa MV is located is characterized by intensive continuous discharge of fluids through the seafloor (Ivanov et al., 1998; Kenyon et al., 2002; Mazzini et al., 2004; Stadnitskaia et al., 2005) and percolation of gas-saturated sediments *via* systems of open faults and fissures, developing vigorous flow of recent sediments downward the slope (Ivanov et al., 1998).

The lipid composition in the Odessa MV notably varies within the Pleistocene-Holocene clay interval, distinguishing their different origins. These changes coincide with the boundary between the Pleistocene and Holocene clay units (Figure 2). Isoprenoidal and branched GDGTs are present along the whole sedimentary section, signifying that organic matter in the sediments from the Odessa MV is derived from both terrestrial and marine sources. In general, the lipid biomarker composition and maturation parameters of the Pleistocene/Holocene clays from the Odessa MV are comparable to those of the mud breccia from the NIOZ MV. This is an indication that organic matter from both the NIOZ and Odessa MVs derived from similar sources.

### 6. Conclusions

Lipid biomarker analyses of mud breccia matrix and sediments from three MVs, the Kazakov, NIOZ, and Odessa, in the Sorokin Trough show that in spite of close location to each other, the Kazakov MV has different sources compared to the NIOZ and Odessa MVs. The data indicate different subsurface-sedimentary depths of defluidization, which are directly linked to the location of fracture zones or diapiric folds formed due to tectonic compression in the area. The mud breccia of the Kazakov MV shows biomarker characteristics of relatively mature organic matter related to the Maycopian Shales, signifying that Maycopian sediments are weakened in this location, enabling fluid discharge through. In contrast, the mud breccias from the NIOZ MV and the sediments from the Odessa MV contain immature organic matter derived from more recent sediments. However, the presence of petroleum-derived compounds in the organic matter of both the NIOZ and Odessa MVs implies that the migrated fluid is partially derived from the deep subsurface, perhaps from the lower part of the MSF or more probably below this sedimentary unit.

The biomarker study also revealed two mud eruption episodes within a single sedimentary sequence from the NIOZ MV. These two mud breccia intervals possess peculiar signatures from unrelated sedimentary facies. The lowermost mud breccia unit is likely related to the “old” terrigenous facies whereas the upper mud breccia interval displays the signature of more recent, probably Quaternary sediments similar to that from the Pleistocene/Holocene clays of the Odessa MVs.

The combination of TOC data with distributions, concentration profiles, and maturation properties of biomarkers can be used as a tool for distinguishing different mud breccia/sedimentary intervals even with similar lithological characteristics and complex sedimentary mixtures. Despite the fact that mud breccia is a complex mixture of different sedimentary facies, a collective biomarker signal from the same mud breccia interval can possess characteristic signatures of those sedimentary sections which contributed most to the migrated fluid.



### **BIOMARKER AND 16S RDNA EVIDENCE FOR ANAEROBIC OXIDATION OF METHANE AND RELATED CARBONATE PRECIPITATION IN DEEP-SEA MUD VOLCANOES OF THE SOROKIN TROUGH, BLACK SEA**

A. Stadnitskaia<sup>a,b</sup>, G. Muyzer<sup>a,c</sup>, B. Abbas<sup>a</sup>, M.J.L. Coolen<sup>a</sup>, E.C. Hopmans<sup>a</sup>, M. Baas<sup>a</sup>, T.C.E. van Weering<sup>a</sup>, M.K. Ivanov<sup>b</sup>, E. Poludetkina<sup>b</sup> and J.S. Sinninghe Damsté<sup>a</sup>

<sup>a</sup>Royal Netherlands Institute for Sea Research (NIOZ), P.O. Box 59, 1790 AB Den Burg, Texel, The Netherlands.

<sup>b</sup>Geological Faculty, UNESCO-MSU Centre for Marine Geosciences, Moscow State University, Vorobjevy Gory, Moscow 119899, Russian Federation.

<sup>c</sup>Department of Biotechnology, Delft University of Technology, Julianalaan 67, 2628 BC Delft, the Netherlands.

Published in *Marine Geology*, 217, 67-96 (2005)

#### **Abstract**

Many mud volcanoes (MVs) were recently discovered in the euxinic bottom waters of the Sorokin Trough (NE Black Sea). Three of them, i.e., NIOZ, Odessa, and Kazakov, were selected for a detailed biogeochemical investigation. Four methane-related carbonate crusts covered with microbial mats, and sediments ('mud breccia') from these MVs were collected during the 11<sup>th</sup> Training-Through-Research cruise (TTR-11) in 2001, the first finding of methanotrophic microbial mats associated with authigenic carbonates in the deep Black Sea. We measured the concentrations and  $\delta^{13}\text{C}$  values of methane and specific archaeal and bacterial lipids, and determined archaeal and bacterial 16S rRNA gene sequences. The  $\delta^{13}\text{C}$  of the microbial lipids reflected the carbon isotopic values of the methane, indicating that methane was the main carbon source for micro-organisms inducing carbonate formation. Anaerobic oxidation of methane (AOM) in these settings was performed by archaea affiliated with the so-called ANME-1 group. None of the identified archaeal sequences were closely related to known methanogens. The combined 16S rRNA gene sequence and biomarker data revealed a distinct difference in archaeal assemblage between the carbonate crusts and mud breccias. Besides gene sequences of sulfate reducing bacteria (SRB), DNA analysis of bacterial communities revealed a diversity of bacteria with apparent contrasting metabolic properties. The methane utilization via AOM processes was detected in the uppermost sediments where it subsequently induces authigenic carbonate precipitation most probably below seafloor. The results of integrated biomarker and 16S rRNA gene study reveal a crucial role of AOM processes in formation of authigenic carbonates in methane-seep environments.

*Keywords:* Black Sea, mud volcanoes, AOM, carbonates, lipids, 16S rRNA.

## 1. Introduction

Mud volcanoes (MVs) represent locations at which subsurface fluids escape from the subsurface through the seafloor. They develop as a result of a strong lateral or vertical compressions, which allow deep-lying sediments to move upward and over the sea floor. MVs can be expressed as mounds, extending up to 100 m above the seabed with diameters of a few kilometers or as negative collapse structures, caused by catastrophic eruption of fluids, especially hydrocarbon gases (predominantly methane), hydrogen sulfide, carbon dioxide, and petroleum products (Ivanov et al., 1998). Generally, fluids (composed of gases, pore water, and sediment) still migrate upwards after the initial eruption. These results in the development of highly diverse and productive ecosystems based on chemosynthesis below and/or at the sea floor. One of the most important biogeochemical processes fuelling these communities at these locations is the anaerobic oxidation of methane (AOM).

Comprehensive biogeochemical, structural, and stable isotope analysis of lipids (Schouten et al., 1998; Thiel et al., 1999, 2001; Hinrichs et al., 1999, 2000a; 2000b; Pancost et al., 2000, 2001a, 2001b; Zhang et al., 2002, 2003) and molecular ecological studies (Boetius et al., 2000; Orphan et al., 2001a, 2001b; Teske et al., 2002; Michaelis et al., 2002) revealed that AOM is generally performed by syntrophic consortia of methanogenic archaea operating in reverse and the sulfate-reducing bacteria (SRB) (Hoehler et al., 1994; Hoehler and Alperin, 1996; Valentine and Reeburg, 2000). It is hypothesized that the use of hydrogen as an electron donor by the SRB results in low partial pressure of H<sub>2</sub>, creating thermodynamically favorable conditions for methanogenic archaea to act as methane-oxidizers (Reeburg, 1976; Zender and Brock, 1979; Alperin and Reeburg, 1985; Hoehler et al., 1994; Hoehler and Alperin, 1996). Phylogenetic analyses of ribosomal RNA (rRNA) gene sequences have revealed two distinct lineages among the *Euryarchaeota* capable of anaerobic methanotrophy: the ANME-1 cluster, which does not contain any cultured relatives (Hinrichs et al., 1999), and the ANME-2 cluster affiliated to the cultured members of the *Methanosarcinales* (Boetius et al., 2000; Orphan et al., 2001a, 2001b). The indication of anaerobic methanotrophy was first demonstrated by compound-specific carbon isotopic study of archaeal lipids: their distinctively depleted  $\delta^{13}\text{C}$  signals indicate that archaea are able to use methane as a carbon source (Hinrichs et al., 1999; Elvert et al., 2000; Hinrichs et al., 2000b; Pancost et al., 2000; Thiel et al., 1999, 2001; Pancost et al., 2001a, 2001b; Aloisi et al., 2002; Teske et al., 2002; Zhang et al., 2002, 2003; Schouten et al., 2003). <sup>13</sup>C-depleted lipids of SRB also indicate their involvement in the AOM process. Collectively, these results indicate a close metabolic association between SRB and methanotrophic archaea (Pancost et al., 2000, 2001b). Conclusive evidence for the co-existence of archaea and SRB, i.e. AOM-consortia was obtained by fluorescence in situ hybridization (FISH) (Boetius et al., 2000; Michaelis et al., 2002) and secondary ion mass spectrometry (SIMS) analyses of individual cell aggregates

(Orphan et al., 2001a). Various studies have also revealed a large variety in distribution and composition of archaea/SRB microbial biomass in gas-venting settings (Boetius et al., 2000; Orphan, 2001a; Pancost et al., 2001a; Michaelis, 2002). For example, sulfate-reducing bacteria affiliated to members of the genera *Desulfosarcina* and *Desulfococcus* have been found in association with ANME-1 and ANME-2 archaeal cells, representing in both cases putative methanotrophic consortia (Boetius et al., 2000; Orphan et al., 2001a, 2001b; Michaelis et al., 2002). An independent *Methanosarcinales*-related ANME-2 lineage composed of bacteria-free archaeal cells has been also reported (Orphan, 2001a).

In spite of the diversity of microbes involved in AOM, the associated or AOM-induced “end-products” are similar in most cases. For example, the co-occurrence of neoformed diagenetic carbonates is a widespread phenomenon in cold-seep settings (Ritger et al., 1987; Roberts and Aharon, 1994; Von Rad et al., 1996; Peckmann et al., 1999a, 1999b, 2001; Aloisi et al., 2000, 2002; Michaelis et al., 2002). These authigenic carbonates exhibit a broad range of morphologies, mineralogy, and stable carbon and oxygen isotopic compositions (Hovland et al., 1987; Roberts and Aharon, 1994; Peckmann et al., 1999a, 1999b, 2001, 2002; Stakes et al., 1999; Aloisi et al., 2000, 2002). Chemical analyses showed that these carbonates are depleted in  $^{13}\text{C}$  which led to the suggestion that carbon in such carbonates is derived from methane (Peckmann et al., 1999a, 1999b, 2001, 2002; Stakes et al., 1999; Aloisi et al., 2000, 2002). It was proposed that the precipitation of authigenic methane-derived bicarbonate is the result of increased alkalinity created by AOM (Ritger et al., 1987; Von Rad et al., 1996; Thiel et al., 1999), i.e. AOM serves as a source of inorganic carbon for the formation of carbonate cement, concretions, crusts, and other carbonate build-ups, which are known in the geological record from the Middle Devonian (Peckmann et al., 1999b). However, only the recent finding of living methanotrophic mats associated with carbonate build-ups in the Black Sea (Michaelis, et al., 2002) directly proved that anaerobic microbial consortia performing AOM indeed induce carbonate precipitation in methane-seepage environments.

Here we report the results of a lipid biomarker study integrated with a survey of 16S rRNA gene sequences to characterize microbial communities in four methane-related carbonate crusts covered by microbial mats and mud volcanic deposits (mud breccia matrix) in an environment where oxygen cannot play a role in the oxidation of methane. Molecular signatures, such as lipids and nucleic acid sequences, have been used in this study as tools to identify the specific microorganisms involved in AOM and revealed microbial ecological relationships, and their metabolic potential, in the context of the specific environments created by migrated fluids. Samples were collected from three MVs at the anoxic seafloor of the Sorokin Trough (NE Black Sea) during the 11<sup>th</sup> Training-Through-Research expedition (TTR-

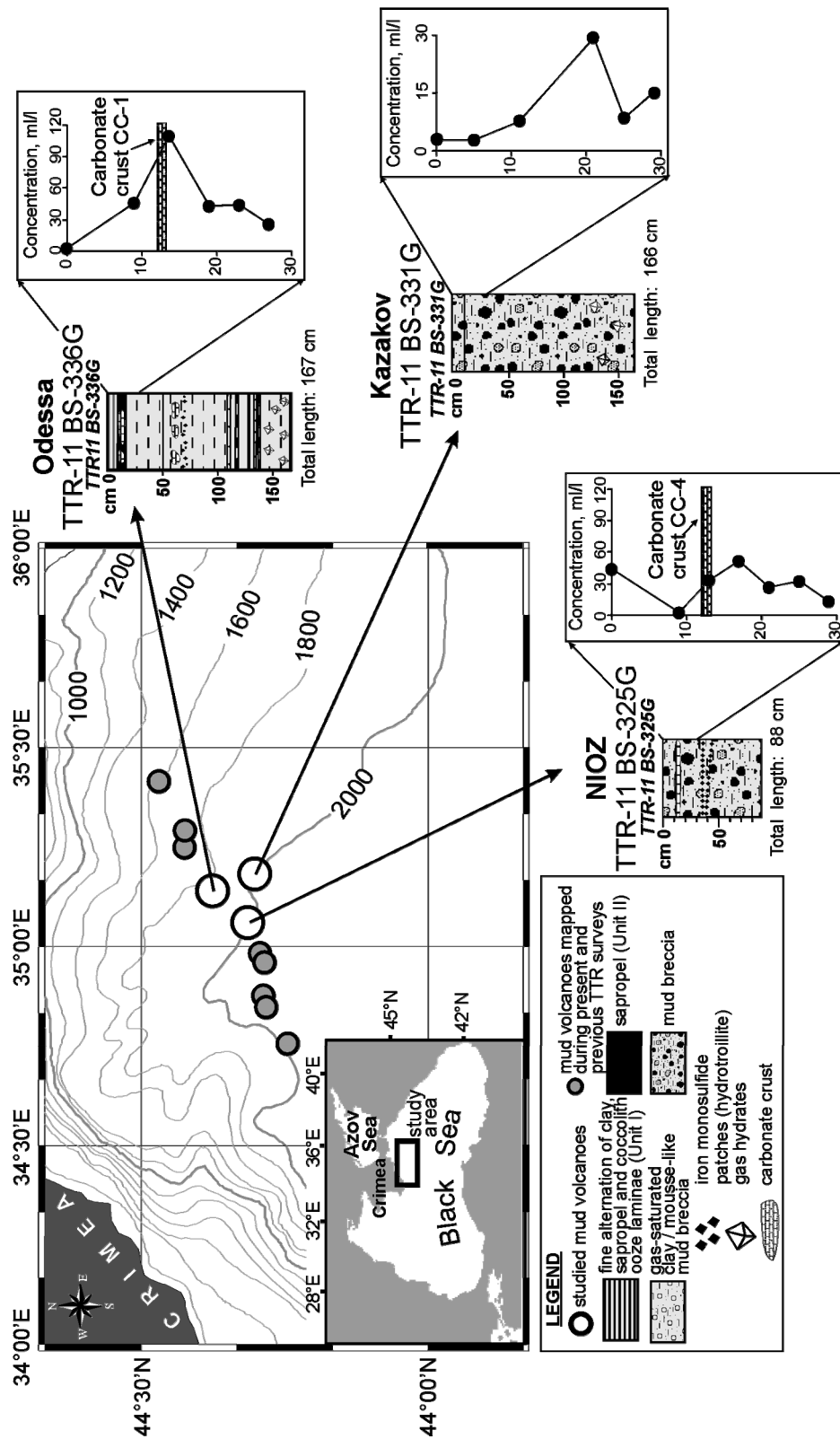


Figure 1. Location of studied mud volcanoes on the Sorokin Trough of the Black Sea and the sediment cores obtained with schematic lithology. The insets show methane concentration profiles measured in the uppermost 30 cm for the studied cores.

11) in 2001 (Kenyon et al., 2002). This is the first finding of methanotrophic microbial mats associated with carbonates in the deep (ca. 2000 m) Black Sea.

## 2. Materials and methods

### 2.1. Samples

On the basis of comprehensive geophysical surveys carried out during the TTR-6 cruise performed in 1996, and the TTR-11 cruise in 2001, a considerable number of MVs were discovered in the Sorokin Trough (Ivanov et al., 1996; Woodside et al., 1997; Ivanov et al., 1998; Bouriak and Akhmetzhnov, 1998; Kenyon et al., 2002). Three of them, i.e., NIOZ (44°19'N; 35°04'E, water depth of ca. 2020 m), Odessa (44°23'N; 35°09'E, water depth of ca. 1830 m) and Kazakov (44°18'N; 35°11'E, water depth of ca. 1920 m), were chosen for a detailed geochemical investigation (Figure 1). These MVs are characterized by a set of characteristic features such as mound morphology (Woodside et al., 1997; Ivanov et al., 1998), composition and sources of hydrocarbon gases (Ivanov et al., 1998), and the occurrence of cold seep-associated features, such as gas hydrates, authigenic carbonates of various types and morphology, and the presence of microbial mats (Ivanov et al., 1998; Bouriak and Akhmetzhanov, 1998; Kenyon et al., 2002).

**Table 1.** General information of samples studied.

Sample ID	Mud volcano	Sampling site	Latitude	Longitude	Water depth (m)	Interval (cm, b.s.f)
<b>Carbonate crusts with microbial mats</b>						
CC-1	Odessa	TTR-11 BS-336G	44°23'	35°09'	1816	12-13
CC-2	NIOZ	TTR-11 BS-328G	44°19'	35°04'	2020	Seafloor surface
CC-3		TTR-11 BS-325G	44°19'	35°04'	2015	12-14
CC-4						
<b>Mud breccia</b>						
MB1A	Kazakov	TTR-11 BS-331G	44°18'	35°11'	1918	2-4
MB1B						8-10
MB1C						20-22
MB2A	NIOZ	TTR-11 BS-325G	44°19'	35°04'	2015	8-12 (above CC-4)
MB2B						16-20 (below CC-4)

Bottom sampling was performed according to standard TTR-procedures (Ivanov et al., 1992). All samples were taken using a 6 m long, 1500 kg gravity corer with an internal diameter of 14.7 cm. Sediments, carbonate crusts, and microbial mats were described, photographed and stored at -20°C until further geochemical and molecular biological analyses were performed.



A carbonate crust, CC-1, was collected from sampling site TTR-11, BS-336G located on the crater of the Odessa MV. The crust appeared at the boundary of the sapropel layer (Unit 2) (Degens and Ross, 1972) and the mud breccia interval (12-13 cm). It is a porous well-cemented precipitate with its lower surface covered by a pink microbial mat (Figure 2a). The same type of biofilm also filled the cavities and pores within the crust.

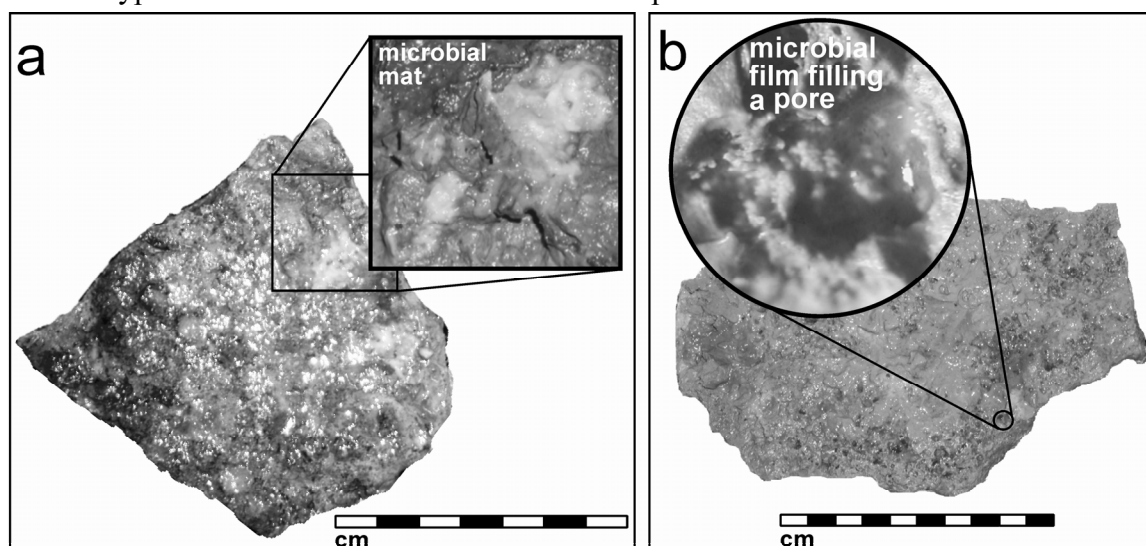


**Figure 2.** Two main types of investigated carbonate crusts and microbial mats. a) the Odessa mud volcano, sampling site TTR-11 BS-336G. The inset assigns the location of the microbial mat. b) the NIOZ mud volcano, sampling site TTR-11 BS-328G. The inset is a binocular image with typical appearance of microbial films within pores and interstices. See page 200 for color figure.

Three carbonate crusts were collected from the crater of the NIOZ MV. Two flat, well-cemented carbonate crusts, CC-2 and CC-3, were found at sampling site TTR-11, BS-328G located on the northern edge of the crater. No sediment was recovered from the site since the core catcher was blocked by the carbonates. These crusts are parts of prolonged carbonate pavements forming a positive seafloor relief. Both of them contained brown, semi-transparent gel-like microbial mats that filled the pores and interstices on the surfaces and within the crusts (Figure 2b). Carbonate crust CC-4 from core TTR-11, BS-325G formed a thin, well-cemented layer, which was confined to the mud breccia at a sub-seabed interval depth of 12-14 cm (Figure 1). Occasional microbial mats similar to these found on the CC-2 and CC-3 crusts were clearly visible within the inner pores of the precipitate. This sampling site was located ca. 500 m to the south from the TTR-11 BS-328G, in the central part of the crater of the NIOZ MV.

All studied carbonate crusts were associated with microbial mats. Therefore, the reader has to be aware that their molecular signatures principally indicate living microbial

communities within these methane-related carbonate crusts. For reasons of conciseness, we decided to name our carbonate/mat samples as CC-1, CC-2, CC-3, CC-4, using predominantly in the text the word “carbonate” rather than “a microbial mat associated with a carbonate” or “carbonate with microbial mat”.

Sediments from the Kazakov MV (TTR-11 BS-331G) were collected from the eastern edge of the crater. They are represented by gas saturated mud breccia containing variety of rock clasts of different lithology and roundness. Drop-sized gas hydrates were found at the base of the core.

### *2.2. Gas measurements*

Hydrocarbon gases were sampled using head-space methods, adapted for shipboard conditions (Bolshakov and Egorov, 1987). The gas phase was transferred into sterile glass jars filled with saturated NaCl solution and stored at  $-5^{\circ}\text{C}$ . A gas chromatograph with a flame-ionization detector was used for quantification of methane.

The results of methane concentration were calculated according to the volume of wet sediment from which gases were extracted. It worth to be noted that in spite of the absolute notations for the methane, significant part of the hydrocarbon had been lost due to active degassing of the recovered sediments. However, in order to see the trend of methane distribution profiles and to show rough level of methane saturation even with its relatively high loss, it was decided to present methane data in ml/l of wet sediments

The stable carbon isotopic composition of methane was measured on a Finnigan Delta S mass spectrometer with a HP 5890 GC and a GC-Combustion interface. Methane was separated on a molsieve 5Å plot column using split- or splitless injection, depending on the concentrations. Results are reported using the delta ( $\delta$ ) notation in per mil (‰), with respect to the Vienna Pee Dee Belemnite (PDB) standard.

### *2.3. Lipid extraction and separation*

About 100-120 g of each carbonate crust and ca. 50 g of each mud breccia sample were freeze-dried, crushed to a fine powder, and extracted with an automatic Accelerated Solvent Extractor (ASE 200/DIONEX) using a solvent mixture dichloromethane (DCM): methanol (MeOH) (9:1, v/v) at 1000 psi and  $100^{\circ}\text{C}$  PT conditions. Elemental sulfur was removed from the total extract by elution over a small pipette filled with activated copper. An aliquot of the total extract was chromatographically separated into apolar and polar fractions using a column with activated (2 h at  $150^{\circ}\text{C}$ )  $\text{Al}_2\text{O}_3$  as stationary phase. Apolar compounds were eluted using hexane:DCM (9:1, v/v), and polar compounds, including glycerol ether core membrane lipids, were obtained with MeOH:DCM (1:1, v/v) as eluent. Alcohols were

transformed into trimethylsilyl-derivatives by addition of 25  $\mu\text{l}$  of pyridine and 25  $\mu\text{l}$  of BSTFA and heating at 60°C for 20 min.

In order to remove saturated normal hydrocarbons and to enrich branched/cyclic compounds, the apolar fraction was filtered over silicalite using cyclohexane as an eluent.

To check for the presence of bacteriohopanepolyol derivatives, fresh extracts of mud breccia from the NIOZ MV were treated with periodic acid and sodium borohydrite according to Rohmer et al. (1984).

#### *2.4. Analysis and identification of biomarkers*

Gas chromatography (GC) was performed using a Hewlett Packard 6890 gas chromatograph equipped with an on-column injector and a flame ionization detector. A fused silica capillary column (CP Sil5 25 m x 0.32 mm,  $d_f = 0.12 \mu\text{m}$ ) with helium as a carrier gas was used. The samples were injected at 70°C. The GC oven temperature was subsequently raised to 130°C at a rate of 20°C/min, and to 320°C at 4°C/min. The temperature was then held constant for 15 min.

All fractions were analyzed by gas chromatography-mass spectrometry (GC-MS) for compound identification. The structural designation of lipids was evaluated by the comparison of their mass spectral fragmentation patterns and Pseudo Kovats retention indices with reported data. GC-MS was conducted using a Hewlett Packard 5890 gas chromatograph interfaced to a VG Autospec Ultima Q mass spectrometer operated at 70 eV with a mass range of  $m/z$  50-800 and a cycle time of 1.8 s (resolution 1000). The gas chromatograph was equipped with a fused silica capillary column (CPSil5 25 m x 0.32 mm,  $d_f = 0.12 \mu\text{m}$ ) and helium as a carrier gas. The temperature program used for GC-MS was the same as for GC.

#### *2.5. Isotope-ratio-monitoring gas chromatography-mass spectrometry (IRM-GC-MS)*

IRM-GC-MS was performed on a Finnigan MAT DELTA <sup>plus</sup> XL instrument used for determining compound-specific  $\delta^{13}\text{C}$  values. The GC used was a Hewlett Packard 6890A series and the same analytical conditions were used as described for GC and GC-MS. With the purpose to achieve better separation and more accurate  $\delta^{13}\text{C}$  values for the cluster of pentamethylcosenes (PMIs), the silicalite non-adducted hydrocarbon fractions isolated from carbonates CC-1 and CC-4 were also analyzed using DB-1MS 60 m x 0.25 mm with  $d_f = 0.25 \mu\text{m}$  capillary column. Samples were injected at 70°C followed by increasing the temperature to 140°C at a rate of 25°C/min, and to 320°C at a rate of 3°C/min. The temperature was then held constant for 20 min. For carbon isotopic correction of the added trimethylsilyl groups, the carbon isotopic composition of the used BSTFA was determined ( $-49.30 \pm 0.5 \text{‰}$ ). Obtained values are reported in ‰ relative to the VPDB standard, and have been corrected for

the addition of Si(CH<sub>3</sub>)<sub>3</sub> group due to the derivatisation procedure. In order to monitor the accuracy of the measurements, the analyses were carried out with co-injection of two standards, C<sub>20</sub> and C<sub>24</sub> *n*-alkanes, which have known carbon isotopic composition.

#### 2.6. High performance liquid chromatography-mass spectrometry (HPLC-MS)

To determine the distribution and composition of intact glycerol dialkyl glycerol tetraethers (GDGTs), carbonate crust and mud breccia samples were analyzed using a HPLC-MS method for their direct analysis (Hopmans, et al. 2000).

#### 2.7. DNA extraction

Table 1 summarizes general details on samples analyzed using molecular biological techniques. Samples of carbonate crusts and sediments were directly stored at -20°C after collection, and at -80°C after return to home institute. Genomic DNA was extracted from about 1 g of sample using the UltraClean Soil DNA Isolation Kit (MoBio, Carlsbad, USA). The quality and quantity of the extracted DNA was checked by standard agarose gel electrophoresis. To reverse sequence of primer Parch519r published by Øvreas et al. (1997) and ARC915r (E.coli positions 915-934; Stahl et al., 1988). The stability of the archaeal 16S rRNA gene fragments in the DGGE was obtained by attaching a 40-bp long GC-clamp (5'-CGC CCG CCG CGC CCC GCG CCC GGC CCG CCG CCC CCG CCC C-3' [Schaefer and Muyzer, 2001]) to the 5'-end of the ARC915r primer (Coolen et al., 2004). PCR conditions included an initial denaturation step of 4 min at 96°C, followed by 35 cycles including a denaturation step for 30 s at 94°C, a primer annealing step for 40 s at 57°C, and a primer extension step for 40 s at 72°C. A final extension was performed for 10 min at 72°C. Partial bacterial 16S rRNA genes were amplified using primers 341f [E.coli positions 341-357; 5'-CCT ACG GGA GGC AGC AG-3' (Muyzer et al., 1993) including the 40-bp GC-clamp and 907r [E.coli positions 907-926; 5'-CCG TCA ATT CCT TTR AGT TT-3' (Lane, 1991)]. PCR conditions were comparable to those described for the amplification of archaeal 16S rRNA genes, except that 32 cycles were applied. The fragment lengths of the archaeal and bacterial PCR products including the 40-bp long GC-clamp were 436 bp and 606 bp, respectively.

All PCR amplifications were performed with a Geneamp PCR System 2400 (Perkin-Elmer) using a mixture of the following components: 5 µl of 10X PCR-buffer (100 mM Tris-HCl [pH 9.0], 15 mM MgCl<sub>2</sub>, 500 mM KCl [Pharmacia Biotechnology, Upsalla, Sweden]), 10 mM of dNTP's, 0.5 µM of each archaeal (Parch-519f, ARC-915r+GC-clamp) and bacterial (341f+GC-clamp, 907r) primers, 20 µg of bovine serum albumine, and 1 unit of Taq DNA polymerase (Pharmacia). Between 2 and 5 ng of template DNA from each carbonate crust, and up to 20 ng from each sediment sample was subjected to PCR. The final volume of the

mixture was adjusted to 50 µl with molecular-grade water (Sigma, Saint Louis, Missouri USA).

### *2.9. DGGE analysis of 16S rRNA genes*

All PCR-products were analyzed by DGGE (Schaefer and Muyzer, 2001), carried out in a Bio-Rad D Gene system (Biorad, München, Germany). PCR samples were applied directly onto 6% (wt/vol) polyacrylamide gels (acrylamide/N,N'-methylene bisacrylamide ratio, 37:1 [w/w]) in 1 x TAE buffer (pH 7.4), which had been prepared from sterile solutions and casted between sterilised glass plates. The gels contained a linear gradient of denaturant from 20-70% (100% denaturant is 7 M urea plus 40% [v/v] formamide). Electrophoresis proceeded for 15 h at 100 V and 60°C. Afterwards, gels were stained for 30 min in sterile double-distilled water containing ethidium bromide, destained for 60 min in sterile double-distilled water, and photographed. DGGE-fragments were excised from the gel with a sterile scalpel and rinsed with molecular-grade water (Sigma, Saint Louis, Missouri USA). The DNA of each fragment was eluted in sterile 10 mM Tris-HCl (pH 8.0) by incubation for 24 h at 2°C and served as template DNA for re-amplification. PCR conditions for re-amplification of PCR bands included an initial denaturation step of 4 min at 96°C, followed by 30 cycles for 40 s at 57°C, and a primer extension step for 40 s at 72°C. A final extension was performed for 10 min at 72°C. Primers without GC-clams were used.

### *2.10. Sequencing of DGGE bands*

Prior to the sequencing reactions, primers were enzymatically removed from the reamplified DGGE-bands using the ExoSAP-IT™ kit (Amersham Bioscience, Roosendaal, the Netherlands) following the descriptions of the manufacturer. Cycle sequencing reactions were performed with the ABI Prism Big Dye Terminator V3.0 kit (Applied Biosystems, Ca. USA) using the forward or reverse primer (without GC clamp) at a final concentration of 0.2 µM, and 10 ng of template DNA. The reaction volume was adjusted to a volume of 20 µl with molecular grade water (Sigma). The following reaction conditions were employed: 1 sec. initial denaturing at 96°C, followed by 25 cycles of 10 s at 96°C, 5 s at 45°C, and 4 min at 60°C. Nucleotide positions were determined using an automated ABI-310 capillary sequencer (Applied Biosystems). Complementary sequences were aligned and manually edited using the AutoAssembler software package (Version 2.1.1; Applied Biosystems).

### *2.11. Comparative analysis of 16S rRNA gene sequences*

The partial sequences were analyzed using BLAST in the NCBI database (<http://ncbi.nlm.nih.gov/BLAST>) and added together with the most important BLAST hits, to an alignment of about 1400 homologous bacterial 16S rRNA gene sequences by using the

aligning tool of the ARB software package. Trees were generated by neighbor-joining, with the correction method of Felsenstein as implemented in ARB. Bootstrap analysis (1000 replicates) was performed in PAUP version 4. Names of the sequences consisted of the prefix DGGE, indicating that the sequences were obtained from excised DGGE bands with ARC for Archaea, BAC for Bacteria, and the number of the excised band. The numbers used in the DGGE are the same as those used in the trees. The accession numbers for the archaeal and bacterial sequences are AY847616 to AY847624 and AY847598 to AY847615, respectively.

### 3. Results and discussion

#### 3.1. Methane

Cold seeps, especially actively degassing MVs, are focal sources of fluids containing methane. The occurrence of gas and its migration through the sediments have been recognized in seismic recordings of the Sorokin Trough in many ways (Ivanov et al., 1998; Bouriak and Akhmetzhanov, 1998). Gas measurements revealed that the main gas components in the area are hydrocarbons, nitrogen, and carbon dioxide, with methane being the most abundant (Ivanov et al., 1998). Hydrocarbon gases from the NIOZ and Odessa MVs are mainly composed of methane (99.1%-99.9% of total hydrocarbon gases). The average carbon isotopic composition of methane is ca. -63‰ at the NIOZ MV and -68‰ at the Odessa MV, indicating the biogenic origin of methane (Rice and Claypool, 1981) at these sites. The abundance of methane in the sediments of the Kazakov MV is ca. 95% of the total hydrocarbon gases and the average  $\delta^{13}\text{C}_{\text{CH}_4}$  value is -56‰. These results indicate a thermogenic contribution to the methane at the Kazakov MV.

The methane distribution in the Kazakov MV displayed the characteristic concave-up-curve at a depth interval of ca. 10-13 cm below sea floor (bsf) (Figure 1), which is consistent with anaerobic methane consumption (Martens and Berner, 1974; Barnes and Goldberg, 1976; Reeburgh, 1976; Alperin and Reeburgh, 1984; Valentine and Reeburgh, 2000). In contrast, methane profiles in the NIOZ and Odessa MVs showed an irregular pattern. Maximum methane concentrations occurred in both settings just below the methane-related authigenic carbonate crust layers (Figure 1). These carbonate crusts were characterized by depleted  $\delta^{13}\text{C}$  values ( $\sim -40\text{‰}$ ), indicating their origin, at least in part, from carbon dioxide produced by AOM (Kovalenko and Belenkaia, 2002; Mazzini et al., 2002).

#### 3.2. Archaeal and bacterial lipid variability

Lipid analysis of the carbonate crusts associated with microbial mats (C1, C2, C3, and C4) and the mud breccias matrix revealed a quite diverse set of biomarkers diagnostic for different archaea and bacteria. A remarkable difference in the molecular composition and

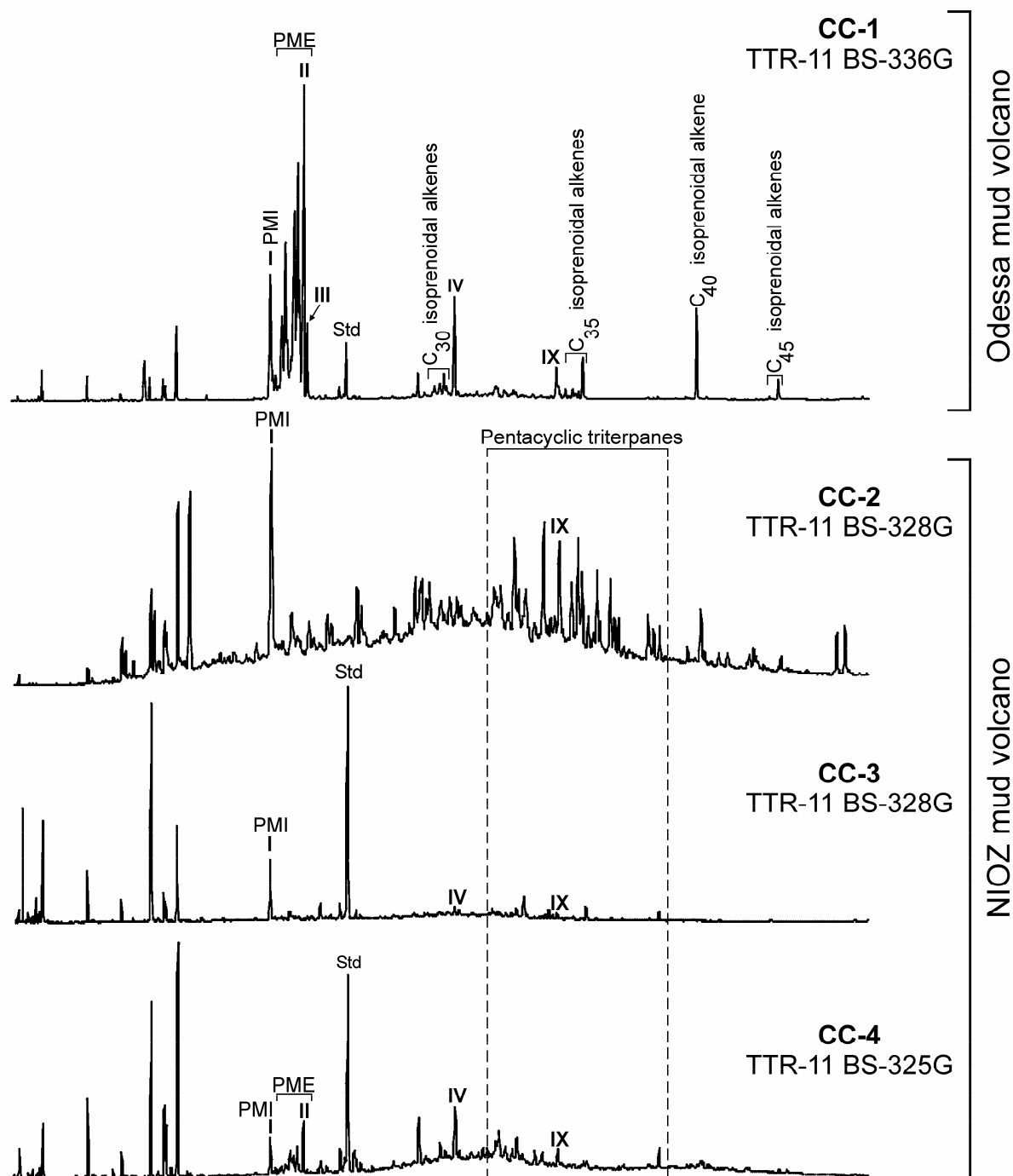


**Figure 3.** Total ion current traces of the silicalite non-adduct (branched and cyclic hydrocarbons of the apolar fraction) of the four carbonate crusts. Roman numbers refer to structures shown in the Appendix.

### 3.2.1. Irregular acyclic isoprenoids

The acyclic isoprenoids in all crusts are dominated by the irregular, tail-to-tail linked C<sub>25</sub> isoprenoid, 2,6,10,15,19-pentamethylcosane (PMI; I, see Appendix for structures) and its unsaturated counterparts (Figures. 3 and 4). PMI is considered to be a specific biomarker for methanogenic Archaea and has been detected in cultures of methanogens, such as *Methanobacterium thermoautotrophicum* and *Methanosarcina barkeri* (Holzer et al., 1979), *Methanosarcina mazei*, and *Methanlobus bombayensis* (Schouten et al., 1997). PMI has also been frequently encountered in marine settings with a high rate of methanogenesis or AOM (Wakeham, 1990; Kohnen et al., 1992; Pancost et al., 2000; Elvert et al., 2000; Thiel et al., 2001). Mono-, di- and polyunsaturated pentamethylcosenes (PMEs) possessing up to five double bonds are also abundant biomarkers in some crusts (Figures. 3 and 4). PME<sub>s</sub> have been identified in the methanogenic archaea *M. mazei*, *M. barkeri* and *M. bombayensis* (Holzer et al., 1979; Tornabene et al., 1979; Schouten et al., 1997; Sinninghe Damsté et al., 1997). Carbon-isotope depleted, PME<sub>s</sub> have also been found in cold-vent sediments, and their origin has been ascribed to archaea involved in AOM (Elvert et al., 1999; Pancost et al., 2000, 2001; Thiel et al., 2001). The distribution of PME<sub>s</sub> in carbonates CC-1 and CC-4 is similar to that reported for the Eastern Mediterranean cold seep sediments (Pancost et al., 2001). They are particularly abundant in crust CC-1, comprising ca. 26 % from the total identified apolar compounds. Crust CC-4 is characterized by less abundant PME<sub>s</sub>, but their composition is similar to that observed in the CC-1 (Figure 4). In both carbonates the most abundant PME is 2,6,10,15,19-pentamethylcosa-2,6,14,18-tetraene (Pseudo Kovats index (CP Sil 5), 2337, II), occurring in the methanogenic archaeon *Methanosarcina mazei* (Schouten et al., 1997; Sinninghe Damsté et al., 1997). The PME with 5 double bonds, pentamethylcosa-2,6,10,14,18-pentaene (Pseudo Kovats index (CP Sil 5), 2346, III), which was previously found in cultures of *M. mazei* and *M. bombayensis* (Schouten et al., 1997; Sinninghe Damsté et al., 1997), was also identified in crusts CC-1 and CC-4. In carbonates CC-2 and CC-3 PMI is abundant but PME<sub>s</sub> are almost absent (Figure 4). The carbon isotopic compositions of PMI range from -101‰ in the crust CC-1 to -89‰ in the crust CC-2 (Table 2). The δ<sup>13</sup>C values of PME<sub>s</sub> in all crusts are quite similar to that of PMI (Table 2). Their depleted δ-values indicate that these compounds are derived from archaea involved in AOM.

In the mud breccias, PMI and PME<sub>s</sub> were only found in the Kazakov MV. In this MV, a mixture of PMI and PME<sub>s</sub> appeared in the uppermost 10 cm of the sediments. Down-core at depth of 20 cm, only PMI and PME (III) were identified. The concentrations of these hydrocarbons decrease with depth and this drop is accompanied with its <sup>13</sup>C enrichment. In the uppermost sediments δ<sup>13</sup>C of PMI is -81‰, while at 20 cm depth δ<sup>13</sup>C values of ca. -71‰



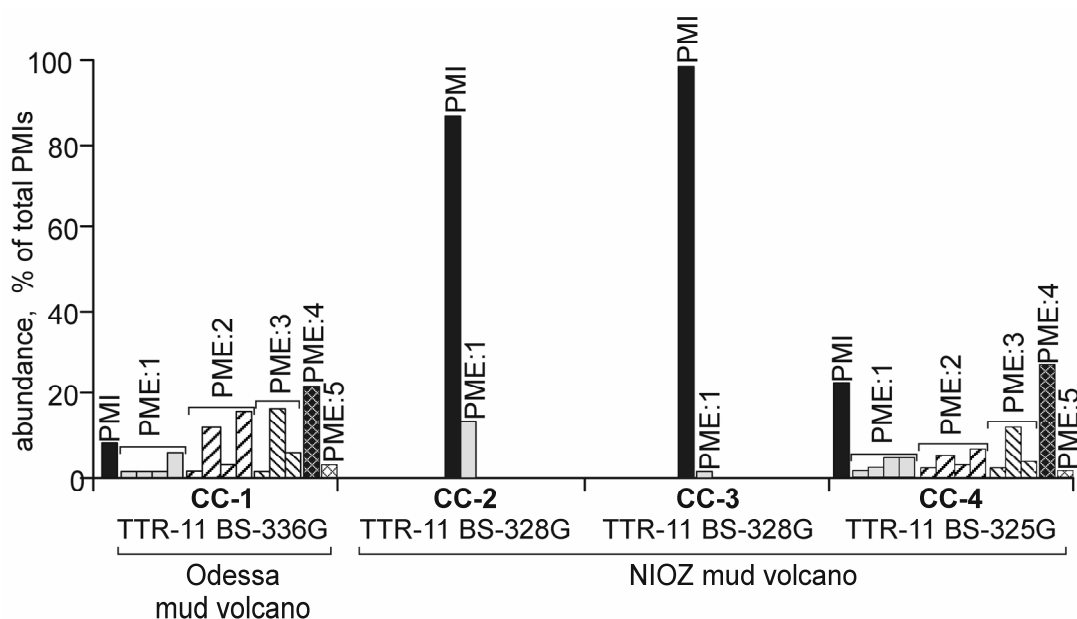


**Figure 4.** The distribution of PMEs in the four carbonate crusts.

( $\pm 3\%$ ) were measured. The distribution of PMI and PMEs in Kazakov mud breccias resembles that of the carbonate crusts CC-1/CC-4.

Another microbial lipid present in the carbonate crusts is the irregular  $C_{30}$  isoprenoid squalene (2,6,10,15,19,23-hexamethyltetracos-2,6,10,14,18,22-hexaene; IV) (Figure 3). Carbon isotopic analyses showed that squalene in carbonate CC-1 is isotopically enriched ( $-71\%$ ) relative to the cluster of PMI and PMEs. Furthermore, this  $\delta^{13}C$  value is the most depleted squalene of all carbonate crusts (Table 2). A distinct feature of CC-1 is the occurrence of relatively high amount of squalene and the presence its  $C_{35}$ ,  $C_{40}$  and  $C_{45}$  pseudo-homologues (Figure 3). None of these “squalene-like” lipids were detected in other carbonate crusts or in the mud breccia. The carbon isotopic compositions of  $\Sigma C_{30}$ ,  $\Sigma C_{35}$ ,  $C_{40}$  and  $C_{45}$  squalene pseudo-homologues were,  $-55\%$ ,  $-74\%$ ,  $-80\%$  and  $-82\%$ , respectively. The isotopic compositions of these components suggest the potential incorporation of methane or methane-derived substrates by the larger bacterial cold-seep community.

### 3.2.2. Isoprenoidal dialkyl glycerol diethers (DGDs)

Analysis of polar fractions of carbonate crusts and mud breccias revealed a suite of isoprenoidal DGDs diagnostic for various archaea (De Rosa and Gambacorta, 1988; Sprott et al., 1990; Nishihara and Koga, 1991; De Rosa et al., 1991; Koga et al., 1993; Sprott et al., 1993) (Figure 5). Archaeol (bis-O-phytanyl glycerol diether, X), *sn*-2- (XI) and *sn*-3- (XII) hydroxyarchaeols (Hinrichs et al., 1999, 2000, Pancost et al., 2000) and two macrocyclic diethers possessing one and two cyclopentane rings within the biphytane chain (XIII and XIV, respectively; Stadnitskaia et al., 2003) were identified (Figure 5). Archaeol is a common

**Table 2.** Carbon isotopic composition ( $\delta^{13}\text{C}$ ) of archaeal and bacterial lipids in carbonate crusts with microbial mats and mud breccia (‰ by PDB standard).

Biomarker	Odessa mud volcano		NIOZ mud volcano		Kazakov mud volcano	
	Carbonate crusts with microbial mats				Mud breccia	
	TTR-11 BS-336G (CC-1)	TTR-11 BS-328G (CC-2)	TTR-11 BS-328G (CC-3)	TTR-11 BS-325G (CC-4)	0-10 cm b.s.f.	10-20 cm b.s.f.
PMI (I) <sup>a</sup>	-101 <sup>b</sup>	-89 <sup>b</sup>	-96 <sup>b</sup>	-99	-81±3‰ <sup>c</sup>	-71±3‰
PME:1	n.d.*	-83	-97	n.d.	n.d.	n.d.
PME:1 ( $\Sigma$ ) <sup>d</sup>	-99	-	-	-	n.d.	-
PME:2 ( $\Sigma$ )	-97	-	-	-	n.d.	-
PME:3 ( $\Sigma$ )	-98	-	-	-92	n.d.	-
PME:4+PME:5 (II, III)	-96	-	-	-103	n.d.	n.d.
Squalene (IV)	-71	-57	n.d.	-40	n.d.	n.d.
Tricos-1-ene (C <sub>23:1</sub> ) (V)	-95	-100	-94	n.d.	n.d.	n.d.
Tetracos-1-ene (C <sub>24:1</sub> ) (VI)	-91	n.d.	n.d.	n.d.	n.d.	n.d.
Diploptene (VII)	-84	-61	-82	n.d.	n.d.	n.d.
<i>Isoprenoidal DGDs</i>						
Archaeol (X)	-106	-116	-102	-107	-85±3‰	-70±3‰
<i>sn</i> -2-hydroxyarchaeol (XI)	n.d.	n.d.	-	n.d.	-79±3‰	n.d.
<i>sn</i> -3-hydroxyarchaeol (XII)	n.d.	n.d.	-112	n.d.		
<i>Macrocyclic DGDs</i>						
XIII	-106	n.d.	-104	-111	-	-
XIV	-115	n.d.	-112	-116	-	-
<i>Non-isoprenoidal DGDs</i>						
XV	-86	-96	-95	-	-70±3‰	-
XVI	-70	-79	-92	-	-72±3‰	-
XVI isomer	-90	n.d.	n.d.	-	-	-
XVII	-87	-	-	-87	-	-
XVIII	-106	-	n.d.	-	-	-
XVIII isomer	-96	-	-	-	-	-

For polar compounds obtained values have been corrected for carbon atoms added by derivatisation.

n.d.\* - not determined

<sup>a</sup>Roman numbers refer to the structures in the Appendix

<sup>b</sup>-89 – co-elution with PME:1 isomer

<sup>c</sup>– mud breccias show considerably lower concentrations of archaeal and SRB lipids compare to the carbonate crusts. Therefore, an error of  $\delta^{13}\text{C}$  measurements of reported compounds for mud breccias increases up to ±3‰.

<sup>d</sup>( $\Sigma$ ) –  $\delta^{13}\text{C}$  values for the sum of C<sub>25</sub> isomers with the same amount of double bonds.

membrane lipid of such ecologically contrasting archaeal groups as thermophiles, halophiles and methanogens (De Rosa and Gambacorta, 1988; De Rosa et al., 1991; Koga et al., 1993). It was detected in all carbonate crusts as the most abundant DGD and in the mud breccias from both MVs. In carbonate crusts CC-2 and CC-3 (from the NIOZ MV), archaeol is the most abundant compound of the polar fractions (Figure 5) with the highest concentration of 5.2 µg/g of dry sediment in CC-2. Unlike archaeol, both the *sn*-2 and *sn*-3 isomers of

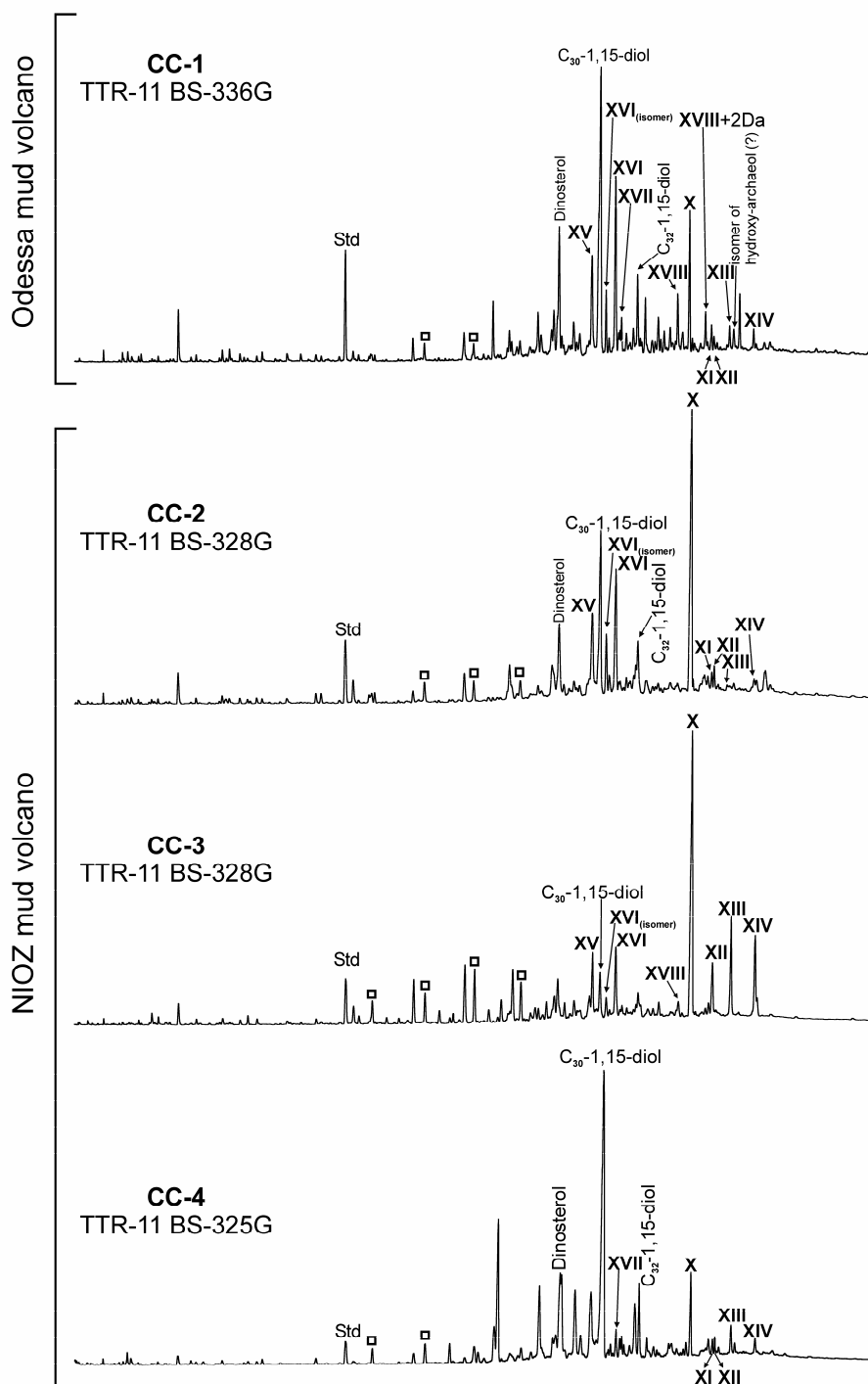


**Figure 5.** Gas chromatograms of the polar fractions of the four carbonate crusts. Roman numerals refer to structures in the Appendix. Open squares indicate straight-chain alcohols. All alcohols were analyzed as their trimethylsilyl derivatives.

hydroxyarchaeol (hydroxydiether lipids) have only been reported to occur in methanogenic archaea, i.e. in all cultured members of the Methanosarcinales (Ferrante et al., 1988; Sprott et al., 1990; Nishihara and Koga, 1992; Koga et al., 1993; Sprott et al., 1993), suggesting that these lipids are a chemotaxonomic characteristic of this genus. It was also reported that hydroxylation at the C-3 position of the *sn*-2 chains is exclusively present in all of the *Methanosarcina* spp., whereas the *sn*-3 isomer has been shown to be produced by a *Methanosaeta* sp. (Sprott et al., 1993). The hydroxyarchaeol isomers occur in all carbonate crusts with abundances substantially lower than that of archaeol and varying between the crusts (Figure 5). In crust CC-3, the *sn*-2-isomer was not detected.

All carbonate crusts are characterized by extremely depleted  $\delta^{13}\text{C}$  values of archaeol and the hydroxyarchaeols. The  $\delta^{13}\text{C}$  of archaeol in crust CC-1 and CC-4 is nearly identical (-106‰ and -107‰, respectively). Crust CC-2 is characterized by a more depleted  $^{13}\text{C}$  value of archaeol (-116‰), whereas archaeol in crust CC-3 is slightly enriched in  $\delta^{13}\text{C}$  value (-102‰) (Table 2). The isotopic composition of *sn*-3-hydroxyarchaeol could only be obtained in crust CC-3 (Table 2) and is 10‰ depleted relative to archaeol.

In the mud breccia from the Kazakov MV archaeol and the *sn*-2 and *sn*-3 isomers of hydroxyarchaeol were only detected in the uppermost 20 cm of the core. Archaeol represents the dominant DGD as observed for the crusts. Its concentration at 10 cm was 1.4  $\mu\text{g/g}$  and decreased to 0.3  $\mu\text{g/g}$  at 20 cm depth. As noticed for PMI and PMEs, deeper sediments show decreasing levels of archaeol and the hydroxyarchaeols. This change was also reflected in their carbon isotopic composition (Table 2). For example, the  $\delta^{13}\text{C}$  of archaeol was -85‰ in the uppermost interval and ca. -70‰ at 20 cm depth. The  $\delta^{13}\text{C}$  value of the composite *sn*-2- and *sn*-3 hydroxyarchaeols was -79 ‰ in the topmost sediment.

In addition to these well-known archaeal DGDs, two macrocyclic diphytanyl glycerol diethers possessing one (XIII) and two (XIV) cyclopentane rings were identified in all carbonate crusts. Although their basic molecular structure is similar to acyclic macrocyclic DGD previously identified in the thermophilic methanogen *Methanococcus jannaschii* (Comita et al., 1984), their occurrence in cold-seep settings suggests that these macrocyclic DGDs are not restricted to thermophilic methanogens (Stadnitskaia et al., 2003). The  $\delta^{13}\text{C}$  of the macrocyclic DGD XIV was 5 to 9‰ depleted relative to macrocyclic DGD XIII, which have similar  $\delta^{13}\text{C}$  values as that of archaeol in all carbonate crusts (Table 2). The macrocyclic DGDs were only found in the carbonate crusts.

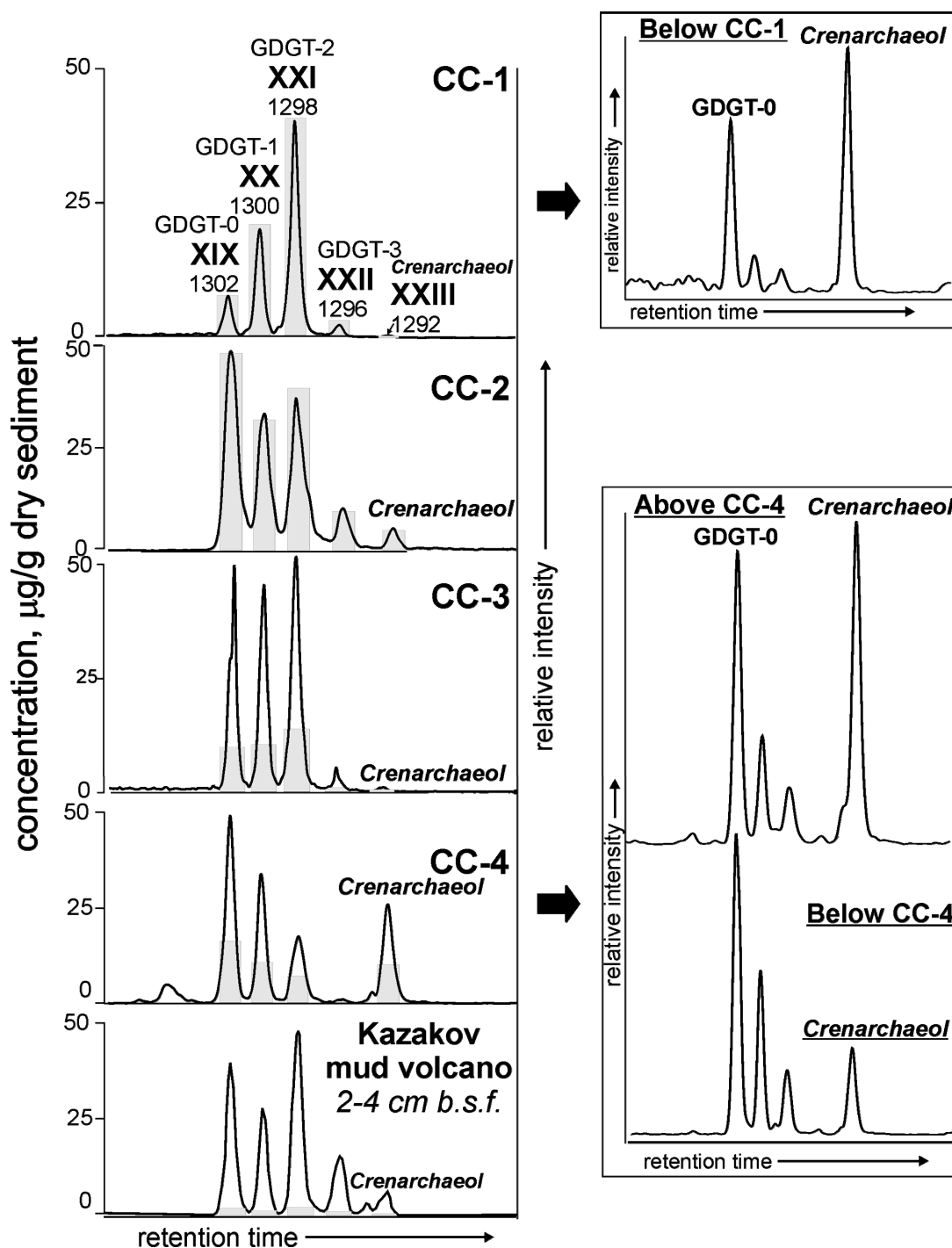


**Figure 6.** Base peak HPLC chromatograms of the polar fractions obtained from the carbonate crusts and mud breccias. The number after «GDGT» indicates the number of cyclopentane rings within the biphytane chains. Roman numbers refer to structures in the Appendix. Arabic numbers below the roman ones indicate the dominant [M+H]<sup>+</sup> ions. Grey bars designate the abundances of GDGTs and refer to the scales at the left side of the plot.

### 3.2.3. *Glycerol Dibiphytanyl Glycerol Tetraethers (GDGTs)*

Isoprenoidal GDGTs are biomarkers for a wide group of archaea. They can represent the main constituents of archaeal membranes and can contain 0 to 8 cyclopentane rings (De Rosa et al., 1983; Langworthy, 1985; De Rosa and Gambacorta, 1988). In the carbonate crusts and mud breccias GDGTs prevail over all other identified archaeal lipids. The total GDGTs in the carbonates ranged from 36 to 136  $\mu\text{g/g}$ . These values are substantially higher than those for total archaeal DGDs (sum of archaeol, OH-archaeols and macrocyclic diethers; 2.1 to 5.6  $\mu\text{g/g}$ ). All GDGT distributions are dominated by GDGTs with 0-2 cyclopentane rings (XIX, XX and XXI) except those of the mud breccias below crust CC-1 and above crust CC-4 (Figure 6), and, thus, reveal AOM “fingerprints”. Such patterns are similar to those previously observed in the Eastern Mediterranean cold seeps, MVs and carbonate crusts (Pancost et al., 2001b; Aloisi et al., 2002), in the Gulf of Mexico methane seepages (Zhang et al., 2003), and in the deep (>700 m) Black Sea water column (Wakeham et al., 2003).

Figure 7 shows the GDGT profiles in mud breccias from the Kazakov and the NIOZ MVs. Although the GDGT concentrations in the Kazakov mud breccias are more than one order of magnitude lower than in the carbonate crusts and substantially lower than in mud breccias from the NIOZ MV, the GDGT distribution profile in the Kazakov mud breccia indicates active anaerobic methanotrophy (Figure 7a). It reveals the predominance of GDGT-0 (XIX) and GDGT-2 (XXI), with the latter as the most prevalent one (Figure 7a). In contrast, the predominance of GDGT-0 (XIX) and crenarchaeol (XXIII) in mud breccias from the NIOZ MV (Figure 7b) and in sediments below crust CC-1 and above crust CC-4 (Figure 6) does not indicate the presence of archaea involved in AOM. Such distributions have previously been observed in sea-water particulate organic matter and in marine sediments from different geographical settings (Schouten et al., 2000; Pancost et al., 2001; Wakeham et al., 2003; Wuchter et al., 2003). Crenarchaeol (XXIII) is a marker of ubiquitous planktonic crenarchaeota (Hoefs et al., 1997; Schouten et al., 1998, 2000, 2001; Sinninghe Damsté et al., 2002a,b; Wakeham et al., 2003), which also produce other GDGTs with 0 and, to a lesser degree, 1-3 cyclopentane rings. The crenarchaeotal GDGTs are most probably indigenous to the mud breccias and, thus, represent fossil material and do not reflect living crenarchaeotal biomass. The presence of crenarchaeol in the carbonate crusts in relatively small amounts is attributed to the inclusion of mud breccia particles during carbonate formation.

### 3.2.4. *Non-isoprenoidal DGDs*

Non-isoprenoidal DGDs, inferred before as a marker of SRB in cold-seep carbonate crusts and MV deposits in the Eastern Mediterranean (Pancost et al., 2001; Werne et al., 2002), were identified in all carbonates and in mud breccia from the Kazakov MV. Two series

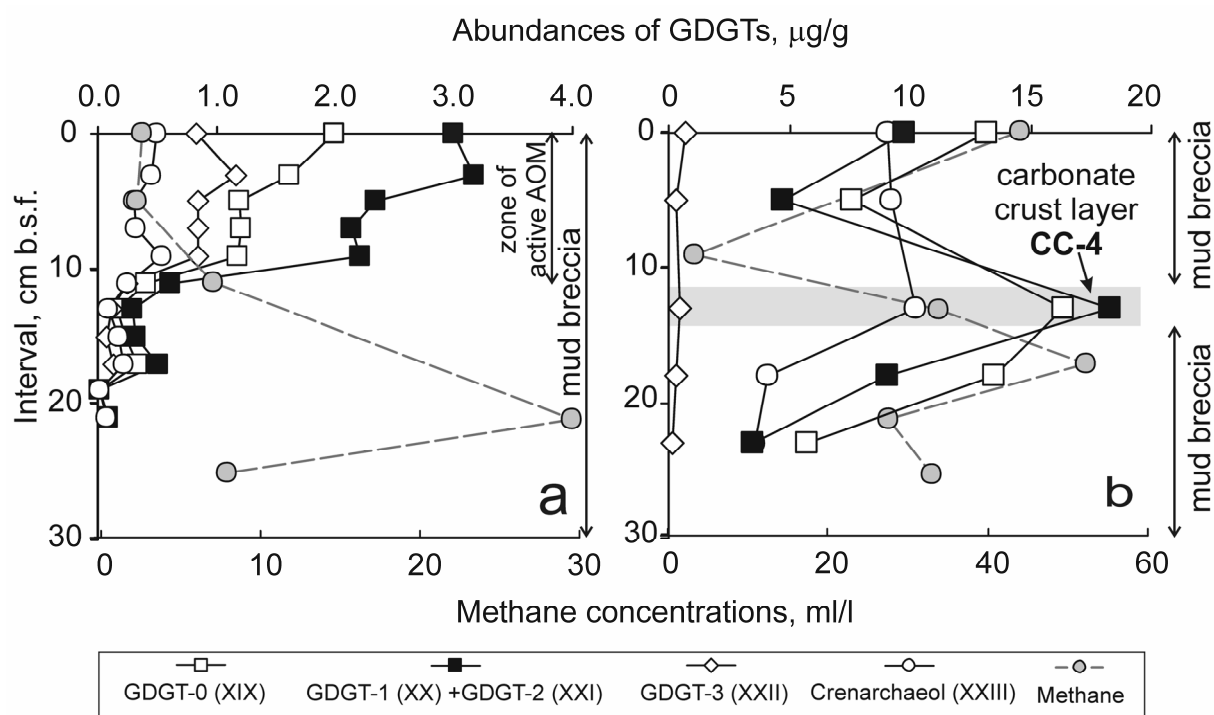


**Figure 7.** Abundances ( $\mu\text{g/g}$  of dry sediment) versus depth of GDGTs and methane (ml/l) for (a) the Kazakov mud volcano, TTR-11 BS-331G; and (b) the NIOZ mud volcano, TTR-11 BS-325G. Roman numbers refer to structures in the Appendix.

of these DGDs were found. The first series includes DGDs possessing anteiso pentadecyl moiety attached at the *sn*-1 position with either an anteiso  $\text{C}_{15}$  alkyl chain ( $\text{C}_{33}$ , XV) or a cyclopropyl-containing  $\text{C}_{16}$  alkyl chain at the *sn*-2 position ( $\text{C}_{34:1}$ , XVI) (Pancost et al., 2001). The second series was represented by DGDs possessing a cyclopropyl-containing  $\text{C}_{17}$  alkyl chain at the *sn*-2 position with either an *n*- $\text{C}_{14}$  alkyl ( $\text{C}_{34:1}$ , XVII; RI=3633) or a  $\text{C}_{17}$   $\omega$ -cyclohexyl alkyl moiety ( $\text{C}_{37:2}$ , XVIII; RI=3927) at the *sn*-1 position (Pancost et al., 2001). With the exception of CC-4, the most abundant diether in the carbonate crusts was XVI and its tentatively identified isomer (Figure 5). The non-isoprenoidal DGD XVII was detected only in crusts CC-1 and CC-4. A novel non-isoprenoidal DGD was tentatively identified in crust CC-1 (Figure 5). Its mass spectrum resembled that of XVIII (Pancost et al., 2001), but the molecular ion is 28 Da higher. The  $\delta^{13}\text{C}$  values of the non-isoprenoidal DGDs in the crusts were generally 10 to 20‰ heavier than those of the isoprenoidal and macrocyclic DGDs (Table 2). An exception is XVIII, which was characterized by a  $\delta^{13}\text{C}$  similar to that of archaeol.

The DGDs XV and XVI were only found in the uppermost interval of the mud breccia from the Kazakov MV. Their carbon isotopic composition was ca.  $-71\text{‰}$ . In the mud breccia

the non-isoprenoidal DGDs co-occurred with archaeal DGDs, PMI and PMEs. It does not indicate a relation of sulfate-reducing bacteria with archaea, but their  $^{13}\text{C}$ -depleted signatures do indicate that the carbon source most probably was methane.

### 3.2.5. Cyclic triterpenes

The hopanoid diploptene (hop-22(29)-ene; VII), widely occurring in the bacterial domain, was detected only in the carbonate crusts (Figure 3). The low  $\delta^{13}\text{C}$  values of diploptene (up to -84‰; Table 2) indicates an incorporation of methane-derived carbon into the biomass of diploptene-biosynthesizing bacteria. The presence of  $^{13}\text{C}$ -depleted diploptene exclusively in the carbonates may suggest specific bacterial populations involved in the process of carbonate precipitation via AOM.

Two other lipids, tetrahymanol (VIII) and bishomohopane-32-ol (IX), were detected in the uppermost 25 cm of the mud breccia of the NIOZ MV. Tetrahymanol and bishomohopane-32-ol were relatively depleted in  $^{13}\text{C}$ , i.e. ca. -49‰ at the interval 16-22 cm bsf. Since bishomohopane-32-ol is probably derived from  $\text{C}_{35}$  bacteriohopanepolyol derivatives, fresh extracts were also subjected to chemical degradation in order to detect all bacteriohopanepolyol derivatives (Rohmer et al., 1984, 1992). However, no indications for the presence of intact  $\text{C}_{35}$  bacteriohopanepolyol derivatives were obtained.

Hopanoids are derived from precursors in the membranes of bacteria. They occur mainly in aerobic bacteria, such as methylo- and methanotrophs, heterotrophs, cyanobacteria, and facultative anaerobic photosynthetic purple non-sulfur bacteria (Rohmer et al., 1984; Rohmer et al., 1992; Kenneth and Moldovan, 1993; Schoell et al., 1994; Summons et al., 1999). Recent biomarker studies revealed the occurrence of hopanoids in anoxic environments (Pancost et al., 2000; Elvert et al., 2001; Thiel et al., 2003), suggesting that the occurrence of hopanoids is not restricted to aerobic bacteria. Recently, it has indeed been shown that strictly anaerobic bacteria capable of anaerobic ammonium oxidation are able to biosynthesize hopanoids, including diploptene and bacteriohopanepolyols (Sinninghe Damsté et al., 2004b).

It is still unclear which microorganisms are capable to biosynthesize tetrahymanol in strict anoxic environments. Tetrahymanol was first isolated from the ciliate protozoan *Tetrahymanella pyriformis* (Mallory et al., 1963). Besides eukaryotes such as in ferns, fungi, and other ciliates, tetrahymanol was found in addition to hopanoids in the phototrophic purple nonsulfur bacterium *Rhodospseudomonas palustris* (Klemann et al., 1990) and in the nitrogen-fixing bacterium *Bradyrhizobium japonicum* (Bravo et al., 2001).



### 3.2.6. Straight-chain alkenes

All carbonate crusts contain *n*-tricosene (C<sub>23:1</sub>; V) and *n*-tetracosene (C<sub>24:1</sub>; VI). Based on the relative retention time, the C<sub>23:1</sub> alkene was tentatively identified as *n*-tricos-10(*Z*)-ene, previously reported in a Black Sea microbial mat (Thiel et al., 2001). The C<sub>24:1</sub> alkene has not been previously reported in AOM settings. The δ<sup>13</sup>C signatures of these alkenes (δ<sup>13</sup>C = ca. -95‰; Table 2) indicated that *n*-C<sub>23:1</sub> and *n*-C<sub>24:1</sub> were biosynthesized by microorganisms involved in AOM (cf. Thiel et al., 2001). It is presently unknown which microorganisms involved in anaerobic methanotrophy are capable to biosynthesize these straight-chain hydrocarbons. However, their presence only in methane-related carbonates and not in mud breccias indicates peculiar trophic association of microorganisms, which may be involved in carbonate precipitation *via* AOM.

### 3.3. 16S rRNA gene sequence analysis

#### 3.3.1. Archaeal sequences

DGGE of PCR products obtained with primers specific for the 16S rRNA encoding gene of Archaea (Coolen et al., 2004) resulted in one intensely stained band at the same position in the gel for carbonate crusts CC-1 and CC-4 (Figure 9, lanes 2 and 5) as well as for CC-2 and CC-3 (Figure 9, lanes 3 and 4). The DGGE profiles of the PCR products obtained with DNA from the mud breccias showed more than one band. The mud breccias from the Kazakov MV showed two bands at 2-4 cm and at 8-10 cm, and three bands at 20-22 cm (Figure 9, lanes 7-9,

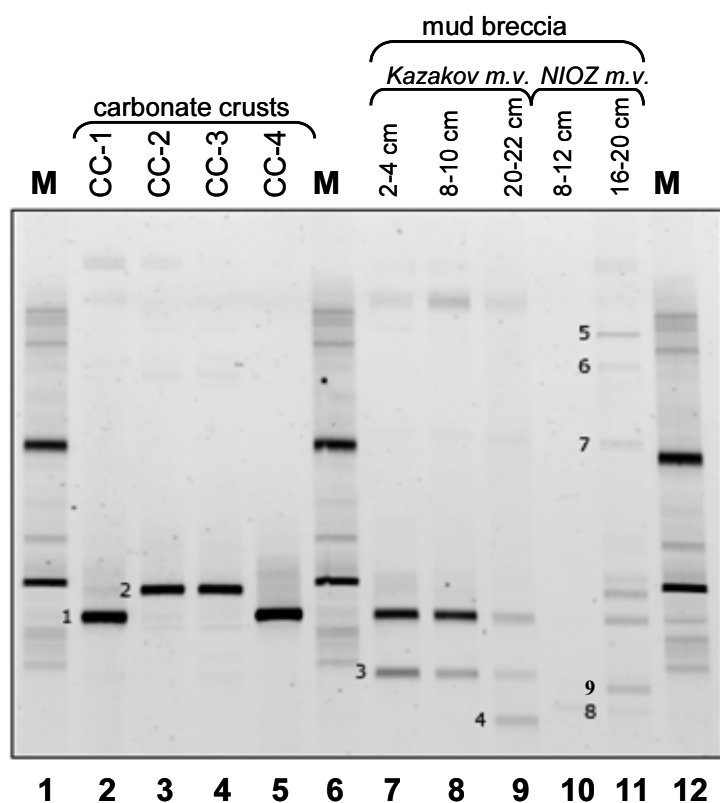


**Figure 8.** DGGE analysis of PCR products obtained with primers specific for the 16S rRNA encoding gene of Archaea and genomic DNA extracted from the carbonate crusts and mud breccias (for detail on the samples, see Table 2). Lanes 1, 6, and 12 are marker fragments. Bands that were excised and sequenced are numbered; band no. 1 is named DGGE-ARC1, band no. 2 is DGGE-ARC2, etc. (see Figure 9 for their phylogenetic position).

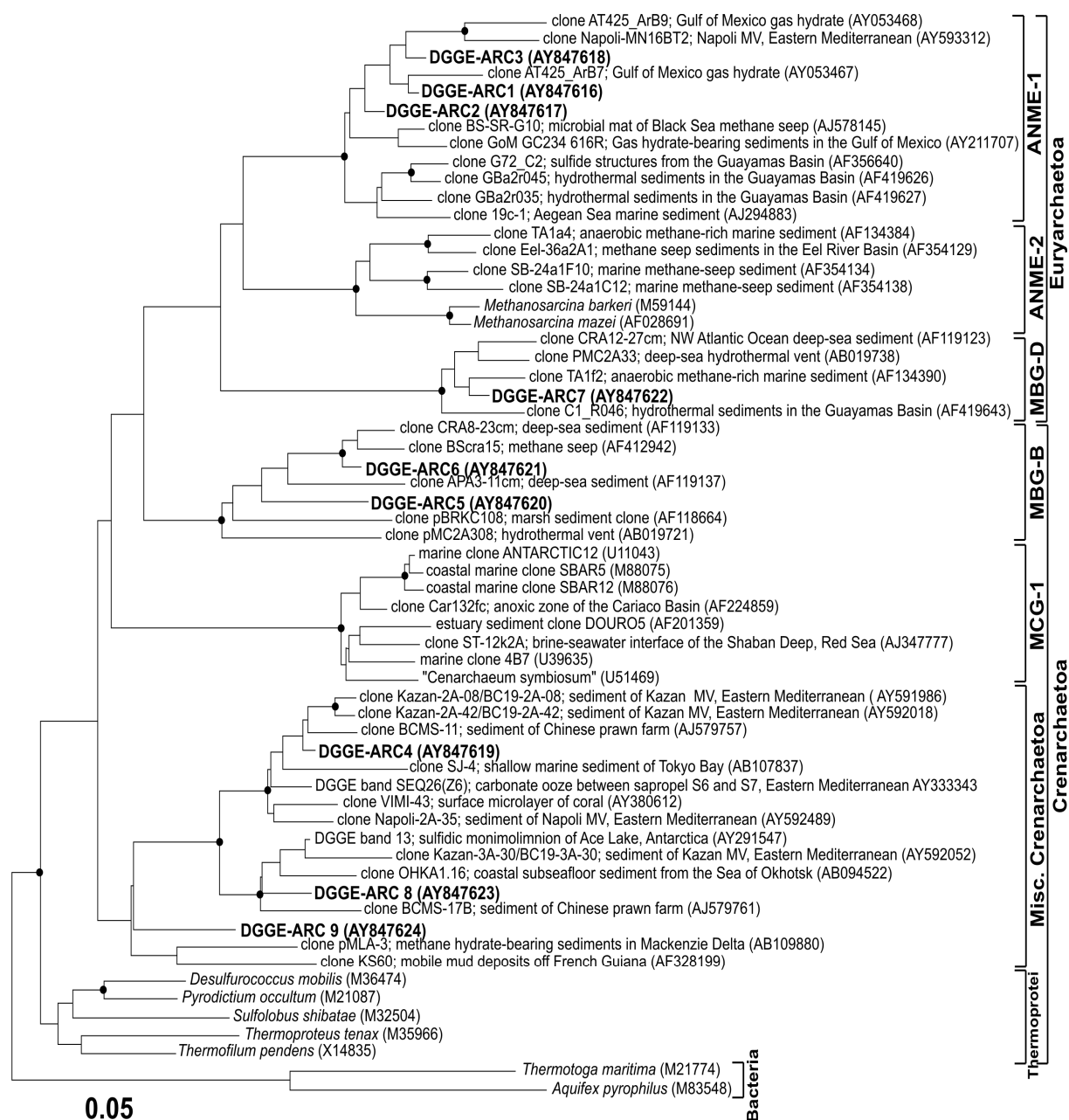


**Figure 9.** Phylogenetic affiliation of Archaea present in the carbonate crusts and mud breccias as revealed by comparative analysis of 16S rRNA gene sequences from bands and those stored in public databases. Bootstrap values are based on 1000 replicates; only values between 90% and 100% are given and indicated by a solid dot on the branches. Sequences determined in this study are shown in bold and refer to the number of the band excised from the gel (see Figure 8). The scale-bar represents 5% sequence divergence. Abbreviations used to indicate the different clusters in the tree: ANME-1 and ANME-2 are two groups of putative anaerobic methane-oxidizing *Archaea*; MBG-D is marine benthic group D; MBG-B is marine benthic group B; MCG-1 is marine crenarchaeotal group -1.

respectively). In contrast, the mud breccias from the NIOZ MV showed no bands at 8-12 cm, just above carbonate crust CC-4, and ca. seven relatively weak bands at 16-20 cm depth, just below the crust (Figure 8, lanes 10- 11).

Most of the bands were excised from the gel, re-amplified, and sequenced to infer the phylogenetic affiliation of the community members. None of the identified archaeal sequences was closely related to known methanogens. Bands at the same position in the gel had identical sequences. Comparative analysis of the sequences obtained from bands no. 1, 2 and 3, and sequences stored in nucleotide databases indicated a close relationship of these populations with Archaea grouped in the ANME-1 cluster (Figure 9). A bootstrap value of 100% confirmed this strong affiliation. The sequence obtained from band no. 7 clustered with sequences of Archaea of the Marine Benthic Group D within the *Euryarchaeota* (Vetriani et al., 1999; Teske et al., 2002). The sequences of the other excised bands grouped with sequences of *Crenarchaeota*. Bands no. 5 and 6 grouped within the Marine Benthic Group B (Vetriani et al., 1999), and bands no. 4, 8, and 9 within the cluster of the Miscellaneous Crenarchaeotal Group (Inagaki et al., 2003). No sequences of mesophilic archaea affiliated with the group of pelagic crenarchaeota were identified (Figure 9).

### 3.3.2. Bacterial sequences

A diversity of bacterial 16S rRNA gene fragments was detected in DNA isolated from the microbial mats associated with carbonate crusts and from mud breccias. DGGE analysis of 16S rRNA gene fragments obtained with bacterial primers (Figure 10) showed a more complex pattern than those for Archaea (Figure 8). To determine the identity of the bacteria, DGGE bands were excised, re-amplified, and sequenced. Comparative sequence analysis indicated the presence of bacteria affiliated to different phylogenetic groups (Figure 11). Three sequences, DGGE-BAC2, -BAC4 and -BAC7, grouped with bacteria for which no cultured representatives have been isolated so far, i.e. the OP8 candidate division (Hugenholz et al., 1998). Two other sequences, i.e. DGGE-BAC1 and -BAC13, grouped with sequences belonging to bacteria from hydrocarbon seeps or benzene-mineralizing consortia within the Haloanaerobiales. Three sequences, DGGE-BAC5, -BAC8 and -BAC12, clustered with SRB within the  $\delta$ -subdivision of the Proteobacteria. These sequences belong to the Desulfobacteraceae, including all the sequences between *Desulfobacterium niacini* and *Desulfostipes sapovorans* with a bootstrap value of greater than 90 %. However, they do not belong to the *Desulfosarcina* cluster. They form a separate group together with the sequence of the uncultured bacterium 63-2 found in the Benguela Upwelling System (Schaefer et al., unpublished data). One sequence, DGGE-BAC17, grouped with members belonging to the genus *Sphingomonas*. Four sequences, DGGE-BAC14, -BAC15, -BAC16, and -BAC18, were affiliated with the  $\alpha$ -subdivision of the Proteobacteria (Figure 11). Interesting is the

affiliation of DGGE-BAC18 with known *Methylobacterium* species, and DGGE-BAC15 with methanotrophic bacteria (Figure 11).

### 3.4. Microbial diversity in carbonate crusts and mud breccia: insight from 16S rDNA sequences and biomarker data

#### 3.4.1. Archaea

Despite the crucial role of archaea in AOM, no species are available in pure culture. Therefore, their precise biomarker composition is still unknown. The combination of the lipid biomarker and 16S rDNA data is, however, a powerful means to identify the main microbial community members involved in AOM. Our 16S rRNA gene sequence survey only revealed archaea related to the ANME-1 cluster (Figure 9). Although this does not prove that archaea from the ANME-2 group are absent, it shows that archaea belonging to the ANME-1 cluster are far more dominant. Both DGGE of PCR amplified archaeal 16S rDNA (Figure 8) and the archaeal biomarker composition (Figs. 3 and 5) show a clear distinction between carbonate crusts CC-1/CC-4 and CC-2/CC-3. Although the DGGE-ARC1 and -ARC2 sequences are relatively closely related (ca. 95%) and both fall in the ANME-1 cluster (Figure 9), the archaeal lipid composition of crusts CC-1/CC-4 and CC-2/CC-3 is quite different. Archaea present in carbonates CC-1/CC-4 predominantly biosynthesize PME<sub>s</sub> and archaeol, while archaea in crusts CC-2/CC-3 produce primarily PMI and, in addition, to archaeol also hydroxyarchaeol. All carbonates contain abundant GDGTs and show the typical pattern (Figure 6) distinctive for AOM (cf. Pancost et al., 2001; Wakeham et al., 2003).

Recent observations of archaeal membrane lipid patterns have typified distinct anaerobic methanotrophic consortia in AOM-driven carbonate reefs with living microbial

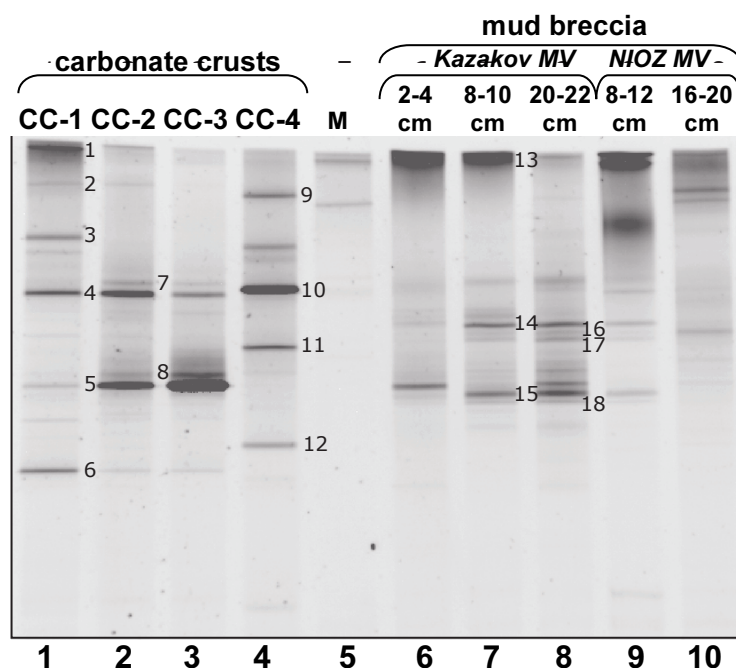
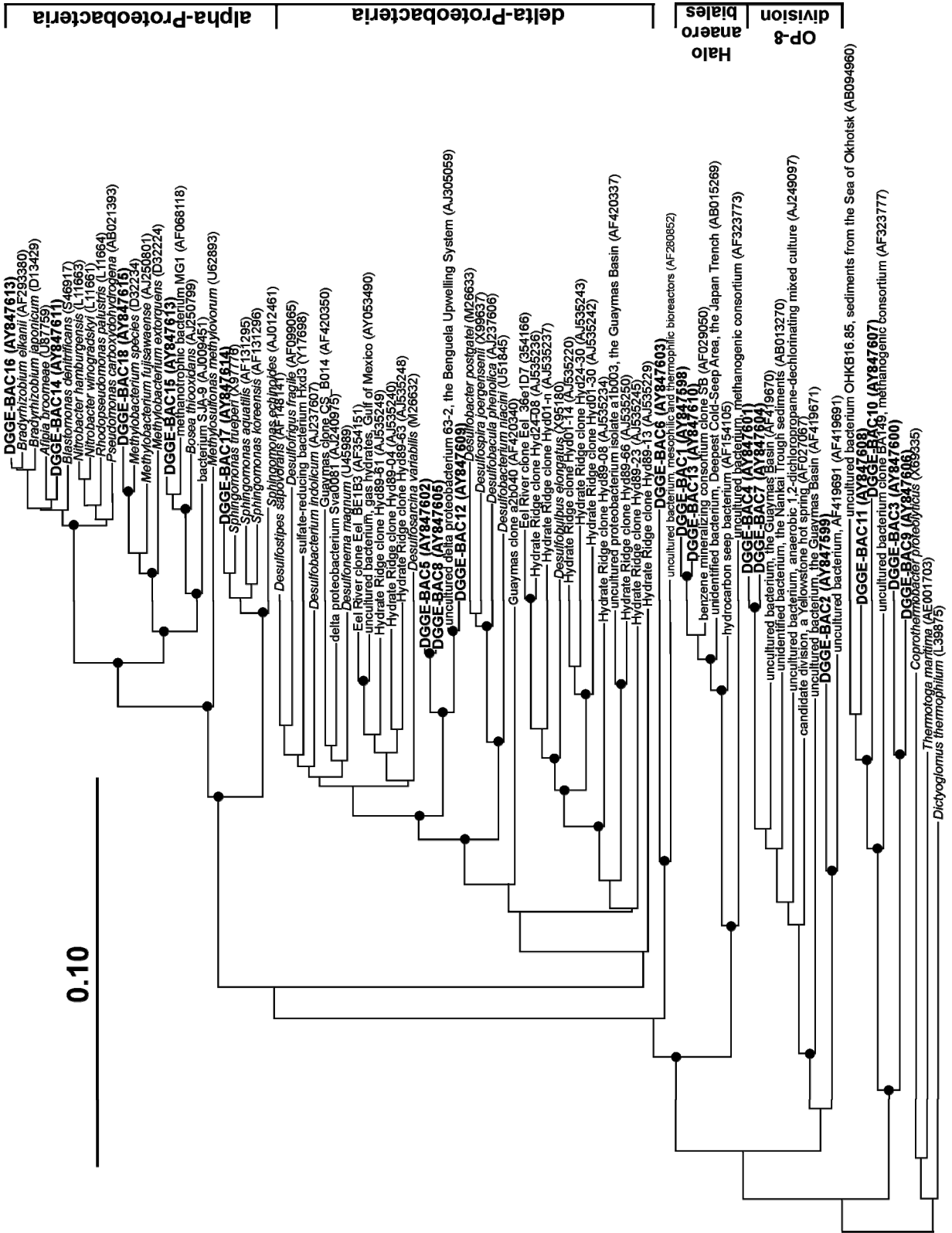


**Figure 10.** DGGE analysis of DNA fragments obtained after PCR-amplification with primers specific for the 16S rRNA genes of Bacteria and genomic DNA extracted from the carbonate crusts and mud breccias (for detail on the samples, see Table 2). Lane 5 represents marker fragments. Bands that were excised and sequenced are numbered; band no. 1 is DGGE-BAC1, band no. 2 is DGGE-BAC2, etc. (see Figure 11 for their phylogenetic position).



mats (Blumenberg et al., 2004). It was shown that microbial communities dominated by archaea from the ANME-1 cluster biosynthesize cyclic GDGTs, archaeol and PMI with relatively low amounts of PMEs, whereas ANME-2 archaea are characterized by the absence of GDGTs, *sn*-2-hydroxyarchaeol in access to archaeol, abundant PMEs relative to PMI and the presence of crocetane and crocetenes (Blumenberg et al., 2004). The tetra- and pentaunsaturated PME isomers were initially thought to be indicative for members of the *Methanosarcinales*-related ANME-2 cluster (Sprott et al., 1990, 1993; Hinrichs et al., 1999) but the data of Blumenberg et al. (2004) do not comply with this. The archaeal lipid distribution in our carbonates is generally consistent with the classification of Blumenberg et al. (2004): GDGTs are relatively abundant, archaeol dominates over the hydroxyarchaeol isomers, and crocetane is absent, all in line with the predominance of ANME-1 archaea. However, despite that the archaea in the carbonate crusts all belong to the ANME-1 cluster, a substantial variation in the amounts of PMI relative to PMEs is observed (Figure 4), indicating that this characteristic should be used cautiously.

In comparison with the carbonate crusts, the mud breccias revealed phylogenetically more diverse archaeal assemblages (Figs. 8 and 9). The mud breccias from the Kazakov MV are characterized by a similar suite of archaeal biomarkers as crusts CC-1 and CC-4, suggesting similar archaeal populations. This was confirmed by DGGE of archaeal 16S rDNA fragments, revealing the predominance of the DGGE-ARC1 sequence, which also characterizes the archaeal community in the crusts CC-1 and CC-4 (Figure 8). Another, but less dominant, sequence (DGGE-ARC3) is phylogenetically closely affiliated with sequences DGGE-ARC2 and -ARC1 found in the carbonates. Sequence DGGE-ARC4, only obtained from the lowermost mud breccia (20-22 cm), is affiliated with the Miscellaneous Crenarchaeota Group of the *Crenarchaeota*. This group of *Crenarchaeota* is comprised of sequences found predominantly in recent sediments (e.g. Inagaki et al., 2003) and mud breccias from the Eastern Mediterranean MVs (Heijs et al., unpublished). In contrast to the Kazakov MV, the mud breccias from the NIOZ MV do not contain sequences affiliated with AOM archaeal groups. They are characterized by a phylogenetically more diverse archaeal community with members within the *Euryarchaeota*, i.e. Marine Benthic Group D (DGGE-ARC7) and *Crenarchaeota*, including Marine Benthic Group B (DGGE-ARC5 and -ARC6)

---

**Figure 11 (page 98).** Phylogenetic affiliation of Bacteria present in the carbonate crusts and mud breccias as revealed by comparative analysis of 16S rRNA gene sequences from DGGE bands and those stored in public databases. Bootstrap values are based on 1000 replicates; only values between 90% and 100% are given and indicated by a solid dot on the branches. Sequences determined in this study are shown in bold and refer to the number of the band excised from the gel (see Figure 10). The accession numbers are given in parentheses. The scale-bar represents 10% sequence divergence.

and the Miscellaneous Crenarchaeota Group (DGGE-ARC4, -ARC8, and -ARC9). Such a variety occurs only in the interval 16-20 cm, below carbonate CC-4 (Figs. 8 and 9). The presence of these crenarchaeotal groups is indicative of sedimentary archaea which is most likely not involved in the anaerobic methanotrophy. The GDGT patterns of these sections of the mud breccias are similar to those in particulate organic matter from the water column derived from pelagic crenarchaeota (e.g. Sinninghe Damsté et al., 2002b; Wakeham et al., 2003). The absence of any archaeal sequences affiliated with marine pelagic crenarchaeota in the mud breccias (Figure 9) indicates that these GDGTs are likely not derived from living archaeal cells. Crenarchaeol (XXII) and the other GDGTs are most likely indigenous to the erupted mud breccia, i.e. they were transported by mud fluid from the subsurface, resulting in a background signal of GDGTs characteristic for pelagic crenarchaeota. This hypothesis is supported by the fact that different mud flows on top of each other may have quite different pelagic crenarchaeotal GDGTs patterns (Stadnitskaia et al., unpublished results). If AOM is taking place, the archaea are producing their characteristic GDGTs, overriding the background signal (Figure 6). In the carbonates the purest AOM signal is found.

#### 3.4.2. Sulfate reducing bacteria

The presence of SRB was mainly detected in the carbonate crusts. Sequences DGGE-BAC5 and -BAC8 grouped within the SRB cluster (Figure 11) and are detected in the carbonate crusts CC-1, CC-2 and CC-3 in association with the occurrence  $^{13}\text{C}$ -depleted non-isoprenoidal diethers (Figure 5), previously inferred as biomarkers of SRB (Pancost et al., 2001a; Werne et al., 2002). Carbonate crust CC-4 reveals relatively low quantities of  $^{13}\text{C}$ -depleted non-isoprenoidal DGDs. However, the presence of sequence DGGE-BAC12 in the crust CC-4 confirms the presence of another species of SRB (Figure 11).

Previous studies have demonstrated that archaea from both the ANME-1 and ANME-2 groups co-occur with members of the *Desulfosarcina/Desulfococcus* phylogenetic cluster (Boetius et al., 2000; Orphan et al., 2001a, 2002; Michaelis et al., 2002). The presence of other groups of SRB from seep-related sediments was recently shown in the Cascadia Margin of Oregon (Knittel et al., 2003). None of the sequences of SRB found in the carbonates belong to these phylogenetic clusters of SRB known to participate in AOM. The sequences, DGGE-BAC5, -BAC8, and -BAC12, form a separate cluster within the Desulfobacteraceae family which possess though *Desulfosarcina/Desulfococcus* group, a potential syntrophic archaeal partner in AOM-consortia as it was previously inferred (Boetius et al., 2000). This indicates that archaea performing AOM in the carbonate crusts are most likely not limited to the known SRB partners but that the SRB diversity is larger than previously anticipated. FISH microscopy should confirm if the new SRB identified here form indeed syntrophic communities as observed previously (Boetius et al., 2000). The positive correlation between

the relative abundance of SRB lipid biomarkers, their carbon isotopic signatures, and the presence of specific SRB-related DGGE bands in the carbonates provides additional evidence to attribute the observed non-isoprenoidal DGDs to SRB involved in AOM microbial communities.

### 3.4.3. Other bacterial assemblages

Sequences belonging to the benzene-mineralizing consortia (Phelps et al., 1998) within the Haloanaerobiales group were only found in the carbonate CC-1 and the mud breccia of the Kazakov MV. The presence of these bacteria is likely related to the abundance of allochthonous aromatic compounds detected in the hydrocarbon gas mixtures and in the lipid extracts of these sediments (Stadnitskaia et al., unpublished data).

The presence of sequences in the mud breccias of the Kazakov and NIOZ MVs (sequences DGGE-BAC18 and -BAC15) that are phylogenetically related to methylotrophic and methanotrophic bacteria in the  $\alpha$ -proteobacteria (Figure 11) is remarkable. This seems to indicate the presence of aerobic bacteria (all cultured bacteria falling in this cluster are aerobes) in an anoxic ecological niche. Alternatively, and perhaps more likely, these findings indicate the existence of microbes in this phylogenetic cluster that are anaerobic. The presence of  $^{13}\text{C}$ -depleted bishomohopan-32-ol in the same sediment intervals where these sequences were detected might indicate that this hopanoid is derived from these bacteria (methanotrophs are known to biosynthesize hopanoids; Rohmer et al., 1992) and that they are actively involved in methane cycling. However, we were not able to detect intact bacteriohopanepolyols in these sediments. Hopanoids have recently been detected in strictly anaerobic bacteria (Sinninghe Damsté et al., 2004b), so this finding is not inconsistent with the hypothesis that the phylogenetic cluster of methanotrophic bacteria in the  $\alpha$ -proteobacteria may contain anaerobes.

The other detected bacterial sequences (Figure 11) can not be directly related to a metabolic reaction or ecological niche. A good example is the presence in the CC-1, CC-2, and CC-3 carbonate crusts of three sequences (DGGE-BAC2, -BAC4, and -BAC7) affiliated with bacterial candidate division OP8. Related sequences of this bacterial division were first detected in a hot spring in Yellowstone National Park, rich in reduced iron, sulfide,  $\text{CO}_2$ , and hydrogen (Hugenholz et al., 1998). Subsequently, related sequences were also obtained from a hydrocarbon-contaminated soil under methanogenic conditions (Dojka et al., 1998) and from the anoxic water column of the Cariaco Basin (Madrid et al., 2001). In all these settings, the representatives of OP8 candidate division co-occurred with various archaea. Although we have no carbon isotopic evidence that implies the involvement of these bacteria in AOM processes, their restricted occurrence in the crusts may indicate an ecologically significant but



as yet unknown role for these bacteria. Another example is the sequence (DGGE-BAC16), closely affiliated with nitrogen-fixing bacteria (*Bradyrhizobium* species; Figure 11), in the mud breccias of the Kazakov MV. *Bradyrhizobium japonicum* biosynthesizes gammacerane derivatives (Bravo et al., 2001) and, thus, may be the biological source for tetrahymanol, but its biogeochemical role in this setting remains to be understood.

### 3.5. AOM processes and the formation of carbonates

A distinctive AOM signal, revealed by the GDGT composition and concentration (Figure 6) and the presence of other  $^{13}\text{C}$ -depleted archaeal and bacterial biomarkers (Table 2), is evident for all carbonate crusts. In contrast, none of the mud breccias hosting the carbonate crusts are characterized by a strong AOM signal (e.g. Figure 6). This is strong evidence that AOM performed by the microbial community of archaea and SRB is indeed directly or indirectly responsible for the precipitation of carbonate. Furthermore, it reveals that AOM is the predominant microbial process within the carbonate crusts, inducing their formation. This is consistent with the 16S rDNA sequence data which revealed ANME-1 archaeal sequences only within the carbonate crusts. By contrast, the mud breccia below the crust CC-4 shows phylogenetically diverse archaeal populations which are not at all affiliated with methanotrophic archaea (Figs. 8 and 9). Most probably, the methanotrophic archaea are present in much lower numbers relative to other archaea in the mud breccia, consistent with the assumption of strongly reduced rates of AOM.

The carbon isotopic compositions of archaeal and bacterial biomarkers in both the carbonates and the mud breccia from the Kazakov MV show extremely depleted  $\delta^{13}\text{C}$  values (Table 2), which is consistent with the data reported for various modern and ancient methane venting areas where AOM took or is taking place (Peckmann et al., 1999, 2002; Thiel et al., 1999, 2001; Elvert et al., 1999; Hinrichs et al., 2000; Pancost et al., 2000, 2001a 2001b; Michaelis et al., 2002; Teske et al., 2002; Zhang et al., 2002, 2003; Werne et al., 2002). PMI is enriched in  $^{13}\text{C}$  relative to archaeol in both the mud breccia and the carbonate crusts. On the other hand, hydroxyarchaeol shows considerable isotopic variation. In the mud breccia it is enriched in  $^{13}\text{C}$  relative to archaeol (by ca. 6 ‰) but depleted in carbonate crust CC3 (by ca. 10 ‰). This is consistent with observations made in Eastern Mediterranean mud volcanic sediments and carbonate crusts (Pancost et al., 2001b). Mud breccias from the Kazakov MV show  $\delta^{13}\text{C}$  values of archaeal and SRB biomarkers of ca. 10‰ to 20‰ enriched relative to those of the same lipids in the carbonate crusts from the other MVs. This enrichment in  $^{13}\text{C}$  is likely related to the enrichment in  $^{13}\text{C}$  of the substrate methane (Kazakov MV:  $\delta^{13}\text{C}_{\text{CH}_4} \sim -56\text{‰}$ ; Odessa MV:  $\delta^{13}\text{C}_{\text{CH}_4} \sim -63\text{‰}$ ; and NIOZ MV:  $\delta^{13}\text{C}_{\text{CH}_4} \sim -68\text{‰}$ ). This indicates that  $\delta^{13}\text{C}$  value of microbial lipids is determined in part by the isotopic composition of methane.

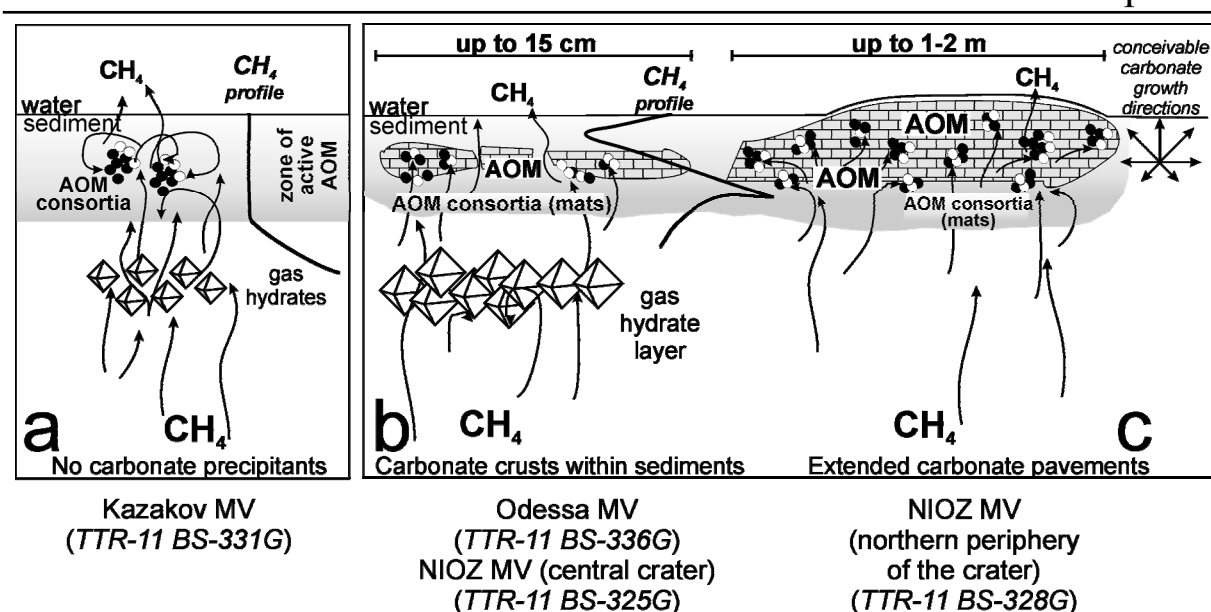


**Figure 12.** Conceptual model showing probable zone of active AOM and related carbonate formation.

It is known, that authigenic carbonates derive their carbon from the pore water  $\Sigma\text{CO}_2$  pool (Suess and Whiticar, 1989). Since the isotopic signal of methane in both the NIOZ and the Odessa MVs is  $^{13}\text{C}$ -depleted, the bicarbonate produced *via* AOM from this methane is also  $^{13}\text{C}$ -depleted. Therefore, the similarities between the  $\delta^{13}\text{C}$  values of the methane,  $\delta^{13}\text{C}$  values of carbonates from the NIOZ and the Odessa MVs (-41 ‰ and -44 ‰, respectively; Mazzini et al., 2002), and  $\delta^{13}\text{C}$  values of the archaeal lipids in the carbonate crusts (Table 2) probably indicate that carbonate precipitation at these sites occurred under relatively constant biogeochemical environments.

Methane concentrations in the NIOZ (TTR-11 BS-325G) and in the Odessa (TTR-11 BS-336G) MVs were highest just below the carbonate crust levels and then tend to decrease within the carbonate interval and just above the crust, indicating its consumption (Figure 7b). Most likely, neofomed carbonates serve as a trap for migrated methane, thus partially reducing its diffusion into the water column. This could explain the settlement of microbial mats at the base of and within the carbonate crusts. Consequently, at sites where authigenic carbonate layers have already been formed (i.e. the NIOZ and the Odessa MVs), AOM occurs predominantly just below or/and within the carbonates.

The data obtained suggest that the studied locations within the NIOZ, the Odessa and the Kazakov MVs were characterized by different intensity and duration of AOM processes. The recovered sedimentary section from the Kazakov MV (TTR-11 BS-331G) was characterized by the absence of overlaying pelagic sediments, indicating that the sampling site was located on a relatively recent mud flow. The presence of only millimeter-sized gas

hydrates suggests inherent limited scale methane diffusion from the subsurface. Low concentrations of GDGTs and the absence of AOM-induced authigenic carbonates suggest that microbial processes in this setting, in particular AOM, are at the “initial stage” of their development (Figure 12 a). Figure 7a shows that, in spite of the relatively low GDGT content in the mud breccias, the distribution of GDGTs is similar to that of the carbonate crust CC-2 (Figure 6). The distinctive concave-up shape of the methane concentration profile relates to the sharp decline in GDGT concentrations at the same depth interval (Figure 7a). This is consistent with the decrease in concentration of SRB and other archaeal lipids (non-isoprenoidal and isoprenoidal DGDs and PME). The DGGE patterns for archaeal 16S rDNA from the uppermost 10 cm (Figure 8) showed the predominance of sequences that are affiliated with the putative methanotrophic archaeal group ANME-1.

Compared with the site from the Kazakov MV (TTR-11 BS-331G), the recovered sedimentary sequences from the NIOZ (TTR-11 BS-325G) and the Odessa (TTR-11 BS-336G) MVs indicate longer methane seepage duration. The presence of pelagic Unit-1 and Unit-2 (Degens and Ross, 1972) at the Odessa MV (TTR-11 BS-336G) indicates that the sampling site was located on a relatively old mud flow, which is in agreement with the presence of a massive gas hydrate layer, indicating excess of methane. The presence of an AOM-related carbonate crusts and associated microbial mats in both the Odessa and NIOZ MVs indicate “long-term” AOM processes and therefore “long-term” methane availability. This might also designate the “next stage” of AOM-resulted diagenetic alterations followed after the “initial stage” observed in the mud breccia of the Kazakov MV (Figure 12 b).

The recovered sedimentary section from the central part of the crater of the NIOZ MV (TTR-11 BS-325G) consists of two different mud breccia intervals, and the carbonate crusts CC-4 found in between (Kenyon et al., 2002). The formation of this crust may have started prior to the second mud breccia effusion. The presence of microbial mats at the base and inside the carbonate crust, however, indicates still on-going microbial processes, resulting in crust development below the sea floor. In the Odessa MV, carbonate crust CC-1 with pink microbial mats is found at the same depth interval as carbonate CC-4. Carbonate crusts CC-2 and CC-3, which are parts of extensive carbonate pavements at the northern edge of the crater of the NIOZ MV (TTR-11 BS-328G), are also intensively colonized by microbes. Underwater camera-surveys revealed that these pavements are covered by pelagic sediments, forming a positive seafloor relief (Kenyon et al., 2002) which implies their formation below the seafloor (Figure 12c). The presence of authigenic carbonates at the subsurface is common for the sediments of the Sorokin Trough and forms an indirect indication of past or present AOM-active horizon.

The strongest AOM signal was detected within carbonates but not in the underlying or covering sediments. This suggests that carbonate was precipitated within the sediments below

the sea-floor surface, and that putative AOM consortia become predominantly concentrated within the carbonates inducing their growth. The carbonate growth direction possibly follows the pathways of the migrated methane, which is mainly laterally and/or upwards. Initially, carbonate precipitation has to correspond to intervals with high AOM rates, i.e. where methane and sulfate are abundant (Figure 12). After precipitation, carbonates may form a good growth substrate for microorganisms due to their large surface and porosity. The upward growth of carbonates in the Black Sea can be explained by partial diffusion of fluids through already formed carbonates. This is demonstrated by the abundant presence of scattered microbial communities within the carbonates investigated (see Material and Methods). Besides, extensive carbonate pavements at the periphery of the NIOZ MV crater form a positive sea floor relief which might indirectly denote their partial upward accretion. On the other hand, we do not reject the idea that in general carbonates can also grow downwards, which might seem more logical. Serving as a trap for the upward migrated methane, carbonate formation may lead the growth of the carbonates downward. However, downward carbonate accretion could be bounded by the methane/sulfate interface.

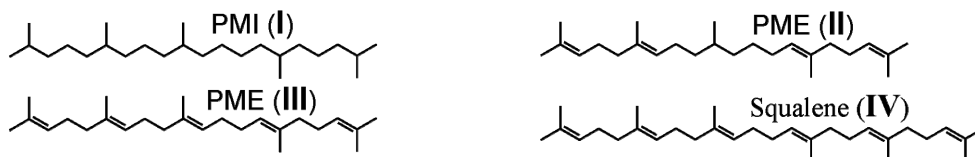
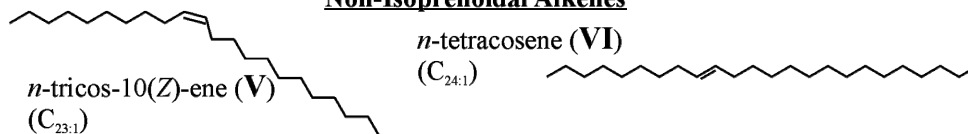
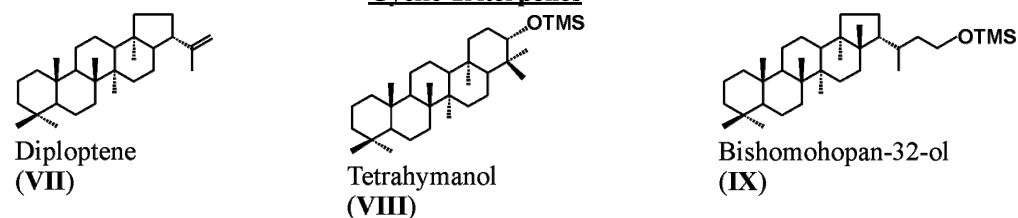
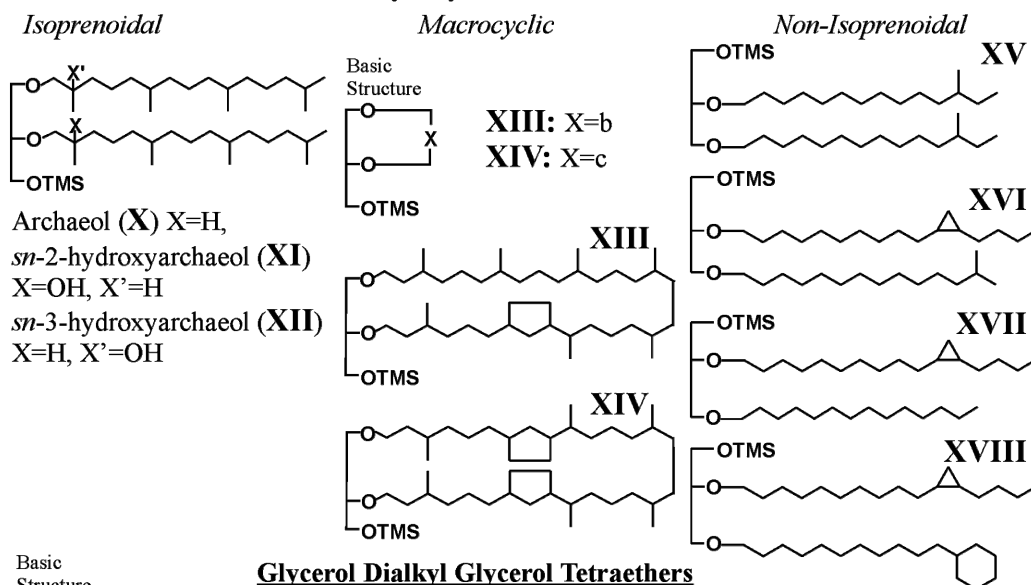
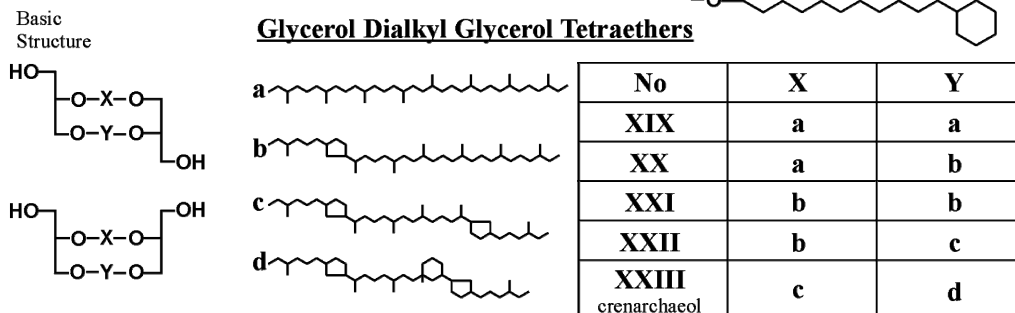
The precipitation of carbonates *via* AOM and their upward growth in the marine environment in the presence of an anoxic/oxic interface will be restricted, because both methanotrophic archaea and SRB are obligate anaerobes. Furthermore, the interaction of sulfide-rich pore fluids, produced due to AOM, with oxygenated seawater results in locally acidic environments (Paull and Neumann, 1987) which may dissolve carbonates at the sediment/water interface. The deep Black Sea environment is strictly anoxic. Actual and active gas seepage into the water column (Michaelis et al., 2002) and active mud volcanism (Ivanov et al., 1992; 1996; 1998; Kenyon et al., 2002) were widely documented within the basin. The finding of 4-meter-high carbonate buildups covered with massive microbial mats in the anoxic waters of the northwestern Black Sea shelf (Michaelis, et al., 2002) can be considered as an example of possible upward carbonate accretion due to AOM. The formation of such build-ups above the sea floor is most probably only possible in an anoxic water column. In an oxygenated-water column, AOM-related carbonates of any shape and morphology will be formed within the oxygen-free intervals below the sea surface. Interestingly, until now no “chimney” shaped carbonate build-ups in the seepage areas of the deep (>1000 m) Black Sea (Woodside et al., 1997; Kenyon et al., 2002) were reported. Probably, the widely observed extensive carbonate pavements in deep-sea fluid venting areas of the Central and the North-eastern parts of the Black Sea might represent an “equivalent” to the shallow-depth “carbonate-chimney-forest” discovered in the Western shelf of the basin (Michaelis, et al., 2002). Such extended carbonate edifices are a characteristic feature related to methane venting in the Sorokin Trough.

#### **4. Conclusions**

Methanotrophic microbial mats associated with carbonates were for the first time found in the deep waters (> 1000 m) of the Black Sea. The combination of methane measurements, biomarker and compound specific isotopic analysis accompanied with a survey of 16S rRNA gene sequences was performed for four methane-derived carbonates with microbial mats and mud breccias collected from the NIOZ, the Odessa and from the Kazakov MVs. Specific lipids for archaea and SRB show a good correlation between their carbon isotopic signatures and the  $\delta^{13}\text{C}$  values of methane, indicating that methane is the dominant carbon source used by microorganisms for their microbial mass. Biomarker and phylogenetic studies of methane-related carbonate crusts and mud breccias show diverse bacterial and archaeal communities, suggesting a wide range of, most probably, novel groups of microorganisms that are directly or indirectly involved in anaerobic methanotrophy. The comparative analysis of archaeal sequences indicate that AOM in these settings is performed predominantly by archaeal populations affiliated with the ANME-1 group. The identified sequences do not belong to the phylogenetic clusters of known methanogenic archaea. A distinction of archaeal strains within the ANME-1 group was detected in carbonates and mud breccia. In combination with biomarker data a clear difference in archaeal assemblages was revealed within the carbonate crusts CC-1/CC-4 and the mud breccias from the Kazakov MV and carbonates CC-2/CC-3. Archaea retrieved from carbonates CC-1/CC-4 and mud breccias from the Kazakov MV predominantly biosynthesise PMEs, and archaea from crusts CC-2/CC-3 mainly produce the PMI. The existence of putative archaea/SRB consortia in the carbonate crusts is suggested by 16S rDNA and biomarker data. However, the identified SRB strains are different from those currently known in archaea/SRB AOM consortia, thus forming a new cluster of SRB within the Desulfobacteraceae family. This could indicate that archaea performing AOM are not limited to the currently known SRB partners.

Our data reveal a different intensity and duration of AOM, most probably forced by intensity of local seepage activity, pathways, and migrated products. Mud breccia from the Kazakov MV, where carbonates were not (yet) formed, uniquely demonstrated the “initial stage” of AOM. In contrast, the strongest signal of on-going AOM was obtained from carbonate crusts CC-1, CC-2 and CC-3, indicating their present formation via anaerobic methanotrophy. The methane, biomarker and 16S rRNA gene sequences data reveal that in these locations AOM processes are most active within the neofomed carbonates and are substantially reduced in the hosting mud breccias. It indicates that in these particular settings carbonate formation within the AOM zone started within the sediment corresponding to the intervals with high AOM rates, i.e. where methane and sulphate are abundant. The carbonate growth direction probably follows the pathways of migrated methane (that is, mainly laterally or/and upwards) due to the presence of anoxic environments in the Black Sea water column.

## Appendix

**Irregular Isoprenoids****Non-Isoprenoidal Alkenes****Cyclic Triterpenes****Dialkyl Glycerol Diethers****Glycerol Dialkyl Glycerol Tetraethers**



---

**NOVEL ARCHAEOAL MACROCYCLIC DIETHER CORE MEMBRANE LIPIDS IN  
A METHANE-DERIVED CARBONATE CRUST FROM A MUD VOLCANO IN THE  
SOROKIN TROUGH, NE BLACK SEA**

A. Stadnitskaia<sup>a,b</sup>, M. Baas<sup>a</sup>, M.K. Ivanov<sup>b</sup>, Tjeerd C.E. van Weering<sup>a</sup> and

Jaap S. Sinninghe Damsté<sup>a</sup>

<sup>a</sup>Royal Netherlands Institute for Sea Research (NIOZ), P.O. Box 59, 1790 AB Den Burg, Texel, The Netherlands.

<sup>b</sup>Geological Faculty, UNESCO-MSU Centre for Marine Geosciences, Moscow State University, Vorobjevy Gory, Moscow 119899, Russian Federation.

Published in *Archaea* 1, 165-173 (2003)

**Abstract**

A methane-derived carbonate crust was collected from the newly discovered NIOZ mud volcano in the Sorokin Trough, NE Black Sea during the TTR-11 cruise of the R/V *Professor Logachev*. Among a number of specific bacterial and archaeal membrane lipids present in this crust, two novel macrocyclic diphytanyl glycerol diethers, containing one or two cyclopentane rings, were detected. Their structures were tentatively identified based on the interpretation of mass spectra, comparison with previously reported mass spectral data, and a hydrogenation experiment. This macrocyclic type of archaeal core membrane diether lipids has so far only been identified in the deep-sea hydrothermal vent methanogen *Methanococcus jannaschii*. However, this is the first time that it is shown that these macrocyclic diethers can also contain internal cyclopentane rings. The molecular structure of the novel diethers resembles those of dibiphytanyl tetraethers in which also biphytane chains occur which contain one and two pentacyclic rings. Such tetraethers were abundant in the crust. Compound-specific isotope measurements revealed  $\delta^{13}\text{C}$  values of -104 to -111‰ for these new archaeal lipids, indicating that they are derived from methanotrophic archaea acting within anaerobic methane-oxidizing consortia, which subsequently induce authigenic carbonate formation.



## 1. Introduction

Geological exploration of the ocean floor has revealed widely occurring fields of submarine fluid discharge, so-called “cold-seeps” or “methane-seeps”, which create specific structures on the sea floor, such as mud volcanoes and pockmarks (Hovland and Judd 1988; Limonov et al., 1994; 1997, Ivanov et al. 1996a,b). In these settings constant and focused fluid supply induce a marked biological activity depending on chemosynthetic nutrition (Hovland and Judd 1988, Sibuet et al. 1988, Corselli and Basso 1996, Olu et al. 1996, 1997, Sibuet and Olu 1998). Specifically, it is manifested in the appearance and diversity of chemoautotrophic microorganisms (bacteria and archaea) thriving in the specific environments created by the strong advection of altered methane-rich fluids (Sassen et al. 1993, Cragg et al. 1996, Lanoil et al. 2001). The most important processes fueling these light-independent biological communities are the aerobic and anaerobic oxidation of methane.

Numerous field and laboratory observations have indicated that in the areas of intensive hydrocarbon gas venting, anaerobic oxidation of methane (AOM) is the dominant pathway for methane consumption. AOM has been proposed to be performed in tandem by methanogenic archaea, acting in reverse, and sulfate-reducing bacteria to consume the formed hydrogen, making the reaction thermodynamically feasible (Reeburgh 1976, Zender and Brock 1979, Alperin and Reeburgh 1985, Hoehler et al. 1994). Recently, multiple lines of investigations have shown the capability of archaea to use methane as a carbon source, i.e. to act as methanotrophic organisms. The light carbon isotopic composition of archaeal membrane lipids revealed that archaea incorporated isotopically light methane-derived carbon into their cell carbon (Hinrichs et al. 1999, Elvert et al. 2000, Hinrichs et al. 2000b, Pancost et al. 2000, Thiel et al. 2001, Pancost et al. 2001a, b, Zhang et al. 2002, Teske et al. 2002). In association with isotopically depleted archaeal membrane lipids, lipids derived from sulfate-reducing bacteria were found in varying distributions (Pancost et al. 2000, 2001a). They are also substantially depleted in  $\delta^{13}\text{C}$  albeit slightly heavier than the archaeal lipids, indicating involvement of sulfate-reducing bacteria in the microbial community performing AOM. The ultimate evidence of an archaeal/sulfate-reducing bacterial consortium was obtained by comparative 16S ribosomal RNA gene sequences and fluorescence *in-situ* hybridization analysis. It was found that the methane-oxidizing archaea are phylogenetically associated with the methanogenic orders of *Methanomicrobiales* (ANME-1) and *Methanosarcinales* (ANME-2) (Hinrichs et al. 1999, 2000b, Boetius et al. 2000, Orphan et al. 2001, Teske et al. 2002), and, that their cell aggregates are surrounded by exosymbiotic, nutritionally versatile sulfate-reducing bacteria (Boetius et al. 2000, Orphan et al. 2001).

The most distinct chemotaxonomic markers of archaea are the presence of ether core membrane lipids composed of isoprenoidal units linked to glycerol moiety (Langworthy et al. 1982, 1985, De Rosa et al. 1983, 1991, Comita et al. 1984, Hoefs et al. 1997, Schouten et al.

1998, Hopmans et al. 2000, Pancost et al. 2000, 2001a, b). Glycerol dibiphytanyl glycerol tetraethers (GDGTs; see the Appendix for structures) are well known to occur in the archaeal membranes and can contain from 0 to 8 cyclopentane rings (De Rosa et al. 1983, De Rosa and Gambacorta 1988). The presence of cyclopentane rings within biphytanyl chains is well known for (hyper)thermophilic archaea whereas methanogenic archaea contain predominantly GDGTs with no cyclopentane rings. Recently, crenarchaeol (**XII**), a GDGT with four cyclopentane rings and one distinctive cyclohexane ring, has been suggested as a specific core membrane lipid for non-thermophilic planktonic Crenarchaeota widely observed in low-temperature marine environments (Schouten et al. 2001b, Sinninghe Damsté et al. 2002a). Glycerol dibiphytanyl glycerol tetraethers with 0-3 cyclopentane rings have been shown to derive from methanotrophic archaea in the Eastern Mediterranean cold seep areas (Pancost et al. 2001b, Aloisi et al. 2002). Diphytanyl glycerol diethers (DGDs; see the Appendix for structures) are also common archaeal core membrane lipids, which could be considered as the archaeal counterparts of the conventional diglycerides of eukaryotic origin. They are characterized by the unusual 2,3-*sn* glycerol stereochemistry compared to that found in bacterial membranes (De Rosa et al. 1991). Archaeol (**IV**) (2,3-bis-*O*-phytanyl glycerol diether) and hydroxyarchaeols (*sn*-2 isomer **V** and *sn*-3 isomer **VI**; see the Appendix for structures) are the universal archaeal core membrane lipid formed by condensation via ether linkage between two C<sub>20</sub> isoprenoid alcohols and a glycerol molecule (De Rosa and Gambacorta 1988, De Rosa et al. 1991). The *sn*-2 and *sn*-3 isomers of hydroxyarchaeol have been identified in cultured members of *Methanosarcinales* (Spratt et al. 1990, Nishihara et al. 1991, Koga et al. 1993). The major producer of *sn*-2-hydroxyarchaeol is *Methanosarcina* sp., while the *sn*-3- isomer was observed in *Methanosaeta concilii* (Spratt et al. 1993). Based on the wide occurrence of these lipids in methane-seepage areas (Hinrichs et al. 1999, 2000a, Elvert et al. 2000, Boetius et al. 2000, Pancost et al. 2001b), and their extremely depleted  $\delta^{13}\text{C}$  values indicating methane-consumption, these archaeal lipids are widely used as indicators of AOM.

Here we report a new type of archaeal core membrane ether lipid in a methane-derived carbonate crust collected from the NIOZ mud volcano recently discovered in the Sorokin Trough, NE Black Sea. The novel macrocyclic isoprenoidal glycerol diethers contain one or two cyclopentyl rings in their biphytanyl chain. The distinct molecular structure of these lipids in combination with compound-specific carbon isotopic data indicate that they derive from the new group of archaea, capable of oxidizing methane anaerobically.

## 2. Geological setting

The Sorokin Trough is one of the large depressions in the deep part of the Black Sea, extending along the south-eastern margin of the Crimea Peninsula with a length of 150 km, a width of 45-50 km, and has a water depth of 600-2100 m (Tugolesov et al. 1985) (Figure 1).

The Trough is well known for the occurrence of mud diapiric structures of Oligocene-Early Miocene age. Some of these diapirs are topped by mud volcanoes (Ivanov et al. 1998). A high gas content was noted in the uppermost part of the sedimentary sequence in the form of both free gas and gas hydrate accumulations

(Bouriak and Akhmetzhanov 1998). Hydrocarbon gas profiles show a

characteristic decrease of the methane concentration in the uppermost part of the sedimentary column (Stadnitskaia 1997). This effect is well documented as a distinctive imprint on the sedimentary geochemical record caused by methane consumption (Barners and Goldberg 1976, Bernard 1979).

During the Training-Trough-Research (TTR-11) expedition of the Russian R/V *Professor Logachev* in July-September 2001 a mud volcano (44°19'N; 35°04'E) was discovered based on MAK-1 high-resolution deep-towed side scan sonar data and named “NIOZ” mud volcano. A total of five sediment cores were subsequently taken from the crater of the NIOZ mud volcano at a water depth of 2020 m. Four of the cores (TTR-11 BS-325G, TTR-11 BS-326G, TTR-11 BS-327G, and TTR-11 BS-328G) recovered carbonate crusts. The carbonate crust we examined and describe here was collected from sampling site TTR-11 BS-328G (Figure 1).

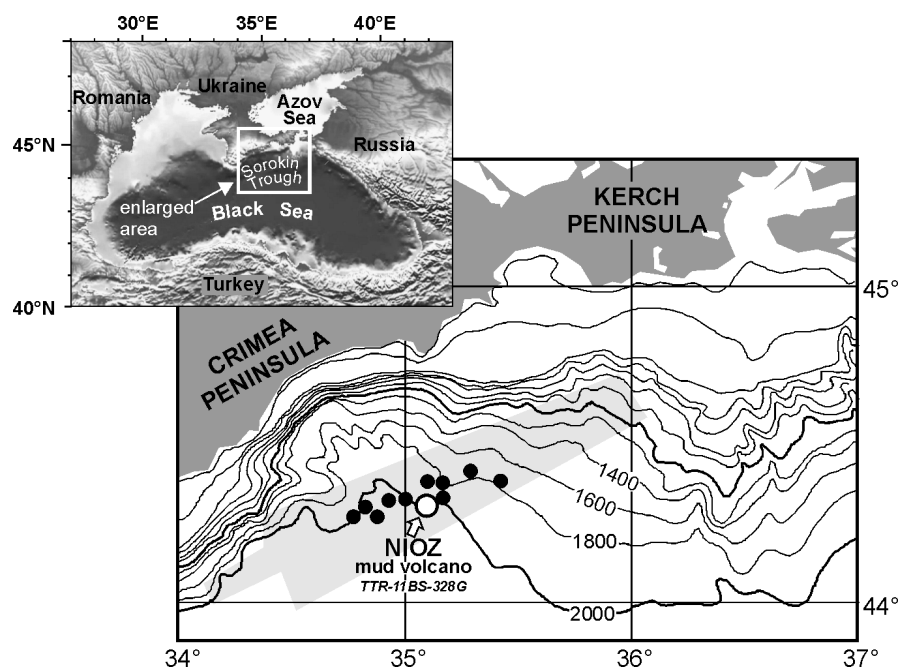


**Figure 1.** Location map of the study area (light gray) within the Sorokin Trough, NE Black Sea. Filled circles indicate the mud volcanoes investigated during the 11<sup>th</sup> Training-Through-Research cruise (July-September 2001); the open circle indicates the position of the NIOZ mud volcano.

The crust (17cm x 9 cm x 1,5 cm) was associated with spherical, drop-sized, brownish microbial mats, which filled the pores and cavities on the surface and inside of the carbonate.

### 3. Methods

#### 3.1. Sample collection

Bottom sampling followed standard TTR procedures, as described in Ivanov et al. (1992). The crust TTR-11 BS-328G-2 was collected from the NIOZ mud volcano using a gravity corer. The sample was described, photographed and stored afterwards at  $-20^{\circ}\text{C}$  until lipid extraction.

#### 3.2. Extraction and separation

About 100 g of the crust was freeze-dried, crushed to a fine powder, and extracted using the Accelerated Solvent Extractor (ASE 200, DIONEX Corporation, USA) using a solvent mixture of dichloromethane (DCM) : methanol (MeOH) (9:1, v/v) at 1000 psi and  $100^{\circ}\text{C}$  PT conditions. Elemental sulfur was removed from the total extract by flushing over a small pipette filled with activated copper. An aliquot of the total extract was chromatographically separated into apolar and polar fractions using a column with activated (for 2 h at  $150^{\circ}\text{C}$ )  $\text{Al}_2\text{O}_3$  as stationary phase. Apolar compounds were obtained using hexane:DCM (9:1, v/v), and polar compounds, including glycerol ether core membrane lipids, were obtained with MeOH:DCM (1:1, v/v) as eluents. A known amount of 2,3-dimethyl-5-(1,1-dideuterohexadecyl)-thiophene ( $\text{C}_{22}\text{H}_{38}\text{SD}_2$ ) was added to each fraction as an internal standard. Alcohols were transformed into trimethylsilyl-derivatives by adding 25  $\mu\text{l}$  of pyridine and 25  $\mu\text{l}$  of BSTFA and heating at  $60^{\circ}\text{C}$  for 20 min.

#### 3.3. Hydrogenation

Hydrogenation was performed in ethyl acetate with  $\text{H}_2$ , a few drops of acetic acid and  $\text{PtO}_2$  for 1 h. Subsequently, the sample was stirred for 8 h at room temperature.

#### 3.4. Gas chromatography

Gas chromatography (GC) was performed using a Hewlett Packard 6890 gas chromatograph equipped with an on-column injector and a flame ionization detector. A fused silica capillary column (CPsil5 25 m x 0.32 mm,  $\text{df} = 0.12 \mu\text{m}$ ) with helium as a carrier gas was used. The samples were injected at  $70^{\circ}\text{C}$  followed by increasing the temperature to  $130^{\circ}\text{C}$  at a rate of  $20^{\circ}\text{C}/\text{min}$ , and then, at  $4^{\circ}\text{C}/\text{min}$  to  $320^{\circ}\text{C}$ , where it was held constant for 15 min.

### 3.5. Gas chromatography-mass spectrometry

The polar fraction was analyzed by gas chromatography-mass spectrometry (GC-MS) for compound identification. GC-MS was conducted using a Hewlett Packard 5890 gas chromatograph interfaced to a VG Autospec Ultima Q (Micromass, Manchester, UK) mass spectrometer operated at 70 eV with a mass range of  $m/z$  50-800 and a cycle time of 1.8 s (resolution 1000). The gas chromatograph was equipped with a fused silica capillary column (CPsil5 25 m x 0.32 mm,  $df = 0.12 \mu\text{m}$ ) and helium as a carrier gas. The temperature program used for GC-MS was the same as for GC.

### 3.6. Isotope ratio monitoring-gas chromatography-mass spectrometry

Isotope ratio monitoring-gas chromatography-mass spectrometry (IRM-GC-MS) was performed on a Finnigan MAT DELTA <sup>plus</sup> XL (Finnigan MAT GmbH, Bremen, Germany) instrument used for determining compound-specific  $\delta^{13}\text{C}$  values. The GC used is a Hewlett Packard 6890A series with the same analytical conditions as those used for GC and GC-MS. For carbon isotopic correction of the added trimethylsilyl groups, the carbon isotopic composition of the used BSTFA was known ( $-49.29 \pm 0.5 \text{‰}$ ). Obtained values are reported in ‰ relative to the PDB standard, and have been corrected for the addition of  $\text{Si}(\text{CH}_3)_3$  group due to the derivatisation procedure. In order to monitor the accuracy of the measurements the analyses are carried out with co-injection of two standards,  $\text{C}_{20}$  and  $\text{C}_{24}$  *n*-alkanes, with known isotopic composition.

### 3.7. High performance liquid chromatography-atmospheric pressure chemical ionization/mass spectrometry

To determine the distribution and composition of intact glycerol dibiphytanyl glycerol tetraethers (GDGTs), the underivatized polar fraction of the carbonate crust was analyzed using the high performance liquid chromatography-atmospheric pressure chemical ionization/mass spectrometry (HPLC-APCI/MS) method for the direct analysis of these compounds according to Hopmans et al. (2000).

## 4. Results

### 4.1. DGDs in the crust

Analysis of the polar fraction of the carbonate crust TTR-11 BS-328G-2 by gas chromatography-mass spectrometry revealed a suite of ether lipids diagnostic for the non-thermophilic group of the euryarchaeota and sulfate-reducing bacteria (Figure 2). Two isoprenoidal DGDs distinctive for methanotrophic archaea (Hinrichs et al. 1999, 2000a) were identified. Archaeol (**IV**) is the most abundant ether lipid. The *sn*-3 isomer of hydroxyarchaeol (**VI**) was also detected in relatively high abundance. Series of non-

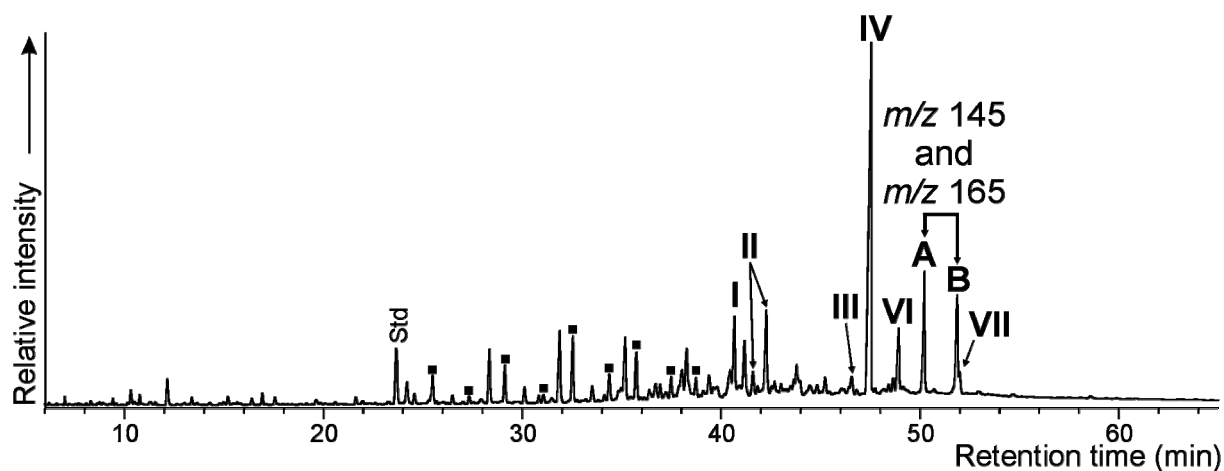


**Figure 2.** Gas chromatogram of the polar fraction extracted from the carbonate crust TTR-11 BS-328G-2. All alcohols were analyzed as their trimethylsilyl derivatives. Black squares indicate straight chain alcohols. Roman numbers and letters refer to Compounds shown in Appendix I.

isoprenoidal DGDs (**I**, **II**, **III**), previously reported as marker of sulfate-reducing bacteria (Pancost et al. 2001a), were also identified in the crust. Diphytanyl glycerol diethers with anteiso alkyl chains (**I**), and with a cyclopropane ring in the alkyl chain attached to the glycerol group at position 2 (**II**) are most abundant. Dicyclic biphytane diol (**VII**; Schouten et al. 1998) was also present in the carbonate crust but it occurs in small amounts relative to the other archaeal and bacterial lipids. It is probably also derived from archaea involved in AOM (Pancost et al. 2001, Teske et al. 2002).

#### 4.2. Novel macrocyclic DGDs in the crust

In addition to these well-known archaeal and bacterial lipids, two relatively abundant, unknown compounds (**A** and **B**) were observed (Figure 2). Their mass spectra (Figure 3) are similar to that of the macrocyclic biphytanyl glycerol diether, the core membrane lipid of the archaeon *Methanococcus jannaschii* (Comita et al. 1984). The mass spectra of compounds **A** and **B** show intense fragment ion at  $m/z$  145, which arise from loss of the entire biphytanyl moiety and a hydroxy group,  $C_3H_4O_2Si(CH_3)_3$ , as was determined by Comita et al. 1984. The presence of relatively abundant fragment ions at  $M^+ - 43$ ,  $M^+ - 57$ , and  $M^+ - 90$  result from loss of  $C_2H_3O$ ,  $C_3H_5O$ , and  $HOSi(CH_3)_3$ , respectively. The fragment ions at  $m/z$  103 and  $M^+ - 103$  are related to the derivatized alcohol-group  $CH_2OSi(CH_3)_3$  (Wood 1980), and those at  $m/z$  130, 131, and 132 to  $C_2H_3O_2Si(CH_3)_3$  moiety, indicating that the  $Si(CH_3)_3$  fragment is attached to the glycerol group at the 1 or 3 position (Pancost et al. 2001a). These mass spectral fragmentation characteristics suggested that **A** and **B** are also macrocyclic biphytanyl glycerol diethers. However, compared to the macrocyclic diphytanyl glycerol diether with a molecular ion at  $m/z$  722 (Comita et al. 1984), the molecular ions of the novel lipids are

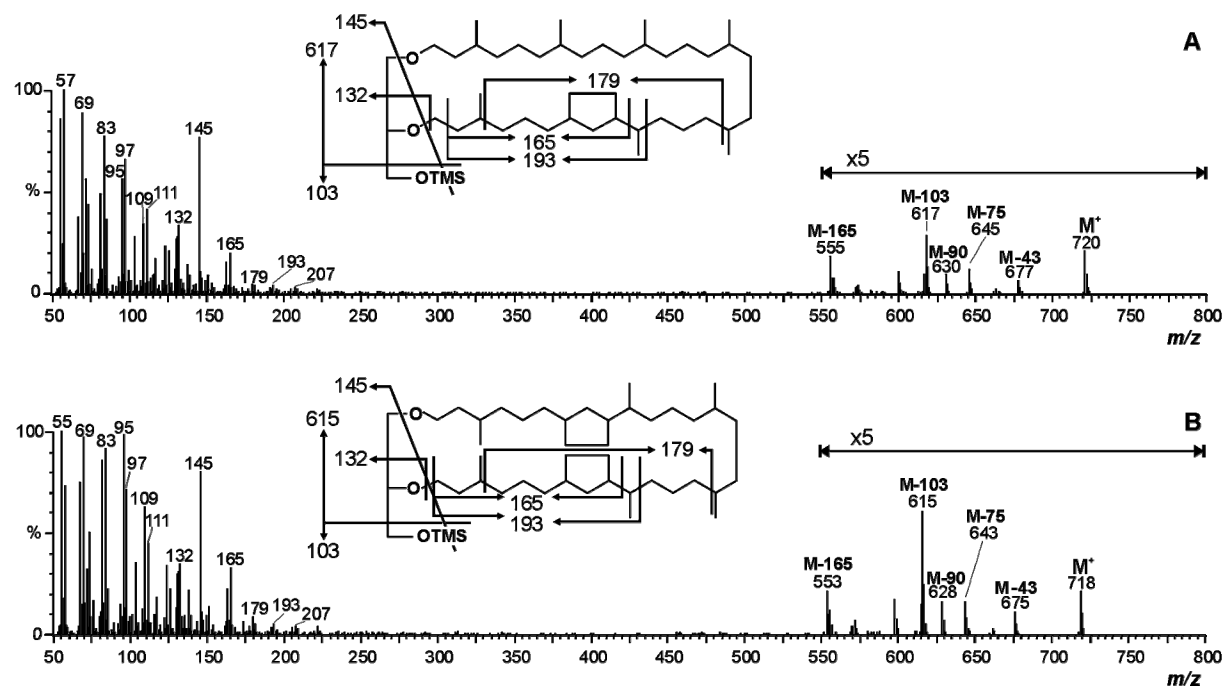


**Figure 3.** Mass spectra (subtracted for background) of novel macrocyclic diethers **A** and **B**.

shifted by 2 Da for **A** ( $M^+ = 720$ ), and by 4 Da for **B** ( $M^+ = 718$ ) (Figure 3). Therefore, it was hypothesized that biphytanyl chains contain either one or two rings or double bonds, respectively. In order to rule out one of these possibilities, the polar fraction was hydrogenated and re-analyzed by GC-MS. This experiment showed no changes in molecular weight of compounds **A** and **B** establishing the absence of double bonds within the biphytanyl skeleton. Consequently, it was concluded that **A** and **B** contain one and two rings, respectively.

Archaeal core membrane lipids have been reported to contain a cyclopentane (De Rosa et al. 1983, 1991, De Rosa and Gambacorta 1988) and, recently, a cyclohexane ring (Sinninghe Damsté et al. 2002a) in their biphytanyl moieties. The presence and location of one and two cyclopentane rings in the biphytanyl chains of **A** and **B**, respectively, is revealed by the distinctive fragment ion at  $m/z$  165 present in both mass spectra (Figure 3). The  $m/z$  165 fragment corresponds to fragmentation associated with the cyclopentyl ring of biphytane derivatives (Schouten et al. 1998). The position of the cyclopentane ring in biphytane moieties has been established by NMR (De Rosa et al. 1977, Sinninghe Damsté et al. 2002b). The mass spectrum of **B** exhibits an enhanced fragment ion of  $m/z$  165 compared to that of **A**, consistent with the presence of two cyclopentane rings.

#### 4.3. GDGTs in the crust

High performance liquid chromatography-atmospheric pressure chemical ionization/mass spectrometry revealed that intact GDGTs in the TTR-11 BS-328G-2

carbonate crust are dominated by GDGTs containing 0 to 2 cyclopentane rings (**VIII**, **IX**, **X**) (Figure 4). This distribution has been reported before in cold seep sediments and crusts of the Eastern Mediterranean (Pancost et al. 2001b, Aloisi et al. 2002) and in the anaerobic water column of the Black Sea (Schouten et al. 2001a, Wakeham et al. 2002), where extensive AOM takes place. Crenarchaeol (**XII**), the GDGT of ubiquitous planktonic crenarchaeota (Hoefs et al. 1997, Schouten et al. 1998, 2001a,b, Sinninghe Damsté et al. 2002a) is nearly absent, which indicates only a minor contribution of pelagic archaeal lipids to the crust.

#### 4.4. Carbon isotopic composition of glycerol diethers

The determination of the carbon isotopic composition of **A** and **B** gave  $\delta^{13}\text{C}$  values of -104‰ and -111‰, respectively. Archaeol and *sn*-3 hydroxyarchaeol are also characterized by extremely depleted  $\delta^{13}\text{C}$  values of -102‰ and -112‰, respectively. The  $\delta^{13}\text{C}$  of non-isoprenoidal dialkyl diethers, **I** and **II**, are 10-20‰ heavier relative to **A**, **B**, archaeol and *sn*-3 hydroxyarchaeol. The carbon isotopic composition of **I** is -95‰, and of **II** is -91‰.

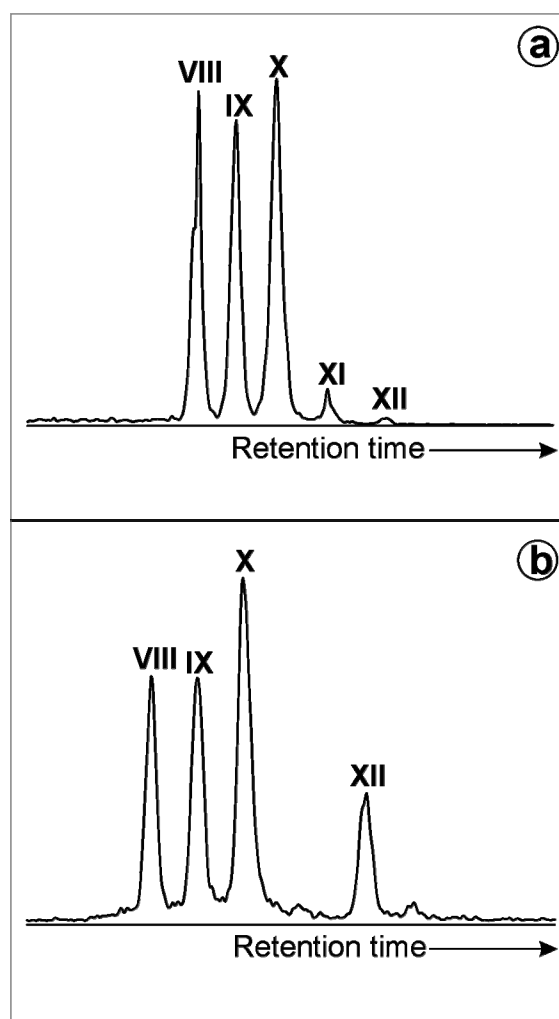


**Figure 4.** Base peak chromatograms of GDGT distribution: (a) carbonate crust TTR-11 BS-328G-2 and (b) Napoli mud volcano, Eastern Mediterranean (Pancost et al., 2001b). Roman numerals refer to GDGT Compounds shown in Appendix I.

## 5. Discussion

The macrocyclic biphytanyl glycerol diethers with one and two cyclopentane rings identified here have, to the best of our knowledge, not been reported to occur in nature. Their molecular structure unites two characteristics reported for ecologically contrasting archaeal groups. The thermophilic methanogen *Methanococcus jannaschii* (Comita et al. 1984) is the only archaeon known to contain the macrocyclic diether as its core membrane lipid. On the other hand, cyclopentane-containing GDGTs are well known for (hyper)thermophilic



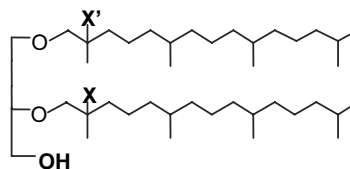
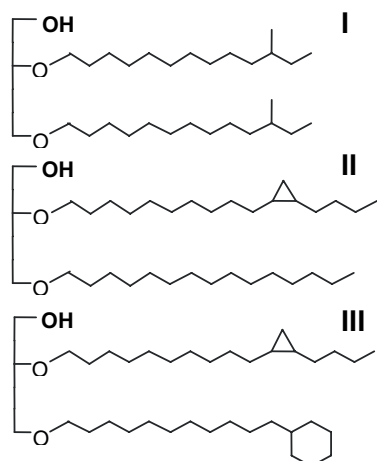
crenarchaeota (Langworthy et al. 1982, De Rosa and Gambacorta 1988), (hyper)thermophilic euryarchaeota (De Rosa and Gambacorta 1988, De Rosa et al. 1991), marine mesophilic crenarchaeota (Sinninghe Damsté et al. 2002a), and mesophilic euryarchaeota capable of AOM (Pancost et al. 2001b, Aloisi et al. 2002), but so far have not been detected in DGDs. This structural information leaves little doubt that the new lipids are derived from archaea. Since archaeal anaerobic methanotrophy results in highly  $^{13}\text{C}$ -depleted lipids, we infer membrane lipids **A** and **B** are derived from methanotrophic archaea. This idea is confirmed by the fact that these type of archaea biosynthesize structurally related GDGT containing biphytane chains with one or two cyclopentane rings (Pancost et al. 2001b, Aloisi et al. 2002, Wakeham et al. 2002). It is not clear why some of the archaeal species capable of AOM present in the NIOZ mud volcano biosynthesize cyclopentane ring containing DGD's instead of GDGT's. This may be related to some sort of adaptation of the physical properties of their cell membranes. It is, however, again consistent with the observed archaeal diversity as observed by lipid composition in cold seep areas (Elvert et al. 2000, Pancost et al. 2001b, Teske et al. 2002). In any case, our data show that archaeal macrocyclic DGD's are not restricted to thermophilic methanogens but are also used by euryarchaeota involved in AOM.

## **6. Conclusions**

Two novel macrocyclic archaeal diether core membrane lipids containing cyclopentane rings were identified in a methane-derived carbonate crust found in the NIOZ mud volcano in the Black Sea. The unprecedented molecular structure and isotopic composition of the novel glycerol diethers **A** and **B** reveal their biosynthesis by archaea performing anaerobic methanotrophy in cold-water environments. The identification of these biomarkers will enable better understanding of AOM-related microorganisms and their metabolic behavior.

## Appendix I

## Dialkyl Glycerol



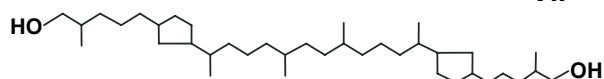
IV: X = H, X' = H (Archaeol)

V: X = OH, X' = H (*sn*-2-

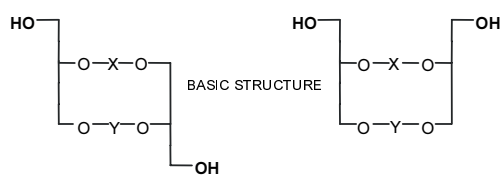
VI: X = H, X' = OH (*sn*-3-

## Biphytane

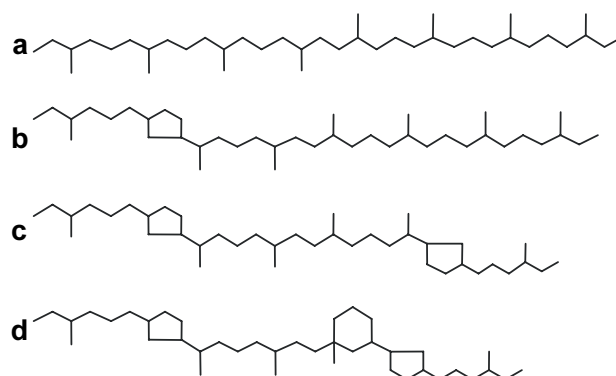
VII



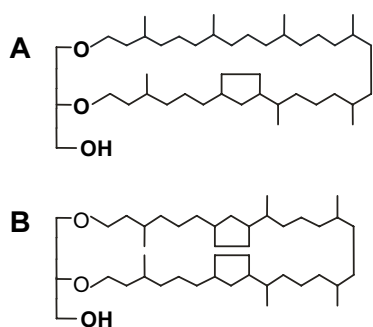
## Glycerol Dialkyl Glycerol



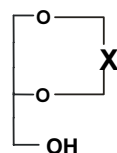
No	X	Y
VIII	a	a
IX	a	b
X	b	b
XI	b	c
XII	c	d



## Macrocyclic



BASIC STRUCTURE



X = a

A: X = b

B: X = VII (-2OH) or c



The Gulf of Cadiz,  
NE Atlantic



**MOLECULAR AND CARBON ISOTOPIC VARIABILITY OF HYDROCARBON GASES FROM MUD VOLCANOES IN THE GULF OF CADIZ, NE ATLANTIC**

A.Stadnitskaia<sup>a,b</sup>, M.K.Ivanov<sup>b</sup>, V. Blinova<sup>b</sup>, R. Kreulen<sup>d</sup> and  
T.C.E.van Weering<sup>a,c</sup>

<sup>a</sup> *Royal Netherlands Institute for Sea Research (NIOZ), P.O.Box 59, 1790 AB, Den Burg, Texel, the Netherlands*

<sup>b</sup> *UNESCO-MSU Centre for Marine Geosciences, Geological faculty, Moscow State University, Vorobjevy Gory, Moscow 119899, Russia*

<sup>c</sup> *Department of Paleoclimatology and Geomorphology, Free University of Amsterdam, de Boelelaan 1085, 1081 HV, Amsterdam, the Netherlands*

<sup>d</sup> *ISOLAB, 1e Tieflaarsestraat 23, 4182 PC, Neerijnen, the Netherlands*

Published in *Marine and Petroleum Geology* 23, 281-296 (2006).

**Abstract**

Investigations of molecular and carbon isotopic variability of hydrocarbon gases from methane through butanes (pentanes) have been performed on six mud volcanoes from two fluid venting provinces located in the Gulf of Cadiz, NE Atlantic. The main aims were to define the basic gas types, to describe their geochemical characteristics in relationship to their sources, and to determine the secondary effects due to migration/mixing and microbial alteration. Hydrocarbon gas data reveal two groups of gases. Despite the different maturation characteristics, both gas groups are allochthonous to the erupted mud breccia and represent a complex of redeposited, secondary migrated, mixed, and microbially altered hydrocarbons. It may possibly imply the presence of hydrocarbon accumulations in the deep subsurface of the Gulf of Cadiz.

## 1. Introduction

In the various manifestations of seeps on and beneath the seafloor, migrated hydrocarbon-rich fluids exert a distinct influence on the biological resources and chemistry of ocean, geology, and environment, consequently linking the lithosphere, biosphere, hydrosphere, and atmosphere. Mud volcanoes (MVs) are representative seepage-related geomorphological features and the most imposing indication of fluid venting (Ivanov et al., 1998). In general, MVs and seeps are direct indicators of hydrocarbon migration providing sign of hydrocarbon potential in the deep sediments (Guliev and Feizullayev, 1997; Ivanov et al., 1998). The connection between seepages and deep-sited hydrocarbon reservoirs has been advocated by Link (1952) who stated that "oil and gas seeps gave the first clues to most oil-producing regions. Many great oil fields are the direct result of seepage drilling". MVs commonly occur in petroliferous regions (Guliev and Feizullayev, 1997). They are expressed in the sea-floor relief either as mounds or as negative collapse structures, caused by catastrophic eruption of fluids, especially hydrocarbon gases (predominantly methane), hydrogen sulfide, carbon dioxide, and petroleum products (Ivanov et al., 1998).

A region of active mud volcanism and gas venting was recently discovered within the Gulf of Cadiz, NE Atlantic (Kenyon et al., 2000; Gardner, 2001; Pinheiro et al., 2003). Previous multidisciplinary investigations in this area, both industrial and scientific, showed a widespread occurrence of hydrocarbon-enriched fluid discharge on the sea floor (Baraza and Ercilla, 1996; Baraza et al., 1999; Ivanov et al., 2000, 2001; Somoza et al., 1999, 2002; Gardner, 2001; Kenyon et al., 2001; Mazurenko et al., 2002, 2003; Pinheiro et al., 2003). Active mud volcanism and associated gas hydrates were for the first time documented in the deep part of the Gulf of Cadiz (from 900 m to over 3000 m of the water depth) during Training Through Research (TTR) cruises of R/V *Professor Logachev* which were carried out within the framework of the UNESCO-IOC "Floating University" Programme (Kenyon et al., 2000).

On the basis of side-scan sonar mosaic and multibeam bathymetry mapping (SEAMAP) by the Marine Physics Branch of the Naval Research Laboratory (USA) in cooperation with the Hawaii Mapping Research Group (HMRG) and the Naval Oceanographic Office (NAVOCEANO) in 1992, detailed geophysical and geological surveys during TTR-9 (1999) cruise led to the discovery of a new mud volcano province along the Moroccan-Spanish continental margin, Western Moroccan Field (WMF; Figure 1) (Kenyon et al., 2000; Ivanov et al., 2000; Gardner et al., 2001). A follow-up study in the Gulf of Cadiz, cruise TTR-10 (2000), discovered an additional mud volcano province on the Deep South Portuguese continental margin, i.e. the Deep South Portuguese Field (DSPF; Figure 1) (Kenyon et al., 2001; Ivanov 2001; Pinheiro et al., 2003).

Until now, detailed investigations of molecular and isotopic characteristics of hydrocarbon gas and organic matter in mud volcanoes (MVs) of the Gulf of Cadiz have not been carried out. Here we report the results on molecular and carbon isotopic characteristics of hydrocarbon gas collected in gas saturated pelagic sediments and mud volcano deposits (mud breccia) from six MVs

in the Gulf of Cadiz (Figure 2). The current investigation concentrated upon two primary objectives. One of the objectives was to

determine the presence of thermogenic hydrocarbons that migrated from the deep subsurface. In addition, it was projected to deduce whether hydrocarbon gases are indigenous to the erupted mud volcano sediments, so called mud breccias, or not. The second major objective of this study is to identify microbial alteration processes related to the presence of hydrocarbon gas, primarily methane, in already erupted mud volcano sediments and in the shallow subsurface. A particular effort was directed towards determination of the content, concentration levels, and correlation between individual hydrocarbons and total organic carbon (TOC) content in the sediments. Hydrocarbon gases have been characterized to their types/maturity, possible sources, and to their alteration due to microbial actions using molecular and stable carbon isotope compositions of C<sub>1</sub>-C<sub>4</sub> alkanes.

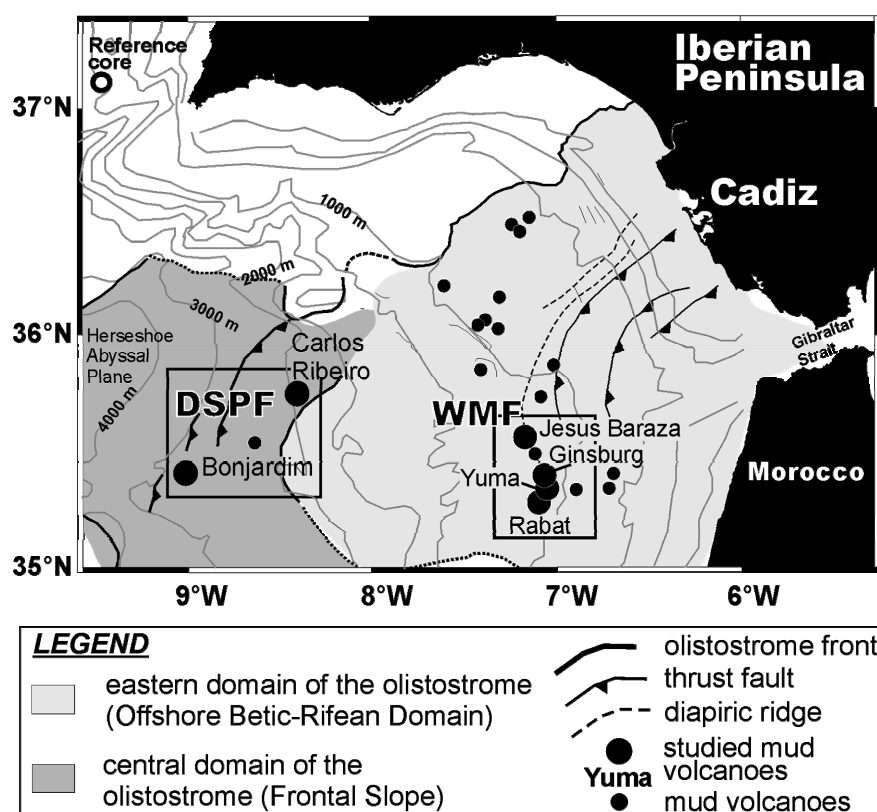


**Figure 1.** Geological map, simplified bathymetry of the Gulf of Cadiz, and the location of studied mud volcanoes (compilation of TTR data 1999-2001 and Medialdea et al., 2004). The boundary of the olistostrome body and names of its structural domains, location of thrusts and diapiric ridges are after Medialdea et al., (2004). DSPF indicates the Deep South Portuguese Field; WMF is the Western Moroccan Field.



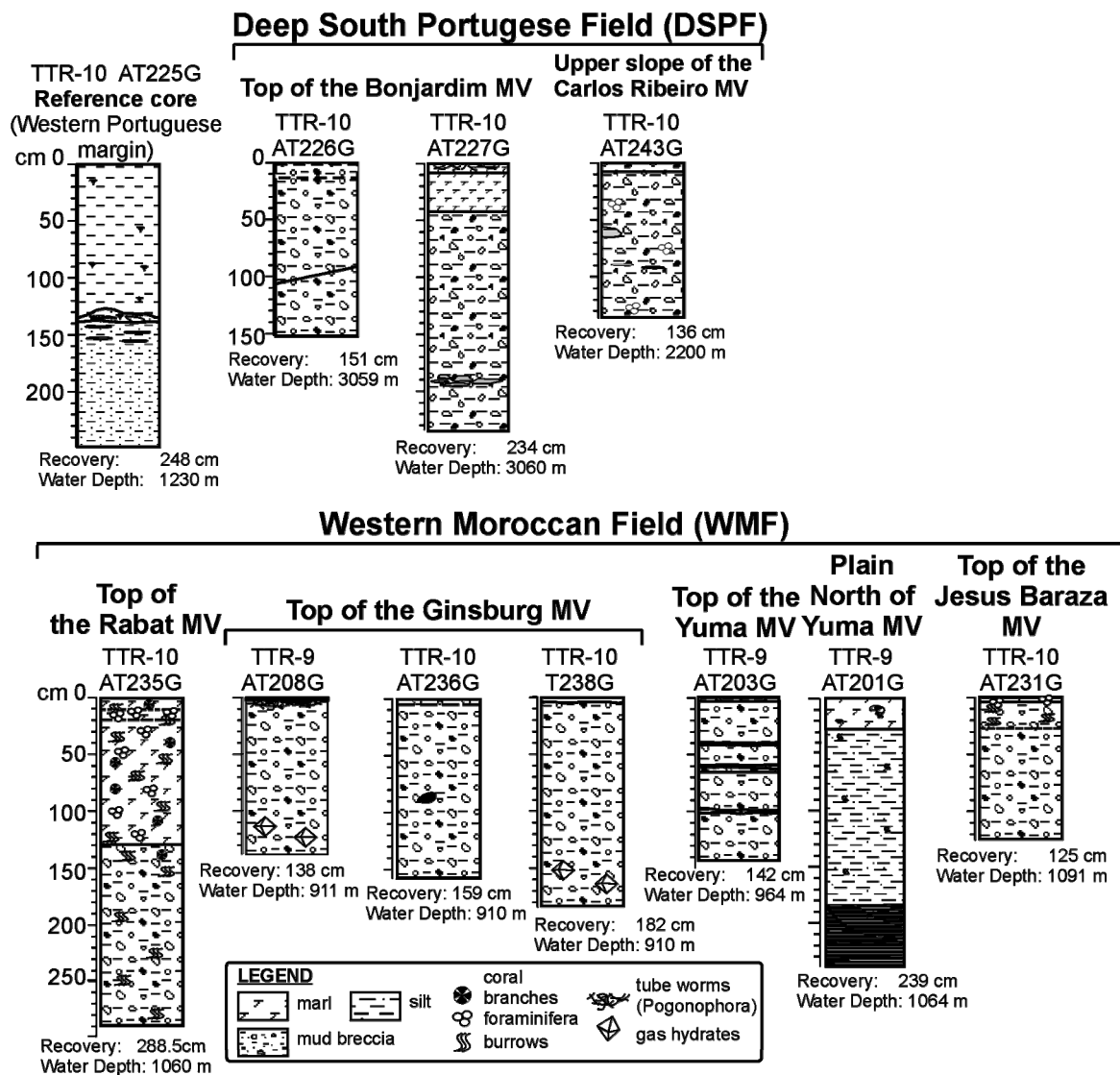


Figure 2. Schematic lithology of the studied cores.

## 2. Geological background

The Gulf of Cadiz is located in the south-western part of the Iberian margin (in the north-eastern Atlantic Ocean), west of Gibraltar Strait. It is positioned on the transition area between the Gloria transform fault zone delineating the African-Eurasian plate boundary in the Atlantic and the western-most part of the Alpine-Mediterranean orogenic belt (Maldonado et al., 1999b; Somoza et al., 2002; Medialdea et al., 2004). The geological evolution of the area is very complex, entailing several phases of rifting, convergence, and strike-slip motions since the Triassic (Srivastava et al., 1990; Maldonado et al., 1999b; Maldonado and Nelson,

**Table 1.** General information on the studied cores from the Gulf of Cadiz (Kenyon et al., 2000, 2001).

Core No	Latitude	Longitude	Geographical Setting	Depth (m)	Recovery (cm)	Remarks
<i>Reference core</i>						
TTR10 AT225G	37°06.002'N	09°28.051'W	Portuguese margin, the Marques de Pombal Area	990	248	Hemipelagic sediments
<i>Western Moroccan Field</i>						
TTR9 AT201G	35°27.305'N	07°06.518'W	Plain to the north of the Yuma MV	1064	239	Pelagic sediments
TTR9 AT203G	35°25.391'N	07°06.026'W	Crater of the Yuma MV	964	142	Mud breccia, gas saturated, strong sulfide smell
TTR9 AT208G	35°22.392'N	07°05.321'W	Crater of the Ginsburg MV	911	138	Mud breccia, gas saturated, strong sulfide smell, gas hydrates
TTR10 AT236G*	35°22.409'N	07°05.328'W	Crater of the Ginsburg MV	910	159	Mud breccia, gas saturated, strong sulfide smell
TTR10 AT238G*	35°22.409'N	07°05.330'W	Crater of the Ginsburg MV	910	182	Mud breccia, gas saturated, strong sulfide smell, gas hydrates
TTR10 AT231G*	35°35.452'N	07°12.048'W	Top of the Jesus Baraza MV	1091	125	Mud breccia, gas saturated, strong sulfide smell, 4 cm of pelagic sediments with Pogonophora tube worms
TTR10 AT235G	35°18.858'N	07°07.997'W	Top of the Rabat MV	1060	288	The upper ca. 130 cm is pelagic sediments, the rest is mud breccia
<i>Deep South Portuguese Field</i>						
TTR10 AT226G*	35°27.603'N	09°00.023'W	Top of the Bonjardim MV	3059	151	Mud breccia, gas saturated, strong sulfide smell. Gas hydrates were recovered from the structure.
TTR10 AT227G*	35°27.851'N	09°00.028'W	Terrace below the top of the Bonjardim MV	3060	234	The top ca. 42 cm is pelagic sediments with Pogonophora tube worms. The rest is mud breccia, gas saturated, strong sulfide smell.
TTR10 AT243G*	35°47.217'N	08°25.313'W	Top of the Carlos Ribeiro MV	2200	136	Mud breccia, gas saturated, strong sulfide smell.

\* Cores chosen for stable isotope study.

1999a). At present, the tectonic regime of the Gulf of Cadiz is characterized by moderate tectonic subsidence and local transpressive tectonics (Maldonado et al., 1999b).

A particular structure in the area is the large olistostrome, extending through the Gulf in a southwest direction (Maldonado et al., 1999b; Figure 1). The main emplacement of the olistostrome close to its present location took place during the late Tortonian as a consequence of a rapid increase of basement subsidence rates (Maldonado, et al., 1999b). The mud volcano provinces discovered and documented during the TTR-9 and TTR-10 cruises, are located “within” the olistostrome body (Figure.1). The WMF (Gardner, 2001; Kenyon et al., 2000; Pinheiro et al., 2003) includes the Rabat, Ginsburg, Yuma, and the Jesus Baraza MVs. These structures are grouped in the eastern domain of the olistostrome body, indicated by Medialdea et al., (2004) as Offshore Betic-Rifean Domain (Figure 1). The presence of the MVs appears to be related to fault systems (Gardner, 2001; Pinheiro et al., 2003) and to diapirs forming a set of parallel ridges with a NE-SW trend (Medialdea et al., 2004). The Bonjardim and the Carlos Ribeiro MVs are the deepest-located structures within the DSPF (Figure 1). These MVs occur in the central domain of the olistostrome, the Frontal Slope of

the Allochthonous Wedge area (Medialdea et al., 2004; Figure 1).

### 3. Materials and Methods

Seismic recording by air gun, profiling by long range OCEAN, and high resolution deep towed OREtech side scan sonar systems, led to recognition of a considerable number of MVs within the WMF and DSPF (Kenyon et al., 2000, 2001). Six of these MVs Rabat, Ginsburg, Yuma, Jesus Baraza (WMF), and Bonjardim and Carlos Ribeiro (DSPF), were selected for sampling and subsequent detailed geochemical analyses (Figure 1). The location of each core site is given in Table 1.

All cores, collected during the TTR-9 and TTR-10 cruises, were obtained using a 6 m long gravity corer (ca. 1500 kg) with an internal diameter of 14.7 cm (Kenyon et al., 2000, 2001). Subsampling for hydrocarbon gas analysis was performed taking into consideration the lithology of the recovered sediments. The standard sub-sampling and degassing procedures of sampled sediments, followed by chromatographic analysis was done. The degassing was accomplished according to the Head-space technique (Bolshakov and Egorov, 1987). To reduce intensive degassing, especially from mud breccias with gas hydrates, the subsampling of such sediments was carried out in a cold-room with a constant temperature of ca. -20°C.

The molecular composition of the C<sub>1</sub> to C<sub>5</sub> hydrocarbons including alkenes (ethene, propene and butene) and alkanes with isomeric molecular structure (*i*C<sub>4</sub> and *i*C<sub>5</sub>) were determined in the laboratory using a gas chromatograph (GC) equipped with an on-column injector and a flame ionization detector. Gas components were separated on a 3 m packed column with activated Al<sub>2</sub>O<sub>3</sub> as a stationary phase. The samples were injected at 40°C and this temperature was held for 10 min. Then the GC oven temperature was subsequently raised to 70°C at a rate of 1°C/min. The temperature was then held constant for 20 min. The results presented here are calculated according to the volume of wet sediment. It is worth to note that in spite of the absolute notations for hydrocarbon gases, part of the gases were lost on deck due to active degassing of the recovered sediments during sectioning and cutting of the cores. Besides, it is well known that the “head-space” technique is a qualitative rather than a quantitative method. In order to indicate the trend of the methane distribution profiles and to indicate a rough level of gas saturation even with its partial loss, we decided to present hydrocarbon gas data in absolute (i.e. ml/l of wet sediment) values.

The carbon isotope ratios from C<sub>1</sub> to C<sub>4</sub> including *i*C<sub>4</sub> hydrocarbon gases were measured on a Finnigan Delta S mass spectrometer with a HP 5890 GC and a GC-combustion interface. Methane was separated on a 5Å molecular sieve plot column using either split- or split-less injection, depending on the concentrations. Alkanes C<sub>2</sub>-C<sub>4</sub> were cryogenically enriched (trapping in liquid nitrogen) and separated on a poraplot-Q column. The carbon stable isotope concentrations are reported in the δ-notation (‰) relative to Vienna Pee Dee

Belemnite (VPDB) standard. The overall precision for stable carbon isotope measurements by parallel definitions was ca. 0.3 ‰ for C<sub>1</sub> and C<sub>2+</sub>.

The determination of the total organic carbon (TOC) content was carried out on samples from the same intervals as used for the hydrocarbon gas analysis. After decalcification of the samples, the measurements were accomplished on a Fisons Instruments NCS-1500 Elemental Analyzer using flash combustion at 1013°C. Standard deviations of duplicate measurements were ca. 0.3 %.

## 4. Results

### 4.1. Sediments

A great variety of sediment types, from both MVs and surrounded areas, were recovered and described during the TTR-9 and TTR-10 cruises in the Gulf of Cadiz (Kenyon et al., 2000, 2001, Pinheiro et al., 2003). These reflect different initial depositional environments, MV activity and complex hydrologic conditions among the two MV provinces. Sediments from all studied MVs showed clear indications of gas saturation. This was manifested by extensive degassing, a strong smell of sulfide and the presence of chemosynthetic fauna such as diverse *Pogonophora* tube worms.

The characteristic feature of the mud breccias from the Ginsburg, the Yuma, and the Bonjardim MVs is the presence of very thin cover of pelagic sediments which indicates that the sampling sites were located on a relatively recent mud flows (Figure 2). Methane-related *Pogonophora* tube worms were found at the surface layers of the Ginsburg (TTR9 AT208G) and the Bonjardim (TTR10 AT227G) MVs and gas hydrates were observed below 1 m sediment depth at the Ginsburg MV (TTR9 AT208G and TTR10 AT238G) (Kenyon et al., 2000, 2001; Gardner, 2001; Pinheiro et al., 2003).

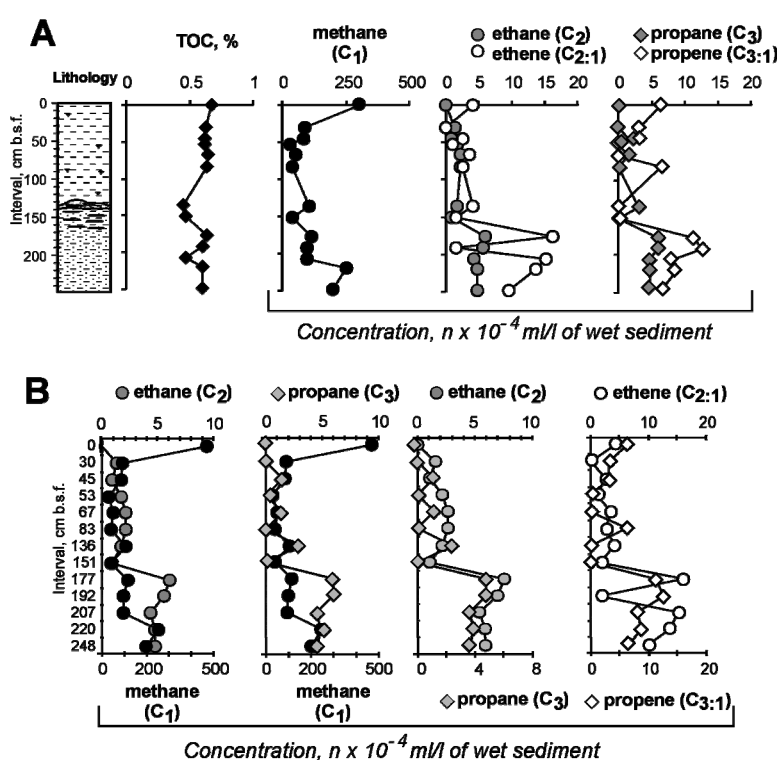


**Figure 3.** Distribution of hydrocarbon gas along sediments of reference core TTR10 AT-225G. (A)- TOC, C<sub>1</sub>-C<sub>3</sub> hydrocarbon gas profiles; (B) - Two-scale plots showing the relationship between C<sub>1</sub>, C<sub>2</sub>, C<sub>3</sub>, C<sub>2:1</sub>, and C<sub>3:1</sub>.

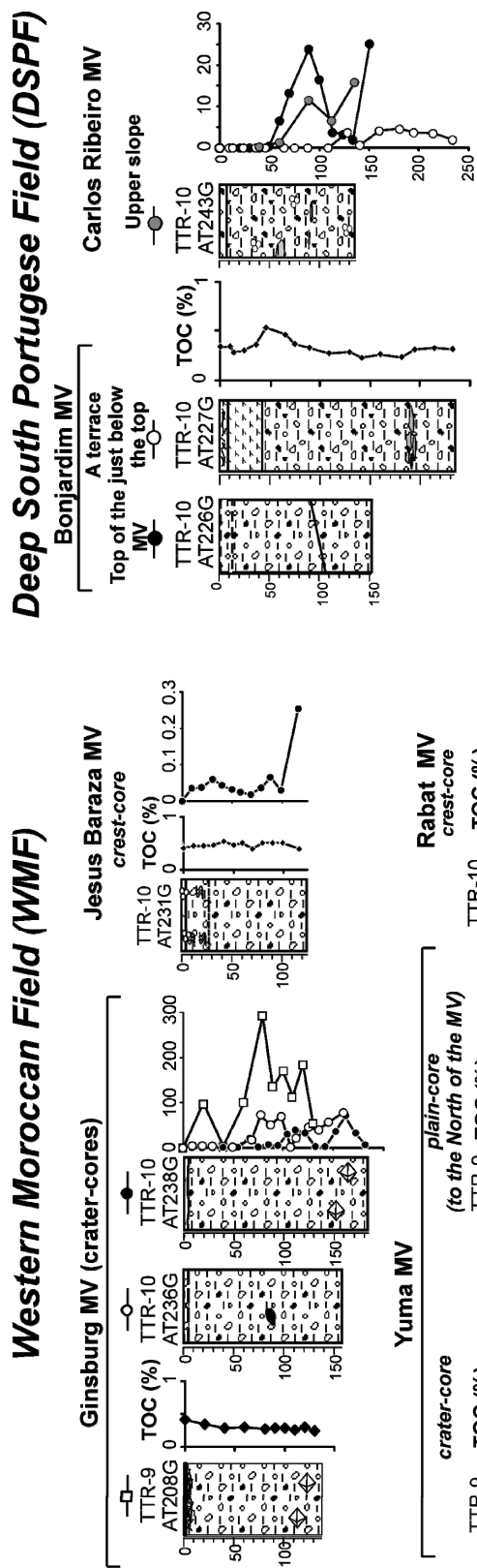


**Figure 4.** Methane concentrations (ml/l) of wet sediments and TOC (%) versus depth in mud volcano sediments from the Western Moroccan Field (WMF) and from the Deep South Portuguese Field (DSPF). For core lithologies see Figure 2.

A reference core, TTR-10 AT225G, was taken in the western Portuguese margin. The core consisted of olive-grey clayey hemipelagic sediments, mainly homogenous and structureless, occasionally bioturbated, with silty admixture and some foraminifera (Table 1, Figure 2).

#### 4.2. Molecular composition of hydrocarbon gas

##### 4.2.1. Reference core

Hemipelagic sediments of core TTR10 AT225G, show methane concentrations several orders of magnitude higher than considered for background methane levels in near-surface sediments (ca. 20-50 ppb; cf. Whiticar, 1994). Unsaturated hydrocarbons, ethene (C<sub>2:1</sub>) and propene (C<sub>3:1</sub>), are generally more abundant than saturated hydrocarbons, ethane (C<sub>2</sub>) and propane (C<sub>3</sub>), which is indicative for recent diagenetic microbial activity (Hunt, 1975; Whiticar et al., 1985;

Whiticar, 1994).

Figure 3a shows that TOC and hydrocarbons are not completely related. The presence of tracks of bioturbation in the uppermost 135 cm and numerous small lenses of silt/sand in a clayey matrix can influence both the distribution and the activity of microorganisms and, as a consequence, hydrocarbon gas profiles. It is unlikely that sediments from the reference core contain petroleum-derived components. This is indicated by the predominance of  $C_{2:1}$  and  $C_{3:1}$ , which can be formed by marine organisms and normally is nearly absent in thermogenic gases (Hunt, 1979). Simultaneously, the reference core shows a good correlation between the  $C_1$ - $C_3$  gas components (Figure 3b). All together imply the *in situ* development of hydrocarbon gas due to microbial organic matter degradation.

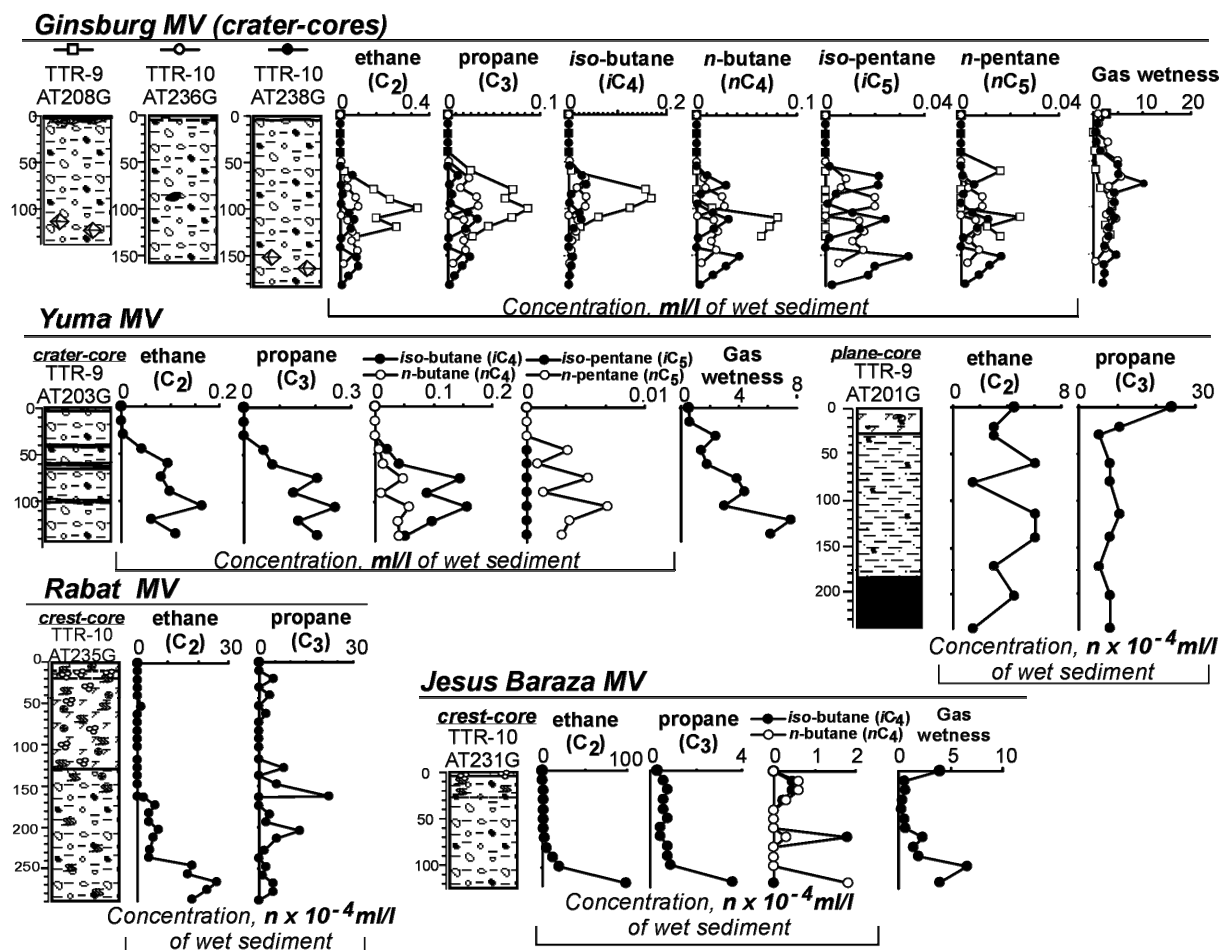
#### 4.2.2. Sediments from MVs

A majority of the sediments from the MVs of the Gulf of Cadiz is characterized by high methane concentrations relative to the reference core. Methane is the dominant hydrocarbon in all samples, comprising from 66 to 99% of the total hydrocarbon gas. The lowest methane content is mainly observed in the uppermost intervals. On average, methane from the WMF and DSPF composes 97 and 92 %, respectively, indicating relatively dry characteristics of the gas in both areas.

The wet gas components ( $C_{2+}$ ) exhibit a different molecular composition and concentration levels in the WMF and in the DSPF provinces. With exception of the sediments collected from the plain to the North of the Yuma MV (TTR9 AT201G) and from the crater of the Rabat MV (TTR10 AT235G), five saturated aliphatic compounds, ethane ( $C_2$ ), propane ( $C_3$ ), *iso*-butane (*iC*<sub>4</sub>), normal butane (*nC*<sub>4</sub>), *iso*-pentane (*iC*<sub>5</sub>), and normal pentane (*nC*<sub>5</sub>) have been identified in the majority of samples. Ethane is the dominant hydrocarbon among the methane homologues, with a highest concentration of 4 ml/l. The maximum concentration of propane is 1.0 ml/l. Butanes (*iC*<sub>4</sub> and *nC*<sub>4</sub>) sometimes exceed the level of propane. Since higher hydrocarbons ( $C_5$ - $C_7$ ) can be significantly fractionated due to condensation effects at surface pressure-temperature conditions, a selection of the data on *iC*<sub>5</sub> and *nC*<sub>5</sub> hydrocarbons is presented.

4.2.2.2. *Western Moroccan Field (WMF). Methane.* Sediments collected from the craters of the Ginsburg (TTR9 AT208G, TTR10 AT236G, and TTR10 AT238G) and the Yuma (TTR9 AT203G) MVs show the highest methane concentrations so far measured in the Gulf of Cadiz, 292 ml/l and 207 ml/l, respectively (Figure 4). These values signify an ample evidence of methane migration or generation. In contrast, methane concentrations in pelagic sediments collected from the plain to the North of the Yuma MV (TTR9 AT201G) are considerably

## Western Moroccan Field (WMF)



## Deep South Portuguese Field (DSPF)

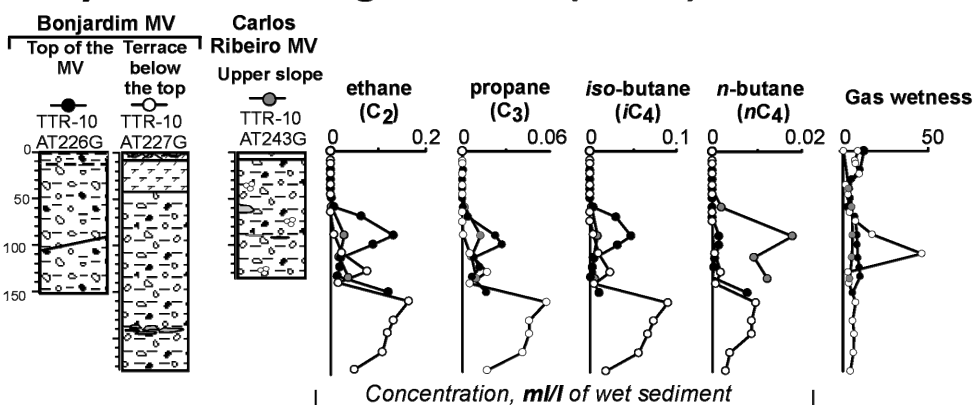


**Figure 5.** C<sub>2+</sub> concentrations versus depth in mud volcano sediments from the WMF and DSPF. For the core lithologies see Figure 2.

lower relative to the mud breccia from the crater (from  $113.0 \times 10^{-4}$  ml/l to 3.7 ml/l). Such a difference in methane levels between the crater and plain areas indicates that active venting is principally concentrated within the central part of the Yuma MV.

Sediments from the crests of the Rabat (TTR10 AT235G) and the Jesus Baraza (TTR10 AT231G) MVs (Figure 1) also demonstrate discernable methane levels. The methane concentrations however are to a great extent lower compared with those in the mud breccias from craters of the Ginsburg and the Yuma MVs (Figure 4). Hence, the methane concentration data indicate that the Ginsburg and the Yuma are the most active MVs among the four investigated within the WMF, and that the present fluid flow is mainly found in these structures.

*Other light hydrocarbons ( $C_{2+}$ ).* The anomalies of  $C_{2+}$  levels, as well as for the  $C_1$ , are related to mud breccias from the main craters of the Ginsburg (sampling sites TTR10 AT236G, TTR10 AT 238G) and the Yuma (TTR9 AT203G) MVs (Figure 5). Gas measurements show that the concentration levels of ethane through pentanes ( $C_2$ - $C_5$ ) in these structures are the highest ever detected in the Gulf of Cadiz. At  $\sim 50$  cm below sea floor (bsf), the mud breccias contain two to three orders of magnitude more of each of the hydrocarbon gases than the reference core (Figure 3a). There is no correlation between hydrocarbon gases and TOC content, indicating the allochthonous nature of  $C_{2+}$  alkanes to the mud breccias.

The plain-core from the Yuma MV (TTR9 AT201G) and the crater-core from the Rabat MV (TTR10 AT235G) are characterized by presence of only  $C_2$  and  $C_3$  hydrocarbons with concentration levels close to the background values. Mud breccia from the Rabat MV is overlaid by ca. 130 cm of pelagic sediments, indicating relatively old mud flow and lack of fluid transport processes. Even though, sediments from both sampling locations show absence of correlation between TOC and hydrocarbon gas distributions. This denotes an allochthonous nature of the gaseous components.

*4.2.2.3. Deep South Portuguese Field (DSPF). Methane.* The deep-seated Bonjardim (sampling sites TTR10 AT226G, TTR10 AT227G) and Carlos Ribeiro (TTR10 AT243G) MVs (Figure 1) show methane concentrations from 0.1 ml/l to 25 ml/l which are considerably higher relative to the measured background values. Compared with the methane concentrations from the cores of the Ginsburg and the Yuma MVs crater (WMF), the methane level in the Bonjardim and the Carlos Ribeiro MVs is lower (Figure 4).

*Other light hydrocarbons ( $C_{2+}$ ).* The  $C_{2+}$  levels in the Bonjardim (TTR10 AT 226G, TTR10 AT 227G) and the Carlos Ribeiro (TTR10 AT 243G) MVs, are similar to those determined in the craters of the Yuma and the Ginsburg MVs (WMF). High concentrations of



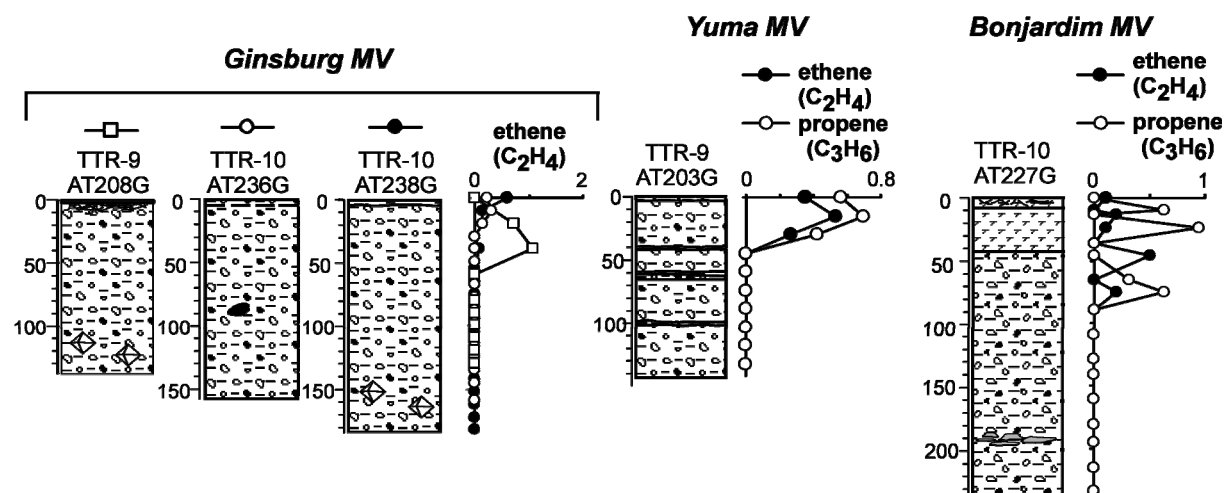


**Figure 6.** Examples of alkene occurrences. Concentrations  $n \times 10^{-4}$  ml/l of wet sediment. Alkenes occur in relation with the “methane’s consumption-signature” and  $C_{2+}$  diminution. This suggests that the formation of unsaturated hydrocarbons is related to the consumption of  $C_{2+}$ . For the core lithologies see Figure 2.

butanes ( $iC_4$  and  $nC_4$ ) and pentanes ( $iC_5$  and  $nC_5$ ) were detected in all sampling locations within the DSPF (Figure 5). None of the distribution profiles show a relationship with the TOC content, implying that  $C_{2+}$  alkanes are not indigenous to the erupted mud breccias.

*Unsaturated hydrocarbon gases in WMF and DSPF.* Appearance of unsaturated gases, ethene ( $C_{2:1}$ ) and propene ( $C_{3:1}$ ), is coherent with  $C_{2+}$  diminutions. Such a tendency is noticed for the sediments from the crater/crest of the Yuma, Ginsburg, Jesus Baraza, and the Bonjardim MVs (Figure 5, 6). It is not clear which peculiar microorganisms and via which pathways are capable to degrade wet gas components and, directly or indirectly, biosynthesize unsaturated hydrocarbon gases. Nonetheless, the occurrence of the alkenes in relation with the “methane’s consumption-signature” and  $C_{2+}$  diminution, additionally may suggest that wet gas components, as well as methane, were selected for microbial intake and that the formation of unsaturated hydrocarbons is related to the consumption of  $C_{2+}$ .

#### 4.3. Carbon isotopic composition of $C_1$ - $C_4$ alkanes

Six cores from the WMF and DSPF were selected for a detailed study of the vertical distribution of the  $C_1$ - $C_4$  stable carbon isotopic composition ( $\delta^{13}C$ ). The obtained data reveal significant variations in carbon isotopic composition within the ca. 50-100 cm sedimentary depth interval, consistent with the compositional changes of the gas as discussed in the previous sections. This leads to caution with regards to the stable carbon isotope data (Table 2).

## 4.3.1. Methane

The methane carbon isotope composition ranges from -23 to -67 ‰ (Table 2). The heaviest  $\delta^{13}\text{C}_{\text{C}_1}$  values were obtained from the mud breccia of the Jesus Baraza MV (WMF) although the values are uneven along the core (see Table 2). The lightest values of  $\delta^{13}\text{C}_{\text{C}_1}$  were obtained from mud breccias of the Bonjardin MV (DSPF). Schoell (1983) proposed that the isotopic composition of methane is not significantly changed after its generation. The changes in isotope signature can be expected when the gas become mixed with another gas during migration (Schoell, 1983) or/and during microbial methane oxidation (Bernard, 1979), which is less likely to be significant at greater depth (James and Burns, 1984). Methane consumption, reflected in  $^{13}\text{C}$  enrichment (Lebedew et al., 1969), is detected in the uppermost sediments from the Ginsburg, Jesus Baraza, Carlos Ribeiro, and the Bonjardim MVs. This correlates well with the methane concentration profiles (Figure 4). In spite of the methane oxidation signature within the uppermost ~ 50-100 cm, Figure 7 shows that the  $\delta^{13}\text{C}_{\text{C}_1}$  values differ between the WMF and the DSPF. This implies that the WMF and DSPF contain methane from two different sources.

Table 2. Stable carbon isotope compositions.

Core No	Interval, cm b.s.f.	Carbon isotopes				
		C <sub>1</sub>	C <sub>2</sub>	C <sub>3</sub>	iC <sub>4</sub>	nC <sub>4</sub>
<i>Western Moroccan field</i>						
	10	-31	-27	-32	-25	-26
Jesus	30	-24	-31	-33	-27	-24
Baraza	50	-27	-30	-27	-29	-27
MV	69	-30	-16	-31	-34	-26
TTR10	79	-32	-25	-27	-27	-22
AT-231G	89	-28	-19	n/d	n/d	n/d
	Average	-29	-25	-30	-28	-25
Ginsburg	10	-54	-16	n/d	n/d	n/d
MV	30	-36	-12	n/d	n/d	n/d
TTR10	88	-42	-23	-22	-25	-24
AT-236G	135	-41	-24	-23	-26	-24
	Average	-43	-19	-23	-25	-24
	0	-35	-23	-22	n/d	n/d
	30	-44	-20	-22	-28	-30
Ginsburg	65	-41	-22	-22	-25	-24
MV	85	-56	-30	-21	-27	-19
TTR10	105	-42	-23	-22	-25	-24
AT-238G	142	-41	-24	-23	-26	-24
	162	-41	-24	-24	-26	-25
	182	-40	-24	-23	-26	-25
	Average	-43	-24	-22	-26	-24
<i>Deep South Portuguese field</i>						
Bonjardi	20	-51	-29	-23	n/d	n/d
m MV	50	-64	-23	-13	n/d	n/d
TTR10	90	-62	-31	-18	-27	n/d
AT-226G	Average	-59	-28	-18		
	24	-51	-34	-25	-30	-27
	36	-63	-26	-27	-28	-22
Bonjardi	46	-57	-28	-26	-27	-25
m MV	75	-58	-24	-24	n/d	n/d
TTR10	141	-52	-28	-21	-28	-20
AT-227G	161	-52	-29	-21	-28	-21
	195	-50	-28	-22	-28	-20
	Average	-55	-28	-24	-28	-22
Carlos	0	-23	n/d	n/d	n/d	n/d
Ribeiro	40	-50	-14	n/d	n/d	n/d
MV	60	-66	-20	-22	-26	-23
TTR10	136	-58	-25	-23	-27	-24
AT-243G	Average	-49	-20	-22	-26	-23

n/d - not determined

4.3.2. Other light hydrocarbons (C<sub>2+</sub>)

The wet gas components also show a significant variability in  $\delta^{13}\text{C}$  composition (Table 2). The  $\delta^{13}\text{C}$  values of C<sub>2</sub> and C<sub>3</sub> have a range of -14 to -34 ‰ and of -13 to -31 ‰,

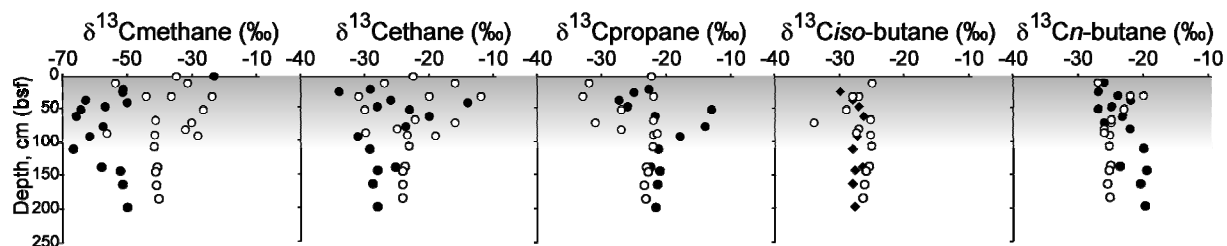


**Figure 7.** Stable carbon isotope composition of C<sub>1</sub>-C<sub>4</sub> alkanes as a function of depth. The grey area indicates interval with irregular δ<sup>13</sup>C<sub>C2-C4</sub> values which resulted from vital microbial actions. Black circles indicate samples from the DSPF, and white circles - from the WMF.

respectively. The highest scatter of the δ<sup>13</sup>C<sub>C2-C3</sub> values is observed within the uppermost ~ 50-100 cm (Figure 7). Compared with C<sub>2</sub> and C<sub>3</sub> alkanes, the δ<sup>13</sup>C values of *i*C<sub>4</sub> and *n*C<sub>4</sub> display less variability within this interval. Figure 7 shows that the carbon isotope values of C<sub>2</sub>-C<sub>4</sub> become more regular below ca. 100 cm bsf, which most likely indicates a reduction of microbial activity with depth.

## 5. Discussion

### 5.1. Compositional variations of C<sub>2</sub>+

The relative proportions of C<sub>1</sub>-C<sub>4</sub> *n*-alkanes in a gas sample provide an initial classification of the natural gas type and may identify the related microbial alteration of the gaseous components. Two molecular ratios, the gas wetness and the Bernard parameter, were applied for gas data to describe the compositional variations of the hydrocarbon gases from the two mud volcano provinces in the Gulf of Cadiz. Commonly, maximum gas wetness is associated with the peak of hydrocarbon generation (Stahl, 1977; Hunt, 1979), while microbial methane oxidation can result in similar (mature) gas wetness characteristics due to an increase of C<sub>2</sub>+ compounds (Coleman et al., 1981). Alternatively, microbial alteration of wet gas components can reduce gas wetness. Figure 8 shows the

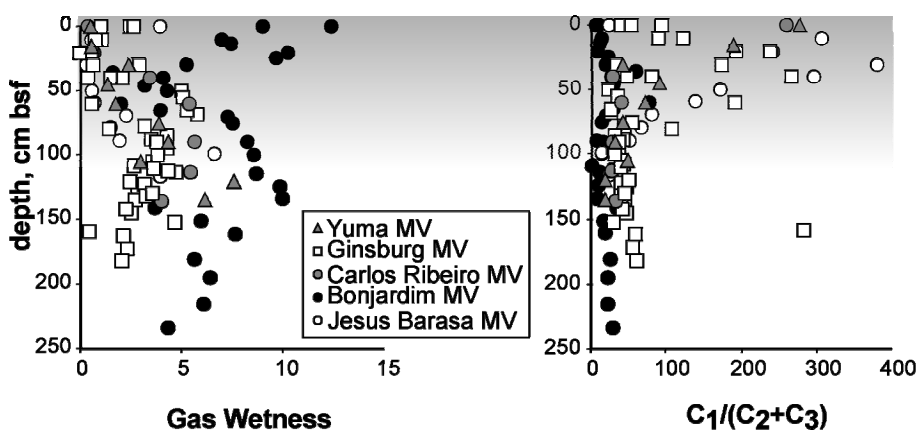


**Figure 8.** Gas wetness and Bernard Parameter as functions of depth. The grey area indicates interval where compositional variations in the hydrocarbon gases forced by microbial interactions are observed.

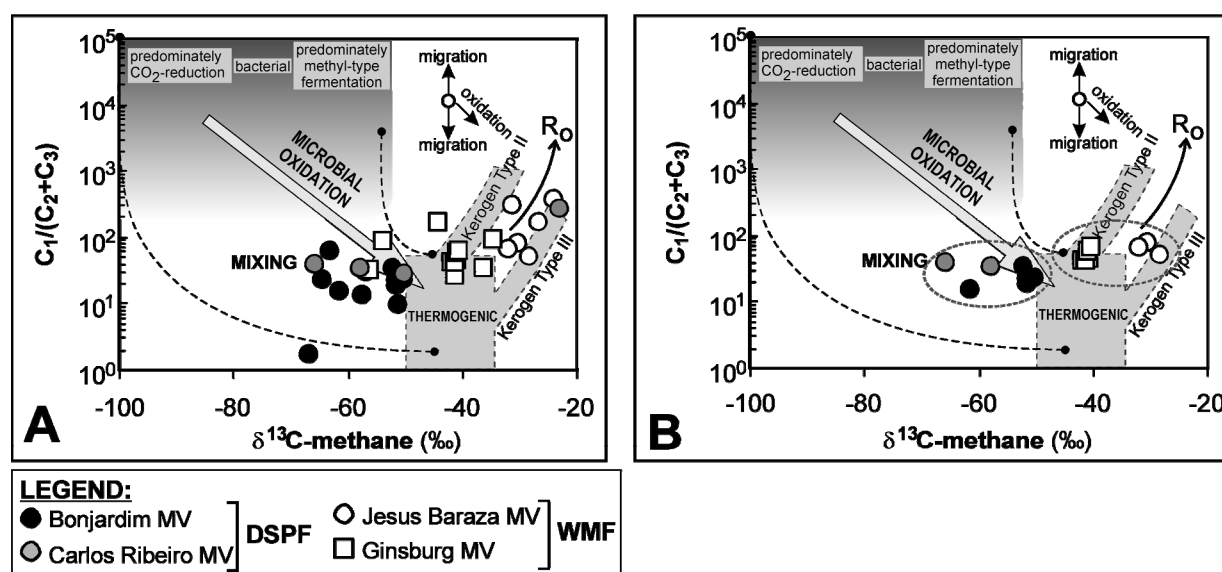


**Figure 9.** Bernard diagram to delineate gas types (after Whiticar, 1994). Two different groups of gases in the WMF and DSPF are recognized. The WMF gas represents mature gases, ( $R_o < 1.2\%$ ), derived from kerogen Type II and/or a mixture of kerogens of Type II and III. The DSPF gas consists of a mixture of thermogenic and bacterial gases. A -the complete suite of gas data; B- the data from the intervals below 60 cm bsf.

compositional variations observed in hydrocarbon gases within the uppermost ca. 50-100 cm below sea floor (bsf). This interval is characterized by a great variability of the molecular gas composition due to diverse microbial actions. Within this interval, methane oxidation is reflected in a significant increase of the gas wetness and  $C_1/(C_2+C_3)$  values, and *vice versa*, a decrease of the gas wetness and  $C_1/(C_2+C_3)$  values most likely implies consumption/degradation of wet gas components (Figure 8).

At the sediment surface the microbial activity, especially at seepage locations, is exceptionally high. Fluid fluxes frequently support highly diverse and productive ecosystems, thriving in response to different environments created by advection of migrated fluids. Microbially-driven anaerobic/aerobic oxidation of methane and degradation of wet gas components can significantly modify the molecular and carbon isotope compositions of the initially migrated gas mixture. A prominent feature of most of the methane curves in the MVs of the Gulf of Cadis is a characteristic concave-up-shape (Figure 4), considered to result from microbial methane consumption (Martens and Berner, 1974; Barnes and Goldberg, 1976; Reeburgh, 1976; Alperin and Reeburgh, 1984). Remarkable, the wet gas components also show a decrease or even deficiency in the uppermost part of the sedimentary column (Figure 5). Their distribution patterns are consistent with the  $C_1$  “concave-up” curve geometry (Figure 4). This implies that together with methane,  $C_{2+}$  gas components were also subjected to consumption.

Summarizing, the gas concentration data, their down-core distribution profiles, and their molecular ratios reveal that the studied mud volcano provinces in the Gulf of Cadiz are characterized by the presence of allochthonous gas with a high input of thermogenically formed hydrocarbons due to anomalous concentrations of C<sub>2+</sub> gas constituents. The data also signify that the molecular composition and concentration of the gas are regulated by upward diffusion and biological oxidation within the subsurface at ca. 50-100 cm bsf. The latter indicates that in the studied locations migrated C<sub>1</sub> and C<sub>2+</sub> components are consumed before they can escape into the overlying water column.

### 5.2. Genetic types of gases

To characterize the hydrocarbon gases from the two mud volcano provinces, we combined molecular concentrations, contents, and stable carbon isotope signatures of C<sub>1</sub>-C<sub>4</sub> alkanes. As was shown in the previous sections, microbial activity in the uppermost 50 to 100 cm resulted in significant changes of concentrations, molecular and carbon isotope composition of the C<sub>1</sub>-C<sub>4</sub> hydrocarbons in both the WMF and DSPF. The δ<sup>13</sup>C values of C<sub>1</sub>-C<sub>4</sub> alkanes below ca. 60 cm of the sediments do not seem to be significantly affected by *in situ* microbial actions. This suggests that hydrocarbon gas samples from the lower intervals could represent an “original” gas mixture, thus containing information on the sources, maturity and microbial alterations in the deeper subsurface. Accordingly, for the characterization of genetic gas types gas data were used only from intervals below ca. 60 cm. The complete gas data though is also presented to the reader for the comparison.

Concentrations of methane and wet gas components in all studied locations of the Gulf of Cadiz are clearly anomalous (Figure 4 and 5). Ethane and propane so far have never been generated in significant quantities by microbial processes (Oremland et al., 1988). Ethane, propane and butanes are formed primarily between 70°C and 150°C with peak generation around 120°C (Hunt, 1995). High concentrations of C<sub>2+</sub> especially C<sub>4</sub> and C<sub>5</sub> hydrocarbons are expected if thermogenic gases are present (Cline and Holmes, 1977; Sandstrom et al, 1983). This signifies that gases from both mud volcano provinces of the Gulf of Cadiz are characterized by input of thermogenic hydrocarbons from deeper sources. Besides, the down-core concentration profiles of C<sub>1</sub>-C<sub>4</sub>(C<sub>5</sub>) hydrocarbons (despite their difference in concentration levels) show an absence of correlation with the TOC content, which also indicates an allochthonous nature of the gas to the hosting mud breccias.

Figure 9 shows the Bernard diagram (Bernard et al., 1978; Faber and Stahl, 1984), modified by Whiticar (1994) to classify hydrocarbon gas. Two distinct genetic gas types can be recognized for the WMF and for the DSPF (Figure 9a). Figure 9b shows gas data from the lowermost parts of the sediments. The uppermost intervals, where microbial alteration of C<sub>1</sub>-

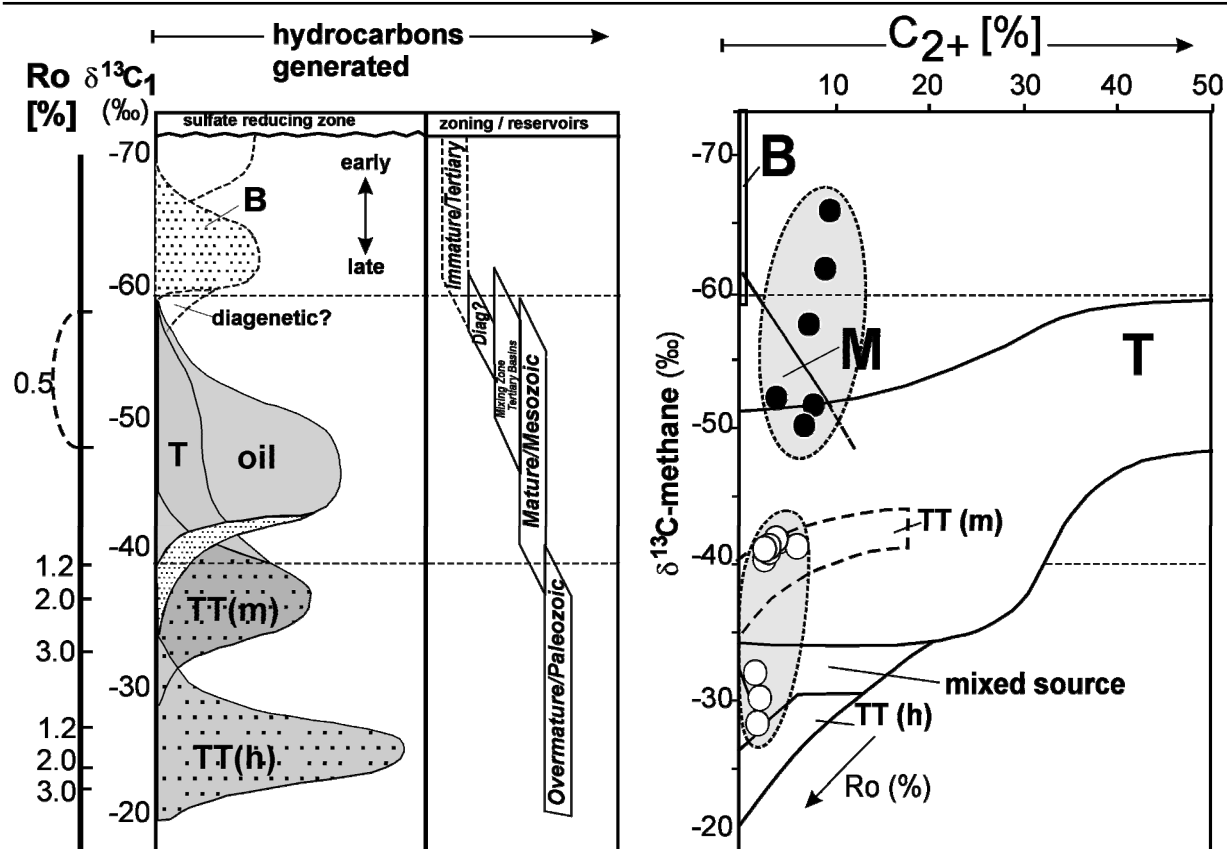


**Figure 10.** Relative concentration of wet gas components in relation to stable carbon isotope composition of methane (after Schoell, 1983) showing two different gas groups in the WMF (white circles) and in the DSPF (black circles). Primary gases (B - bacterial, T - thermogenic associated, and TT (m) - nonassociated dry gases from sapropelic liptinic organic matter, TT(h) - nonassociated gases from humic organic matter) are distinguished on the basis of fields determined by Schoell (1983). Mixing of primary gases (M - mixed gases) reflects in the different proportions of thermogenic and bacterial gases. The data set includes values from intervals below 60 cm.

C<sub>4</sub> alkanes is taking place, have been excluded. As a result, two different gas groups is more clearly highlighted (Figure 9b).

MVs from the WMF, the Ginsburg and the Jesus Barasa, depict mature gas characteristics with  $\delta^{13}\text{C}_{\text{C}_1}$  values ranging from -28 to -42 ‰ (Table 2). The C<sub>2+</sub> content varies between 1 and 6 % from the total hydrocarbon gases. Concurrently, MVs from the DSPF, the Bonjardim and the Carlos Ribeiro, are characterized by less mature gas signatures (Figure 9). These gases have  $\delta^{13}\text{C}$  values of methane between ca.-50 and -67 ‰ although the C<sub>2+</sub> content ranges from 3 to almost 10 %.

The stable carbon isotope composition of methane is dependent on type and maturity of the initial source (Galimov, 1968; Stahl, 1977, 1979). Migration and/or mixing may be a mechanism of carbon isotope fractionation, and is reflected in either enrichment or depletion with  $^{12}\text{C}$  (Galimov, 1967; Lebedev and Syngayevski, 1971). Figure 9 show, that the composition characteristic of gas from the MVs of the WMF falls in the “thermogenic gas field”. Besides, the source, from which the gas was derived, is indicated on the diagram as kerogen of Type II for the Ginsburg MV and as a mixture of kerogens II and III for the Jesus Baraza MV.

Hydrocarbon gas from the DSPF represents a mixture of gases of various origins. We consider that an admixture of bacterial gases is the reason for an immature characteristic of the methane, whereas the relatively high content of wet gas components indicates the presence of thermogenic hydrocarbons (Figure 9).

Using another principle for genetic characterization of gases outlined by Schoell (1983), two different gas groups can also be distinguished. Applying the same parameters (i.e.  $\text{C}_{2+}$  versus  $\delta^{13}\text{C}_{\text{C1}}$ ), Schoell (1983) considered only three processes, maturation, mixing, and migration, which may influence the methane carbon isotope composition and  $\text{C}_{2+}$  concentration. In fact, the data (Figure 10) confirm the interpretation of the Bernard diagram and also clearly indicate the presence of two different groups of gases in the WMF and DSPF. The WMF gas represents two mature gases, ( $R_o < 1.2\%$ ), derived from kerogen Type II (the Ginsburg MV) and a mixture of kerogens of Type II and III (Jesus Boraza MV). The DSPF gas is a mixture of thermogenic and bacterial gases with relatively immature characteristics (the beginning of the oil window;  $R_o \leq 0.5\%$ ) (Figure 10). In fact, the mature characteristics of the gas from the WMF coincide with geochemical data obtained from a gas reservoir in a faulted anticline in the Arkoma basin, Oklahoma (Stahl et al., 1981).

### 5.3. Secondary processes

#### 5.3.1. Mixing

The evidence of gas mixing for both the WMF and DSPF is shown in Figure 11, which reflects an almost linear relation between the  $\text{C}_{2+}$  contents and the

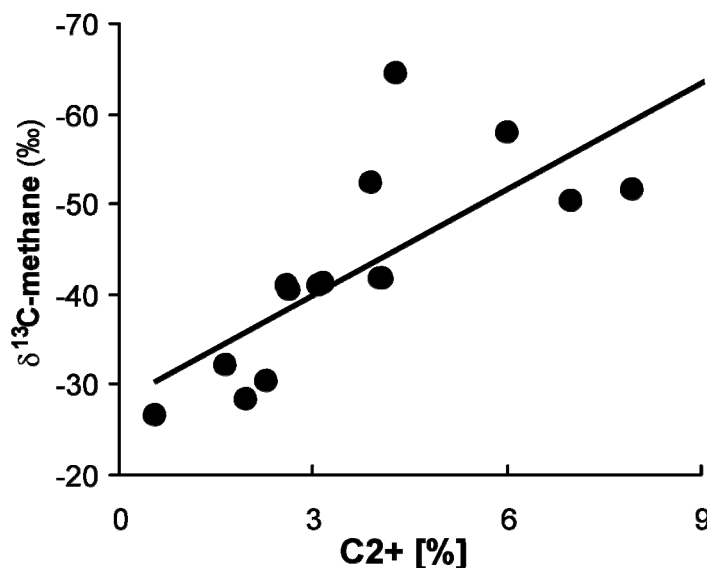


**Figure 11.** Gases of mixed bacterial and thermogenic origin. Compositional variations are caused by various mixing proportions of the gases (after Schoell, 1983).

$\delta^{13}\text{C}$  signatures of methane (Schoell, 1983). Mixing of gases of different origins is a common phenomenon (Whiticar, 1994), which indicates that gas components are not necessarily co-genetic. In a thermogenic co-genetic  $\text{C}_1\text{-C}_2$  pair, methane is depleted in  $^{13}\text{C}$  between 5 and 10 ‰ relatively to the ethane (Silverman, 1971; Deines, 1980). An admixture of a biogenic gas will be reflected in a significant carbon isotope difference between methane and the other wet gas components, i.e. methane will appear much lighter relative to  $\text{C}_2\text{-C}_4$ . The average value of  $\delta^{13}\text{C}_{\text{C}_1}$  in the DSPF is -57 ‰ while the average value of  $\delta^{13}\text{C}_{\text{C}_1}$  in the WMF is -38 ‰ (Table 2). If a

$\delta^{13}\text{C}$  of -70 ‰ is assumed for pure biogenic methane (Chung et al., 1988), a proportion of ca. 50 % of biogenic gas in DSPF can be calculated as mixed with thermogenic gas of -30 ‰ (Schoell, 1983) from humic source materials. Nevertheless, it is difficult to recognize the source or sources for the methane from the DSPF. Mixing of early-formed biogenic gas and later formed thermogenic gas results in a lack of abilities to differentiate the thermogenic gas due to compositional changes caused by mixing (Rice and Claypool, 1981). Besides, the earliest formed thermogenic methane is isotopically light,  $\delta^{13}\text{C}$  values are -55 ‰ (Sackett, 1978; Stahl et al., 1979).

Figure 12 shows that in general methane is not co-genetic with ethane. Besides, the  $\delta^{13}\text{C}$  values of ethane from the DSPF are on average -27 ‰, which is the signature of ethane in mixed gases (Matavelli et al., 1983). In contrast, the ethane from the WMF has a more

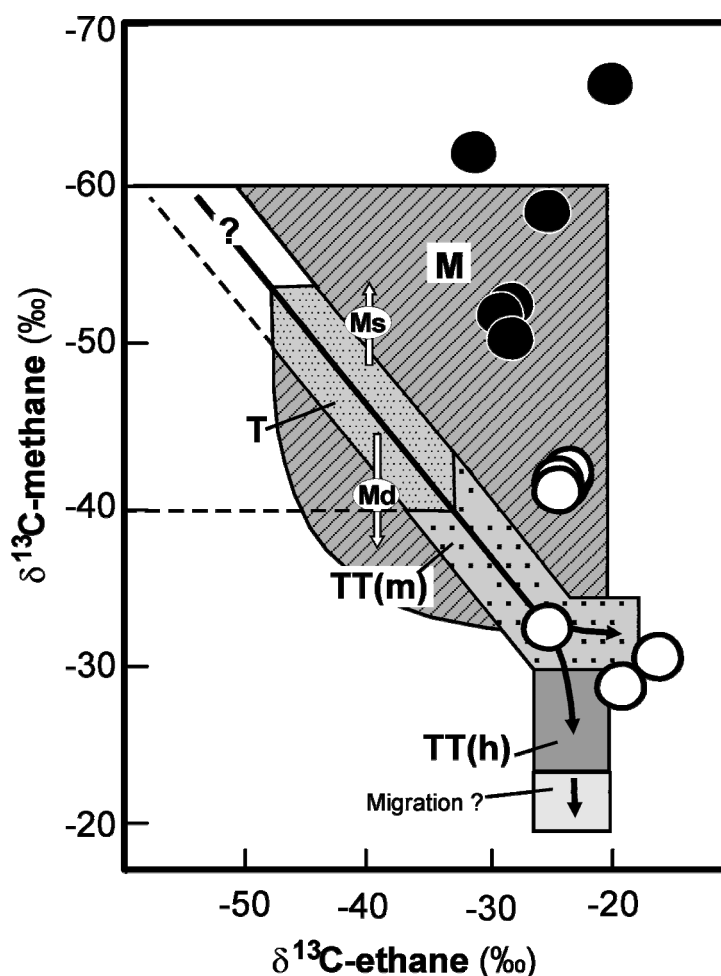


**Figure 12.** Mixing/migration diagram. Genetical definition of hydrocarbon gas by relation of  $\delta^{13}\text{C}$  changes in ethane and methane (after Schoell, 1983). Gas from the WMF (white circles) is characterized by mixture of two thermogenic gases. Gas from the DSPF represents a mixture of thermogenic and bacterial gases.



positive carbon isotopic composition, on average -23 ‰. Furthermore, the C<sub>1</sub>-C<sub>2</sub> pair from the Ginsburg MV demonstrates a close relation between methane and ethane on the basis of the small differences in their carbon isotopic compositions (Table 2). The decrease in  $\delta^{13}\text{C}$  difference between C<sub>1</sub> and C<sub>2</sub> is a result of an increase of the thermal maturity (James, 1983). This is consistent with Figure 10, showing mature characteristics of the gas from the Ginsburg MV.

### 5.3.2. *Microbial alteration*

The level of maturity and the original gas source is reflected in the carbon isotopic composition of C<sub>2</sub>-C<sub>4</sub> gas components (James, 1990). Microbial alteration extensively affects the maturity relationship as shown in the  $\delta^{13}\text{C}$  signal of gaseous alkanes, especially in the topmost decimeters of marine sediments. In unaltered gases, the carbon isotopic compositions of C<sub>1</sub>-*n*C<sub>4</sub> (excluding *i*C<sub>4</sub>) follow a smooth progression from C<sub>1</sub> to *n*C<sub>4</sub> (James 1983), which is not the case for our gas data set (Table 2). Mud volcanoes from both provinces show reduction of ethane, which is reflected in its <sup>13</sup>C enrichment (Table 2). Anomalously enriched ethane was detected in the topmost parts of the Ginsburg MV (WMF) and Carlos Ribeiro MV (DSPF), which is in conjunction with ethane concentration profile indicating its consumption in the uppermost decimeters of sediments (Table 2, Figure 5). In this aspect, obtained ethane data partly supports the findings of Clayton et al., (1997) and Pallasser (2000), where authors showed most positive  $\delta^{13}\text{C}$  values of ethane as a consequence of its microbial alteration together with relatively unaltered  $\delta^{13}\text{C}$  signatures of propane (Clayton et al, 1997; Pallasser, 2000). Enriched in <sup>13</sup>C ethane was detected in the deeper intervals from the Jesus Baraza MV (WMF), which is probably also result from selective uptake of this alkane by unknown type of ethane-degrading microorganisms.

In contrast, James and Burns (1984) reported microbial alteration of subsurface reservoir gas by the selective removal of propane. This resulted in an anomalous heavy propane carbon isotopic composition and ethane was relatively unaffected (James and Burns, 1984). In the unaltered gases, the  $\delta^{13}\text{C}$  values of propane constitute ca. -27 to -28 ‰ (James, 1983). Hence, both the WMF and the DSPF, also show propane alteration,  $\delta^{13}\text{C}_{\text{C}_3}$  comprises by a mean -23 ‰ and -21 ‰, respectively (Table 2). Except sediments from the Bonjardim MV,  $\delta^{13}\text{C}$  values of propane remain similar along the sediments. This can imply that measured propane was microbially changed in the subsurface before it was transported by fluid upward.

Microbial alteration is also clearly illustrated in the butane dataset (Figure 13). Although the  $\delta^{13}\text{C}$  values of *iso*- and *n*-butanes are generally in the same range in the gases from both mud volcano provinces, the butanes from the DSPF display a greater variability in their  $\delta^{13}\text{C}$  values (Figure 13; Table 2). Hence, the isotopically heavy values of *n*-butane from

the DSPF suggest that there has been a reduction of  $nC_4$  likely as a result of its microbial consumption. In contrast, butanes from the WMF have relatively steady stable carbon isotope characteristics, indicating their possible co-genetic nature and absence of a microbial alteration signal.

Thus, propanes from both locations and  $n$ -butane from DSPF have been microbially altered in the deeper subsurface, which makes the interpretation of their maturity/sources difficult.

#### 5.4. Geological and tectonic controls

Both the WMF and the DSPF are located within the olistostrome unit representing huge allochthonous deposits emplaced in the Gulf of Cadiz in the late Tortonian (Maldonado et al., 1999b; Somoza et al., 1999). Taking into consideration the sedimentary cover and the present structure of the Gulf (Medialdea et al., 2004), it is quite possible that olistostrome deposits could possess subsurface gas accumulations, representing a re-deposited mixture of hydrocarbons migrated from below. The sediments of the olistostrome masses include Miocene units from Langhian to Messinian and are composed of various clays with some intervals of limestone and sand lenses (Maldonado et al., 1999b). MVs from the DSPF appear within the central domain of the olistostrome (Figure 1), which includes the complete Miocene depositional sequences and constitutes the bulk of the sedimentary infill of the slope basis including fragments of Mesozoic and plastic Triassic materials (Medialdea et al., 2004). The area is characterized by compressive deformation, thrusting and the presence of deep faults which could act either as pathways for fluid migration or as a structural trap for hydrocarbons, or may provide a link between sedimentary units from different stratigraphic horizons with different physical properties.

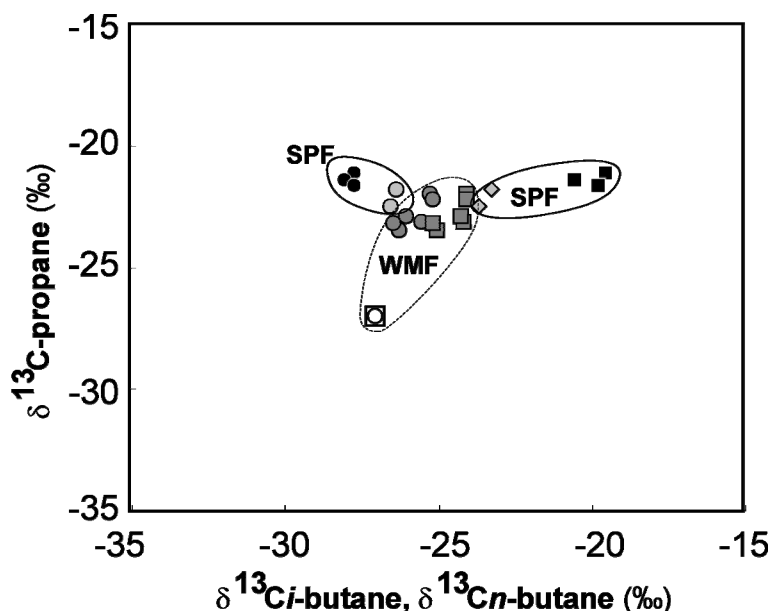


**Figure 13.** Relationship of carbon isotope ratios for propane versus  $i$ -butane and  $n$ -butane.  $iso$ -Butane/propane: DSPF: (●) Bonjardim MV; (○) Carlos Ribeiro MV; WMF: (●) Ginsburg MV; (○) Jesus Baraza MV.  $n$ -Butane/propane: DSPF: (■) Bonjardim MV; (◇) Carlos Ribeiro MV; WMF: (■) Ginsburg MV; (□) Jesus Baraza MV. The data set includes selection of values below ca. 60 cm.

The tectonic regime in the eastern domain of the olistostrome, where the WMF is located, is different. Here extensive mud diapirism and mud volcanism is a characteristic feature. The Yuma, Ginsburg, Jesus Baraza, and the Rabat MVs have a linear orientation, reflecting their relation with a NW-SE orientated strike-slip fault system observed on the seafloor (Gardner, 2001). The trend of this fault system is coherent with the direction of convergence between the African and the Eurasian plates (Diaz-del-Rio et al., 2003), suggesting that mud volcanism and mud diapirism is triggered by the tectonic forces related to plate movements (Gardner, 2001).

### *5.5. Migration*

The presence of particular tectonic regimes in the Gulf of Cadiz may be additional evidence for the presence of mixed hydrocarbon gases. Mattaveli et al., (1983) stated that formation of mixed gases appears generally bound to areas of faulting. The hydrocarbon gas from both mud volcano provinces is relatively dry, with  $C_{2+}$  contents in the WMF and in the DSPF of on average 3 and 8 %, respectively. Predominance of woody-coaly organic matter (i.e. kerogen Type III) over the more lipid-rich oil-prone sources (i.e. kerogen Type II) can be a reason for high production of dry gas. In contrast, migration can be important for redistribution of hydrocarbons due to their apparent diffusion coefficients (Leythaeuser et al., 1980, 1984). This leads to the  $C_{2+}$  depletion and therefore dry gas characteristics (Silverman, 1971). Migration processes, without any doubts, were active in the past and are still active at present in the Gulf of Cadiz. The occurrence of MVs is already ample corroboration of vertically focused fluid transport. Vertical-migration distances in the Gulf of Cadiz can be considerable, depending on vertical faulting, changes in permeability as a result of facies variation, possibilities of combined vertical and lateral migrations, active tectonics, etc. However, as a consequence of both tectonic disruption and facies changes, related to the past and present tectonic events in the Gulf, the lateral continuity of migration-carrier beds should be relatively poor. This indicates a lack of long-distance lateral migration of deep generated hydrocarbons from the DSPF to the WMF. Different tectonic regimes and thicknesses of the sedimentary cover in the central and the eastern domains of the olistostrome (Medialdea et al., 2004) also suggest a distinctive level and distribution of heat flow, which is one of the main factors causing hydrocarbon generation. For that reason, the same sedimentary unit may show different maturity characteristics in the DSPF and in the WMF. In this context, the identified gas types may belong to the same source beds, being under a different heat stress within these two MV provinces. As was shown above, both gas types are dry gases with generally similar  $C_{2+}$  compositions.

### *5.6. A possible locality of hydrocarbon gas accumulations*

An independent geochemical study of rock clasts from the Yuma MV (WMF) shows generally immature characteristics of kerogen belonging to the types II and III (Kozlova et al, 2004) which is consistent with the kerogen types established for the hydrocarbon gas in the area. The age of these rock clasts varies from the Middle Eocene to the Late Miocene (Ovsyannikov et al., 2003) which is consistent with the age of the olistostrome deposits (Maldonado et al., 1999b). The contrast between maturities of the clasts and the gas, however, may indicate that the source rocks with similar kerogen types belong to deeper horizons, since the gas generation window locates from ca. 105-155 °C to 175-220 °C (Pepper and Corvi, 1995). It implies possible redeposition of migrated thermogenic gas within the olistostrome or/and even within the Pliocene-Quaternary sediments in the WMF.

Gas from the DSPF represents a mixture of thermogenic and biogenic gases as reflected by its immature signal. This also may indicate redeposition of the migrated/mixed gas at shallow depths, possibly within the olistostrome or/and Pliocene-Quaternary units.

In addition, the recognized microbial consumption of propanes in both areas and *n*-butane in the Bonjardim MV (DSPF) is an additional confirmation of secondary processes which may occur in the deep subsurface. Similar gas alterations were reported in the reservoired hydrocarbon gas and also in a variety of geological settings, both onshore and offshore (James and Burns, 1984).

## 6. Conclusions

The Gulf of Cadiz is an area of active mud volcanism and fluid venting. This implies active processes of fluid migration from the deep sited horizons. MVs from two provinces, WMF and DSPF, have been studied to identify peculiarities of hydrocarbon gas composition, to classify hydrocarbon gases to their types/maturity, possible sources, and to trace their alteration due to secondary effects, such as migration, mixing, diverse microbial actions or combination of them. Obtained results revealed that among studied MVs, the Ginsburg and the Yuma are the most active structures currently known in the Gulf of Cadiz.

The molecular gas composition shows relatively dry gas characteristics; the C<sub>2+</sub> content is 3 and 8% in the WMF and the DSPF, respectively. Changes in gas composition and curves of concentration profiles from both MV areas show (i) absence of strong upward gas transport and (ii) active biological processes within ca. 50-100 cm bsf. This means that in the studied locations C<sub>1</sub> and C<sub>2+</sub> are consumed before they can escape into the overlying water column.

The combination of gas concentration data, stable carbon isotope composition of C<sub>1</sub>-C<sub>4</sub> alkanes, and molecular ratios revealed the presence of two different groups of gases in the WMF and DSPF. Both gas groups represent allochthonous to the erupted mud breccia gas with high input of thermogenically formed hydrocarbons as shown by anomalous concentrations of C<sub>2+</sub> gas components. The WMF gas represents mature gases, (Ro<1.2%), derived from kerogen Type II (the Ginsburg MV) and a mixture of kerogens of Type II and III (Jesus Boraza MV). The DSPF gas is a mixture of thermogenic and bacterial gases which cause of its relatively immature characteristics (the beginning of the oil window; Ro ≤ 0.5%). A source and maturation characteristic of gas from the DSPF is difficult to determine due to migration, biodegradation, and mixing processes.

The combination of molecular and stable carbon isotopic signatures of the C<sub>1</sub>-C<sub>4</sub> alkanes provides geochemical evidence that besides methane, C<sub>2</sub>-C<sub>4</sub> hydrocarbons can be also microbially consumed within first decimeters below the seafloor. Further, microbial activity in the first top ca. 60 cm reflects in the formation of unsaturated ethene and propene which appearance coincided with the vanishing of saturated hydrocarbon gases.

Microbial consumption of ethanes and propanes in both areas and of *n*-butane in the Bonjardim MV (DSPF) makes identification of source and maturity for these alkanes difficult. Simultaneously it can be an indicator of secondary microbial processes previously observed in suite of natural gases (James and Burns, 1984, Clayton et al., 1997; Pallasser, 2000) and seepages (Sassen et al., 2004).

The studied MVs appear within the olistostrome body, the WMF is located in the eastern domain and the DSPF – in the central part. Different tectonic regimes and thicknesses of the sedimentary cover within the olistostrome domains (Medialdea et al., 2004) suggest

distinctive fluid venting environments as well as distinctive distribution patterns of heat flows. This should be reflected in the geochemical behaviour/properties of migrating fluids, which is consistent with the different peculiarities of the erupted mud breccias and the recognition of two gas groups in the WMF and DSPF. This study reveals that despite the discrete maturation characteristics, both gas types are a complex of secondary migrated, microbially altered and mixed hydrocarbons, most likely redeposited within the olistostrome /Pliocene-Quaternary sedimentary units. It may possibly imply the existence of hydrocarbon accumulations in the subsurface and probable association of mud volcanoes with the olistostrome body.



**APPLICATION OF LIPID BIOMARKERS TO DETECT SOURCES OF ORGANIC MATTER IN MUD VOLCANO DEPOSITS AND POST-ERUPTIONAL METHANOTROPHIC PROCESSES IN THE GULF OF CADIZ, NE ATLANTIC.**

A. Stadnitskaia<sup>a,b</sup>, M.K. Ivanov<sup>b</sup>, J.S. Sinninghe Damsté<sup>a</sup>

<sup>a</sup> *Royal Netherlands Institute for Sea Research (NIOZ), P.O.Box 59, 1790 AB, Den Burg, Texel, the Netherlands*

<sup>b</sup> *UNESCO-MSU Centre for Marine Geosciences, Geological faculty, Moscow State University, Vorobjevy Gory, Moscow 119899, Russia*

To be submitted to the Special Issue of the TTR Programme in  
*Marine and Petroleum Geology*

**Abstract**

The Gulf of Cadiz is known as an active mud volcano (MV) and fluid venting region discovered during the Training Through Research (TTR) expeditions in 1999 (TTR-9). Here we report a study of lipid biomarkers in the mud breccia matrix from three MVs in this region. The lipid biomarker composition revealed strong compositional resemblance as well as similar thermal maturity properties for the studied MVs. This indicates that the primary source of the erupted material for these MVs is located in similar litho-stratigraphic units. In both areas, upward migrated fluid went through the sedimentary series of the allochthonous Olistrostrome and through the Upper Cretaceous horizons. The relatively immature characteristics of organic matter from both mud breccia rock clasts and matrix together with the more mature properties of hydrocarbon gases from the same sampling locations indicate that source strata for the initial fluid are located deeper in the subsurface than the source strata for the erupted sedimentary material.

The presence of microbial lipid biomarkers derived from archaea and sulfate reducing bacteria in the mud breccias revealed anaerobic oxidation of methane (AOM) as a dominant microbial process in these habitats. The low concentrations of AOM-related biomarkers in these MVs suggest relatively low intensities of AOM in the studied MV deposits. The distribution of biomarkers suggests an abrupt and brief cold seep activity in the past and the absence of a continuous methane influx in the studied locations.



## **1. Introduction**

Discharge of hydrocarbon-rich fluids is a widespread phenomenon in the Gulf of Cadiz (Baraza and Ercilla, 1996; Baraza et al., 1999; Ivanov et al., 2000, 2001; Somoza et al., 1999, 2002; Gardner, 2001; Kenyon et al., 2000, 2001; Mazurenko et al., 2002, 2003; Pinheiro et al., 2003; Stadnitskaia et al., 2006a). Petroleum exploration on the continental margin of the gulf (up to 1000 m of the water depth) resulted in the drilling of two commercial wells by 1999 and revealed the presence of natural gas (Somoza et al., 2001). Later on, during the international multidisciplinary Training Through Research (TTR) cruises carried out within the framework of the UNESCO-IOC "Floating University" Programme, the deep part of the Gulf of Cadiz (from 700 to >3000 m water depth) was demonstrated to be an active mud volcano province. Numerous mud volcanoes (MVs), diapiric ridges, gas-saturated sediments, gas hydrates, chemosynthetic communities, and "graveyards" of authigenic carbonates have been discovered, sampled and described during six TTR cruises to the region in the period between 1999 and 2005 (Kenyon et al., 2000, 2001; Ivanov et al., 2000, 2001; Gardner, 2001; Pinheiro et al., 2003; Terrinha et al., 2003; Mazurenko et al., 2002, 2003; Somoza et al., 2003; Ovsyannikov et al., 2003; Murton and Biggs, 2003; Van Rensbergen et al., 2005; Stadnitskaia et al., 2006a).

Because hydrocarbons are often dominant components of the migrated fluid, MVs and seeps in general are direct indicators of hydrocarbon migration and, thus, hydrocarbon potential in the subsurface (Link, 1952; Guliev and Feizullayev, 1997; Ivanov et al., 1998; Stadnitskaia et al., 2006a). Concurrently, upward migrating fluids contain organic and inorganic components providing sources of energy to the microbial communities in the deep sea. Microbial methane utilization in anoxic environments or anaerobic oxidation of methane (AOM) has been considered as one of the most important and effective biological filters preventing methane emissions from the sea floor into the hydrosphere and to the atmosphere (see for review Hinrichs and Boetius, 2002). The process is accomplished in anoxic marine environments with sulfate as the terminal electron acceptor (Barnes and Goldberg, 1976). Molecular ecological studies using ribosomal DNA revealed that AOM is performed by consortia of specific groups of archaea and sulfate reducing bacteria (Boetius et al., 2000; Orphan et al., 2001a,b; Michaelis et al., 2002; Knittel et al., 2003, 2005). Lipid biomarker investigations of seepage-related anoxic sediments and authigenic carbonates revealed that methane acts as an important carbon source in these environments (Elvert et al., 1999, 2000, 2003; Hinrichs et al., 1999, 2000a,b, Pancost et al., 2000, 2001b; Zhang et al., 2003; Peckman and Thiel, 2004; Stadnitskaia et al., 2005). Thus, fluids expelled from mud volcanoes and from other venting related structures not only portray the products of generation and migration from the deep subsurface, but also provide constraints on microbial processes at the seafloor in such habitats.

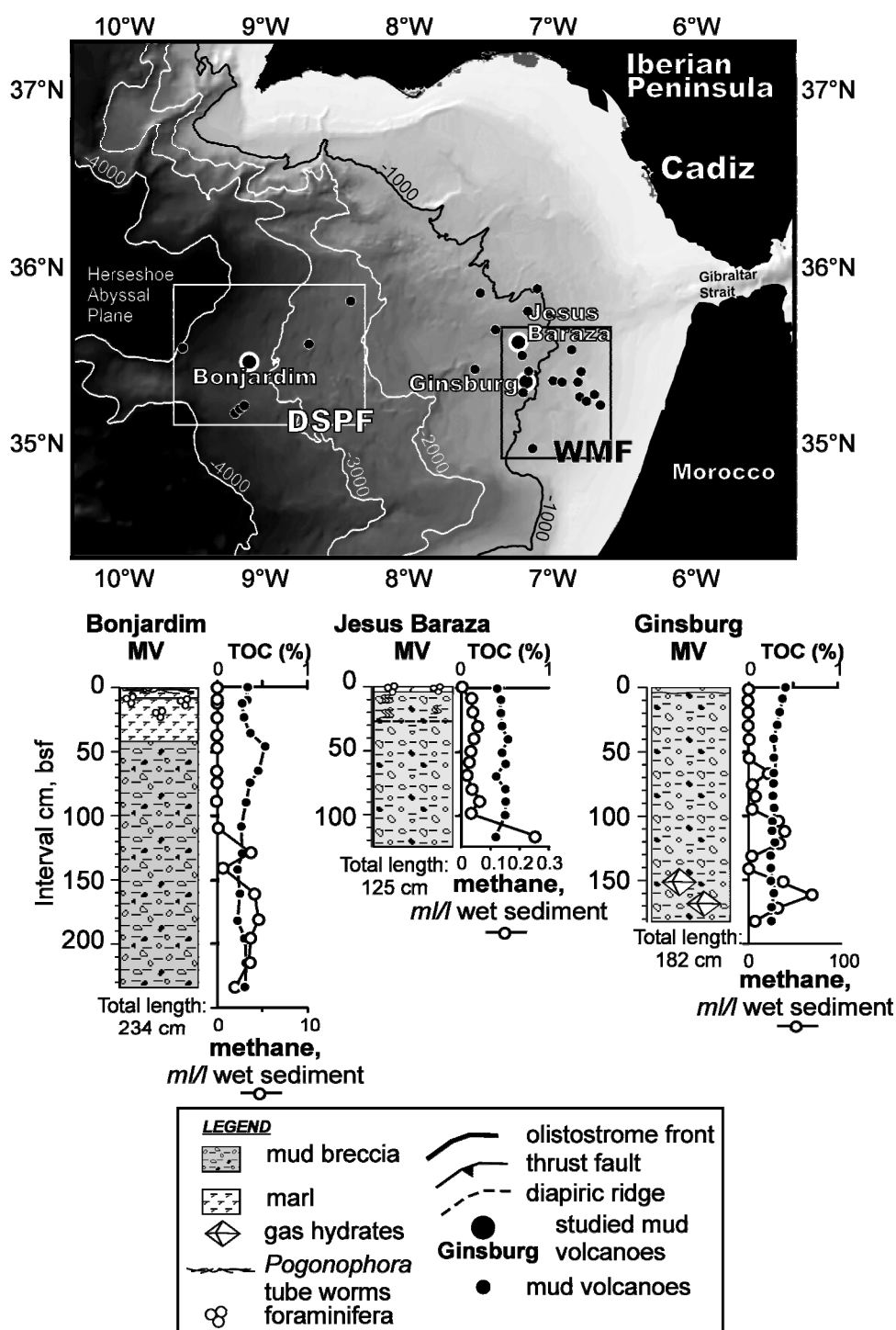


**Figure 1.** Geological map with location of studied mud volcanoes (modified after Akmetzhanov, SOC, UK) and schematic lithology (Kenyon et al., 2001), TOC and methane vertical profiles (Stadnitskaia et al., 2006) of the studied sedimentary cores. DSPF is the acronym for the Deep South Portuguese Field; WMF is the acronym for the Western Moroccan Field.

Two mud volcano provinces (Figure 1), along the Moroccan-Spanish (Western Moroccan Field; WMF) and Deep South Portuguese (Deep South Portuguese Field; DSPF) continental margins, were discovered during the TTR-9 cruise in 1999 and the TTR-10 cruise in 2000, respectively (Kenyon et al., 2000, 2001; Ivanov et al., 2000, 2001; Gardner, 2001; Pinheiro et al., 2003). Here, we applied molecular and stable carbon isotope measurements of lipid biomarkers to mud breccia matrix from three MVs, the Ginsburg and Jesus Baraza MVs located within WMF, and the Bonjardim MV located within the DSPF (Figure 1). The composition of hydrocarbon gases and their stable carbon isotope signatures from these MVs was previously reported in Stadnitskaia et al. (2006). Hence, the aim of this study is to make a contribution towards the assessment of the source-strata for the erupted sedimentary material and the microbiological processes associated with the transport of methane from the subsurface. The results are compared with similar studies for mud breccia matrixes from MVs in the Sorokin Trough, NE Black Sea. Besides the mud breccia sources assessment, our objectives are also the identification of microorganisms involved in methanotrophic activity, in particular AOM, using lipid signatures associated with methanotrophic processes.

## **2. Geological background**

The Gulf of Cadiz is located in the south-western part of the Iberian Peninsula margin, representing a wide embayment of the Atlantic Ocean from Cape Saint Vincent (Portugal) to the Gibraltar Strait (Figure 1). It extends for ca. 300 km and is characterized by a complex geological evolution entailing several phases of rifting, convergence, and strike-slip motions since the Triassic (Srivastava et al., 1990; Maldonado et al., 1999b; Maldonado and Nelson, 1999a). Tectonically, the Gulf of Cadiz region straddles the east-west-trending segment of African-Eurasian plate boundary from the Azores to the Mediterranean between the Gloria transform fault and the Gibraltar Arc (Maldonado et al., 1999b; Somoza et al., 2002; Pinheiro et al., 2003; Medialdea et al., 2004). During the Late Tortonian, the Gibraltar Arc migrated westward, which resulted in the formation of the Gulf of Cadiz as a forearc basin and forced the emplacement of the Olistostrome, which ended in the Late Miocene (Maldonado et al., 1999b). Both WMF and DSPF are attributed to the Olistostrome (Figure 1), extending through the Gulf in a southwest direction (Maldonado et al., 1999b; Medialdea et al., 2004). Three MVs were chosen for lipid biomarker investigations. The Bonjardim MV (35° 28' N; 09° 00' W, water depth ca. 3060 m) represents one of the deepest structures and appears within the DSPF, in the Central domain of the Olistostrome (Figure 1). This region is characterized by compressive deformation, thrusting and the presence of deep faults (Medialdea et al., 2004). The Ginsburg (35° 22' N; 07° 05' W, water depth ca. 910 m) and the Jesus Baraza (35° 35' N; 07° 12' W, water depth ca. 1091 m) MVs locate within the WMF, in the Eastern domain of the Olistostrome (Figure 1). In contrast to the Central domain, this

region is characterized by extensive mud diapirism and mud volcanism which are structurally controlled and likely triggered by the tectonic forces related to the convergence of the African and the Eurasian plates (Gardner, 2001).

### 3. Material and methods

#### 3.1. Sample collection and storage

During the TTR-10 expedition in July-August 2000, mud breccias were collected using a 6 m long, 1500 kg gravity corer with an internal diameter of 14.7 cm (Kenyon et al., 2001). The extraction of the core from the plastic liner was followed by a lithological description and sub-sampling procedure for lipid biomarkers. For optimal correlation, the subsampling for the lipid biomarker study was accomplished in close concert with subsampling for hydrocarbon gas measurements, obtaining identical sampling intervals along mud breccia sections (Stadnitskaia et al., 2006). Directly after sub-sampling, sediments were frozen and stored at -20°C until solvent extraction.

#### 3.2. Extraction and separation

Samples of 20-50 g were freeze-dried, crushed in an agate mortar to a fine powder, and extracted with an automatic Accelerated Solvent Extractor (ASE 200/DIONEX) using a solvent mixture comprised of dichloromethane (DCM): methanol (MeOH) (9:1, v/v) at 1000 psi and 100°C. Elemental sulfur was removed from the total extracts by adding ca. 30 mg of activated copper and stirring the sample over night. An aliquot of the total extract was used for total lipid analysis. To this end, fatty acids in the extract were methylated by heating at 60°C for 5 min in boron trifluoride-MeOH complex (in excess MeOH, ca.12 wt.% BF<sub>3</sub>), and alcohols were transformed into trimethylsilyl (TMS)-derivatives by adding 25 µl of pyridine and 25 µl of *N,O*-bis(trimethylsilyl)trifluoroacetamid (BSTFA) and heating at 60°C for 20 min. Another aliquot of the total extract was chromatographically separated into apolar and polar fractions using a column with activated (2 h at 150°C) Al<sub>2</sub>O<sub>3</sub> as stationary phase. Apolar compounds were eluted using hexane:DCM (9:1, v/v), and polar compounds, including glycerol diethers and glycerol dialkyl glycerol tetraethers (GDGTs) core membrane lipids, were obtained with MeOH:DCM (1:1, v/v) as eluent. To calculate absolute concentrations of biomarkers in mud breccia matrixes, a known amount of 2,3-dimethyl-5-(1,1-dideuterohexadecyl)-thiophene (C<sub>22</sub>H<sub>38</sub>SD<sub>2</sub>) was added to each fraction as an internal standard.

To analyze the ether-linked biphytanes in GDGTs, aliquots of the polar fractions were subjected to ether cleavage using 57% HI (1 h at 110°C). The reduction of the resulting

iodides was accomplished by using  $\text{LiAlH}_4$ . The full procedure is described elsewhere (Schouten et al., 1998).

### *3.3. Analysis and identification of lipid biomarkers*

Gas chromatography (GC) was performed using a Hewlett Packard 6890 gas chromatograph equipped with an on-column injector and a flame ionization detector. A fused silica capillary column (CP Sil-5 25 m x 0.32mm,  $d_f=0.12 \mu\text{m}$ ) with helium as a carrier gas was used. The samples were injected at 70° C. The GC oven temperature was subsequently raised to 130° C at a rate of 20° C  $\text{min}^{-1}$ , and then to 320° C at 4° C  $\text{min}^{-1}$ . The temperature was then held constant for 15 min.

All fractions were analyzed by gas chromatography-mass spectrometry (GC-MS) for compound identification. GC-MS was conducted using a Hewlett Packard 5890 gas chromatograph interfaced to a VG Autospec Ultima Q mass spectrometer operated at 70 eV with a mass range of  $m/z$  50–800 and a cycle time of 1.8 s (resolution 1000). The gas chromatograph was equipped with a fused silica capillary column (CP Sil-5, 25 m x 0.32 mm,  $d_f=0.12 \mu\text{m}$ ) and helium as a carrier gas. The temperature program used for GC-MS was the same as for GC. The structural designation of lipids was evaluated by the comparison their mass spectral fragmentation patterns and Pseudo Kovats retention indices with reported data.

Isotope-ratio-monitoring gas chromatography-mass spectrometry (IRM-GC-MS) was performed on a Finnigan MAT DELTA plus XL instrument used for determining compound-specific  $\delta^{13}\text{C}$  values. The GC used was a Hewlett Packard 6890 A series and the same analytical conditions were used as described for GC and GC-MS. For carbon isotopic correction of the added trimethylsilyl groups, the carbon isotopic composition of the used BSTFA was determined ( $-49.3 \pm 0.5 \text{‰}$ ). Obtained values are reported in per mil relative to the VPDB standard, and have been corrected for the addition of TMS group due to the derivatisation procedure. In order to monitor the accuracy of the measurements, the analyses were carried out with co-injection of two standards,  $\text{C}_{20}$  and  $\text{C}_{24}$  *n*-alkanes, which have known carbon isotopic composition.

To determine the distribution and composition of intact glycerol dialkyl glycerol tetraethers (GDGTs), samples were analyzed using a high performance liquid chromatography-mass spectrometry (HPLC-MS) method for their direct analysis (Hopmans et al., 2000). GDGTs were analyzed using an Agilent 1100 series / 1100 MSD series instrument, with auto-injection system and HP-Chemstation software. The quantification of GDGTs by HPLC-MS-analysis using single ion monitoring was accomplished as described by Weijers et al., (2006).

## 4. Results

### 4.1. Sedimentary lithologies and geochemistry of the studied locations

Figure 1 shows the lithology of the cores studied (Kenyon et al., 2001), concentration profiles of methane and TOC content (Stadnitskaia et al., 2006). The sediments are predominantly composed of mud breccia, which is different in the WMF and DSPF (Kenyon et al., 2001). MVs from the WMF showed relatively fine mud breccias intensively bioturbated at the top, possessing semi-consolidated rock clasts within a clayey matrix with high carbonate content (Kenyon et al., 2000, 2001; Pinheiro et al., 2003). MVs from the DSPF were characterized by stiff non-stratified mud breccias, only occasionally bioturbated, having well-lithified clasts within clayey matrix with insignificant carbonate admixture (Kenyon et al., 2000, 2001; Pinheiro et al., 2003). Mud breccias from the Jesus Baraza MV showed two mud breccia intervals of the same lithology, probably representing different mud flows (Kenyon et al., 2001; Pinheiro et al., 2003).

Pelagic sediments overlay the top of the recovered mud breccia section for two of the three MVs studied. The upper 42 cm of the sedimentary section of the Bonjardim MV comprised of pelagic marl (Figure 1). This marl was bioturbated at the top, and rich in Foraminifera and Pogonophora (mainly *Polybrachia* sp.) tube worms (Kenyon et al., 2001; Pinheiro et al., 2003). A similar pelagic cover was recovered from the Jesus Baraza MV, where it constituted a 4 cm thick interval rich in Foraminifera (Kenyon et al., 2001). Compared with the Bonjardim MV, only a few Pogonophora tube worms (*Siboglinum* sp.) were found within this marl. Mud breccias recovered from the Ginsburg MV showed no pelagic cover at the top (Kenyon et al., 2001). Gas hydrates were detected in this MV below 1 m (Figure 1).

Study of the gas hydrates and pore waters of the mud breccias showed deep sources of upcoming fluids (Mazurenko et al., 2003). Molecular and stable carbon isotope signatures of C<sub>1</sub>-C<sub>5</sub> alkanes revealed high input of thermogenic gaseous hydrocarbons and two different groups of gases in the WMF and DSPF (Stadnitskaia et al., 2006). The WMF gas represents mature gases with methane  $\delta^{13}\text{C}$  values between -28 and -42 ‰. In contrast, the DSPF gas is a mixture of thermogenic and bacterial gases with relatively immature characteristics and methane  $\delta^{13}\text{C}$  signatures between -50 and -67 ‰ (Stadnitskaia et al., 2006). High concentrations of methane and C<sub>2+</sub> components and relatively low TOC values indicate an allochthonous nature of the C<sub>1</sub>-C<sub>5</sub> alkanes to the host mud breccias (Figure 1; Stadnitskaia et al., 2006).

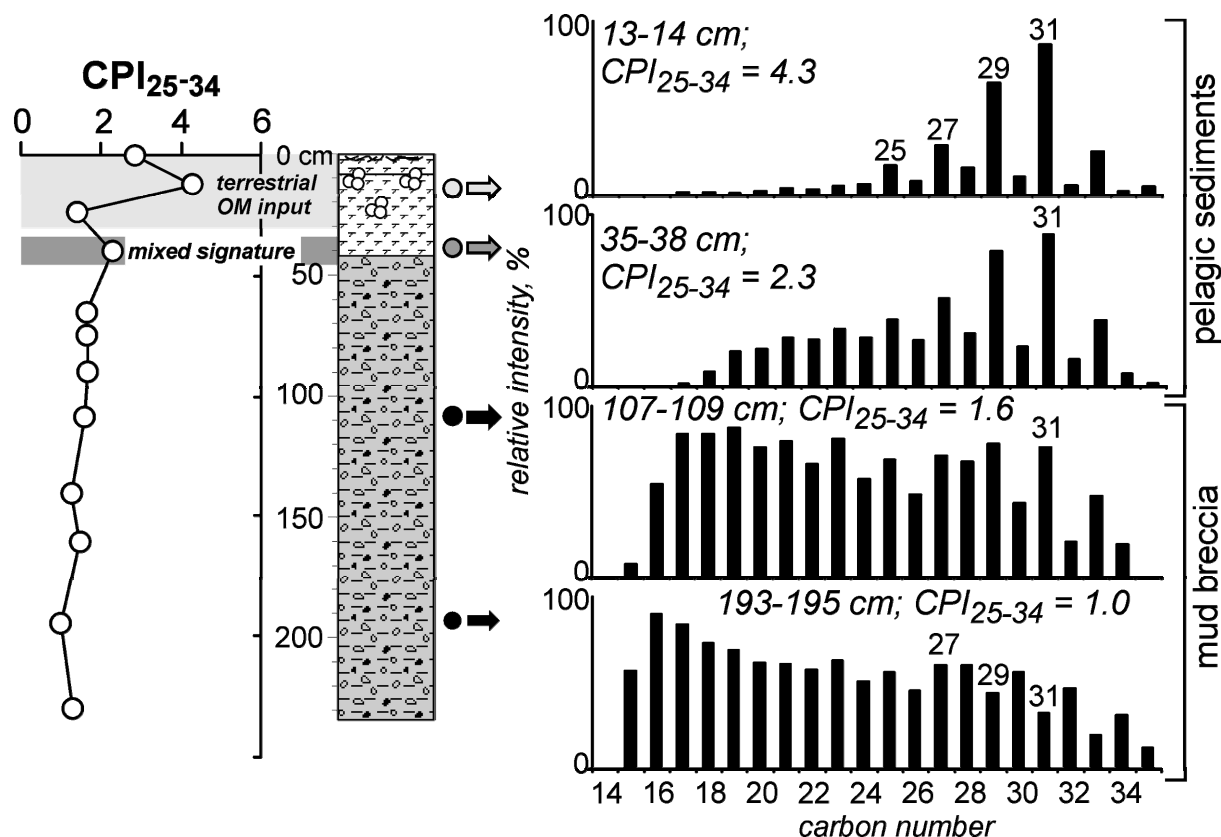


**Figure 2.** Distribution of *n*-alkanes and CPI profile along the sedimentary core from the Bonjardim MV. The *n*-alkane patterns show clear difference between the organic matter from the pelagic sediments and from the mud breccia. Arabic numbers denote alkanes with the given carbon chain length.

#### 4.2. General lipid characteristics of MV deposits

The pelagic sediments and mud breccias are characterized by different lipid distributions (e.g. Figure 2). Mud breccia matrixes from the Bonjardim MV (DSPF) and from the Ginsburg and Jesus Baraza MVs (WMF) showed almost identical lipid biomarker compositions (e.g. Figure 3). Apolar compounds strongly dominated the total extract. Polar constituents were mainly represented by bacterial and archaeal lipids, marking *in situ* microbial processes, mainly AOM.

The lipid extracts from all MVs contained abundant of *n*-alkanes ranging in carbon number from C<sub>15</sub> to C<sub>35</sub> with an odd-over-even carbon-number predominance in the C<sub>23</sub>-C<sub>35</sub> range. In all mud breccias, C<sub>25</sub>-C<sub>31</sub> components dominate *n*-alkane distributions to a variable extent, signifying an admixture of terrestrial organic matter. The Carbon Preference Index (CPI; Bray and Evans, 1961) for C<sub>25</sub>-C<sub>34</sub> *n*-alkanes slightly fluctuates along the mud breccias. The CPI values for the mud breccia of the Bonjardim MV (DSPF) are on average 1.4, and for the mud breccias of the Jesus Baraza and Ginsburg MVs (WMF) are on average 1.6 and 1.5, respectively (Table 1). Figure 2 shows that in the Bonjardim MV, the *n*-alkane distributions

and  $CPI_{25-34}$  values clearly distinguish the pelagic section from the mud breccia. This interval is characterized by a pronounced signal of the odd-numbered  $C_{25}$ - $C_{31}$   $n$ -alkanes (Figure 2, the topmost light grey area) and the  $CPI_{25-34}$  values increase up to 4.3 (Table 1). This indicates that the organic matter in the pelagic sediments received a substantial contribution from higher plants (Eglinton and Hamilton, 1967; Kolattukudy, 1980; Simoneit, 1977; Gagosian et al., 1981, 1987). The  $n$ -alkane distribution from the deeper pelagic sediments below showed a “mixed” signal of  $n$ -alkanes from the pelagic sediments above and from the mud breccia below (Figure 2, darker grey area). The mud breccia interval clearly shows the presence of petroleum-derived  $n$ -alkanes (Figure 2).

The  $C_{25}$  highly branched isoprenoid (HBI; 2,6,10,14-tetramethyl-7-(3-methylpentyl)-pentadecane) alkane, a diagenetic product of HBI alkenes produced by two specific phylogenetic clades of diatoms (Sinninghe Damsté et al., 2004a), was present in all mud breccia sections in noticeable amounts (e.g. Figure 3). The steroid composition was dominated by  $C_{27}$ ,  $C_{28}$ , and  $C_{29}$   $5\alpha,14\alpha,17\alpha(H)$ -steranes with the  $C_{29}$  sterane as the dominant member. Low amounts of 20S- and 20R-epimers of  $13\alpha,17\beta$ -diacholestanes were also detected (Figure 3; Table 2).

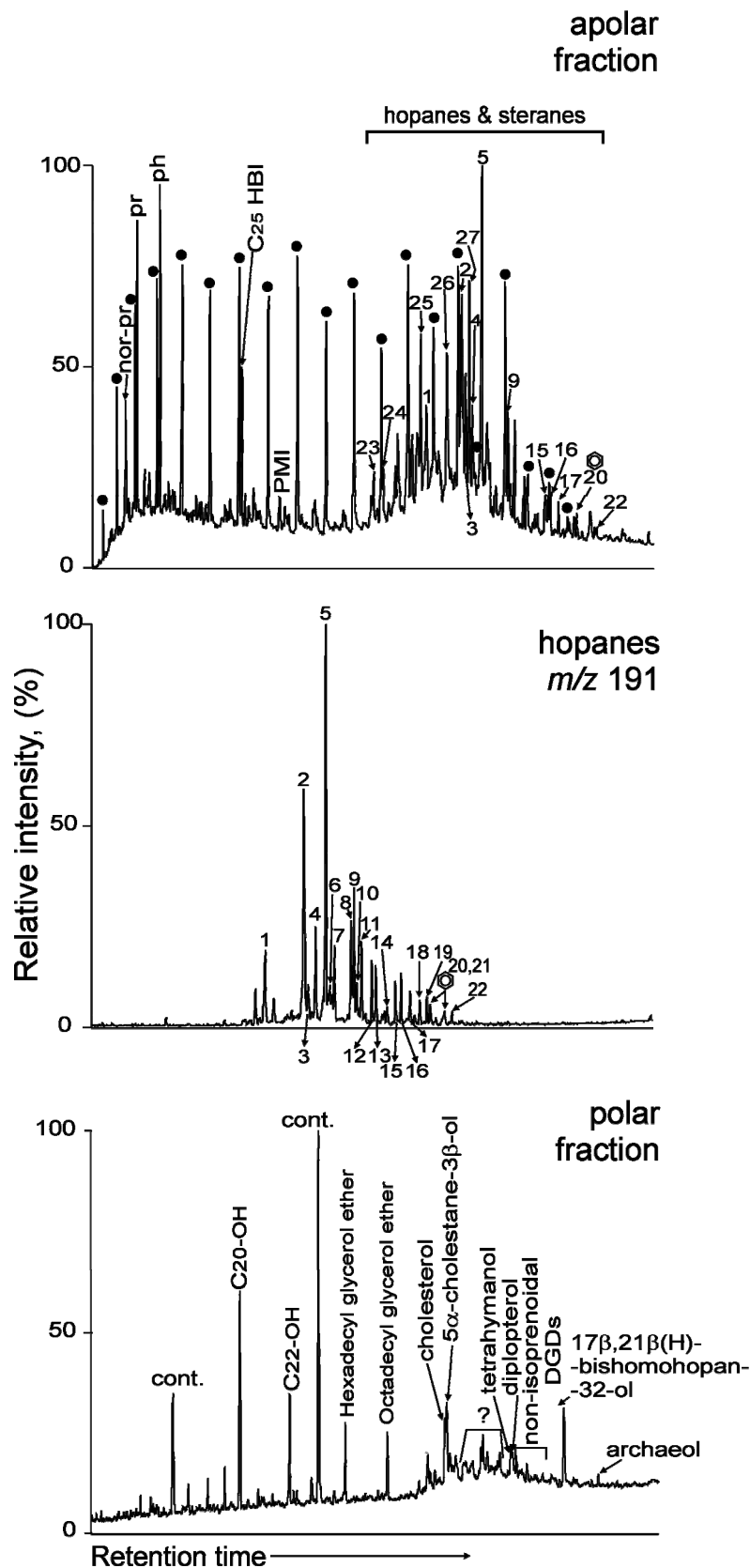
The pentacyclic triterpanes showed a similar distribution in the different MVs (e.g. Figure 3; Table 2). Hopanes were the main constituents.  $C_{30}$ - $C_{32}$  hopanes with  $\beta\alpha$ - and  $\beta\beta$ -configurations were present in smaller amounts relative to their  $\alpha\beta$ -epimers (Table 1). The

medium intervals, (cm b.s.f.)	TOC <sup>a</sup> (wt %)	Compound indexes				
		n-Alkanes		Hopanes		
		$CPI_{25-34}$	$C_{31}$ 22S/(22S+22R)	$C_{32}$ 22S/(22S+22R)	$C_{30}$ $\beta\alpha/(\alpha\beta+\beta\alpha)$	$C_{31}$ $\beta\beta/(\beta\beta+\alpha\beta+\beta\alpha)$
<b>Jesus Baraza MV (WMF)</b>						
10	0.5	1.7	0.50	0.54	0.15	0.06
30	0.5	1.8	0.50	0.53	0.14	0.06
50	0.5	1.6	0.51	0.55	0.16	0.06
69	0.4	1.5	0.49	0.51	0.14	0.10
89	0.5	1.5	0.44	0.56	0.18	0.06
116	0.4	1.6	0.42	0.51	0.25	0.12
Average	0.4	1.6	0.5	0.5	0.2	0.1
<b>Ginsburg MV (WMF)</b>						
0	0.4	1.9	0.50	0.50	0.20	0.12
30	0.4	1.5	0.40	0.50	0.30	0.12
65	0.4	1.2	0.40	0.50	0.20	0.12
85	0.4	1.4	0.50	0.50	0.20	0.12
105	0.3	1.5	0.50	0.40	0.20	0.12
142	0.4	1.3	0.50	0.50	0.20	0.12
Average	0.4	1.5	0.5	0.5	0.2	0.1
<b>Bonjardim MV (DSPF)</b>						
0	0.3	2.8	n/d	n/d	n/d	n/d
13	0.3	4.3	n/d	n/d	n/d	n/d
24	0.3	1.4	0.50	0.53	0.21	0.22
36	0.4	2.3	0.48	0.56	0.21	0.12
65	0.5	1.6	0.43	0.50	0.23	0.13
75	0.4	1.7	0.45	0.53	0.21	0.32
89	0.3	1.6	0.48	0.54	0.21	0.13
109	0.3	1.6	0.47	0.57	0.22	0.16
141	0.2	1.2	0.47	0.57	0.22	0.16
161	0.3	1.4	0.52	0.56	0.19	0.10
195	0.3	1.0	0.46	0.52	0.23	0.12
234	0.3	1.3	0.52	0.51	0.20	0.13
Average	0.3	1.8	0.5	0.5	0.2	0.2

<sup>a</sup> - Stadnitskaia et al., 2006

**Table 1.** TOC content and compound indexes.





dominant component was  $17\alpha,21\beta(H)$ -hopane, followed by  $17\alpha,21\beta(H)$ -30-norhopane.  $C_{32}$  to  $C_{34}$  benzohopanes were prominent members among the pentacyclic triterpanes. Unsaturated hopanoids were represented by diploptene (hop-22(29)-ene) and  $C_{29}$  and  $C_{30}$  neohop-13(18)-enes. The variety of polar triterpenoids included the functionalized hopanoid diplopterol ( $17\beta,21\beta(H)$ -hopan-22-ol) and the non-hopanoid, tetrahymanol (gammaceran- $3\beta$ -ol; ten Haven, et al., 1989). The  $17\beta,21\beta(H)$ -bishomohopan-32-ol, and  $\alpha\beta$ - and  $\beta\beta$ -epimers of bishomohopanoic acid were also detected. These constituents were mainly identified in the uppermost 60 cm of the studied sedimentary sections and were present in low amounts.

**Figure 3.** Typical lipid distribution patterns by the example of mud breccia from the Bonjardim MV. Numbers refer to compounds listed in Table 2. Abbreviations: nor-pr. - nor-pristane; pr - pristane; ph - phytane;  $C_{25}$  HBI -  $C_{25}$  highly branched isoprenoid; PMI - pentamethylcosane; cont. - contamination.

Peak number	Compound name	Carbon number
1	17 $\alpha$ (H)-trisorhopane	27
2	17 $\alpha$ ,21 $\beta$ (H)-30-norhopane	29
3	18 $\alpha$ (H)-30-norneohopane	29
4	17 $\beta$ ,21 $\alpha$ (H)-30-norhopane	29
5	17 $\alpha$ ,21 $\beta$ (H)-hopane	30
6	17 $\alpha$ (H)-30-nor-29-homohopane	30
7	17 $\beta$ ,21 $\alpha$ (H)-hopane (moretane)	30
8	17 $\alpha$ ,21 $\beta$ (H)-homohopane 22S	31
9	17 $\alpha$ ,21 $\beta$ (H)-homohopane 22R	31
10	17 $\beta$ ,21 $\alpha$ (H)-homohopane	31
11	Diploptene (hop-22(29)-ene)	30
12	17 $\alpha$ ,21 $\beta$ (H)-bishomohopane 22S	32
13	17 $\alpha$ ,21 $\beta$ (H)-bishomohopane 22R	32
14	17 $\beta$ ,21 $\beta$ (H)-homohopane	31
15	17 $\alpha$ ,21 $\beta$ (H)-trishomohopane 22S	33
16	17 $\alpha$ ,21 $\beta$ (H)-trishomohopane 22R	33
17	17 $\beta$ ,21 $\alpha$ (H)-trishomohopane	33
18	17 $\alpha$ ,21 $\beta$ (H)-tetrakishomohopane 22S	34
19	17 $\alpha$ ,21 $\beta$ (H)-tetrakishomohopane 22R	34
20	20,32-cyclo-32-methyl-17 $\alpha$ -bishomohopane-20,22,31-triene 22 S/R	33
21	20,32-cyclo-32-ethyl-17 $\alpha$ -bishomohopane-20,22,31-triene 22S/R	34
22	17 $\alpha$ ,21 $\beta$ (H)-pentakishomohopane 22S/R	35
23	13 $\beta$ ,17 $\alpha$ (H)-diacholestane 20S	27
24	13 $\beta$ ,17 $\alpha$ (H)-diacholestane 20R	27
25	5 $\alpha$ -cholestane	27
26	5 $\alpha$ -ergostane	28
27	5 $\alpha$ -stigmastane	29

**Table 2.** Hopanes and steranes identified in apolar fractions from mud breccia matrixes.

In the mud breccia from the Jesus Baraza MV,  $\delta^{13}\text{C}$  values of diplopterol varied from -41 to -67 ‰ and of 17 $\beta$ ,21 $\beta$ (H)-bishomohopane-32-ol from -36 to -48 ‰ (Table 3). In contrast, pelagic sediments from the Bonjardim MV showed less depleted  $\delta^{13}\text{C}$  signatures of both hopanoids, i.e. -31 and -26 ‰, respectively (Table 3). Initially, these lipids were detected in many chemoorganotrophic bacteria which are mainly related to aerobic microorganisms (Rohmer et al., 1984, 1992; Summons et al., 1999). The presence of hopanoids in fluid venting anoxic sediments (Pancost et al., 2000; Stadnitskaia et al., 2005) together with their identification in strictly anaerobic bacteria performing the anaerobic ammonium oxidation (Sinninghe Damsté et al., 2004b) and in the sulfate reducing bacteria (SRB) of the genus

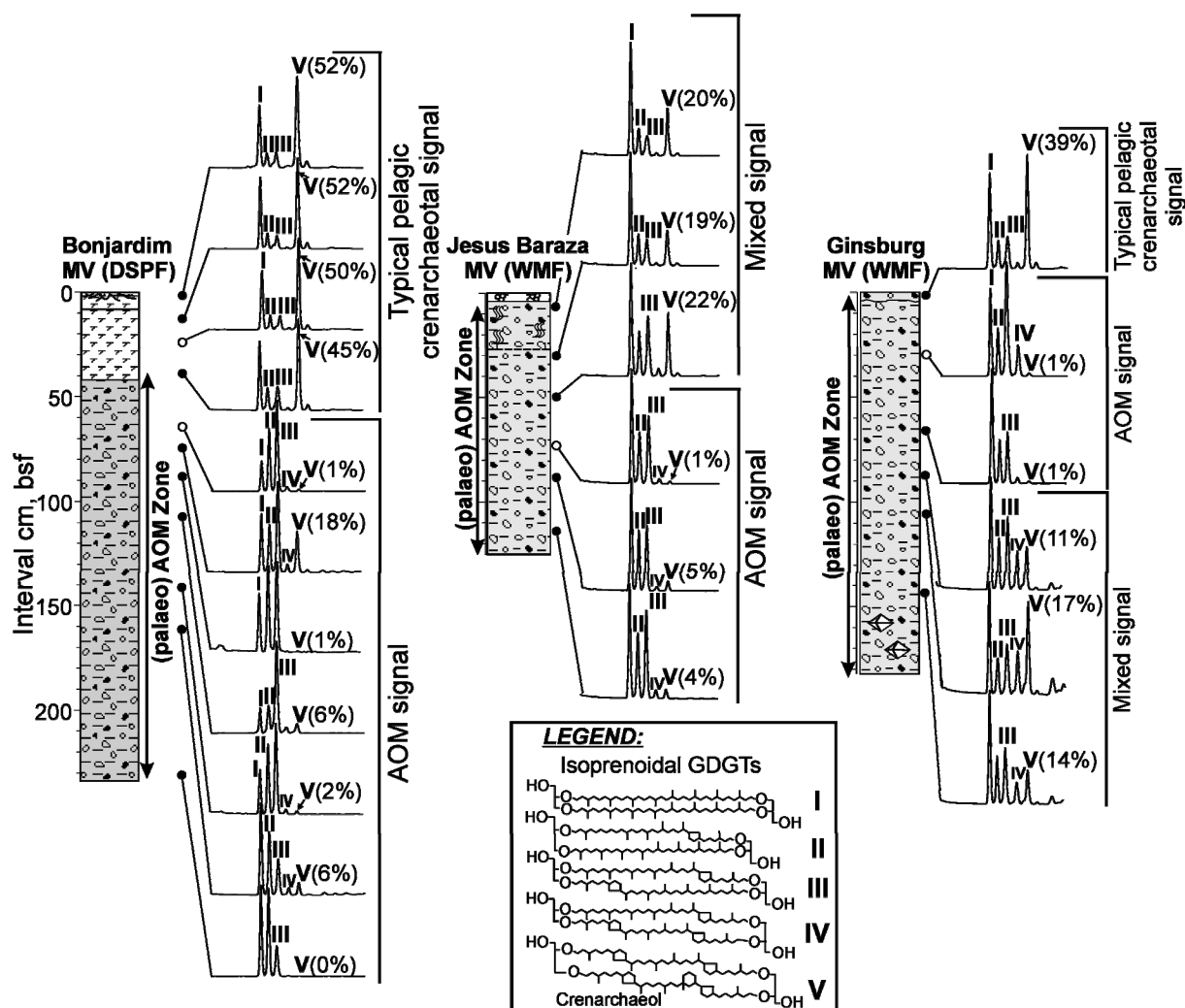


**Figure 4.** Base peak HPLC chromatograms of the polar fractions from mud breccia matrixes showing compositional variations among the GDGTs along the sedimentary successions. Circles indicate subsampling interval. White circles specify samples, which were selected to cleave ethers in GDGTs through the HI-treatment (see Table 3). Roman numbers refer to structures in the legend. Percentage values in parentheses next to "V" denote the content of crenarchaeol from the total identified GDGTs.

*Desulfovibrio* (Härtner et al., 2005; Blumenberg et al., 2006) provided evidence that anaerobic bacteria also significantly contribute to the sedimentary hopanoid pool.

Isoprenoid biomarkers derived from archaea were found in all locations. The irregular acyclic hydrocarbons such as 2,6,11,15-tetramethylhexadecane (crocetane), mono- and di-unsaturated crocetenes, 2,6,10,15,19-pentamethylcosane (PMI), trace amounts of dialkyl glycerol diethers (DGDs) such as archaeol, hydroxyarchaeol, and glycerol dibiphytanyl glycerol tetraethers (GDGTs) were detected up to 234 cm below the sea floor.

Figure 4 reveals the distributions of GDGTs in all studied sedimentary sections. The pelagic cover of the Bonjardim MV possessed the typical “marine” GDGT distribution previously detected in seawater particulate organic matter and marine sediments (Schouten et al., 2000; Pancost et al., 2001a,b; Sinninghe Damsté et al., 2002a,b; Wakeham et al., 2003; Wuchter et al., 2003). This distribution is characterized by the abundance of crenarchaeol, the characteristic GDGT of pelagic crenarchaeota (Sinninghe Damsté et al., 2002b), which comprises 45-52 % of the total amount of GDGTs within this interval (Figure 4). Below this level, the GDGT distribution is completely different, and is dominated by GDGTs with 0-2 cyclopentane rings and crenarchaeol is almost absent (Figure 4). This distribution is typical for euryarchaeota involved in AOM (i.e. Pancost et al., 2001 a,b; Aloisi et al., 2002; Zhang et al., 2003; Wakeham et al., 2003; Stadnitskaia et al., 2005). This interpretation is confirmed by the stable carbon isotope signatures of the biphytanes formed after ether bond cleavage from these GDGTs (cf. Schouten et al., 1998). In a sample (24 cm) from the pelagic section,  $\delta^{13}\text{C}$  values for acyclic, bicyclic and tricyclic biphytanes are -21‰, -20‰, and -19‰, respectively (Table 3). These are typical for pelagic crenarchaeotal membrane lipids (Hoefs et al., 1997). In contrast, in a sample from the mud breccia (75 cm),  $\delta^{13}\text{C}$  values of the acyclic, monocyclic and bicyclic biphytanes are -70‰, -87‰, and -89‰, respectively, and substantially depleted relative to the average  $\delta^{13}\text{C}$  values of *in situ* methane (-55‰), the carbon source for the archaea involved in AOM. In the mud breccia from the Jesus Baraza MV the GDGT distribution in the upper 50 cm represented a mixture of the AOM and pelagic crenarchaeotal distributions due to enhanced relative amounts of both crenarchaeol and the GDGTs with 1 and 2 cyclopentane rings primarily derived from methanotrophic archaea (Figure 4). Below this interval a GDGT distribution derived from archaea involved in AOM was observed. This was confirmed by the  $\delta^{13}\text{C}$  values for the acyclic, monocyclic and bicyclic biphytanes from a sample (69 cm) from this section, i.e. -83‰, -91‰, and -81‰, respectively (Table 3), which are substantially depleted relative to that of *in-situ* methane (-29‰). In the mud breccia from the Ginsburg MV, the GDGT pattern varied along the mud breccia section. A pelagic crenarchaeotal distribution was observed in the uppermost interval, whereas a clear “AOM” distribution was evident in the 30-65 cm interval (Figure 4). Biphytanes derived from GDGTs from this interval were characterized by the most depleted  $\delta^{13}\text{C}$  signatures, e.g. -105‰ for the acyclic, -82‰ for the monocyclic, and -104‰ for the bicyclic biphytanes (Table 3). The distribution of GDGTs in combination with their  $^{13}\text{C}$ -depleted composition provided clear-cut evidence for (palaeo) AOM in all three MVs.

The isoprenoid DGDs, archaeol and hydroxyarchaeol, derived from archaea were detected in all MVs but their concentrations (e.g. Figures 3 and 5) are much lower than those in the mud breccias from the Eastern Mediterranean (Pancost et al., 2000 2001a, b) and from

PART II: The Gulf of Cadiz, NE Atlantic

Interval, cm b.s.f.	Methane <sup>a</sup>	Biomarker										
		PMI <sup>b</sup>	Phytane+crocetane	Archaeol	Non-isopren. DGD	17 $\beta$ ,21 $\beta$ (H)-bishomohopan-32-ol	Diplopterol	Diploptene	Biphytane a	Biphytane b	Biphytane c	Biphytane d
<b>Jesus Baraza MV (WMF)</b>												
10	-31	-54	n.d.	-39	n.d.	n.d.	n.d.	-45	-	-	-	-
30	-24	-54	n.d.	-45	n.d.	-36	-41	n.d.	-	-	-	-
50	-27	-46	n.d.	-45	-34	-33	-41	n.d.	-	-	-	-
69	-30	-62	n.d.	-76	-46	-48	-67	-62	-86	-91	-81	n.d.
89	-32	-61	n.d.	n.d.	n.d.	n.d.	n.d.	n.d.	-	-	-	-
116	-28	n.d.	n.d.	n.d.	n.d.	n.d.	n.d.	n.d.	-	-	-	-
Average	-29											
<b>Ginsburg MV (WMF)</b>												
65	-41	n.d.	n.d.	n.d.	n.d.	n.d.	n.d.	n.d.	-104	-82	-91	n.d.
<b>Bonjardim MV (DSPF)</b>												
0	-	n.d.	n.d.	n.d.	n.d.	n.d.	n.d.	n.d.	-	-	-	-
13	-	n.d.	n.d.	n.d.	n.d.	n.d.	n.d.	n.d.	-	-	-	-
24	-51	n.d.	n.d.	n.d.	n.d.	n.d.	n.d.	n.d.	-21	-21	-20	-19
36	-63	-67	-63	n.d.	n.d.	-26	-31	n.d.	-	-	-	-
46	-57	-	-	n.d.	n.d.	n.d.	n.d.	n.d.	-	-	-	-
65	-	-42	-36	n.d.	n.d.	n.d.	n.d.	n.d.	-	-	-	-
75	-58	-41	-32	n.d.	n.d.	n.d.	n.d.	n.d.	-70	-88	-56	n.d.
89	-	-53	-39	n.d.	n.d.	n.d.	n.d.	n.d.	-	-	-	-
109	-	-74	-66	n.d.	n.d.	n.d.	n.d.	n.d.	-	-	-	-
141	-52	-71	-53	n.d.	n.d.	n.d.	n.d.	n.d.	-	-	-	-
161	-52	-40	-33	n.d.	n.d.	n.d.	n.d.	n.d.	-	-	-	-
195	-50	n.d.	n.d.	n.d.	n.d.	n.d.	n.d.	n.d.	-	-	-	-
234	-	n.d.	n.d.	n.d.	n.d.	n.d.	n.d.	n.d.	-	-	-	-
Average	-55											

<sup>a</sup> - Stadnitskaia et al., 2006

<sup>b</sup> - the concentrations of archaeal and bacterial biomarkers in mud breccia matrixes were low.

Therefore, the error of  $\delta^{13}\text{C}$  measurements is estimated to be  $\pm 3\%$ .

n.d. - not determined

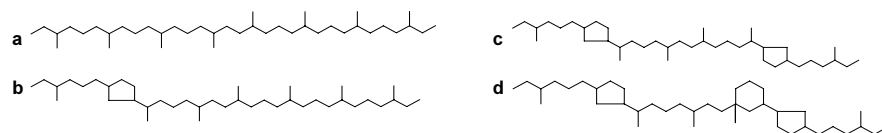


**Table 3.** Carbon stable isotope compositions of selected biomarkers, methane, and biphytanes retrieved from GDGTs of selected samples.  $\delta^{13}\text{C}$  values in ‰ vs Vienna PeeDee Belemnite.

the Black Sea (Stadnitskaia et al., 2006). Therefore, it was only possible to measure the  $\delta^{13}\text{C}$  values of archaeol in the Jesus Baraza MV (Table 3). At the interval with the highest archaeol concentration (69 cm; Figure 5) a substantially depleted value (-76‰) was recorded; at other intervals archaeol was much less enriched.

Acyclic archaeal isoprenoids were also detected in all MVs. PMI, a typical biomarker for archaea involved in AOM (Holzer et al., 1979; Wakeham, 1990; Kohlen et al., 1992; Schouten et al., 1997; Pancost et al., 2000; Elvert et al., 2000; Thiel et al., 2001), was present in all three MVs and was in the Bonjardim MV, one of the most abundant apolar archaeal lipids in sediments at a depth >40 cm. Its  $\delta^{13}\text{C}$  value varied between -40 and -74‰ (Figure 5b). In the Jesus Baraza MV, its  $\delta^{13}\text{C}$  value varied between -46 and -62‰ with the most depleted values at the highest concentrations of PMI (Figure 5a). Crocetane, also a typical

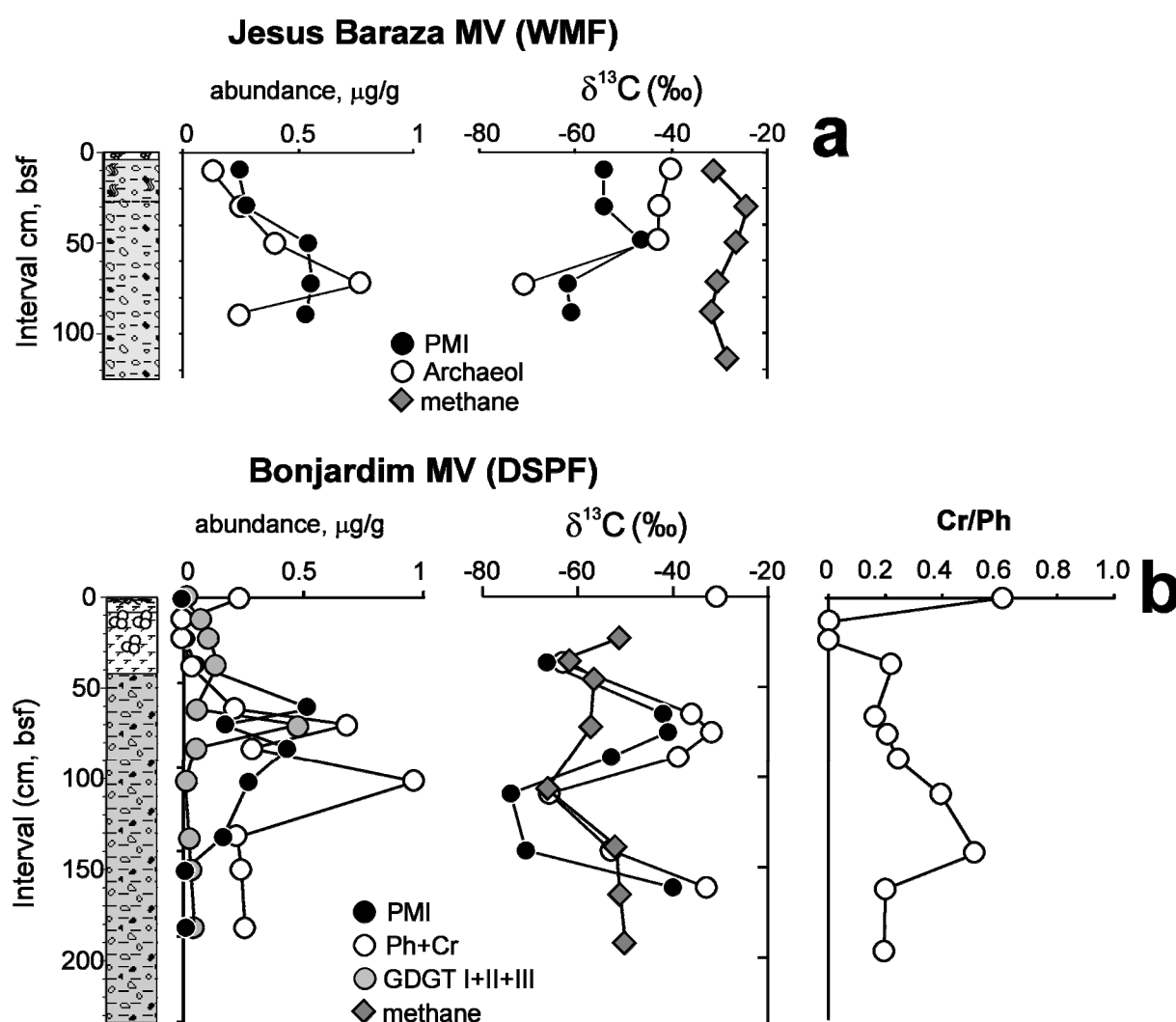


**Figure 5.** Abundances of archaeal lipids (  $\mu\text{g/g}$  of dry sediments),  $^{13}\text{C}$  values of PMI, phytane+crocetane, methane (Stadnitskaia et al., 2006), and crocetane/phytane ratio vs. depth. For the structures of GDGT I, II, and III see Figure 4.

biomarker for archaea involved in AOM (Elvert et al., 2000; Pancost et al., 2000; Bian et al., 2001), and its mono- and di-unsaturated counterparts were only detected in the Bonjardim MV, with substantially higher concentrations in the mud breccia section of the core (Figure 5b). Crocetane is also carbon isotopically depleted (Figure 5b) but this determination is complicated by a coelution with phytane. Using mass spectrometry (i.e.  $m/z$  183 as a diagnostic fragment ion for the phytane and  $m/z$  169 for the crocetane) the crocetane/phytane ratio was determined and this revealed that enriched  $\delta^{13}\text{C}$  values for the phytane/crocetane peak correlate with a decreased crocetane/phytane ratio, suggesting that

crocetane is isotopically light and phytane isotopically heavy (Figure 5b). This would indeed be consistent with an origin of crocetane from archaea involved in AOM.

Another  $^{13}\text{C}$ -depleted compound group is the non-isoprenoidal DGDs with monomethyl-branched and linear carbon chain structures. The DGD with two anteiso *ai*- $\text{C}_{15}$  ether bond chains was the most prominent one. These non-isoprenoid DGDs are presumably of SRB origin (Pancost et al., 2001 a,b; Werne et al., 2002; Stadnitskaia et al., 2005) and were found in trace amounts in all mud breccias together with archaeal lipids. Only in the mud breccia from the Jesus Baraza MV  $\delta^{13}\text{C}$  values (-34 to -46 ‰) could be obtained for this DGD (Table 3).

## 5. Discussion

### 5.1. Sources of organic matter in the mud breccias

Mud volcano deposits or mud breccia consist of a clayey matrix with a varying terrigenous admixture (silt, sand, gravel) and a variety of rock fragments often arising from sedimentary depth up to 10 kilometers (Camerlinghi et al., 1995; Akhmanov and Woodside, 1998; Ovsyannikov et al., 2003; Kozlova, 2003; Kozlova et al., 2004). Mud breccia comprises the solid part of the erupted material. The gaseous-liquid part of the migrated fluid contains hydrocarbon gases (predominantly methane), hydrogen sulfide, carbon dioxide, pore waters, and often petroleum products. After an eruption of a MV, this complex material appears at the seafloor surface providing unique information on the basin development, stratigraphy, paleoenvironments, and hydrocarbon potential of the MV area. However, knowledge regarding the sources of erupted sediments is still limited. The reason is that often mud breccia rock clasts, mud breccia matrix, and gaseous-liquid fraction of the fluid are not syngenetic. Previous study of hydrocarbon gases and pore-waters from MV deposits and gas hydrates revealed deep sources for the migrated fluids (Mazurenko et al., 2003; Stadnitskaia et al., 2006a). In contrast, studies of mud breccia rock clasts from the same MVs showed diverse lithologies and ages of these rock fragments with different thermal maturation characteristics within a single mud breccia interval and between the studied MVs (Kozlova, 2003; Ovsyannikov et al., 2003; Kozlova et al., 2004). Hence, rock clasts possess information about sedimentary horizons brought up by eruption of a MV but they do not necessarily mark the primary origin of the source-strata for the erupted sediments. The matrix holds an integrated signal of mechanically assimilated rocks, sediments, as well as organic matter inherited from diverse lithofacies passed by fluid. Consequently, the mud breccia matrix possibly is the most reliable, although complicated, sedimentary material, that can contain molecular signatures of the primary source-strata for the erupted sediments. This hypothesis was checked on the mud breccia matrices from the Black Sea MVs (Stadnitskaia et al., 2006b). In these MVs, lipid biomarker data from mud breccia matrices revealed different

sources for the erupted material and different mud eruption episodes within a sedimentary section, which was not apparent from the visual lithological description.

In the mud breccia matrices from the studied MVs in the Gulf of Cadiz, lipid analysis show similar suites of biomarkers, indicating related sources for the erupted material in DSPF and WMF, despite their distant location from each other (Figure 1). In addition, TOC data and biomarker indices (Table 1) suggest that each collected mud breccia section from the Ginsburg and Bonjardim MVs is part of a single mud flow within the MV. Hence, despite visual differences in lithologies, the organic matter from mud breccia matrices of the three MVs suggests a common source.

#### *5.1.1. Degree of thermal maturation of the organic matter*

The mud breccias of the three studied MVs all contain molecular signatures implying a mixture of moderately mature and immature organic matter. The degree of 22S/(22S+22R) homohopane epimerization for both the C<sub>31</sub> and C<sub>32</sub> 17 $\alpha$ ,21 $\beta$ (H)-homohopanes for all MVs is ca. 0.5 (Table 1). This is close to the thermodynamic equilibrium ratio of ca. 0.6, signifying a relatively mature character for these biomarkers (van Duin et al., 1997; Peters et al., 2005). The CPI values for *n*-alkanes also imply moderately mature organic matter and an admixture of petroleum-derived compounds, for instance in the mud breccia from the Bonjardim MV (Figure 2; Table 1). Nevertheless, the abundance of terrestrial C<sub>27</sub>-C<sub>33</sub> *n*-alkanes, as reflected in the CPI values, indicates an admixture of immature bitumen. An admixture with thermally immature components is also evident from the presence of hopenes and 17 $\beta$ ,21 $\beta$ (H) stereoisomers for the C<sub>30</sub> and C<sub>31</sub> hopanes (Figure 3). These stereoisomers do not co-occur with 17 $\alpha$ ,21 $\beta$ (H)-hopanes, when 22S/(22S+22R) hopane ratios are close to the value reached at thermodynamic equilibrium (van Duin et al., 1997). This must indicate that organic matter with various degrees of thermal maturation is brought to the surface during the eruption of the MVs.

A high hydrocarbon potential in the Gulf of Cadiz was detected in mud breccia rock fragments represented by clay-stones of the Upper Cretaceous age: TOC is ca. 6.7 % and HI is ca. 560-577 mg HC/g TOC (Kozlova, 2003). Pyrolysis data revealed that these clays are moderately mature and mostly at the beginning of the oil window: T<sub>max</sub> = 430-440° C (Kozlova, 2003). This is consistent with the maturity estimation for the mud breccia matrixes from MVs in the WMF and DSPF, and assumes that in both provinces fluid could pass through the Upper Cretaceous horizons of the sedimentary formations of the Gulf of Cadiz.



*5.1.2. Probable source-strata for the erupted mud breccias*

The similarities in lipid composition and degree of thermal maturation of the organic matter in the mud breccias from the studied MVs suggest common source-strata for erupted material in both DSPF and WMF. This is in contrast with the results obtained for mud breccia matrices from the MVs in the Sorokin Trough, NE Black Sea. In this area, the studied MVs are situated rather close to each other but lipid biomarker signatures revealed different sources of the organic matter in the mud breccias from these MVs (Stadnitskaia et al., 2006b). The similarity in lipid composition in the MVs of the Gulf of Cadiz indicates the presence of sedimentary unit extending through the whole Gulf, which is consistent with the understanding of the main tectonic structures and sedimentary content in the area (Maldonado et al., 1999b; Medialdea et al., 2004). The complete stratigraphic filling in the Gulf of Cadiz includes several major sedimentary units (see Medialdea et al., 2004 for a review). The presence of an upper Cretaceous–lower Eocene unit, consisting of shales with chert layers and limestones (Hayes et al., 1972), is in agreement with the age and lithology of the mud breccia rock fragments, varying in age from the Upper Cretaceous to Pliocene (Kozlova, 2003; Ovsyannikov et al., 2003). An upper Cretaceous origin is consistent with the presence of the C<sub>25</sub> HBI alkane in all mud breccias. The C<sub>25</sub> HBI alkane was previously reported in crude oils, rock and sediment extracts as old as Cretaceous (Robson and Rowland, 1986; Sinninghe Damsté et al., 1999; Rowland and Robson, 1990). Recently, Sinninghe Damsté et al. (2004) showed that this biomarker appears in the sediments and petroleum that are Upper Turonian (Upper Cretaceous) in age or younger. HBIs were previously found in diatoms (Volkman et al., 1994), and recently (Sinninghe Damsté et al., 2004) a phylogenetic study of >120 marine diatom cultures showed that biosynthesis of HBIs is restricted to two specific phylogenetic clusters. One of these clusters evolved in the Upper Turonian age (Sinninghe Damsté et al., 2004). This finding postulated C<sub>25</sub> HBI alkane as age-related biomarker (Sinninghe Damsté et al., 2004). Its abundance (Figure 3) suggests that in both WMF and DSPF, the source-strata for the erupted material are at least partly Upper Turonian or younger in age.

The moderate mature-immature characteristics of the organic matter from both mud breccia rock clasts and matrix together with mature properties of hydrocarbon gases from the same sampling locations (Stadnitskaia et al., 2006a) indicate that source-strata for the initial fluid are likely located much deeper than the source-strata for the organic matter in the erupted sedimentary material.

*5.2. Microbial processes induced by upward migrating fluids*

Fluid venting areas are “hot-spots” for a variety of microbes dwelling in specific niches of these environments. The metabolism of these microbes in such settings are determined by a number of factors, such as the chemistry and physics of migrated fluids,

temperature and pressure, the presence of inorganic and organic substances required for microbial functioning and growth. In cold seeps, methane is often the most important substance as a source for energy and carbon. Aerobic methane consumption is restricted to a much narrow sedimentary interval than AOM since sulfate penetrates much deeper than oxygen (Krüger et al., 2005) and only bioturbation can enhance oxygen diffusion into suboxic/anoxic sediments (Zorn et al., 2006). In comparison with oxygen-dependent methanotrophy, AOM is thought to be one of the most efficient barrier for methane release from marine sediments (Hinrichs and Boetius, 2002; Krüger et al., 2005).

Lipids biosynthesized by microbes involved in anaerobic methanotrophy are strongly depleted in  $^{13}\text{C}$ , signifying methane, which is commonly depleted in  $^{13}\text{C}$ , as their source of carbon (Hinrichs et al., 1999, 2000b; Elvert et al., 1999, 2000; Boetius et al., 2000; Thiel et al., 2001; Pancost et al., 2000). The specific GDGT distributions in the mud breccias (Figure 4) in combination with substantially  $^{13}\text{C}$ -depleted biphytanes from these GDGTs in these intervals (Table 3) provide evidence for the occurrence of AOM in all studied mud breccias. This is confirmed by the presence of other specific  $^{13}\text{C}$ -depleted biomarkers for archaea and SRB (Figure 5 and Table 3) although their  $\delta^{13}\text{C}$  values are more enriched than the biphytanes and more variable. The presence of  $^{13}\text{C}$ -depleted diplopterol and  $17\beta$ ,  $21\beta(\text{H})$ -bishomohopan-32-ol in the MV deposits from the Jesus Baraza MV also denotes incorporation of methane-derived carbon into hopanoid-producing microbes. The occurrence of  $^{13}\text{C}$ -depleted non-isoprenoidal DGD (Table 3), a lipid hypothetically marking SRB, together with archaeal biomarkers could suggest the presence of SRB. AOM was not detected in the pelagic sediments from the Bonjardim MV (Figure 4 and Table 3).

Methanotrophic euryarchaeota from seep environments fall in three different groups: ANME-1 (Hinrichs et al., 1999), ANME-2 (Boetius et al., 2000; Orphan et al., 2001a,b), and ANME-3 (Knittel et al., 2005) as revealed by molecular ecological studies. ANME-1 and ANME-2 archaeal groups are characterized by a specific lipid composition (Blumenberg et al., 2004). The occurrence of crocetane and crocetenes in the mud breccias of the Bonjardim MV is diagnostic for ANME-2 archaea (Blumenberg et al., 2004). However, AOM-derived GDGTs with 0-2 cyclopentane rings (Figure 4) are indicative of the dominance of the ANME-1 members (Blumenberg et al., 2004). In the mud breccia from the Ginsburg MV, the composition of AOM-specific biomarkers varies with the depth implying a mixed AOM archaeal community. The presence of PMI and GDGTs with 0-3 cyclopentane rings (Figure 4) along the whole mud breccia interval suggests that ANME-1 archaea are likely the most dominant methanotrophs at this site. Similarly, in the mud breccia from the Jesus Baraza MV, the set of AOM-related components lack of crocetane/crocetenes and hydroxyarchaeol while PMI, archaeol (Figure 5a) and GDGTs with 0-2 cyclopentane (Figure 4) rings are present.

This suggests the main archaeal methanotrophs in the mud breccia from the Jesus Baraza MV are likely also predominantly members of the ANME-1 archaeal group (Blumenberg et al., 2004).

Changes in the methane flux and temperature can have a selective effect on the AOM community (Treude, 2003; Nauhaus et al., 2002; 2005; Krüger et al., 2005). Previous studies have shown that ANME-1 and ANME-2 often co-occur, but depending on the environments, one of these groups tends to dominate the microbial population (Nauhaus et al., 2005). Hence, the observed variations of archaeal lipid compositions may indicate changes in the environmental conditions through time resulting in an adaptational response of the archaea involved in AOM.

Biomarkers indicative for AOM were detected in the whole interval of the mud breccias of the three MVs. AOM only occurs in the zone where downward diffusing methane and upward migrating methane, i.e. the sulfate-methane transition zone (SMT), meet. This is typically only a small interval in the sediment. Therefore, our data suggest that the biomarker lipids indicative for microbes involved in AOM are, at least in part, fossil in origin (i.e. they do not reflect active AOM communities) and thus reflect AOM activity in these MVs integrated over time. The position of the SMT is likely to shift in depth after the eruption of a MV and the formation of a mud breccia flow as the result of changes in the depth of sulfate penetration and methane flux (cf. Hoehler et al., 1994). This probably explains the “noisy” appearance of the concentration profiles (Figure 5) and changes in the  $\delta^{13}\text{C}$  values of the biomarkers with depth. It also indicates that a comparison of the  $\delta^{13}\text{C}$  values of the fossil biomarkers with in-situ methane is not always useful.

Compared to the presently active fluid venting provinces and related flourishing of AOM in the Black Sea (Ivanov et al., 1998; Michaelis et al., 2002; Blumenberg et al., 2004; Stadnitskaia et al., 2005), in the cold seeps from the Gulf of Mexico (Zhang et al., 2003), in the Eastern Mediterranean MVs (Pancost et al., 2000), in the Tommeliten seep area in the Central North Sea (Niemann 2005a) and in the Håkon Mosby MV on the Norwegian margin of the Barents Sea (Niemann, 2005b), low concentrations of AOM-biomarkers are evident for the three MVs from the Gulf of Cadiz. This likely relates to brief period of methane seeping and thus to the absence of continuous methane/fluid influx. This is consistent with hydrocarbon gas data (Stadnitskaia et al., 2006a) and measured AOM activity in MVs from the Gulf, which is estimated as low to mid range in comparison to other fluid flow environments of the World oceans (Niemann, et al., 2006). Nevertheless, this does not indicate that the studied MVs are dormant since gas hydrates were repeatedly recovered from these structures (Kenyon et al., 2000, 2001, 2002; Pinheiro et al., 2003).

The lowest concentrations of AOM-related lipid biomarkers were found in the mud breccias from the Ginsburg MV. This is somewhat surprising since in this MV methane

concentrations are the highest of the three MVs (Figure 1). The mud breccia from the Ginsburg MV has no pelagic cover at the top (Kenyon et al., 2001) and gas hydrates were found at depths greater than 120 cm (Kenyon et al., 2001; Mazurenko et al., 2003). This indicates recent MV activity and the availability of methane. In this particular setting, the low concentration of AOM biomarkers may possibly be explained by the fact that AOM activity started only recently due to a recent mud eruption episode in combination with long doubling times of methanotrophic archaea cells (Treude, 2003). By contrast, the low concentrations of AOM-related lipid biomarkers in the Bonjardim and Jesus Baraza MVs have a different reason than in the Ginsburg MV. The pelagic cover at both sampling sections indicates relatively old mud breccia flows. The reduction of methane supply reflects in the significantly lower methane concentrations compared with the Ginsburg MV (Figure 1). The Ginsburg MV can thus be considered as one of the most active structure in the Gulf at present and is indeed located within the tectonically active part of the Gulf, suggesting intensive fluid transport (Kenyon et al., 2000, 2001; Stadnitskaia et al., 2006a).

## **6. Summary**

Lipid biomarker analysis was for the first time performed for MV deposits collected from three MVs, the Bonjardim, Ginsburg and Jesus Baraza, from the Gulf of Cadiz. The obtained data showed similar suite of biomarkers and maturity properties of organic matter implying common sources for the mud breccias in both MV provinces. The combination of existing geochemical data for the mud breccia rock fragments and our lipid biomarker data from the mud breccia matrixes reveals that in both MV areas, the source of organic matter from mud breccias is likely located below the Olistostrome deposits, possibly Upper Turonian or younger sedimentary beds. The moderate mature-immature properties of organic matter from both mud breccia rock clasts and matrix and mature characteristics of hydrocarbon gases from the same sampling sites (Stadnitskaia et al., 2006) indicate that source strata of the primary fluid are located deeper than the source strata of the organic matter from the erupted sedimentary material.

The presence of  $^{13}\text{C}$ -depleted lipid biomarkers derived from methanotrophic archaea in the mud breccias revealed that AOM is or has been a dominant microbial process in these habitats. The low concentrations of AOM-related biomarkers suggest low AOM rates within all studied MV deposits and may even indicate that AOM was only a predominant process at the time of active mud volcanism. The occurrence of  $^{13}\text{C}$ -depleted non-isoprenoidal DGD, a lipid hypothetically marking SRB, together with archaeal biomarkers supports the presence of SRB in all mud breccias.

### CARBONATE FORMATION BY ANAEROBIC OXIDATION OF METHANE IN THE GULF OF CADIZ (NE ATLANTIC)

A. Stadnitskaia<sup>a,b</sup>, D. Nadezhkin<sup>b</sup>, B. Abbas<sup>a</sup>, V. Blinova<sup>b</sup>,  
M.K. Ivanov<sup>b</sup> and J. S. Sinninghe Damsté<sup>a</sup>.

<sup>a</sup> *Royal Netherlands Institute for Sea Research (NIOZ), P.O.Box 59, 1790 AB, Den Burg, Texel, the Netherlands*

<sup>b</sup> *UNESCO-MSU Centre for Marine Geosciences, Geological faculty, Moscow State University, Vorobjevy Gory, Moscow 119899, Russia*

In preparation

#### **Abstract**

Detailed investigation of fluid venting and mud volcanism in the Gulf of Cadiz, carried out during several cruises of the Training Trough Research (TTR) programme, revealed that carbonate chimneys and crusts occur widespread. Their presence likely reflects fluid escape events in the geological past, possibly in the Early Pleistocene. We studied a carbonate crust from the Kidd mud volcano collected in the Gulf during the TTR-14 cruise in 2004. Concentrations of microbial lipids, their stable carbon isotope composition, determination of 16S rRNA gene sequences of anaerobic methanotrophic archaea in combination with mineralogical composition and  $\delta^{13}\text{C}$  and  $\delta^{18}\text{O}$  composition of carbonate were obtained for seven different horizons of the crust and used to reconstruct microbiological processes and biogeochemical conditions during the formation of the carbonate crust. The combination of molecular organic, molecular biological and inorganic methods revealed good correlation among the various independent parameters and indicated that the formation of the crust took place in two phases and in a downward direction. Archaeal lipid biomarkers and 16S rRNA gene sequence data revealed the dominance of archaeal ANME-2 group and elevated methane flux during the formation of the top part of the crust. The lower part of the carbonate likely was formed in the environments with less intensive methane flux in comparison with the top part, which probably reflected in the dominance of ANME-1 archaeal members.

## **1. Introduction**

Anaerobic Oxidation of Methane (AOM) is an important sink for methane in marine settings controlling, in part, atmospheric concentrations of methane. Although geochemical evidence for AOM exists for decades (Martens and Berner, 1974; Reeburgh, 1976; Barnes and Goldberg, 1976; Zender and Brock, 1979; Alperin and Reeburgh, 1984, 1985; Hoehler et al., 1994; Hoehler and Alperin, 1996), it is only recently that we start to identify the microbes responsible for AOM. The first unequivocal evidence for an involvement of archaea in AOM came from the detection of <sup>13</sup>C-depleted archaea-specific lipid biomarkers in methane seep environments (Hinrichs et al., 1999). Observations of conspicuous aggregates of archaea and sulfate reducing bacteria (SRB) by microscopy made by Boetius et al. (2000), complemented and strengthened this work. It showed that AOM can be accomplished by microorganisms belonging to the domain of Archaea occurring mostly in a consortium with SRB belonging to different phylogenetic groups developing in symbiotic aggregations of unknown functioning (Boetius et al., 2000; Orphan et al., 2001 a,b; Teske et al., 2002; Michaelis et al., 2002).

AOM results in the production of sulfide and bicarbonate in anoxic sediments (Reeburgh, 1976). Precipitation of carbonate, as a consequence of oversaturation of bicarbonate in pore waters, is one of the most visually evident consequences of AOM in cold-vent settings (Hovland et al., 1987; Ritger et al., 1987; 1993; Suess and Whiticar 1989; LePichon et al., 1990; Buczynski and Chafetz, 1991; Jørgensen, 1992; Roberts and Aharon, 1994; Von Rad et al., 1996; Peckmann et al., 1999 a, b, 2001; Aloisi et al., 2000, 2002; Michaelis et al., 2002; Stadnitskaia et al., 2005). Such AOM-related carbonates can occur in the form of crusts, concretions, pavements and chimneys, varying in size from precipitates of only a few millimetres to meters-high chimneys and carbonate pavements of hundred square meters on the sea floor. Methane-related carbonates have been documented in sediments ranging in age from Recent (Paul et al., 1992; Campbell, 1993; Roberts et al., 1994; Clari et al., 1994; Michaelis et al., 2002; Stadnitskaia et al., 2005; Reitner et al., 2005) to up to the Middle Devonian (Beauchamp, et al., 1989; Gaillard et al., 1992; Peckmann et al., 1999b; Kauffman et al., 1996; Thiel, et al., 1999; Campbell et al., 2002; Peckmann et al., 2002, 2003, 2004). However, only the recent discovery of living methanotrophic mats in relationship with carbonate chimneys and active methane emanation in the north-western Black Sea established the direct relationship of carbonate formation in such habitats and AOM (Michaelis et al., 2002). It is presently unknown how much methane is “trapped” in the carbonate during AOM and how environmental conditions play a role in this conversion.

About twenty MVs have been discovered since 1999 during the five Training Through Research (TTR) expeditions in the area of the Gulf of Cadiz (Kenyon et al., 2000, 2001, 2000; Ivanov et al., 2000, 2001; Gardner, 2001; Pinheiro et al., 2003; Terrinha et al., 2003; Mazurenko et al., 2002, 2003; Somoza et al., 2003; Ovsyannikov et al., 2003; Murton and

Biggs, 2003; Van Rensbergen et al., 2005; Stadnitskaia et al., 2006). The TTR cruises were focused on mud volcanism and related phenomena such as gas hydrates, methane-related carbonates and seepage-associated benthic chemosynthetic communities. A wide variety of carbonate chimneys, slabs, crusts and concretions was discovered and sampled in the Gulf (Kenyon et al., 2002; Diaz-del-Rio, et al., 2003; Ivanov et al., 2004). Most of these carbonates are spatially distributed on the top and slopes of diapiric ridges occurring in 800 to 1100 m of the water depth (Kenyon et al., 2002; Ivanov et al., 2004). Diaz-del-Rio et al. (2003) showed similar petrographic characteristics among the carbonate chimney from several areas within the Gulf of Cadiz. Simultaneously,  $\delta^{13}\text{C}$  and  $\delta^{18}\text{O}$  data from these chimneys showed significant differences, indicating distinct sources of migrated fluids (Diaz-del-Rio, et al., 2003). U/Th dating revealed that chimneys were formed in the Early Pleistocene during glacials (Ivanov et al., 2004).

To learn more about complex environmental factors responsible for the development of such carbonates and the associated microbiological processes, we studied in detail one methane-related carbonate crust collected from the Kidd MV during the TTR-14 (2004) cruise in the Gulf of Cadiz (Figure 1). The idea of this work was to reveal the “carbonate precipitation history” within the local methane-seepage environment *via* the combination of molecular geochemical tools with mineralogical and stable isotopes techniques. We analyzed vertical distribution profiles of (i) lipid biomarkers derived from anaerobic methanotrophic archaea and sulfate-reducing bacteria (SRB) responsible for AOM at different seepage habitats, (ii)  $\delta^{13}\text{C}$  and  $\delta^{18}\text{O}$  signatures from bulk carbonate accompanied with mineralogical

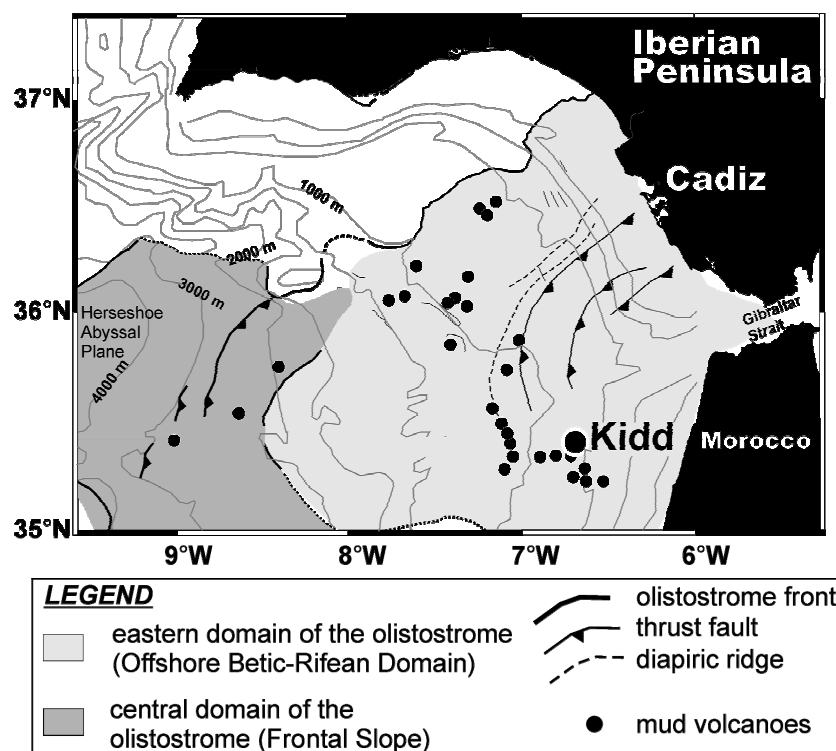


**Figure 1.** Geological map, simplified bathymetry of the Gulf of Cadiz, with the location of the Kidd MV and other MVs discovered during TTR cruises (compilation of TTR data 1999-2001 and Medialdea et al., 2004).



composition studies, and (iii) 16S rRNA gene sequence to characterize communities of ANaerobic MEthanotrophs (ANME) during the development of the crust.

## **2. Material and methods**

### *2.1. Sampling location and the carbonate crust*

The Kidd MV is located on the Western Moroccan continental margin (Figure 1; Kenyon et al., 2000; 2003; Medialdea et al., 2004). This part of the Gulf is known for extensive mud diapirism and mud volcanism, which are structurally controlled and probably triggered by the tectonic forces related to the convergence between the African and the Eurasian plates (Gardner, 2001). Seismic and acoustic data revealed that the Kidd MV sits at the top of the Vernadsky Ridge and has a diapiric nature (Kenyon et al., 2003). It disturbs adjacent Quaternary age units, indicating its recent emplacement (Kenyon et al., 2000).

The sampling site was chosen on the basis of the data from previous TTR-9 (1999) geophysical surveys in the Gulf (Kenyon et al., 2000). The carbonate crust was collected from the top of the Kidd MV (35°25'W; 06°44'W) during the TTR-14 (2004) expedition using a TV-controlled grab sampler. The crust represents ca. 30 x 15 cm irregularly shaped, elongated, porous at the top and well-cemented precipitate (Figure 2). The topmost 12 cm are brownish-beige in colour with intensively porous the outer surface and with signs of erosion caused by the presence of chemosynthetic fauna, e.g. cemented borrows and a number of shell debris. The intermediate part of the crust, from 12 to 17 cm, is darker, brownish-grey, less porous, and with no visual indication of the chemosynthetic biota presence. Below this interval, the crust is grey in colour and massive (Figure 2).

For the set of analytical measurements outlined below, the crust was split into seven intervals taking into consideration the visual differences in color and surface structure of the precipitant.

### *2.2. Mineralogy and stable isotope composition of the carbonate*

The mineralogy was determined using an X-ray diffraction (XRD) technique of dried and powdered sub-samples of the crust (Shlikov and Kharitonov, 2001). The carbon and oxygen stable isotope measurements were performed for the bulk carbonate material, liberating CO<sub>2</sub> by the phosphoric acid techniques as described in McCrea, (1950) and in Sharma and Clayton (1965). Measurements were made at the Laboratory of Isotope Geology of Fluids in the St.-Petersburg State University (Russia) with a modernized AEI instrument linked with MS-20 mass spectrometer. The carbon and oxygen stable isotope concentrations are reported in the  $\delta$ -notation (‰) relative to the Vienna PeeDee Belemnite (VPDB) standard and relative to the Standard Mean Ocean Water (SMOW), respectively. The precision of the analysis is 0.1 – 0.2‰ for carbon and 0.1 – 0.3‰ for oxygen (Prasolov et al., 2002).

### 2.3. Lipid biomarker study

#### 2.3.1. Preparation and extraction

Samples of ca. 20 g were crushed in an agate mortar to a fine powder, and extracted with an automatic Accelerated Solvent Extractor (ASE 200/DIONEX) using a solvent mixtures of dichloromethane (DCM): methanol (MeOH) (9:1, v/v) at 1000 psi and 100°C. Elemental sulfur was removed from the total extracts by adding ca. 30 mg of activated copper and stirring the sample over night. In accordance to the weight difference of total lipid extracts before and after sulfur removal, a rough estimation of the concentration of elemental sulphur in the crust was calculated. Afterwards, fatty acids were methylated by heating at 60°C for 5 min in BF<sub>3</sub>-MeOH complex (in excess MeOH, ca.12 wt.% BF<sub>3</sub>), and alcohols were transformed into trimethylsilyl-derivatives by adding 25 µl of pyridine and 25 µl of BSTFA and heating at 60°C for 20 min. A known amount of 2,3-dimethyl-5-(1,1-dideuterohexadecyl)-thiophene (C<sub>22</sub>H<sub>38</sub>SD<sub>2</sub>) was added in each fraction as an internal standard.

An aliquot of the total lipid extract (TLE) was chromatographically separated into apolar and polar fractions using a column with activated (2 h at 150°C) Al<sub>2</sub>O<sub>3</sub> as stationary phase. Apolar compounds were eluted using hexane:DCM (9:1, v/v), and polar compounds, including glycerol ether core membrane lipids, were obtained with MeOH:DCM (1:1, v/v) as eluent.

#### 2.3.2. Instrumental analysis

Gas chromatography (GC) was performed using a Hewlett Packard 6890 gas chromatograph equipped with an on-column injector and a flame ionization detector. A fused silica capillary column (CP Sil-5 25 m x 0.32mm, *d*<sub>f</sub>=0.12 µm) with helium as a carrier gas was used. The samples were injected at 70° C. The GC oven temperature was subsequently raised to 130° C at a rate of 20° C min<sup>-1</sup>, and then to 320° C at 4° C min<sup>-1</sup>. The temperature was then held constant for 15 min.

All fractions were analyzed by gas chromatography-mass spectrometry (GC-MS) for compound identification. GC-MS was conducted using a Termofinnigan TRACE gas chromatograph with the same temperature program as for GC. The column was directly inserted into the electron impact ion source of a Thermofinnigan DSQ quadrupole mass spectrometer operated with ionization energy 70 eV with a scanning mass range of *m/z* 50–800 at 3 scans per second. The structural designation of lipids was evaluated by the comparison their mass spectral fragmentation patterns and Pseudo Kovats retention indices with reported data.

Isotope-ratio-monitoring gas chromatography–mass spectrometry (IRM–GC–MS) was performed on a Finnigan MAT DELTA plus XL instrument used for determining compound-specific  $\delta^{13}\text{C}$  values. The GC used was a Hewlett Packard 6890 A series and the same analytical conditions were used as described for GC and GC–MS. For carbon isotopic correction of the added trimethylsilyl groups, the carbon isotopic composition of the used BSTFA was determined ( $-49.30 \pm 0.5 \text{ ‰}$ ). Obtained values are reported in per mil (‰) relative to the VPDB standard, and have been corrected for the addition of  $\text{Si}(\text{CH}_3)_3$  group due to the derivatisation procedure. In order to monitor the accuracy of the measurements, the analyses were carried out with co-injection of two standards,  $\text{C}_{20}$  and  $\text{C}_{24}$  *n*-alkanes, which have known carbon isotopic composition.

To determine the distribution of intact glycerol dialkyl glycerol tetraethers (GDGTs), the polar fractions were analyzed using a high performance liquid chromatography–mass spectrometry (HPLC–MS) method for their direct analysis (Hopmans et al., 2000). GDGTs were analyzed using an Agilent 1100 / 1100 MSD series instrument, with auto-injection system and HP-Chemstation software. An Alltech Prevail Cyano column (150 mm x 2.1 mm, 3  $\mu\text{m}$ ) was used with hexane:propanol (99:1, 13 v) as a mobile phase. For the first 5 min the flow rate of eluent was  $0.2 \text{ ml min}^{-1}$ . In the following 45 min, the flow rate was used with a linear gradient to 1.8 % propanol. MS-analysis and quantification of isoprenoidal GDGTs followed methods reported in Weijers et al. (2006).

### 2.3.3. DNA extraction

Genomic DNA was extracted from ca. 4 g of sample using a modified method described by Hurt et al. (2001). Using standard agarose gel electrophoresis, the genomic DNA quality and quantity were evaluated. The genomic DNA from all samples mainly consisted of high molecular weight DNA (>20 kilobases).

### 2.3.4. PCR amplification of 16S rRNA genes

Amplification of 16S rRNA gene fragments specific for ANME archaeal groups, appropriate in size for analysis by denaturing gradient gel electrophoresis (DGGE) (Schäfer and Muyzer, 2001), was accomplished using combination of published primers (Schubert et al., 2006), ANME111f (*E. coli* positions 111–128; Thomsen et al., 2001) and the general archaeal primer ARCH915r (*E. coli* positions 915–934; Stahl and Amann, 1991). To ensure the stability of 16S rRNA gene fragments during DGGE analysis, a 40-bp long GC-clamp (5'-CGC CCG CCG CGC CCC GCG CCC GGC CCG CCG CCC CCG-3') (Schäfer and Muyzer, 2001) was added to the 5'-end of the ARCH915r primer (Coolen et al., 2004).

For the detection of ANME-specific 16S rRNA gene fragments, a two-step amplification was applied. The first amplification (without GC-clamp) was performed in

realtime using PCR conditions with an initial denaturation step of 4 min at 95°C, followed by 32 cycles including a denaturation step for 30 s at 94°C, a primer annealing step for 40 s at 64°C, a primer extension step of 60 s at 72°C, and a final extension (photomoment) of 25 s at 80°C. The reaction was stopped when the first products of PCR appeared above a threshold. In order to attach the GC-clamp to the fragments and increase the sensitivity by at least a factor of 10, a re-amplification was performed using a similar protocol, but with only 15 cycles and a final extension of 30 min at 72°C to prevent double banding in DGGE. All PCR amplifications were performed with a iCycler real-time PCR machine (Bio-Rad). To prevent impaired-fragment-running behaviour during the DGGE analysis, the first round amplifications and re-amplifications were observed in realtime and non-realtime, respectively. The PCR-reaction setup contained 2 µl of 10X Picomaxx High Fidelity buffer (Stratagene, USA), 250 µM of each dNTP's (Eurogentec, Belgium), 250 pM of each primer, 2.5 units of Picomaxx enzyme, 8 µg of bovine serum albumin (BSA, Sigma-Aldrich) and 0.4 µl of genetic DNA template. For the realtime setup, extra components were added: 1.0 mM MgCl<sub>2</sub>, 10 nM Fluorescein (supplied by Bio-Rad) and 50k diluted Sybr-Green (molecular probes, invitrogen). The final volume of the mixture was adjusted to 20 µl with molecular-grade water (Sigma, Saint Louis, MO, USA). PCR resulted in fragment lengths (including GC-clamp) of 834-847 bp. As positive controls, genetic DNA and diluted purified PCR product of *Methanosarcina mazei* were used. Two types of negative controls, an extraction control (used ultra pure H<sub>2</sub>O in stead of sample) and a PCR negative (added ultra pure H<sub>2</sub>O) were also included.

Prior to performing PCR amplifications for DGGE, a PCR reaction was setup to determine inhibition and maximum sensitivity. The setup was as followed: three five-fold dilutions (1-5-25x) were made from genetic DNA. Amplifications were observed in realtime and Ct (threshold cycles) were noted. All reactions were slightly inhibited when undiluted template was used. In the case of the 5x and 25x diluted template, inhibition seemed minimal while a signal was still possible to observe (around  $1 \times 10^2$ - $10^3$  copies). The sediment sample from 25 cm (Table 1) was diluted 625x to normalize for Ct value compared to the other samples. Using the realtime PCR setup, the amount of gene copies per extracted sample was determined using a diluted reference of a full-16s rRNA amplicon (*Methanosarcina mazei*) from  $1 \times 10^6$  copies till  $1 \times 10^0$ . Amounts between  $5 \times 10^4$  to  $5 \times 10^5$  copies/gram crust were measured.

All PCR reactions of carbonate samples and positive controls yielded product of a single length of sufficient quantity. All negative controls remained negative.

### *2.3.5. DGGE analysis of 16S rRNA genes*

All PCR-products were analyzed by DGGE (Schäfer and Muyzer, 2001) with a Bio-Rad DGene system (Biorad, München, Germany). PCR products were quantified by gel electrophoresis using a mass molecular DNA marker (Smartladder, Eurogentec). For analysis about 100 ng was applied directly onto 6% (wt/ vol.) polyacrylamide gel (acrylamide/N,NV-methylene bisacrylamide ratio, 37:1 [w/w]) in 1xTAE buffer (pH=8.3), which was prepared from sterile solutions and casted between glass plates. The gel contained a linear gradient of denaturant from 20 to 70% Urea-formamide (100% denaturant is 7 M urea plus 40%[v/v] formamide). Electrophoresis proceeded for 5 h at 200 V at 60°C. Afterwards, the gels were stained by overlaying with 5 ml staining solution, consisting of a 2xTAE buffer containing 10k diluted Sybr-Green (molecular probes, invitrogen) for 20 min. Destaining was done by rinsing with MQ-quality water. Gels were visualized using a Darkreader (Clare Chemical Research, Inc. Dolores, CO 81323, USA) to prevent DNA damage and photographed using a FluorS imaging system (Bio-Rad). DGGE fragments were excised from the gel with a sterile scalpel and the DNA containing fragment was submerged in sterile 10 mM Tris-HCl (pH=8.0) for >48 h at 2-8°C. Re-amplification of the eluted DNA was performed using a standard, non-realtime setup, by using 0.4 µl of eluted DNA in a final 20 µl PCR volume as described above, with the exception that 1 unit enzyme was used and a protocol consisted of only 25 cycles.

### *2.3.6. Sequencing of DGGE bands*

Prior to performing cycle sequencing reactions, PCR products were purified using a PCR purification kit (Qiagen, Benelux). After purification, products were quantified on an agarose gel as previously described. Cycle sequencing reactions were performed using the ABI Prism Big Dye Terminator V1.1 kit components (Applied Biosystems, CA, USA), the forward or reverse primer (without GC clamp) at a final concentration of 0.2 µM and 10 ng of template DNA. The reaction volume was adjusted to a volume of 20 µl with molecular grade water (Sigma). The following reaction conditions were set: 1 min initial denaturing at 95°C followed by 25 cycles of 10 s at 95°C, 5 s at 55°C, and 4 min at 60°C. An isopropanol mediated purification was used for purifying DNA, pellets were dissolved in HiDi formamide ready for sequencing. Sequencing was performed on an automated ABI-310 capillary sequencer (Applied Biosystems). Complementary sequences were aligned and manually edited using the AutoAssembler software package (Version 2.1.1; Applied Biosystems).

### *2.3.7. Comparative analysis of 16S rRNA gene sequences*

The partial sequences were aligned with sequences present in the database and added by parsimony to a recently published extensive phylogenetic tree by Knittel et al. (2004) and

Jurgens et al. (2005) containing about 200-300 target sequences of Eury-, and Crenarchaeota using Crenarchaeota as an out-group. Phylogenetic trees were generated by using maximum likelihood method, with a filter for valid columns installed as implemented in ARB. Names of the sequences consist of the prefix DGGE, indicating that the

Crust intervals (cm)	$\delta^{13}\text{C}$ (‰)	$\delta^{18}\text{O}$ (‰)	Crust intervals (cm)	Extractable organic matter (mg/g)	Total genomic DNA content (ng/g)
top	-26.2	+1.0	0-1	0.12	50-250
5	-20.2	+0.3	5-6	0.14	50-250
12	-25.1	+0.1	9-10	0.11	20-120
15	-25.9	+1.1	10-12	0.07	<20
20	-27.0	+1.3	15-16	0.11	20-120
25	-26.7	+2.1	18-23	0.12	50-250
28	-24.9	+1.3	25-28	0.13	50-250

**Table 1.** Bulk parameters of the studied carbonate crust.

sequences were obtained from excised DGGE bands with ANME-#(1-40) indicating ANME Euryarchaeota. The numbers used in the DGGE are the same as those used in the tree.

### 3. Results

#### 3.1. Mineralogy and stable isotopes

XRD analyses revealed that the carbonate crust consists of aragonite and quartz with an admixture of calcite, high-magnesium calcite, dolomite, ankerite, plagioclase and halite (Figure 2). The magnesium content is in the range of 15-19 mole %  $\text{MgCO}_3$ , increasing downwards the crust. The quartz content also showed an increase with increasing depth (Figure 2).

The bulk carbonate from the crust is strongly depleted in  $^{13}\text{C}$ . Carbon stable isotope composition varies from -20.2 to -27.0 ‰ (Table 1). Oxygen stable isotopes change vary from +0.3 to +2.1 ‰ (Table 1). Figure 2 shows distribution profiles of  $\delta^{13}\text{C}$  and  $\delta^{18}\text{O}$  values from bulk carbonates, revealing their variations along the crust.

#### 3.2. Composition of lipid biomarkers

Figure 3 shows two representative gas chromatograms of total lipid extracts (TLEs) from two intervals of the crust. The compounds identified include  $\text{C}_{14}$  to  $\text{C}_{17}$  *n*-alkanes,  $\text{C}_{14}$  to  $\text{C}_{18}$  straight-chain fatty acids and straight-chain  $\text{C}_{14}$  to  $\text{C}_{18}$  alcohols. All these compound classes are present in subordinate amounts.

All samples lack biomarkers for aerobic methanotrophic bacteria. Instead, TLEs show a set of compounds diagnostic for archaea. Among the apolar components, the irregular, tail-to-tail linked isoprenoid acyclic  $\text{C}_{20}$  (2,6,11,15-tetramethylhexadecane or crocetane; **I**, see Appendix for structures) and  $\text{C}_{25}$  [2,6,10,15,19-pentamethylcosane, PMI; **II**] hydrocarbons, are the dominant members. Crocetane and PMI were present in similar absolute amounts

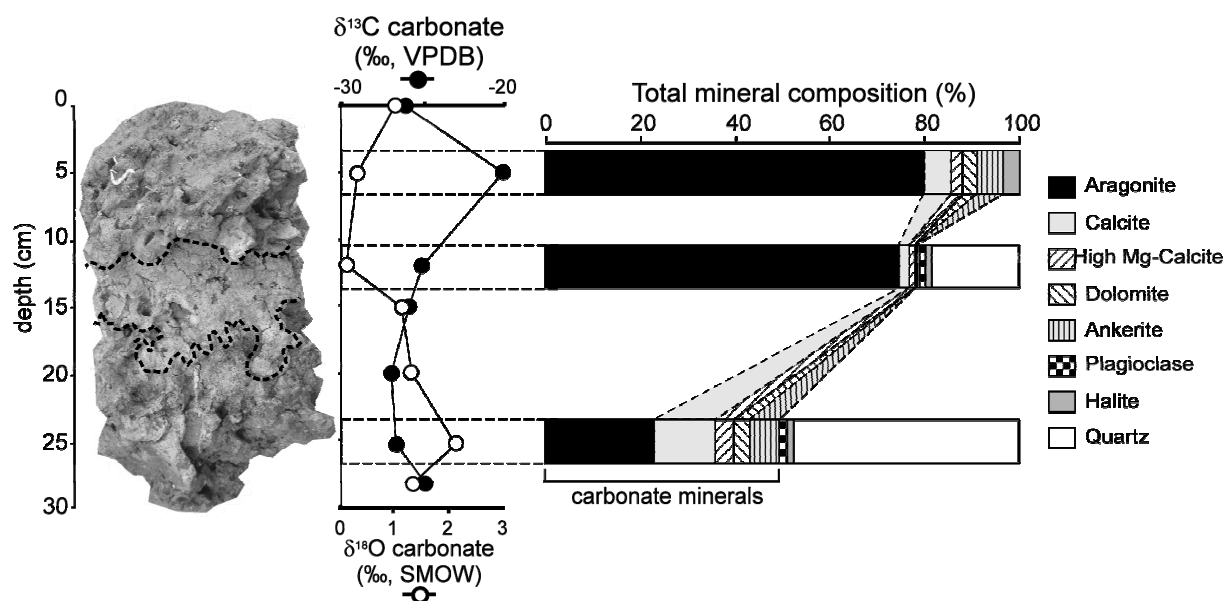


**Figure 2.** Stable carbon and oxygen isotope profiles and mineralogical composition of the crust. See page 201 for color figure.

varying from 0.1 to 0.5  $\mu\text{g/g}$  and from 0.1 to 0.6  $\mu\text{g/g}$ , respectively, with their highest abundances in the uppermost 10 cm of the carbonate crust (Figure 4). The unsaturated derivatives of PMI, pentamethylcosenes (PMEs; **III**) with 1 to 5 unsaturations, were also detected throughout the crust although they occur in trace amounts (Figure 3).

For the polar components, the topmost 10 cm of the carbonate showed the dominance of archaeol (2,3-di-*O*-phytanyl-*sn*-glycerol; **IV**) and *sn*-2-OH-hydroxyarchaeol (2-*O*-3-hydroxyphytanyl-3-*O*-phytanyl-*sn*-glycerol; **V**) and its dehydration product, mono-TMS derivative, previously described in Hinrichs et al. (2000). Along the crust, their concentrations vary from 0.7 to 4.6  $\mu\text{g/g}$  and from 0.1 to 5.5  $\mu\text{g/g}$ , respectively (Figure 4). GDGT distributions were dominated by GDGTs with 0-2 cyclopentane moieties (**VII**, **VIII**, **IX**; Figure 3). These patterns are similar to those previously reported in the Eastern Mediterranean (Pancost et al., 2001b; Aloisi et al., 2002) and in the Black Sea MVs (Stadnitskaia et al., 2005) as well as in the Black Sea water column (Wakeham et al., 2003). The total concentration of GDGTs varied along the crust from 1.2 to 8.3  $\mu\text{g/g}$  (Figure 4). Concentrations of all archaeal lipids are noticeably lower within the intermediate part (10-12 cm) of the crust (Figure 4) and the proportions between the compounds become different, i.e. the summed concentration of the most abundant GDGTs (i.e. **VII-IX**) is comparable to those of archaeol and hydroxyarchaeol (Figure 4). Further down the carbonate, archaeol and hydroxyarchaeol become less dominant and the GDGTs turn out to be the most abundant polar components, with the GDGT possessing two cyclopentane moieties (**IX**) as the dominant one (Figure 3).

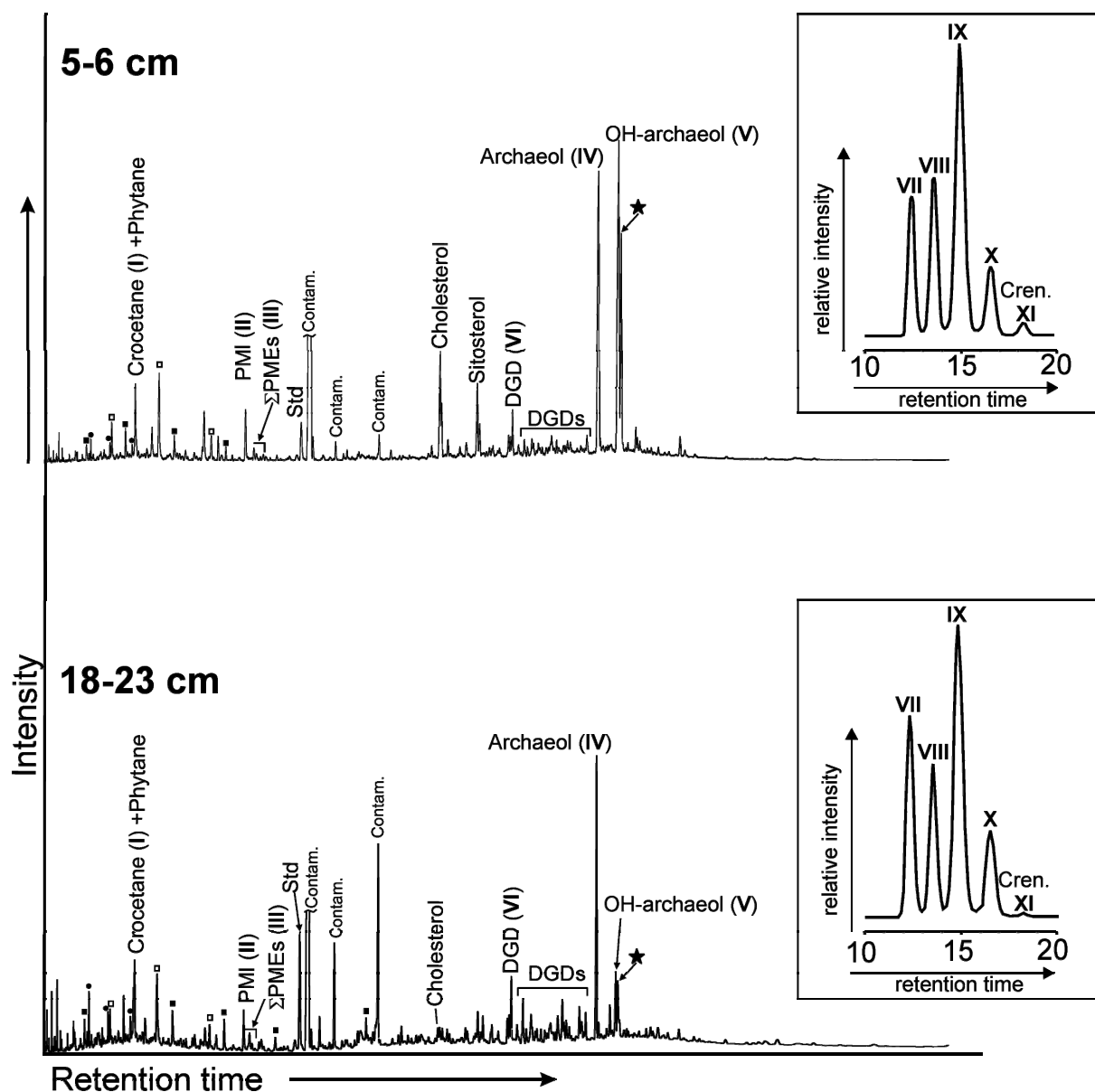


**Figure 3.** Gas chromatograms of the total lipid extracts from 5 cm and 20 cm depth intervals. Black circles are *n*-alkanes, black squares are straight-chain alcohols, open squares are straight-chain fatty acids, and the star is the dehydration product of the hydroxyarchaeol. Roman numerals refer to structures in the Appendix.

Another distinct group of compounds detected are non-isoprenoidal DGDs, tentatively inferred previously as a marker of uncharacterized SRB (Pancost et al., 2001a; Werne et al., 2002). The concentration of the most abundant DGD (VI), possessing anteiso pentadecyl moieties attached at both the *sn*-1 and *sn*-2 position (Pancost et al., 2001a), varied from 0.1 to 0.4  $\mu\text{g/g}$  (Figure 4), which is similar to concentration levels of crocetane



Crust intervals, cm	Crocetane + phytane	PMI	archaeol	OH-archaeol	DGD VI
0-1	-61	-100	-103	-107	-89
5-6	-93	-106	-104	-109	-90
9-10	-44	-98	-102	-107	-87
10-12	-38	-98	-100	-105	-84
15-16	-53	-99	-101	-107	-86
18-23	-38	-100	-101	-104	-86
25-28	-42	-101	-100	-115	-83

and PMI. The depth profile of the DGD is similar to those of crocetane, PMI, archaeol and hydroxyarchaeol.

### 3.3. Stable carbon isotope signatures of microbial lipids

**Table 2.** Stable carbon isotope composition (in ‰ vs VPDB) of selected biomarkers in the studied carbonate crust.

PMI, archaeol, *sn*-2 hydroxyarchaeol and the non-isoprenoidal DGD VI were strongly depleted in <sup>13</sup>C (Table 2, Figure 4), indicating that methane was used as the carbon source for their biosynthesis. Hydroxyarchaeol was ca. 10 ‰ more depleted in comparison with archaeol (Table 2). Crocetane is more enriched in <sup>13</sup>C likely due to an admixture of isotopically less depleted phytane.

<sup>δ13</sup>C values of the non-isoprenoidal DGD were 14-17 ‰ heavier than those of archaeol (Table 2; Figure 4). Non-isoprenoidal DGDs are typically enriched relative to archaeal DGDs (Pancost et al., 2001a,b; Stadnitskaia et al., 2005) and these values do indicate that the carbon source for the organism which biosynthesized this compound was likely also methane.

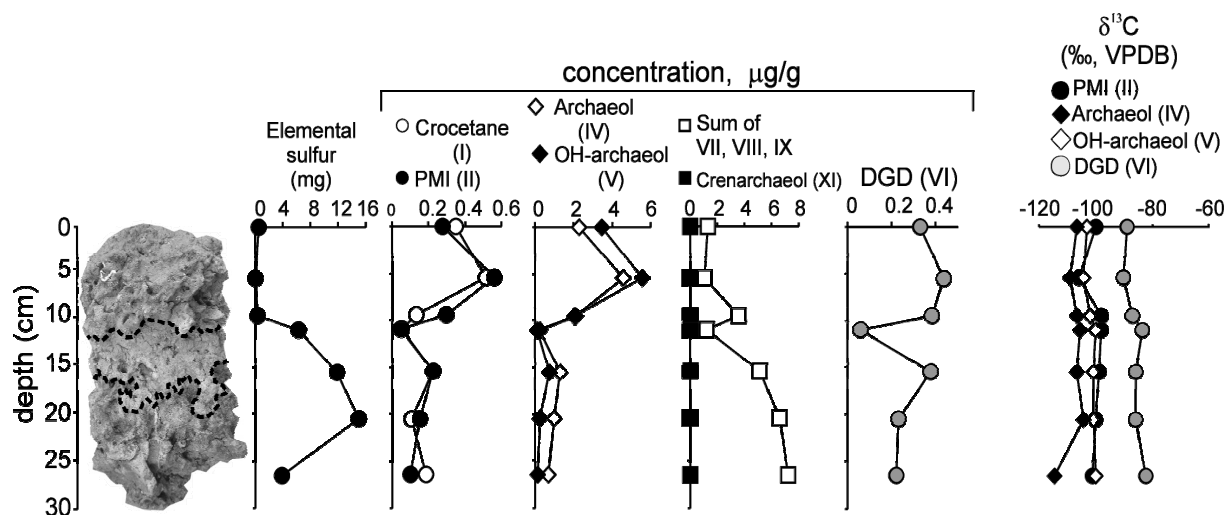


**Figure 4.** Distribution profiles of abundances (g/g of dry sediment) and <sup>13</sup>C values of archaeal and SRB lipid biomarkers along the crust. Roman numbers refer to structures in the Appendix.

### 3.4. Diversity of anaerobic methanotrophic archaea as revealed by 16S rRNA gene sequence analysis

The diversity of anaerobic methanotrophs varied along the carbonate crust. Figure 5 shows DGGE of PCR products obtained with primers specific for the 16S rRNA encoding gene from ANME archaeal groups. The PCR products reveal the diversity reflected in the appearance of a number of intensely stained bands (Figure 5). Comparative analysis of the sequences obtained from 40 bands with sequences from nucleotide databases indicated the presence of sequences belonging to both ANME-1 and ANME-2 groups (Figure 6). Sequences belonging to ANME-1 are affiliated with the ANME-1a and ANME-1b subgroups. Sequences clustered within the ANME-2 fall in the subgroups ANME-2a and ANME-2c. The sequences of the excised bands falling within the ANME-2 group are most abundant in the top 5 cm of the crust and below 15 cm these sequences were not detected. Simultaneously, the ANME-1 archaea were identified only in samples from 9 cm and deeper in the crust. According to the sequences obtained from bands within the interval of 9-12 cm, both ANME-1 and ANME-2 archaeal populations are present

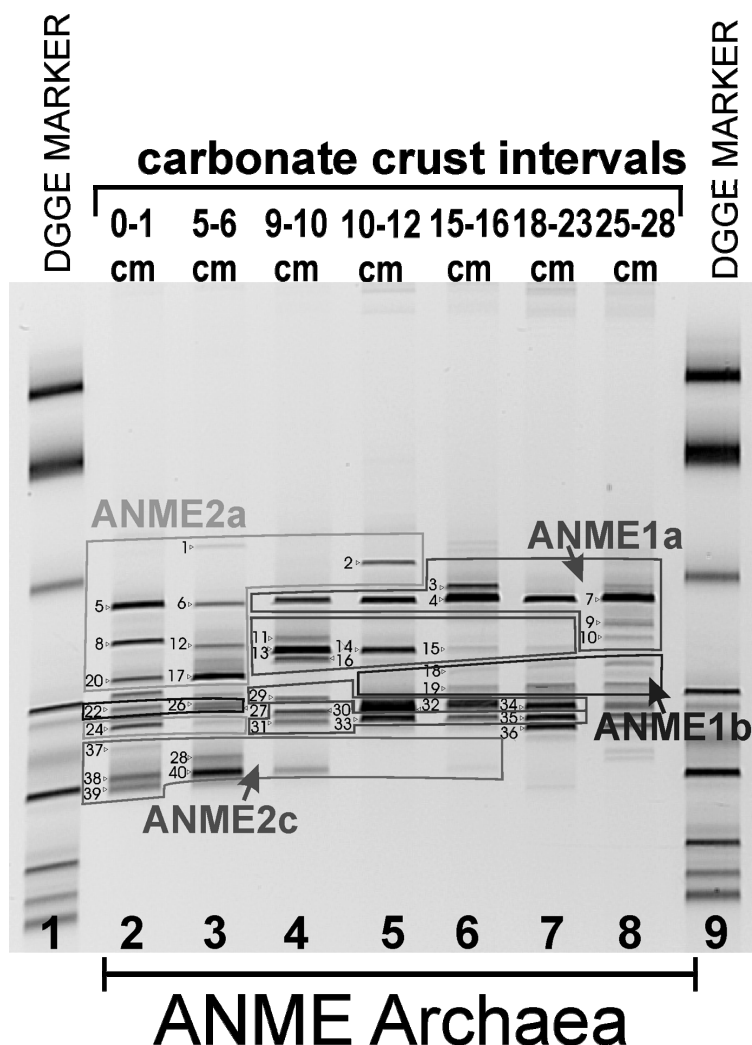
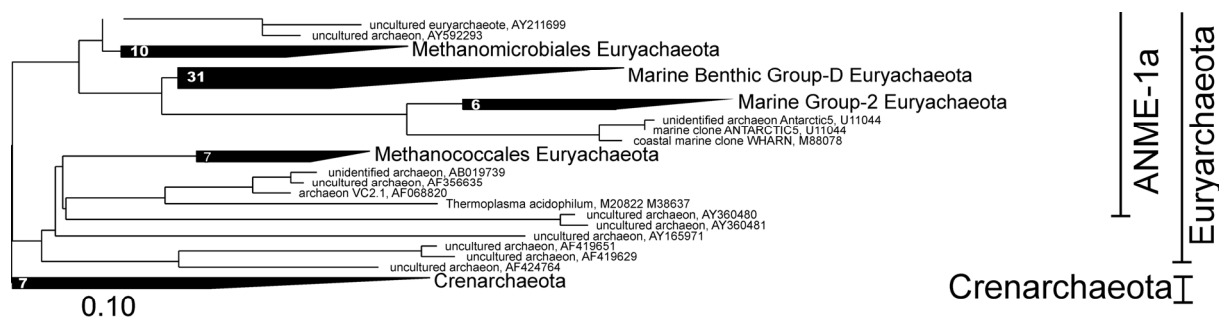


**Figure 5.** DGGE analysis of PCR products obtained with primers specific for the 16S rRNA encoding genes of anaerobic methanotrophs (ANME). Lanes 1 and 9 are marker fragments. The excised bands are numbered and named as DGGE ANME1 for the band no 1, DGGE ANME2 for the band no. 2, etc. (See Figure 6 for their phylogenetic affiliation). The green and orange selections on the gel are affiliated with ANME-2a and ANME-2c, respectively, archaeal subgroups. The pink and blue selections are related to ANME-1a and ANME-1b, respectively, archaeal subgroups (See Figure 6). See page 201 for color figure.



Continuation:



\* previous published data, Stadnitskaia et al., 2005

**Figure 6.** Phylogenetic affiliation of anaerobic methanotrophs in the carbonate crust. The light blue sequences in the tree are those found in the carbonate crusts and related microbial mats in the deep Black Sea mud volcanoes (Stadnitskaia et al., 2005).

(Figures 5 and 6). Hence, the DGGE profiles of PCR products from the carbonate crust reveal changes in the archaeal community structure during the formation of the crust.

## 4. Discussion

### 4.1. Anaerobic methanotrophy as the process for the crust formation

The first observation indicating that AOM processes induced the formation of the studied carbonate crust is the depletion in  $^{13}\text{C}$  of the bulk carbonate (Brooks et al., 1986; Hovland et al., 1987; Paull et al., 1992; Von Rad et al., 1996; Aharon et al., 1997; Bohrmann et al., 1998; Peckmann et al., 1999 a,b, 2001, 2002; Stakes et al., 1999; Aloisi et al., 2000, 2002; Diaz-del-Rio et al., 2003; Peckmann et al., 2001; Michaelis et al., 2001; Mazzini et al., 2004). The  $\delta^{13}\text{C}$  values vary between -20 and -27 ‰ (Table 1), which is substantially depleted relative to typical values for marine carbonates. Such a depleted  $^{13}\text{C}$ -content of the carbonate is likely related to methane oxidation since its composition can only be explained to derive in part from isotopically depleted bicarbonate formed during microbial oxidation of isotopically depleted methane (Ritger et al., 1987; Von Rad et al., 1996; Thiel et al., 1999; Peckmann et al., 1999 a,b, 2001, 2002; Stakes et al., 1999; Aloisi et al., 2000, 2002). The absence of lipid biomarkers derived from aerobic methanotrophs indicates that methane oxidation was a strict anaerobic process and that aerobic methanotrophy did not play a role in the formation of the crust. The occurrence of strongly  $^{13}\text{C}$ -depleted archaeal lipid biomarkers in the crust, the dominance of these components among the lipids extracted from this carbonate (Figure 3) and the 16S rDNA sequence data, which revealed the presence of anaerobic methanotrophs throughout the crust (Figure 5), confirm that bicarbonate used for carbonate precipitation is

partially derived from AOM accomplished by methanotrophic archaea (cf. Boetius et al., 2000; Pancost et al., 2000, 2001; Hinrichs and Boetius, 2002).

The occurrence of the  $^{13}\text{C}$ -depleted non-isoprenoidal DGD may indicate that SRB were possibly also involved in AOM (Pancost et al., 2001 a,b; Werne et al., 2002; Stadnitskaia et al., 2005). The distribution profile of DGD correlates well with distribution profiles of archaeal lipids (Figure 4) and the difference between the  $\delta^{13}\text{C}$  values of archaeal lipids and the DGD is constant throughout the crust which is consistent with previous finding of such carbon isotope difference detected in the Eastern Mediterranean cold seeps (Pancost et al., 2001 a,b; Werne et al., 2002) and in the methane related carbonates from the Black Sea MVs (Stadnitskaia et al., 2005). The similar concentrations levels of the crocetane and PMI and the non-isoprenoidal DGD, may support the presence of a consortium of archaea with SRB. This is also consistent with results of *in vitro* experiments, which revealed that AOM communities use methane and sulfate in a stoichiometry of about 1:1 (Nauhaus et al., 2002).

#### 4.2. *Changes in the diversity of anaerobic methanotrophs along the crust*

Figure 4 shows marked changes in the biomarker distributions along the crust. Based on the lipid biomarker concentration profiles (Figure 4), the top, intermediate and the bottom parts of the crust are characterized by different amounts of crocetane, PMI, archaeol, hydroxyarchaeols, and GDGTs derived from archaea involved in AOM. The distribution of archaeal lipids in the crust indicates the presence of both ANME-1 and ANME-2 archaeal groups. Archaea in the ANME-II group are thought to mainly produce DGDs as their membrane lipids with concentrations of *sn*-2-hydroxyarchaeol exceeding those of archaeol (Blumenberg et al., 2004). GDGTs have been proposed to constitute the majority of membrane lipids in archaea in the ANME-1 group, but occur in ANME-2 group in small amount (Blumenberg, et al., 2004). The predominance of *sn*-2 hydroxyarchaeol and archaeol in the uppermost 9 cm of the crust over the other archaeal lipids, the relatively low concentrations of GDGTs **VII-IX**, and the relatively high concentrations of crocetane and PMI, also thought to be characteristic for ANME-2 archaea (Blumenberg, et al., 2004), suggests the dominance of archaea of the ANME-2 group (Figure 4). Towards the bottom of the crust, concentrations of cyclized GDGTs increase (Figure 4) and archaeol is more abundant than hydroxyarchaeol. This suggests the dominance of the ANME-1 archaeal group (Blumenberg et al., 2004) at the lowermost part of the crust during its formation. Thus, the lipid biomarkers seem to indicate a shift in the archaeal community structure during the development of the crust. This is confirmed by the DGGE patterns of 16S rDNA specific for ANME groups which indeed reveal a dominance of ANME-2 archaea in the uppermost 9 cm of the crust, of ANME-1 archaea in the bottom section and a mixed ANME-1/ANME-2

archaeal population in the transition zone (Figure 5). The combined biomarker lipid and 16S rDNA record thus reveal two different phases in the formation of the carbonate crust.

The mechanism controlling the preferential development of seepage-related anaerobic methanotrophs is still uncertain. Recently, it was shown that changes in the methane flux and *in situ* temperature can influence AOM rates and the AOM community structure (Treude, 2003; Nauhaus, et al., 2002, 2005). Archaea of the ANME-1 and ANME-2 groups can co-exist (Nauhaus et al., 2005). Nevertheless, archaea from the ANME-2 group were found to have a preferential niche in habitats of elevated methane partial pressures, whereas ANME-1 archaea are found when methane levels are lower (Blumenberg et al., 2004). The combined biomarker lipid and 16S rRNA gene sequence data reveal the dominance of the ANME-2 archaeal members at the top of the crust (Figure 4, 5). This suggests that the top of the crust was formed under conditions with higher in-situ methane concentrations and that during further build-up of the crust, which apparently was extending in a downward direction, methane levels ceased and ultimately resulted in conditions more favourable for archaea affiliated with the ANME-2 group. Depth profiles of  $\delta^{13}\text{C}$  values of archaeal and SRB lipids (Figure 4) show rather constant values throughout the crust. This indicates that, despite apparent changes in the methane flux, the  $\delta^{13}\text{C}$  values of the supplied methane, and, thus, likely its source, remained the same during the various stages of carbonate crust growth.

#### 4.3. Stable carbon and oxygen isotopes and authigenic minerals in the crust

Despite the relative constant  $\delta^{13}\text{C}$  values of the methane during formation of the crust, the  $\delta^{13}\text{C}$  of the bulk carbonate varies along the carbonate (Figure 2). This is probably caused by different degrees of mixing of methane-derived bicarbonate with other sources of bicarbonate such as in-situ oxidation of organic matter *via* sulfate reduction, mixture with bicarbonate from the sea water or with migrated bicarbonate-bearing deep fluids.

The relatively  $^{18}\text{O}$ -enriched signatures in the carbonate crust (Figure 2) which fits with the  $\delta^{18}\text{O}$  values from other carbonates in the Gulf (Figure 7; Diaz-del-Rio et al., 2003) may indicate low temperatures during the carbonate formation. The fluctuations in  $\delta^{18}\text{O}$  values along the crust (Figure 2) may be caused by fluctuations in the pore water compositions, and by water formed by decomposition of gas hydrates since gas hydrates are known to be enriched in  $^{18}\text{O}$  (Bohrmann et al., 1998; Aloisi et al., 2000; Campbell et al., 2002; Mazurenko et al., 2003; Campbell et al., 2002, 2006 and references therein).

The mineralogical composition of the crust shows substantial variation with depth. The lack of terrigenous admixture as indicated by the presence of quartz in the top part of the crust is noteworthy. Perhaps, this phenomenon indicates a relatively fast rate of carbonate precipitation within the sediments, indicating local seepage environments with elevated

methane fluxes and AOM rates. This is consistent with lipid biomarker and 16S rDNA data, revealing the presence of ANME-2 archaea, which were found predominantly in environments with high methane partial pressures (Blumenberg et al., 2004). The noticeable increase in terrigenous minerals, quartz and plagioclase, downwards the carbonate may signify a drop in the rates of carbonate precipitation resulting from the reduction of the methane flux and rates of AOM. These terrigenous minerals are likely presented in abundance within the sediment and were entrained due to protracted downward accretion of the carbonate. The presence of almost 50 % of quartz in the lower part of the crust probably indicates the completion phase of the carbonate formation. The changes in the archaeal community structure within the lower part of the crust, as was revealed by lipid biomarkers and 16S rRNA gene sequence data, support the notion of two phases of the crust development induced by the local environmental changes, e.g. methane flux.

The set of carbonate minerals dominates by aragonite, which is similar to methane-related carbonates from the Eastern Mediterranean MVs (Aloisi et al., 2002). The process of aragonite formation in methane-venting environments is still unknown. Zong and Mucci (1989) showed that aragonite and calcite can precipitate at all salinities but that their formation requires high sulfate environments. The dolomite group of minerals is represented by dolomite and ankerite. The presence of dolomite and its slight increase downwards the crust is considered to be an indicator of low-sulfate anoxic solutions (Walter, 1986) due to an activity of SRB (Jørgensen, 1992). Its relatively small content may indicate a moderate sulfate reduction (Figure 2). Van Lith et al. (2003) revealed that bacterial sulfate reduction and elevated salinity are the most important factors enhancing the kinetic of dolomite formation. Sulfate reduction increases carbonate ion activity, and decrease the hydration energy of magnesium in water, promoting dolomite formation in the microenvironment around the bacterial cells (Van Lith et al., 2003). The existence of sulfate reduction, especially during precipitation of the lower part of the crust, can perhaps be related to the increase of the elemental sulfur content in the lipid extracts (Figure 4). Accordingly, a slight increase in the dolomite content in the lower part of the precipitant might record changes in the rates of bacterial sulfate reduction and perhaps somewhat higher salinities compare to the top of the carbonate.

Previous studies of microbial mats and associated carbonates from the Black Sea (Stadnitskaia et al., 2005) revealed the strongest AOM signal within the carbonates and not within the surrounded sediments, indicating the formation of such carbonates below the seafloor surface. This is consistent with our lipid data from MVs in the Gulf of Cadiz (Chapter 7), suggesting low AOM rates in the MV deposits, and the present lipid biomarker results, showing the absence of biomarkers associated with aerobic microbes. AOM-performing consortia are obligate anaerobes and the consequence of the interaction between

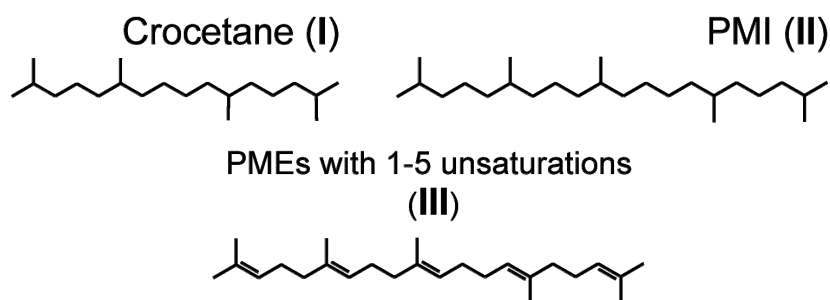
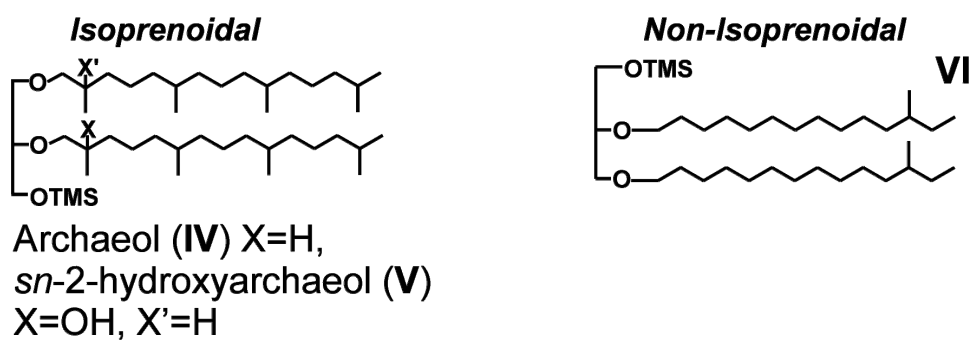
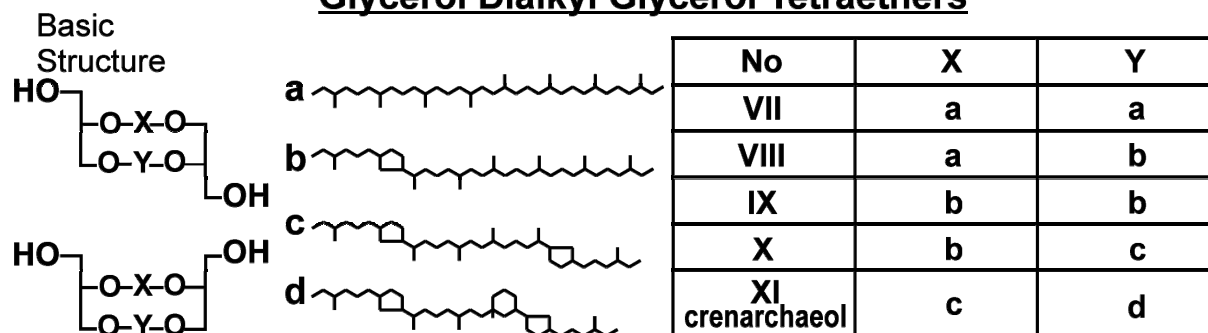
AOM-resulted sulfide-enriched pore waters and oxygenated seawater is acidic environments (Paull and Neumann, 1987), which are harmful for the carbonate precipitation. Taking into consideration that the Gulf of Cadiz possesses oxygenated bottom waters and never experienced anoxic episodes during its geological history, the formation of the crust was indeed taken place within the sediments below the sediment-water interface and the growth direction was in this case most likely downwards.



## **5. Conclusions**

A combination of molecular organic, molecular biological and inorganic methods was applied to a methane-related carbonate crust collected from the Kidd mud volcano in the Gulf of Cadiz. The data revealed that AOM is the process that induced the formation of the crust. The obtained multidisciplinary data are well correlated with each other, indicating two phases in the development of the crust caused by changes in the local microenvironments, most likely methane fluxes, during the crust growth. These changes likely affected the archaeal community structures at the upper and in the lower parts of the carbonate crust. In the top part of the crust, archaeal lipid biomarkers and 16S rRNA gene sequence data indicate the dominance of archaeal ANME-2 group, whereas the intermediate and the bottom part of the carbonate likely indicate the dominance of archaeal ANME-1 members and likely lower methane fluxes in comparison with the top part of the crust. The presence of aragonite as the main carbonate mineral may indicate sulphate-rich environment during the formation of the crust. Besides, vertical distribution profiles of  $\delta^{13}\text{C}$  values of archaeal and bacterial lipids show that during the carbonate crust growth, the methane source remained the same, whereas  $\delta^{18}\text{O}$  signatures of the total carbonates together with mineralogical composition revealed inconstancy of environmental conditions in the local environments. This close examination showed and proved an advantage of “vertical-profile-study-strategy” and the advantage of the combination of organic and inorganic methods to understand palaeo-processes that resulted in the development of the carbonate fabrics.

## Appendix

**Irregular Isoprenoids****Dialkyl Glycerol Diethers****Glycerol Dialkyl Glycerol Tetraethers**



## Synthesis

The goal of this research was to compare geological and biogeochemical processes occurring in two MV provinces, which are located in the Gulf of Cadiz (NE Atlantic) and in the Sorokin Trough (NE Black Sea). These areas are characterized by fundamentally different geological histories and present-day ecological environments. Both are known for the presence of gas hydrates, seep ecosystems, and methane-related carbonates. In each of these MV provinces, an experimental program, which comprised a spectrum of modern geochemical and molecular ecological techniques was applied. An effort was made to determine the possible sources of migrated fluids, especially methane, and to disclose a link between the occurrence of microbes in such extreme environments and their symbiotic partnerships and relation to migrated components from deep subsurface (methane, petroleum products or their mixtures). Microbial anaerobic oxidation of methane (AOM) process and AOM-related carbonate-shaping ecosystems in the geological past (in the Gulf of Cadiz) and within currently active fluid venting environments (in the Sorokin Trough) were investigated. A wide set of hydrocarbon gases and lipid biomarkers was investigated and stable carbon isotope and 16S rRNA gene sequence analyses for MV deposits, pelagic sediments, carbonates and microbial mats collected from different fluid-venting settings within these two areas were performed.

In this thesis it was aimed:

- (1) to integrate and interpret the same set of biogeochemical data from both MV provinces to gain an understanding of deep-fluid dynamics in these areas and to reveal the sources for fluids (hydrocarbon gases) and MV deposits (mud breccias);
- (2) to investigate the environmental impact of seepage phenomena, i.e. study of *in situ* microbial processes involved in the methane cycle, predominantly AOM, and related carbonate formation;
- (3) to compare the obtained information for the Gulf of Cadiz and for the Sorokin Trough in order to understand relationship between geological and biogeochemical regulatory mechanisms of the fluid venting and mud volcanism as well as factors controlling the occurrence, distribution and activity of methane-dependent microbial populations and related carbonate fabrics in both areas.

### 9.1. Sources of hydrocarbon gas and mud breccias

The Sorokin Trough and the Gulf of Cadiz are characterized by different geological histories, tectonic regimes, and the lithology of sedimentary cover. These affect the

composition of the initially formed fluid, fluid venting activity, fluid migration history and, as a result, the fluid composition as it appears at the near-surface sediments. Hydrocarbon gas is one of the dominant components in the MV fluid system. In both MV provinces, the molecular and carbon stable isotope compositions of C<sub>1</sub>-C<sub>5</sub> hydrocarbons are significantly affected by secondary alterations due to migration, mixing and microbial degradation. Despite the first evidence for different maturity properties of gas among the MVs in the Sorokin Trough, the wet gas components in all mud breccias and gas hydrates are related to each other. In general, these wet hydrocarbon gases can be recognized as originally derived from oil cracking and/or biodegradation in the subsurface. In contrast, hydrocarbon gases from two MV provinces within the Gulf of Cadiz can be considered as a consequence of secondary microbial alteration in the subsurface, which affected the  $\delta^{13}\text{C}$  values of C<sub>2+</sub> hydrocarbons. This complicated the assessment of the level of maturity and the original gas source. Nevertheless, the presence of high molecular weight gaseous hydrocarbons indicated that gases are in part thermally mature.

Hence, the hydrocarbon gas data indicate that an admixture of non-microbial, thermogenic hydrocarbon gases characterize migrated fluid from both areas. This indicates that the original source for gaseous fluids in both MV provinces locates in the deep subsurface since the gas generation window was established at ca. 105-155°C to 175-220°C (Pepper and Corvi, 1995). Hydrocarbon gases from both MV provinces represent a complex of redeposited, secondary migrated, mixed with biogenic gas, and microbially altered gas mixtures. In this respect, the redeposition of hydrocarbon gas in the Gulf of Cadiz would be expected within the Olistostrome or in relation with the diapir bodies or with submarine escarpments. The redeposition of the hydrocarbon gas at shallow subsurface in the Sorokin Trough already proved by numerous geophysical surveys in the area which detected many signs of the gas presence at ~ 250-300 m below the seafloor surface (Ivanov et al., 1998; Bouriak and Akhmetzhanov, 1998; Krastel et al., 2003).

The organic matter composition of the mud breccia matrixes in the MVs from the Sorokin Trough and the Gulf of Cadiz exhibit clear differences. These differences reflect the location of source strata of the erupted material. Despite the proximate location of the studied MVs in the Sorokin Trough, biomarker lipid distributions revealed different mud breccia sources in these structures. This indicates different subsurface-sedimentary depths of defluidization, which are directly linked to the location of fracture zones or diapiric folds. MVs from the Gulf of Cadiz are located relatively distant from each other within tectonically different parts of the Gulf. The lipid biomarker compositions from mud breccia matrixes in all studied MVs showed strong compositional resemblance and similar thermal maturity properties of the organic matter. This indicates related source strata for the erupted material,

similar depths of defluidization, and the extension of common litho-stratigraphic units through the Gulf.

Comparison of lipid biomarkers and hydrocarbon gas data from both areas sheds new light on the question what triggers the eruption of a MV: (i) hydrocarbons or (ii) fluidized sediments or (iii) a mixture of both? The maturity properties of organic matter in mud breccias from MVs in the Gulf of Cadiz and in the Sorokin Trough generally indicate that the source strata for the erupted sediments are located at shallower depth of burial than the source strata for the hydrocarbon gases. Accordingly, our results support the notion that the formation of the MV fluid starts with the release of overpressured hydrocarbons, followed by the mechanical entrainment of encountered sediments.

### *9.2. Anaerobic oxidation of methane*

At cold vents, the composition of fluids and seepage rates generally varies considerably. This directly affects the diversity and abundance of seep-thriving biota. The anoxic water column in the Black Sea eliminates the possibility for the presence of oxygen-dependent macro- and microorganisms, thus limiting microbial inhabitants to only obligate anaerobic species. In contrast, oxygenated waters in the Gulf of Cadiz promote the development of substantially more diverse suite of (micro)organisms. The main outcome of the applied lipid biomarker and 16S rDNA sequence study is that AOM is the dominant biogeochemical process in MVs from both areas and archaea of the ANME groups have been detected in all studied locations. However, the intensity of AOM processes, which was tentatively suggested from the distribution and contents of AOM-derived lipid biomarkers, and the location of AOM zones within the sediments are notably different in the MVs from the Sorokin Trough and from the Gulf of Cadiz. Presently active fluid venting characterizes the Sorokin Trough. In gas saturated mud breccias and sediments with gas hydrates, the highest AOM activity was detected. Besides, lipid biomarker distribution profiles and 16S rRNA gene sequence data revealed that in the MV deposits from the Sorokin Trough, AOM is restricted within the ca. 20 cm zone with archaea belonging to the ANME-1 cluster. The ANME-2 archaeal group was not detected, which does not prove their total absence; it indicates a significant dominance of archaea from the ANME-1 guild in these presently active methane-venting habitats. In contrast, the lack of strong upward fluid transport and the absence of gas escape into the overlying water column characterize the Gulf of Cadiz. In the studied locations, MV deposits showed unexpectedly low concentrations of lipids specific to AOM, suggesting lower intensities of anaerobic methanotrophy. AOM-derived lipid biomarkers were detected through the ca. 240 cm of the mud breccia section, tracing the presence of both archaeal clades. In the site where methane concentration was the highest,

AOM zone was close located to the sediment surface. In contrast, sampling locations with relatively low methane concentrations showed shift of AOM deeper into the sediments. Hence, the results of this study and inspection of published data suggest that the distribution and composition of anaerobic methanotrophs in the studied MV deposits are ruled by the fluid inflow, i.e. methane flux.

### *9.3. Carbonate shaping ecosystems*

In local seepage environments in the Sorokin Trough and in the Gulf of Cadiz, microbial system development results in the growth of specific seep-carbonate fabrics. Carbonates were collected from principally different methane-seepage settings and include: (i) carbonate crusts associated with two different types of living microbial mats from active seepage and gas hydrate localities from the Sorokin Trough and (ii) a carbonate crust from a non-active MV in the Gulf of Cadiz. Compared with the studied Black Sea's carbonates/microbial mats, the crust from the Gulf of Cadiz was considered to be a relict of the past seepage activity.

The common feature among all studied carbonates is the significant role of AOM-related microorganisms in their formation. However, the diversity of anaerobic methanotrophs varied among the crusts. Lipid biomarkers and 16S rDNA sequence data revealed the presence of archaea affiliated with the ANME-1 clade in all carbonates from the Sorokin Trough, whereas carbonate crust from the Gulf of Cadiz shows the presence of both guilds. Since the crust from the Gulf of Cadiz was examined in detail, changes in the archaeal communities were traced along the carbonate, evaluating changes in the local environments during the precipitation of the crust.

The difference in sulphate concentration is likely one of the causes for the different suite of authigenic minerals present in the AOM-carbonates of the Sorokin Trough and in the Gulf of Cadiz. For instance, compositional analyses of numerous carbonates from the Sorokin Trough revealed the presence of calcite, with the predominance of high Mg-calcite, and dolomite (Mazzini et al., 2004). Aragonite, which is common carbonate mineral in seepage locations, was not detected at all. In contrast, aragonite is the dominate carbonate mineral in the carbonate crust from the Gulf of Cadiz. At fluid venting sites, the precipitation of calcite is favoured over aragonite when low sulphate concentrations occur in the system (Burton, 1993; Naehr et al., 2000; Aloisi et al., 2002). Low sulfate environments (ca. 18 mM compare with the ocean of 30 mM) are typical for the Black Sea bottom waters (Murray et al., 1991). Accordingly this observation indicates that anaerobic methanotrophy only serves as a partial source for the bicarbonate and the compositional variety for the resulted carbonates are partially dictated by the sulphate reduction and probably by other microbial activities impacting on cycles of other elements.

In both areas the methane, lipid biomarker and 16Sr rRNA gene sequence data revealed that the carbonate forming ecosystems are located below the seafloor and the precipitation of methane-related carbonates *via* AOM takes place beneath the sediment water interface, i.e. where methane and sulfate are abundant. AOM processes are most active within the neoformed carbonates and are substantially reduced in the hosting sediments. The carbonate growth direction likely follows the pathways of migrated methane although the presence of anoxic water column in the Black Sea allows the upward accretion of carbonate. In the Gulf of Cadiz, the carbonate growth is ultimately happening in a downward direction.

Overall, the study of different fluid venting environments in the Sorokin Trough and in the Gulf of Cadiz revealed different intensities and duration of AOM, most likely forced by intensity of local seepage activity and by composition of migrated fluid.

#### *9.4. Factors that regulate biogeochemical processes in the Sorokin Trough and in the Gulf of Cadiz*

The major cause for different fluid venting activity reflected in AOM intensities and carbonate formation is the different marine geotectonic settings of the studied areas. The regional topography and distinctiveness of the seafloor at the Sorokin Trough and at the Gulf of Cadiz can be indicative for type and modes of seepages. For instance, the occurrence of pock-marks, fissure outflows of mud breccias, or mud volcanoes at the seafloor specifies different physical factors leading the formation of such different seep-system scenery. In other words, relatively low-pressure events with less dense fluid will cause pock-marks topography. A high-pressure event with outburst of high-density material is required for the formation of a mud volcano. Thus, development of mud volcanoes is related to episodic high-pressure relief of deep fluids.

Both areas are known for mud volcanism and associated phenomena. However, the AOM signal in the mud breccias from the Gulf of Cadiz is considerably lower than in the MV deposits from the Sorokin Trough. This suggests low AOM rates which indicate the absence of intensive fluid venting and methane influxes in the Gulf, confirmed by the hydrocarbon gas data. The Sorokin Trough is known to be a currently active fluid venting area which results in dense AOM communities. Gas saturated sediments are ubiquitous in the Trough and AOM even takes place in the water column. Unlike, in the Gulf of Cadiz, fluid venting activity is distributed locally and often the most active sites are the craters of MVs. The phases of MV activity in response to past and present geo-tectonic regimes or/and (palaeo) environmental events are not known for both MV provinces. Fields of outcropping methane-related carbonate material in the Gulf of Cadiz mark the episode of active defluidisation in the geological past. Besides, this period of seeping should last over a relatively long time span,



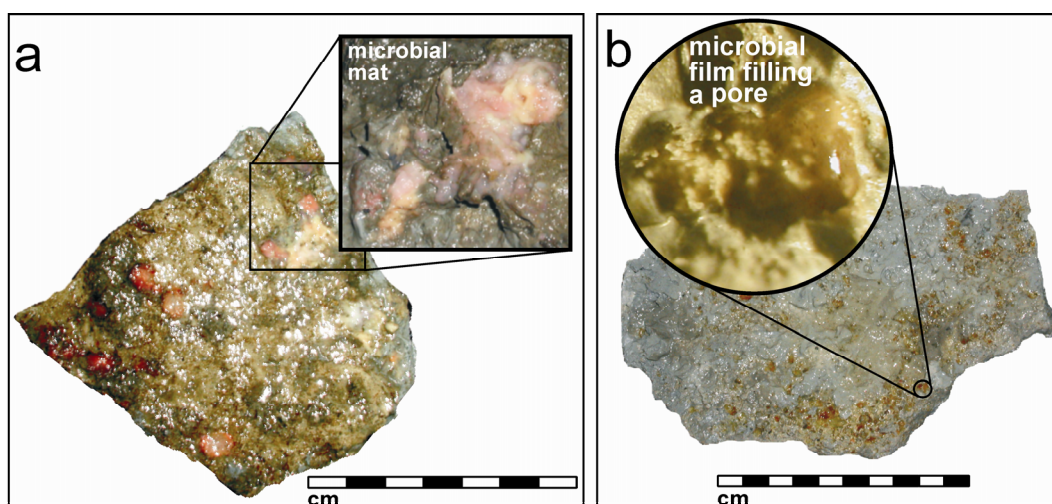
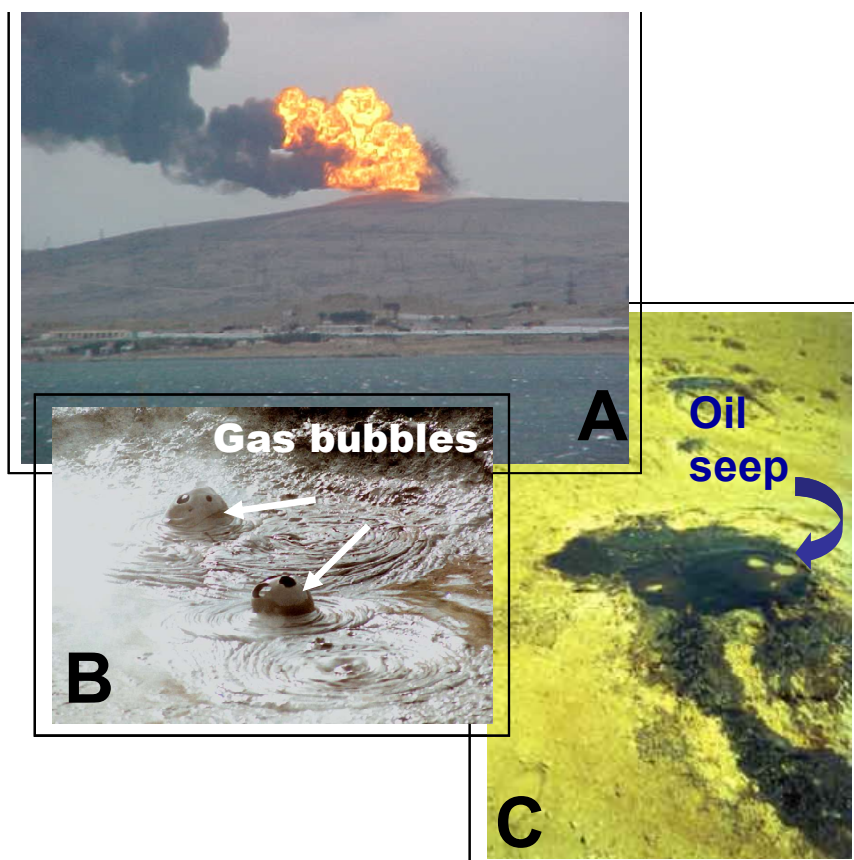
since the length of these chimneys are in some cases reach 0.5 m (Kenyon et al., 2002; Díaz-del-Río et al., 2003). It is still enigmatic when such episode took place in the Gulf's history, and which factors acted as a trigger. Nevertheless, this can testify different modes of fluid venting in the Gulf of Cadiz and in the Sorokin Trough. Likely, the absence of fluid supply in the mud breccias from the MV in the Gulf of Cadiz can be explained by an abrupt and brief period of MV eruptions associated with emissions of fluid saturated mud breccias followed by fast consumption of introduced methane and other organic and inorganic components. Accordingly, after some time, mud breccias in the Gulf are in "fluid-flux-starvation" environments. In the Sorokin Trough, gas saturated sediments are ubiquitous and AOM even take place in the water column. The fluid inflow is constant and some parts of the Trough are characterized by the presence of so called "gas front" (Ivanov et al., 1998). This determines the presently steady energy source environments and thus flourishing of chemosynthetic biota and associated mineral formation.

---

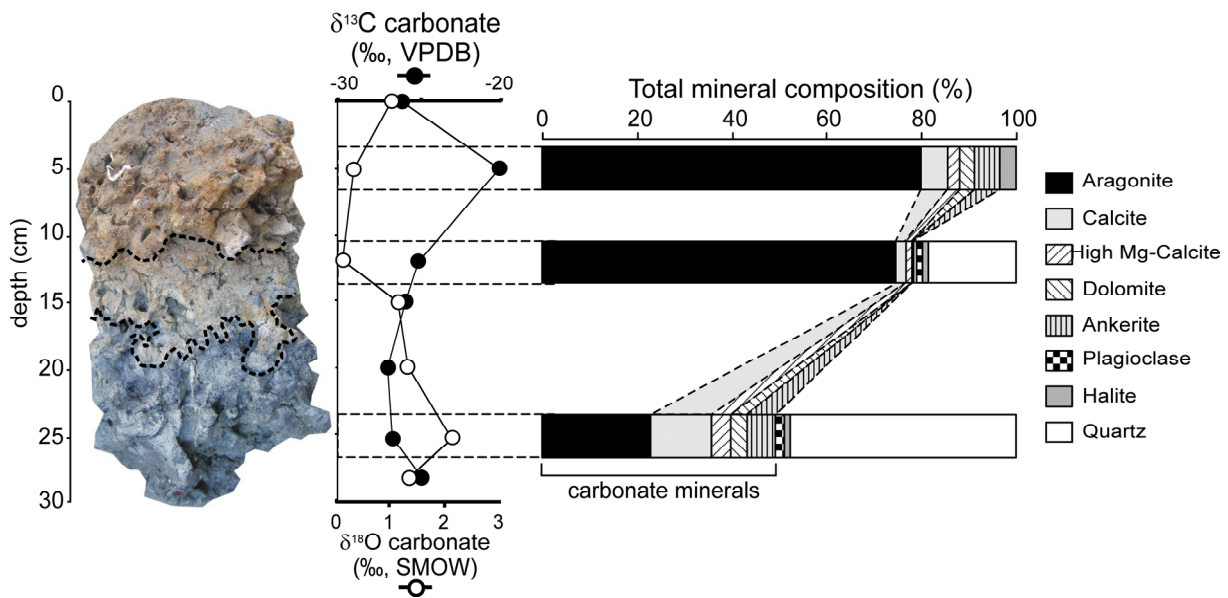
## Color figures

## Color figures

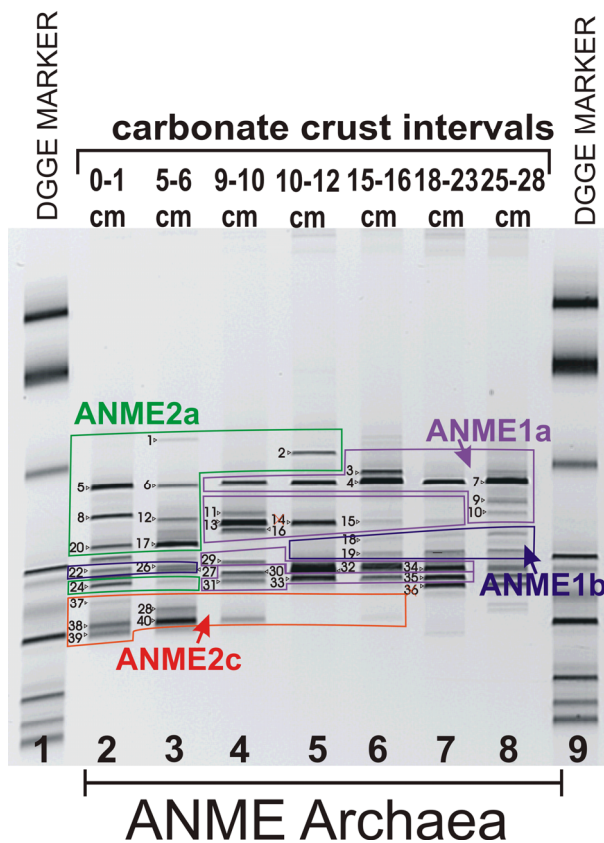
**Chapter 1, Figure 1.** Examples of on-land mud volcano and seepages. **A** – Eruption of the mud volcano at Lokbatan, near Baku (October 10, 2001; Photo: Phil Hardy); **B** – small gas seepage (Bulganak MV field, Kerch Peninsular); **C** – small oil seepage near Baku, Azerbaijan.



**Chapter 4, Figure 2.** Two main types of investigated carbonate crusts and microbial mats. a) the Odessa mud volcano, sampling site TTR-11 BS-336G. The inset assigns the location of the microbial mat. b) the NIOZ mud volcano, sampling site TTR-11 BS-328G. The inset is a binocular image with typical appearance of microbial films within pores and interstices.



**Chapter 8, Figure 2.** Stable carbon and oxygen isotope profiles and mineralogical composition of the crust.



**Chapter 8, Figure 5.** DGGE analysis of PCR products obtained with primers specific for the 16S rRNA encoding genes of anaerobic methanotrophs (ANME). Lanes 1 and 9 are marker fragments. The excised bands are numbered and named as DGGE ANME1 for the band no. 1, DGGE ANME2 for the band no. 2, etc. (See Chapter 8, Figure 6 for their phylogenetic affiliation). The green and orange selections on the gel are affiliated with ANME-2a and ANME-2c, respectively, archaeal subgroups. The pink and blue selections are related to ANME-1a and ANME-1b, respectively, archaeal subgroups (See Chapter 8, Figure 6).



## References

---

- Abikh, G.V., 1873. Geologicheskii obzor poluostrovov Kerchi i Tamani. Zap. Kavk.otd.Rus.Geogr. Obshstva, 8, 1-17 (in Russian).
- Aharon, P., Schwarcz, H.P., Roberts, H.H., 1997. Radiometric dating of submarine hydrocarbon seeps in the Gulf of Mexico. *Geol. Soc. Amer. Bull.* 109, 568-579.
- Akhmanov, G.G., 1996. Lithology of mud breccia clasts from the Mediterranean Ridge. *Marine Geology* 132, 151-164.
- Akhmanov G.G., Woodside J.M., 1998. Mud Volcanic Samples in the Content of the Mediterranean Ridge Mud Diapiric Belt. In: Robertson, A.H.F., Emeis, K.-C., Richter, C., Camerlenghi, A. (Eds.), *Proc. ODP, Scientific Results*, 160. College Station, Texas, pp. 597-605.
- Aloisi, G., Pierre, C., Rouchy, J.-M., Foucher, J.-P., and the MEDINAUT Scientific Party, 2000. Methane-related authigenic carbonates of eastern Mediterranean Sea mud volcanoes and their possible relation to gas hydrate destabilization. *Earth and Planetary Science Letters* 184, 321-338.
- Aloisi, G., Bouloubassi, I., Heijs, S.K., Pancost, R.D., Pierre, C., Sinninghe Damsté, J.S., Gottschal, J.C., Forney, L.J., Rouchy, J.-M., 2002. CH<sub>4</sub>-consuming microorganisms and the formation of carbonate crusts at cold seeps. *Earth and Planetary Science Letters* 203, 195-203.
- Alperin, M.J., Reeburgh, W.S., 1984. Geochemical observations supporting anaerobic methane oxidation, in: Crawford, R.L., Hanson, R.S. (Eds.), *Microbial Growth on C-1 Compounds*. American Society of Microbiology, pp. 282-298.
- Alperin, M.J., Reeburgh, W.S., 1985. Inhibition experiments on anoxic marine sediments suggests methane is not directly oxidized by sulfate-reducing bacteria. In *Book monograph: 7<sup>th</sup> International Symposium on Environmental Biogeochemistry*, 6 p.
- Ambar, I., Howe, M.R., 1979a. Observation of the Mediterranean outflow -I: Mixing in the Mediterranean outflow. *Deep Sea Research* 26A, 535-554.
- Ambar, I., Howe, M.R., 1979b. Observation of the Mediterranean outflow -II: The deep circulation in the vicinity of the Gulf of Cadiz. *Deep Sea Research* 26A, 555-568.
- Anders, D.F., Claypool, G.E., Lubrek, C.M., Patterson, J.M., 1978. Preliminary results, organic geochemical investigation of Black Sea sediments: Deep Sea Drilling Project Leg 42B. In: Ross, D.A., Neprochnov et al., (Eds.), *Initial Reports of the Deep Sea Drilling Project* 42, 755-763.
- Arkhangel'skii, A.D., 1925. Neskol'ko slov o genesise gryazevikh vulkanov Apsheronskogo poluostrova I Kerchensko-Tamanskoy oblasti. *BMOIP. Otd. Geolog.*, 33, 3/4, 269-285 (In Russian).
- Baker, P.A., Kastner, M., 1981. Constraints on the formation of sedimentary dolomite. *Science* 213, 215-216.
- Baraza, J., Ercilla, G., 1996. Gas-charged sediments and large pockmark-like features on the Gulf of Cadiz slope (SW Spain). *Marine and Petroleum Geology*, 13 (2), 253-261.
- Baraza, J., Ercilla, G., Nelson, C.H., 1999. Potential geologic hazards on the eastern Gulf of Cadiz slope (SW Spain). In: A. Maldonado and C.H. Nelson (Eds.), *Marine Geology of the Gulf of Cadiz. Marine Geology Special Issue*, 155, 191-216.
- Barners, R.O., Goldberg, E.D., 1976. Methane production and consumption in anoxic marine sediments. *Geology* 4: 297-300.
- Beauchamp, B., Savard, M., 1992. Cretaceous chemosynthetic carbonate mounds in the Canadian Arctic. *Palaios* 7, 434-450.
- Belousov, V.V., Volvovsky, B.S., Arkhipov, I.V., Buryanova, B.V., Evsyukov, Y.D., Goncharov, V.P., Gordienko, V.V., Ismagilov, D.E, Kislov, G.K., Kogan, L.I., Kondyurin, A.V., Kozlov, V.N., Lebedev, L.I., Lokholatnikov, V.M., Malovitsky, Y.E, Moskalenko, V.N., Neprochnov,

## References

---

- Y.R., Otisty, B.K., Rusakov, O.M., Shimkus, K.M., Shlezinger, A.E., Sochelnikov, V.V., Sollogub, V.B., Solovyev, V.D., Starostenko, V.I., Starovoitov, A.F., Terekhov, A.A., Volvovsky, I.S., Zhigunov, A.S. and Zolotarev, V.G., 1988. Structure and evolution of the earth's crust and upper mantle of the Black Sea. *Boll. Geofis. Teor. Appl.* 30, 117-118, 109-196.
- Bernard, B.B., Brooks, J.M., Sackett, W.M., 1976. Natural gas seepage in the Gulf of Mexico. *Earth and Planetary Science Letters* 31, 48-54.
- Bernard, B.B., Brooks, J.M., Sackett, W.M., 1978. Light hydrocarbons in recent Texas continental shelf and slope sediments. *Journal of Geophysical Research* 83, 4053-4061.
- Bernard, B.B., 1979. Methane in marine sediments. *Deep-Sea research*, 26A, 429-443.
- Bian, L., Hinrichs, K.-U., Xie, T., Brassell, S.C., Iversen, N., Fossing, H., Jørgensen, B.B., Hayes, J.M., 2001. Algal and archaeal polyisoprenoids in a recent marine sediment: molecular isotopic evidence for anaerobic oxidation of methane. *Geochemistry Geophysics, Geosystems* 2, No 2000GC000112.
- Blinova, V., Ivanov, M., Bohrmann, G., 2003. Hydrocarbon gases in deposits from mud volcanoes in the Sorokin Trough, northeastern Black Sea. *Geo-Marine Letters* 23, 250-257.
- Blumenberg, M., Krüger, M., Nauhaus, K., Talbot, H.M., Oppermann, B.I., Seifert, R., Pape, T., Michaelis, W., 2006. Biosynthesis of hopanoids by sulfate-reducing bacteria (genus *Desulfovibrio*). *Environmental Microbiology* 8, 1220-1227.
- Blumenberg, M., Seifert, R., Reitner, J., Pape, T., Michaelis, W., 2004. Membrane lipid patterns typify distinct anaerobic methanotrophic consortia. *PNAS* 101, 11111-11116.
- Boetius, A., K. Ravenschlag, C.J Schubert, D. Rickert, F. Widdel, A. Gieske, R. Amann, B.B. Jørgensen, U. Witte and O. Pfannkuche. 2000. A marine anaerobic consortium apparently mediating anaerobic oxidation of methane. *Nature* 407: 623-626.
- Bohrmann, G., Greinert, J., Suess, E., Torres, M., 1998. Authigenic carbonates from the Cascadia subduction zone and their relation to gas hydrate stability. *Geology* 26, 647-650.
- Bohrmann, G., Ivanov, M., Foucher, J.P., Spiess, V., Bialas, J., Weinrebe, W., Abegg, F., Aloisi, G., Artemov, Y., Blinova, V., Drews, M., Greinert, J., Heidersdorf, F., Krastel, S., Krabbenhöft, A., Polikarpov, I., Saburova, M., Schmale, O., Seifert, R., Volkonskaya, A., Zillmer, M., 2003. Mud volcanoes and gas hydrates in the Black Sea - new data from Dvurechenskii and Odessa mud volcanoes. *Geo-Marine Letters* 23, 239-249.
- Bolshakov, A.M., Egorov, A.V., 1987. Using a phase-equilibrium degassing method for gasometric studies. *Oceanology* 27, 861-862.
- Borowski, W.R., Paull, C.K. and Ussler III, W., 1999. Global and local variations of interstitial sulfate gradients in deep-water, continental margin sediments: Sensitivity to underlying methane and gas hydrates. *Marine Geology* 159, 31-154.
- Bouriak, S.V., Akhmetzhanov, A.M., 1998. Origin of gas hydrate accumulations on the continental slope of the Crimea from geophysical studies. In *Gas hydrates: Relevance to World Margin Stability and Climatic Change*. Eds. J-P. Henriot and J.Mienert. The Geological Society, London, Special Publications, No 137, pp 215-222.
- Bouriak, S., Vanneste, M., Saoutkine, A., 2000. Inferred gas hydrates and clay diapirs near the Storrega slide on the southern edge of the Vøring Plateau, offshore Norway. *Marine Geology* 163, 125-148.
- Bravo, J.-M., Perzl, M., Härtner, T., Kannenberg, E.L., Rohmer, M., 2001. Novel methylated triterpenoids of the gammacerane series from the nitrogen-fixing bacterium *Bradyrhizobium japonicum* USDA 110. *European Journal of Biochemistry* 268, 1323-1331.
- Bray, E.E., Evans, E.D., 1961. Distribution of *n*-paraffins as a clue to recognition of source beds. *Geochimica et Cosmochimica Acta* 22, 2-15.

## References

---

- Brooks, J.M., Cox, H.B., Bryan, W.R., Kennicutt II, M.C., Mann, R.G., McDonald, T.J., 1986. Association of gas hydrates and oil seepage in the Gulf of Mexico. *Organic Geochemistry* 10, 221-234.
- Buczynski, C., Chafetz, H.S., 1991. Habit of bacterially induced precipitates of calcium carbonate and the influence of medium viscosity on mineralogy. *Journal of Sedimentary Petrology* 61, 226-233.
- Burton, E.A., 1993. Controls on marine carbonate cement mineralogy: review and reassessment. *Chemical Geology* 105, 163-179.
- Camerlenghi, A., Cita, M.B., Della Vedova, B., Fusi, N., Mirabile, L., Pellis, G., 1995. Geophysical evidence of mud diapirism on the Mediterranean Ridge accretionary complex. *Marine Geophysical Research* 17, 115-141.
- Campbell, K.A., Bottjer, D.J., 1993. Fossil cold seeps. *Natl. Geog. Res. Explor.* 9, 326–343.
- Campbell, K.A., Bottjer, D.J., 1995. Brachiopods and chemosymbiotic bivalves in Phanerozoic hydrothermal vent and cold seep environments. *Geology* 23, 321–324.
- Campbell, K.A., Farmer, J.D., Des Marais, D., 2002. Ancient hydrocarbon seeps from the Mesozoic convergent margin of California: Carbonate geochemistry, fluids and paleoenvironments, *Geofluids* 2, 63-94.
- Campbell, K.A., 2006. Hydrocarbon seep and hydrothermal vent paleoenvironments and paleontology: past developments and future research directions. *Palaeogeography, Palaeoclimatology, Palaeoecology* 232, 362-407.
- Chung, H. M., Gormly, J. R., Squires, R. M., 1988. Origin of gaseous hydrocarbons in subsurface environments: Theoretical considerations of carbon isotope distribution. *Chemical Geology* 71(1-3), 97-104.
- Cita, M.B., Ryan, W.B.F., Paggi, L., 1981. Prometheus mud breccia. An example of shale diapirism in the Western Mediterranean Ridge. *Annales Géologiques des Pays Héliéniques* 30, 543-569.
- Claypool, G.E., and Kaplan, I.R., 1974. The origin and distribution of methane in marine sediments. In Kaplan, I.R. (Ed.), *Natural Gases in Marine Sediments: New York (Plenum)*, 99–139.
- Clayton, C.J., Hay, S.J., Baylis, S.A., Dipper, B. 1997. Alteration of natural gas during leakage from a North Sea salt diapir field. *Marine Geology* 137, 69-80.
- Cline, J.D., Holmes, M.L., 1977. Submarine seepage of natural gas in Norton Sound, Alaska. *Science* 198, 1149-1153.
- Coleman, D.D., Lin, C., Keogh, R.A., 1977. Isotopic identification of leakage gas from underground storage reservoirs – a progress report. *Illinois State Geological Survey, Illinois Petroleum* 111, 1-10.
- Coleman, D.D., Risatte, J.B., Schoell, M., 1981. Fractionation of carbon and hydrogen isotopes by methane-oxidizing bacteria. *Geochimica et Cosmochimica Acta* 45, 1033–1037.
- Comita, P.B., Gagosian, R.B., Pang, H., Costello, C.E., 1984. Structural elucidation of a unique macrocyclic membrane lipid from a new, extremely thermophilic, deep-sea hydrothermal vent archaeobacterium, *Methanococcus jannaschii*. *Journal of Biological Chemistry* 259, 15234-15241.
- Coolen, M.J.L. Hopmans, E.C., Rijpstra, W. I.C., Muyzer, G., Schouten, S., Volkman, J.K., Sinninghe Damsté, J.S., 2004. Evolution of the methane cycle in Ace Lake (Antarctica) during the Holocene: response of methanogens and methanotrophs to environmental change. *Organic Geochemistry* 35, 1151-1167
- Corselli, C. and D. Basso. 1996. First evidence of benthic communities based on chemosynthesis on the Napoli mud volcano (Eastern Mediterranean). *Marine Geology* 132, 227-239.
- Cragg, B.A., R.J. Parkes, J.C. Fry, A.J. Weighman, P.A. Rochelle and J.R. Maxwell. 1996. Bacterial populations and processes in sediments containing gas hydrates (ODP Leg 146: Cascadia margin). *Earth and Planetary Science Letters* 139, 497-507.



## References

---

- Daniels, L., Sparling, R., Sprott, G.D., 1984. The bioenergetics of methanogenesis. *Biochimica et Biophysica Acta* 768, 113-163.
- De Leeuw, J.M., van Bergen, P.F., van Aarsen, B.G.K., Gatellier, J.-P.L.A., Sinnighe Damsté, J.S., Collinson, M.E., 1991. Resistant biomacromolecules as major contributors to kerogen. *Philosophical Transactions of the Royal Society of London B333*, 329–337.
- De Rosa, M., de Rosa, S., Gambacorta, A., 1977. Chemical structure of the ether lipids of thermophilic acidophilic bacteria of the *Caldariella* group. *Phytochemistry* 16, 1961-1965.
- De Rosa, M., A. Gambacorta, B. Nicolaus, B. Chappe and P. Albrecht. 1983. Isoprenoid ethers: backbone of complex lipids of the archaeobacterium *Sulfolobus solfataricus*. *Biochimica et Biophysica Acta* 753, 249-256.
- De Rosa, M., Gambacorta, A., 1988. The lipids of archaeobacteria. *Progress in Lipid Research* 27,153–175.
- De Rosa, M., Trincone, A., Nicolaus, B., Gambacorta, A., 1991. Archaeobacteria: lipids, membrane structures, and adaptation to environmental stresses, in: Di Prisco, G. (Ed.), *Life Under Extreme Conditions*. Springer-Verlag, Berlin, Heidelberg, pp 61-87.
- Degens, E. T., Ross, D. A., 1972. Chronology of the Black Sea over the last 25,000 years. *Chemical Geology* 10, 1-16.
- Degens, E.T., Ross, D.A. (Eds.), 1974. *The Black Sea – Geology, Chemistry and Biology*. Memoir No. 20, American Association of Petroleum Geologists, Oklahoma, 633 pp.
- Deines, P., 1980. The isotopic composition of reduced organic carbon. In: Fritz, P., Fontes, J.Ch., (Eds.). *Handbook of environmental isotope geochemistry. The terrestrial Environment*. Amsterdam, Elsevier Scientific Publishing Co., 1, 329-406.
- DeLong, E.F., Wickman, G.S., Pace, N.R., 1989. Phylogenetic stains: ribosomal RNA-based probes for the identification of single cells. *Science* 243, 1360-1363.
- Diaz-del-Rio, V., Somoza, L., Martinez-Frias, J., Mata, M.P., Delgado, A., Hernandez-Molina, F.J., Lunar, R., Martin-Rubi, J.A., Maestro, A., Fernandez-Puga, M.C., Leon, R., Llave, E., Medialdea, T., Vazquez, J.T., 2003. Vast fields of hydrocarbon-derived carbonate chimneys related to the accretionary wedge/olistostrome of the Gulf of Cadiz. *Marine Geology*, 125, 177-200.
- Dojka, M.A., Hugenholtz, P., Haack, S.K., Pace, N.R., 1998. Microbial diversity in a hydrocarbon- and chlorinated-solvent-contaminated aquifer undergoing intrinsic bioremediation. *Applied and Environmental Microbiology* 64, 3869-3877.
- Drozd, R.J., Pazdersky, G.J., Jones, V.T., Weismann, T. J., 1981. Use of compositional indicators in prediction of petroleum production potential (abs.). American Chemical Society Meeting, Atlanta, GA, March 29-April 3.
- Eglinton, G., Hamilton, R.J., 1967. Leaf epicuticular waxes. *Science* 156, 1322–1335.
- Egorov, A.V., Ivanov, M.K., 1998. Hydrocarbon gases in sediments and mud breccia from the Central and Eastern part of the Mediterranean Ridge. *Geo-Marine Letters* 18, 139-145.
- Elvert, M., Suess, E., Whiticar, M. J., 1999. Anaerobic methane oxidation associated with marine gas hydrates: superlight C-isotopes from saturated and unsaturated C<sub>20</sub> and C<sub>25</sub> irregular isoprenoids. *Naturwissenschaften* 86, 295-300.
- Elvert, M., Suess, E., Greinert, J., Whiticar, M.J., 2000. Archaea mediating anaerobic methane oxidation in deep-sea sediments at cold seeps of the eastern Aleutian subduction zone. *Organic Geochemistry* 31, 1175-1187.
- Elvert, M., Boetius, A., Knittel, K., Jørgensen, B.B., 2003. Characterization of specific membrane fatty acids as chemotaxonomic markers for sulfate-reducing bacteria involved in anaerobic oxidation of methane. *Geomicrobiology Journal* 20, 403-419.

## References

- Faber, E., Stahl, W., 1984. Geochemical surface exploration for hydrocarbons in North Sea. AAPG Bulletin 68, 363-386.
- Ferreira, A.M., Miranda, A., Caetano, M., Baas, M., Vale, C., Sinninghe Damsté, J.S., 2001. Organic Geochemistry 32, 271–276.
- Frank, D.J., Gormly, J.R., Sackett, W.M., 1974. Reevaluation of carbon isotope compositions of natural methane, AAPG Bulletin 58, 2319-2325.
- Gagosian, R.B., Peltzer, E.T., Zafiriou, O.C., 1981. Atmospheric transport of continentally derived lipids to the tropical North Pacific. Nature 291, 312-314.
- Gagosian, R.B., Peltzer, E.T., Merrill, J.T., 1987. Long-range transport of terrestrially derived lipids in aerosols from the South Pacific. Nature 325, 800-803.
- Gaillard, C., Bourseau, J.P., Boudeulle, M., Pailleret, P., Rio, M., Roux, M., 1985. Les pseudo-bioherms de Beauvoisin (Drome): un sitenhydrothermal sur la marge tethysienne a l'Oxfordien Bull. Soc. Geol. Fr. 8, 69-78.
- Galimov, E.M., 1967. Effect obogasheniya izotopom  $^{13}\text{C}$  ugleroda metana v processe filtracii ego v gornih porodah (in Russian). Geohimiya, 12.
- Galimov, E.M., 1968. Izotopnyi sostav ugleroda gazov zemnoj kory (in Russian). Izvestiya Akademii Nauk SSSR, serija geologicheskaya, 5.
- Galimov, E.B., Kvenvolden, K.A., 1983. Concentrations and Carbon Isotopic Compositions of CH<sub>4</sub> and CO<sub>2</sub> in Gas from Sediments of the Blake Outer Ridge, Deep Sea Drilling Project Leg 76. In Initial Reports of the Deep Sea Drill. Project. 76, 493-407.
- Gardner, J.M., 2001. Mud volcanoes revealed and sampled on the Western Moroccan continental margin. Geophysical Research Letters 28, 339–342.
- Gelin, F., Volkman, J.K., de Leeuw, J.W., Sinninghe Damsté, J.S., 1997. Mid-chain hydroxy long-chain fatty acids in microalgae from the genus *Nannochloropsis*. Phytochemistry 45, 641–646.
- Gelmersen, G.P., 1886. Issledovaniya gryazevikh vulkanov i neftyanikh istochnikov v Krimu I na Tamanskom poluostrove. Zap. Imperat. Mineral. Obshestva, 1, 294-295 (In Russian).
- Ginsburg, G., Kremlev, A., Grigoriev, M., 1990. Fil'trogennye gasovije gidrati v Chernom More. Geologiya i Geofisika 3, 10-19 (In Russian).
- Ginsburg, G., Soloviev, V., 1997. Methane migration within the submarine gas-hydrate stability zone under deep-water conditions. Marine Geology 137, 49-57.
- Golubyatnikov, D.V., 1923. Fossil mud volcano at the Ilich oil field. Neftyan. Slantsev. Khozyaistvo, 3 7-8 (In Russian).
- Grantham, P.J., Posthuma, J., de Groot, K., 1980. Variation and significance of the C<sub>27</sub> and C<sub>28</sub> triterpane content of a North Sea core and various North Sea crude oils. In: Douglas, A.G., Maxwell, J.R. (Eds.), Advances in Organic Geochemistry 1979. Pergamon Press, New York, pp. 29–38.
- Gubkin, I.M., 1913. Review of geological formations in the Taman Peninsula. Izvest. Geol. Com., 31, 803-859 (In Russian).
- Gubkin, I.M., 1932. Uchenie o nefi, Moscow, USSR (In Russian).
- Guliev, I.S., Feizullayev, A.A., 1997. All about mud volcanoes. Nafta-Press, Baku.
- H Schäfer, G Muzzer, 2001. Denaturing gradient gel electrophoresis in marine microbial ecology. In Methods in Microbiology, Marine Microbiology, vol. 30, JH Paul (Ed.), Academic Press, pp. 425-468.
- Han, M. W., Suess, E., 1989. Subduction induced pore fluid venting and the formation of authigenic carbonates along the Cascadia continental margin: Implications for the global Ca cycle. Palaeogeography Palaeoclimatology Palaeoecology 71, 97–118.

## References

---

- Haq, B.U., Hardenbol, J., Vail, P.R., 1987. Chronology of fluctuating sea levels since the Triassic. *Science* 235, 1156–1167.
- Härtner, T., Straub, K.L., Kannenberg, E., 2005. Occurrence of hopanoid lipids in anaerobic *Geobacter* species. *FEMS Microbiol Lett.* 243, 59-64.
- Harvey, H.R., McManus, G.B., 1991. Marine ciliates as a widespread source of Tetrahymanol and hopan-3 $\beta$ -ol in sediments. *Geochimica et Cosmochimica Acta* 55, 3387–3390.
- Hayes, D. E., Pimm, A. C., Beckmann, J. P., Benson, W. E., Berger, W. H., Roth, P. H., Supko, P. R., and von Rad, U., 1972. Site 135. Pimm, A. C. (ed.), Initial Reports of the Deep Sea Drilling Project, Vol. XIV, JOIDES.
- Henriet, J.-P., Mienert, J., (Eds), 1998. Gas hydrates. Relevance to world margin stability and climatic change. Geological Society, London, Special Publications 137, pp. 338.
- Hinrichs, K-U., Hayes, J.M., Sylva, S.P., Brewer, P.G., De Long, E.F., 1999. Methane-consuming archaeobacteria in marine sediments. *Nature* 398, 802-805.
- Hinrichs, K-U., Pancost, R.D., Summons, R.E., Sprott, G.D., Sylva, S.P., Sinninghe Damsté, J.S., Hayes, J.M., 2000a. Mass spectra of Sn-2-hydroxyarchaeol, a polar lipid biomarker for anaerobic methanotrophy. *Geochemistry, Geophysics, Geosystems* 1, May 26.
- Hinrichs, K-U., R.E. Summons, V. Orphan, S.P. Sylva and J.M. Hayes. 2000b. Molecular and isotopic analysis of anaerobic methane-oxidizing communities in marine sediments. *Organic Geochemistry* 31, 1685-1701.
- Hinrichs, K.U., Boetius, A.B., 2002. The anaerobic oxidation of methane: new insights in microbial ecology and biogeochemistry. In *Ocean Margin Systems*. Wefer, G., Billett, D., Hebbeln, D., Jørgensen, B.B., Schlüter, M., and van Weering, T. (eds), Heidelberg: Springer-Verlag, 457-477.
- Hoefs, M.J.L., Schouten, S., de Leeuw, J.W., King, L.L., Wakeham, S.G., Sinninghe Damsté, J.S., 1997. Ether lipids of planktonic archaea in the marine water column. *Applied and Environmental Microbiology* 63, 3090–3095.
- Hoehler, T.M., Alperin, M.J., Albert, D.B., Martens, C.S., 1994. Field and laboratory studies of methane oxidation in an anoxic marine sediment: Evidence for a methanogen-sulfate reducer consortium. *Global Biogeochemical Cycles* 8, 451-463.
- Hoehler, T.M., Alperin, M.J., 1996. Anaerobic methane oxidation by a methanogen-sulfate reducer consortium: geochemical evidence and biochemical considerations, in: Lidstrom, M.E., Tabita, R.F. (Eds.), *Microbial growth on C-1 compounds*. Kluwer, Dordrecht, The Netherlands, pp. 326–333.
- Holzer, G., Oro, J., Tornabene, T.G., 1979. Gas chromatographic-mass spectrometric analysis of neutral lipids from methanogenic and thermoacidophilic bacteria. *Journal of Chromatography* 186, 795-809.
- Hopmans, E.C., Schouten, S., Pancost, R.D., van der Meer, M.T.J., Sinninghe Damsté, J.S., 2000. Analysis of intact tetraether lipids in archaeal cell material and sediments by high performance liquid chromatography/atmospheric pressure chemical ionization mass spectrometry. *Rapid Communications in Mass Spectrometry* 14, 585–589.
- Hopmans, E.C., Weijers, J.W.H., Schefuss, E., Herfort, L., Sinninghe Damsté, J.S., Schouten, S., 2004. A novel proxy for terrestrial organic matter in sediments based on branched and isoprenoid tetraether lipids. *Earth and Planetary Science Letters* 224, 107–116.
- Hovland, M., Talbot, M., Qvale, H., Olausson, S., Aasberg, L., 1987. Methane related carbonate cements in pockmarks of the North Sea. *Journal of Sedimentary Petrology* 57, 881-892.
- Hovland, M., Judd, A.G., 1988. Seabed pockmarks and seepages. Impact on geology, biology and the marine environment. Graham & Trotman, Alden Press, Great Britain, Oxford.
- Hugenholtz, P., Pitulle, C., Hershberger, K.L., Pace, N.R., 1998. Novel division level bacterial

## References

---

- diversity in a Yellowstone Hot Spring. *Journal of Bacteriology* 180, 366-376.
- Hunt, J.M., 1975. Origin of gasoline range alkanes in the deep sea. *Nature*, 254, 411–413.
- Hunt, J.M., 1979. *Petroleum geochemistry and geology*. San Francisco, W.H. Freeman, 617 p.
- Hunt, J.M., 1995. *Petroleum geochemistry and geology*. New York, W.H. Freeman and Co., 743 p.
- Inagaki, F., Suzuki, M., Takai, K., Oida, H., Sakamoto, T., Aoki, K., Nealson, K.H., Horikoshi, K., 2003. Microbial communities associated with geological horizons in coastal subseafloor sediments from the Sea of Okhotsk. *Applied and Environmental Microbiology* 69, 7224-7235.
- Ivanov, M.K., Konyukhov, A.I., Kul'nitskii, L.M., Musatov, A.A., 1989. Gryazevie vulkani v glubokovodnoy chasti Chernogo moria. *Vestn. Mosc. Univ. ser. Geol.*, 3, 48-54 (In Russian).
- Ivanov, M.K., van Weering, T.C.E., and Krugljakova, R.P., 1992a. Abstract. Mud volcanoes in the Black Sea. Second Conference on Gas in Marine Sediments, North Sea Centre, Hirshals, Denmark, p. 31–32.
- Ivanov, M.K., A.F. Limonov and J.M. Woodside (Eds). 1992b. Geological and geophysical investigations in the Mediterranean and Black Seas. Initial results of the “Training-through-Research” Cruise of R/V Gelendzhik in the Eastern Mediterranean and the Black Sea (June/July 1991). UNESCO Rep. Mar. Sci. 56, pp 208.
- Ivanov, M.K., A. Limonov and B. Cronin. 1996a. Mud volcanism and fluid venting in the eastern part of the Mediterranean Ridge. In UNESCO reports in Marine Science. UNESCO, Paris.
- Ivanov, M.K., A. Limonov and T. van Weering. 1996b. Comparative characteristic of the Black Sea and Mediterranean Ridge mud volcanoes. *Marine Geology* 132: 253-271.
- Ivanov, M.K., A.F. Limonov and J.M. Woodside. 1998. Extensive fluid flux through the sea floor on the Crimean continental margin (Black Sea). In *Gas hydrates: Relevance to World Margin Stability and Climatic Change*. Eds. J-P. Henriot and J. Mienert. The Geological Society, Special Publications No 137, London, pp 195-213.
- Ivanov, M.K., Kenyon, N., Nielsen, T., Wheeler, A., Monteiro, J., Gardner, J., Comas, M., Akhmanov, G., Akhmetzhanov, A., and Scientific Party of the TTR-9 cruise, 2000. Goals and principle results of the TTR-9 cruise. In: *Geological processes on European Continental Margin (TTR-9)*. International conference and eighth post-cruise meeting of the Training-Trough-Research Programme, Granada, Spain, 31 January – 3 February, 2000. Intergovernmental Oceanographic Commission, Workshop report No 168, 3-4.
- Ivanov, M., Pinheiro, L., Stadnitskaia, A., Blinova, V., 2001. Hydrocarbon Seeps on Deep Portuguese Margin. In: XI Meeting of European Union of Geosciences (EUG). Abstract book, Strasbourg, France, 2001, 160.
- Ivanov, M., Pinheiro, L., Stadnitskaia, A., Blinova, V., 2001. Hydrocarbon Seeps on Deep Portuguese Margin. In: XI Meeting of European Union of Geosciences (EUG). Abstract book, Strasbourg, France, 2001, 160.
- Ivanov, M., Blinova, V., Belenkaya, I., Eisenhauer, A., Pinheiro, L., 2004. Methane-derived carbonate chimneys in the Gulf of Cadiz, their composition and possible way of formation. *Geophysical Research Abstracts* 6, EGU04-A-05128.
- James, A.T., 1983. Correlation of natural gas by use of carbon isotopic distribution between hydrocarbon components. *AAPG Bulletin*, 67, 1176-1191.
- James, A.T., 1990. Correlation of reservoir gases using the carbon isotopic compositions of wet gas components. *AAPG Bulletin*, 74, 1441-1458.
- James, A.T., Burns, B.J., 1984. Microbial alteration of subsurface natural gas accumulations. *AAPG Bulletin*, 68 (8), 957-960.
- Jones, V.T., Drozd, R.J., 1979. Predictions of oil or gas potential by near-surface geochemistry. *AAPG Bulletin* 63, 699.
- Jones, V.T., Drozd, R.J., 1983. Prediction of oil or gas potential by near-surface geochemistry. *AAPG Bulletin* 67, 932-952.

## References

---

- Jørgensen, N.O., 1992. Methane-derived carbonate cementation of marine sediments from the Kattegat, Denmark: Geochemical and geological evidence. *Marine Geology* 103, 1-13.
- Kalinko, M.K., 1964. Osnovnije zakonomernosti raspredeleniya nefi i gasa v zemnoy kore. Moscow, Nedra (In Russian).
- Kalitskii, K.P., 1910. The mode of oil occurrence in the Cheleken Island. *Trudy Geol. Com. Ser.* 59.
- Katz, B.J., Elrod, L.W., 1983. Organic geochemistry of DSDP Site 467, offshore California, Middle Miocene to Lower Pliocene strata. *Geochimica et Cosmochimica Acta* 47, 389–396.
- Kauffman, E.G., Arthur, M.A., Howe, B., Scholle, P.A., 1996. Widespread venting of methane-rich fluids in Late Cretaceous (Campanian) submarine springs (Tepee Buttes), Western Interior seaway, USA. *Geology* 24, 799–802.
- Kenneth, E.P., Moldovan, J.M., 1993. The biomarker guide: interpreting molecular fossils in petroleum and ancient sediments. Prentice-Hall, Inc. A Simon and Schuster Company, Englewood Cliffs, New Jersey, pp. 363.
- Kenyon, N., Ivanov, M.K., Akhmetzhanov, A., Akhmanov, G. (Eds.), 2000. Multidisciplinary study of geological processes on the North East Atlantic and Western Mediterranean margins. Preliminary results of geological and geophysical investigations during TTR-9 cruise of R/V Professor Logachev, June-July, 1999. Intergovernmental Oceanographic Commission technical series vol. 56, p. 56.
- Kenyon, N., Ivanov, M.K., Akhmetzhanov, A., Akhmanov, G. (Eds.), 2001. Geological processes in the Mediterranean and Black Seas and North East Atlantic. Preliminary results of investigations during the TTR-11 cruise of R/V Professor Logachev, July-September 2001. Intergovernmental Oceanographic Commission technical series vol. 62, p. 63.
- Kenyon, N.H., Ivanov, M.K., Akhmetzhanov, A.M., Akhmanov, G.G. (Eds.), 2002. Geological Processes in the Mediterranean and Black Seas and North East Atlantic: Preliminary Results of Investigations during the TTR-11 cruise of RV Professor Logachev July-September, 2001. Intergovernmental Oceanographic Commission technical series 62, pp. 113.
- Kenyon, N.H., Ivanov, M.K., Akhmetzhanov, A.M., Akhmanov, G.G. (Eds.), 2003. Interdisciplinary geoscience research on the North East Atlantic margin, Mediterranean Sea and Mid-Atlantic Ridge. Intergovernmental Oceanographic Commission technical series 67, pp. 114.
- Kholodov, V.N., 1983. Postsedimentacionniye preobrazovaniya v elizionnikh basseinakh (na primere Vostochnogo Predkavkaz'ya). Moscow, Nauka (In Russian).
- Kholodov, V.N., 1990. Problem of the genesis of minerals in elision basins: communication 1. The South Caspian elision basin. *Lithol. Polez. Iskop.*, 6, 3-26.
- Kholodov, V.N., Nedumov, R.I., 1991. On the geochemical criteria of hydrosulfide pollution occurrence in waters of ancient basins. *Izvestia Akademii Nauk SSSR, Seria Geologicheskaya* 12, 62–78.
- Kholodov, V.N., 2002a. Mud volcanoes, their distribution regularities and genesis: communication 1. Mud volcanic provinces and morphology of mud volcanoes. *Lithology and Mineral Resources* 37, 3, 197-209.
- Kholodov, V.N., 2002b. Mud volcanoes: distribution regularities and genesis (Communication 2. Geological-geochemical peculiarities and formation model). *Lithology and Mineral Resources* 37, 4, 193-309.
- Kleemann, G., Poralla, K., Englert, G., Kjösen, H., Liaaen-Jensen, S., Neunlist, S., Rohmer, M., 1990. Tetrahymanol from the phototrophic bacterium *Rhodospseudomonas palustris*: first report of a gammacerane triterpene from a prokaryote. *Journal of General Microbiology* 136, 2551-2553.
- Knittel, K., Boetius, A., Eilers, A.L.H., Lochte, K., Linke, O.P.P., 2003. Activity, distribution, and diversity of sulfate reducers and other bacteria in sediments above gas hydrate (Cascadia Margin, Oregon). *Geomicrobiology Journal* 20, 269-294.

## References

---

- Knittel, K., Lösekann, T., Boetius, A., Kort, R., and Amann, R. 2005. Diversity and distribution of methanotrophic archaea at cold seeps. *Applied and Environmental Microbiology* 71, 467-479.
- Koga, Y., Akagawa-Matsushita, M., Ohga, M., Nishihara, M., 1993. Taxonomic significance of the distribution of component parts of polar ether lipids in methanogens. *Systematic and Applied Microbiology* 16, 342-351.
- Kohnen, M.E.L., Schouten, S., Sinninghe Damsté, J.S., de Leeuw, J.W., Merritt, D., Hayes, J.M., 1992. Recognition of paleobiochemicals by a combined molecular sulfur and isotope geochemical approach. *Science* 256, 358-362.
- Kolattukudy, P.E., 1980. Cutin, suberin and waxes. In: Stumpf, P.K. (Ed.), *The Biochemistry of Plants*, Vol. 4, Academic Press, pp. 571–641.
- Kovalenko, O., Belenkaia, I., 2002. Methane-induced precipitation of authigenic carbonates in mud volcano deposits of the Black Sea, in: *Geosphere/biosphere/hydrosphere coupling processes, fluid escape structures and tectonics at continental margins and ocean ridges*. Intergovernmental Oceanographic Commission Workshop Report 183, pp. 14-15.
- Kozlova, E.V., 2003. Petroleum potential revealed from geochemical study of mud volcano deposits. PhD thesis. Moscow State University, Russia. (In Russian).
- Kozlova, E., Ivanov, M.K., Baudin, F., Largeau, C., Derenne, S., 2004. Composition and maturity of organic matter in the rock clasts of mud volcanic breccia. Abstract. North Atlantic and Labrador Sea Margin Architecture and Sedimentary Process. International Conference and Twelfth Post-Cruise Meeting of the Training-Trough-Research programme, Copenhagen, Denmark. Intergovernmental Oceanographic Commission Workshop Report No 191, pp. 24–25.
- Krastel, S., Spiess, V., Ivanov, M., Weinrebe, W., Bohrmann, G., Shashkin, P., Heidersdorf, F., 2003. Acoustic investigations of mud volcanoes in the Sorokin Trough, Black Sea. *Geo-Marine Letters* 23, 230-238.
- Krüger, M., Treude, T., Wolters, H., Nauhaus, K., Boetius, A., 2005. Microbial methane turnover in different marine habitats. *Palaeogeography, Palaeoclimatology, Palaeoecology* 227, 6-17.
- Kutas, R.I., Kobolev, V.P., Tsvyashchenko, V.A., 1998. Heat flow and geothermal model of the Black Sea depression. *Tectonophysics* 291, 91–100.
- Kvenvolden, K.A., Frank, T.J., Golan-Bac, M., 1990. Hydrocarbon gases in Tertiary and Quaternary sediments offshore Peru-results and comparisons. In Suess, E., von Huene, R., et al., *Proc. ODP, Sci. Results*, 112: College Station, TX (Ocean Drilling Program), 505-515.
- Kvenvolden, K.A., Ginsburg, G., Soloviev, V., 1993. Worldwide distribution of subaquatic gas hydrates. *Geo-Marine Letters* 13, 32-40.
- Lallemant, S. J. C., Henry, P., Le Pichon, X., Foucher, J.-P., 1990. Detailed structure and possible fluid paths at the toe of the Barbados accretionary wedge (ODP Leg 110 area). *Geology* 18, 9, 854–857.
- Langworthy, T.A., Tornabene, T.G., Holzer, G., 1982. Lipids of Archaeobacteria. *Zentralbl. Bakteriol. Mikrobiol. Hyg. Abt.1 Orig. C* 3, 228-244.
- Langworthy, T.A. 1985. Lipids of archaeobacteria. In: Woese, C.R., Wolfe R.S. (Eds.), *The Bacteria*. Vol. VIII. Academic Press, New York, pp. 459–497.
- Lanoil, B.D., R. Sassen, M.T. La Duc, S.T. Sweet and K.H. Neilson. 2001. Bacteria and Archaea physically associated with Gulf of Mexico gas hydrates. *Applied and Environmental Microbiology* 67: 5143-5153.
- Larter, S., di Primio, R., 2005. Effects of biodegradation on oil and gas field PVT properties and the origin of oil rimmed gas accumulations. *Organic Geochemistry* 36, 299-310.
- Layell, Ch., 1850. *Principles of geology*. 8<sup>th</sup> edition. London: John Murray.
- Le Pichon, X., Henry, P., Lallemant, S., 1990. Water flow in the Barbados accretionary complex. *J. Geophys. Res.*, 95, 8945-8967.

## References

---

- Lebedew, W.C., Owsjannikow, W.M., Mogilewskij, G.A., Bogdanov, W.M., 1969. Fraktionierung der kohlenstoffisotope durch microbiologische prozesse in der biochemischen zone. *Angew. Geol.*, 15, 621-624.
- Lebedev, V.S., Syngayevski, E.D., 1971. Razdelenije izotopov ugleroda pri sorbcionnih processah (in Russian). *Geohimija*, 5.
- Lebedev, L.N., 1978. Stroenie I neftegasonosnost' sovremennikh geterogennikh depressii. Moscow, Nauka (In Russian).
- Leythaeuser, D.R., Schaefer, R.G., Yüklér, 1980. Diffusion of light hydrocarbons through near-surface rocks. *Nature* 284, 522-525.
- Leythaeuser, D.R., Mackenzie, A., Schaefer, R.G., Bjørøy, M., 1984. A novel approach for recognition and quantification of hydrocarbon migration effects in shale-sandstone sequences. *AAPG Bulletin* 68, 196-219.
- Limonov, A., M. Ivanov and J. Woodside. 1994. Mud volcanism in the Mediterranean and Black Seas and shallow structure of Eratosthenes Sea-mount. In UNESCO reports in Marine Science. UNESCO, Paris.
- Limonov, A.F., Woodside, J.M., Cita, M.B., Ivanov, M.K., 1996. The Mediterranean Ridge and related mud diapirism; a background. *Marine Geology* 132, 7-19.
- Limonov, A., T.C.E. van Weering, N. Kenyon, M. Ivanov and L. Meisner. 1997. Seabed morphology and gas venting in the Black Sea mud volcano area: observations with the MAK-1 deep-tow side-scan sonar and bottom profiler. *Marine Geology* 137: 121-136.
- Link, W.K., 1952. Significance of oil and gas seeps in World oil exploration. *AAPG Bulletin* 36, 1505-1541.
- Loncke, L., Gaullier, V., Bellaiche, G., Mascle, J., 2002. Recent depositional patterns of the Nile deep-sea fan from echo-character mapping. *AAPG Bulletin* 86, 1165-1186.
- Lovley, D.R., Dwyer, D.F., Klug, M.J., 1982. Linetic analysis of competition between sulfate reducers and methanogens for hydrogen in sediments. *Applied and Environmental Microbiology* 43, 6, 1373-1379.
- Luth, C., Luth, U. Gebruk, A.V, Thiel, H., 1999. Methane gas seeps along the oxic/anoxic gradient in the Black Sea: manifestations, biogenic sediment compounds, and preliminary results on benthic ecology. *Marine Ecology* 20, 221-249.
- MaCrea, J.M., 1950. On isotope chemistry of carbonates and paleotemperature scale. *Journal of Chemical Physics* 18, 849– 857.
- Madigan, M.T., Martinko, J.M., Parker, J., 2000. Brock biology of microorganisms. Prentice-Hall, Inc. Madrid, V.M., Taylor, G.T., Scranton, M.I., Chistoserdov, A.Y., 2001. Phylogenetic diversity of bacterial and archaeal communities in the anoxic zone of the Cariaco Basin. *Applied and Environmental Microbiology* 67, 1663-1674.
- Maldonado, A., Nelson, C.H., 1999a. Interaction of tectonic and depositional processes that control the evolution of the Iberian Gulf of Cadiz margin. *Marine Geology* 155, 217-242.
- Maldonado, A., Somoza, L., Pallarés, L., 1999b. The Betic orogen and the Iberian-African boundary in the Gulf of Cadiz: geological evolution (central North Atlantic). *Marine Geology* 155, 9-43.
- Mallory, F.B., Gordon, J.T., Conner, R.L., 1963. The isolation of a pentacyclic triterpenoid alcohol from a protozoan. *Journal of the American Chemical Society* 85, 1362–1363
- Martens, C.S., Berner, R.A., 1974. Methane production in the interstitial waters of sulfate-depleted marine sediments. *Science* 185, 1167-1169.
- Mascle, J., Zitter, T., Bellaiche, G., Droz, L., Gaullier, V., Loncke, L. and Prised Scientific Party, 2001. The Nile deep sea fan: preliminary results from a swath bathymetry survey. *Marine and Petroleum Geology* 18, 4, 471-477.
- Mattavelli, L., Ricchiuto, T., Grignanu, D., Schoell, M., 1983. Geochemistry and habitat of natural gases in Po Basin, Northern Italy. *AAPG Bulletin* 67, 2239-2254.

## References

---

- Mazurenko, L.L., Soloviev, V.A., Belenkaya, I., Ivanov, M.K., Pinheiro, L.M., 2002. Mud volcano gas hydrates in the Gulf of Cadiz. *Terra Nova* 14, 321-329.
- Mazurenko, L.L., Soloviev, V.A., Gardner, J.M., Ivanov, M.K., 2003. Gas hydrates in the Ginsburg and Yuma mud volcano sediments (Moroccan Margin): results of chemical and isotopic studies of pore water. *Marine Geology* 195, 201-210.
- Mazzini, A., Cronin, B.T., Parnell, J., 2002. Carbonate crust stratigraphy from the Black Sea, in: *Geosphere/biosphere/hydrosphere coupling processes, fluid escape structures and tectonics at continental margins and ocean ridges*. Intergovernmental Oceanographic Commission Workshop Report 183, pp. 15-16.
- Mazzini, A., Ivanov, M.K., Parnell, J., Stadnitskaia, A., Cronin, B.T., Poludetkina, E., Mazurenko, L., van Weering, T.C.E., 2004. Methane-related authigenic carbonates from the Black Sea: geochemical characterisation and relation to seeping fluids. *Marine Geology* 212, 153–181.
- Medialdea, T., Vegas, R., Somoza, L., Vázquez, J. T., Maldonado, A., Díaz-del-Río, V., Maestro, A., Córdoba, D., Fernández-Puga, M. C., 2004. Structure and evolution of the "Olistostrome" complex of the Gibraltar Arc in the Gulf of Cadiz (eastern Central Atlantic): evidence from two long seismic cross-sections. *Marine Geology* 209, 173-198.
- Méjanelle, L., Sanchez-Gargallo, A., Bentaleb, I., Grimalt, J.O., 2003. Long chain n-alkyl diols, hydroxy ketones and sterols in a marine eustigmatophyte, *Nannochloropsis gaditana*, and in *Brachionus plicatis* feeding on the algae. *Organic Geochemistry* 34, 527-538.
- Michaelis, W., Seifert, R., Nauhaus, K., Treude, T., Thiel, V., Blumenberg, M., Knittle, K., Gieseke, A., Peterknecht, K., Pape, T., Boetius, A., Amann, R., Jorgensen, B. B., Widdel, F., Peckmann, J., Pimenov, N. V., Gulin, M. B., 2002. Microbial reefs in the Black Sea fueled by anaerobic oxidation of methane. *Science* 297, 1013-1015.
- Moskalenko, V.N., Neprochnov, Y.R., Otisty, B.K., Rusakov, O.M., Shimkus, K.M., Shlezinger, A.E., Sochelnikov, V.V., Sollogub, V.B., Solovyev, V.D., Starostenko, V.I., Starovoitov, A.F., Terekhov, A.A., Volvovsky, I.S., Zhigunov, A.S., Zolotarev, V.G., 1988. Structure and evolution of the earth's crust and upper mantle of the Black Sea. *Boll. Geofis. Teor. Appl.* 30, 109-196.
- Mousseau, R.J., Williams, J.C., 1979. Dissolved hydrocarbons in coastal waters of North America (abs). *AAPG Bull.*, 63, 699-700.
- Murray, J.W., Top, Z., O' zsoy, E., 1991. Hydrographic properties and ventilation of the Black Sea. *Deep Sea Research* 38, 663– 689.
- Murton, B.J., Biggs, J., 2003. Numerical modelling of mud volcanoes and their flows using constraints from the Gulf of Cadiz. *Marine Geology* 195, 223-236.
- Nauhaus, K., Boetius, A., Krüger, M., Widdel, F., 2002. In vitro demonstration of anaerobic oxidation of methane coupled to sulfate reduction in sediment from a marine gas hydrate area. *Environmental Microbiology* 4, 296-305.
- Nauhaus, K., Treude, T., Boetius, A., Krüger, M., 2005. Environmental regulation of the anaerobic oxidation of methane in ANME-I or –II dominated communities: A comparison. *Environmental Microbiology* 7, 98-106.
- Nedumov, R.I., 1994. Problems of the lithology, geochemistry and paleogeography of the Cenozoic sediments of the Ciscaucasus. Report 2: Influence of paleorivers on peculiarities of sedimentation in basins of the Ciscaucasus. *Litologia i Poleznije Iskopaemie* 1, 69–78.
- Neumayr, M., 1889. *Istoriya Zemli*. St.Petersburg, Prosveshenie.
- Niemann, H., Elvert, M., Hovland, M., Orcutt, B., Judd, A., Suck, I., Gutt, J., Joye, S., Damm, E., Finster, K., Boetius, A., 2005a. Methane emission and consumption at a North Sea gas seep (Tommeliten area). *Biogeosciences* 2, 335-351.



## References

---

- Nieman, H., 2005b. Rates and signatures of methane turnover in sediments of continental margins. PhD thesis, Bremen University, Germany.
- Nieman, H., 2005c. Rates and signatures of methane turnover in sediments of continental margins. PhD thesis, Bremen University, Germany.
- Niemann, H., Duarte, J., Hensen, C., Omorigie, E., Magalhães, V.H., Elvert, M., Pinheiro, L.M., Kopf, A., Boetius, A., 2006. Microbial methane turnover at mud volcanoes of the Gulf of Cadiz. *Geochimica et Cosmochimica Acta*, accepted.
- Nikishin, A. M., Korotaev, M.V., Ershov, A.V., Brunet, M.-F. 2003. The Black Sea basin: tectonic history and Neogene-Quaternary rapid subsidence modeling. *Sedimentary Geology* 156, 149–168.
- Nishihara, M., Koga, Y., 1991. Hydroxyarchaeetidylserine and hydroxyarchaeetidyl-myo-inositol in *Methanosarcina barkeri*: polar lipids with a new ether core portion. *Biochimica et Biophysica Acta* 1082, 211-217.
- Olu, K., M. Sibuet, F. Harmegnies, J-P. Foucher and A. Fiala-Medioni. 1996. Spatial distribution of diverse cold seep communities living in various diapiric structures of the southern Barbados prism. *Progress in Oceanography* 38, 347-376.
- Olu, K., Lance, S., Sibuet, M., Henry, P., Fiala-Medioni, A., Dinet, A., 1997. Cold seep communities as indicator of fluid expulsion patterns through mud volcanoes seaward of the Barbados accretionary prism. *Deep-Sea Research* 44, 811-841.
- Oremland, R.S., Whiticar, M.J., Strohmaier, F.E., Keine, R.P., 1988. Bacterial ethane formation from reduced, ethylated sulfur compounds in anoxic sediments. *Geochimica et Cosmochimica Acta*, 52, 1895-1904.
- Orphan, V.J., House, C.H., Hinrichs, K-U., McKeegan, K.D., DeLong, E.F., 2001a. Methane-consuming archaea revealed by directly coupled isotopic and phylogenetic analysis. *Science* 293, 484-487.
- Orphan, V.J., Hinrichs, K.-U., Ussler III, W., Paull, C.K., Taylor, L.T., Sylva, S.P. Hayes, J.M., Delong, E.F., 2001b. Comparative analysis of methane-oxidizing archaea and sulfate-reducing bacteria in anoxic marine sediments. *Applied and Environmental Microbiology* 67, 1922-1934.
- Orphan, V.J., House, C.H., Hinrichs, K-U., McKeegan, K.D., DeLong, E.F., 2002. Multiple archaeal groups mediate methane oxidation in anoxic cold seep sediments. *Proc. Natl. Acad. Sci.* 99: 7663-7668.
- Ourisson, G., Albrecht, P., Rohmer, M., 1979. The hopanoids. *Palaeochemistry and biochemistry of a group of natural products. Pure and Applied Chemistry* 51, 709–729.
- Ovsyannikov, D. O., Sadekov, A. Yu., Kozlova, E. V., 2003. Rock fragments from mud volcanic deposits of the Gulf of Cadiz: an insight into the Eocene–Pliocene sedimentary succession of the basin. *Marine Geology* 195, 211-221.
- Pallasser, R.J. 2000. Recognizing biodegradation on gas/oil accumulations through the  $\delta^{13}\text{C}$  compositions of gas components. *Organic Geochemistry*, 31, 1363-1373.
- Pancost, R.D., J.S. Sinninghe Damsté, S. De Lint, M.J.E.C. van der Maarel, J.C. Gottschal and the Medinaut shipboard scientific party. 2000. Biomarker evidence for widespread anaerobic methane oxidation in Mediterranean sediments by a consortium of methanogenic archaea and bacteria. *Applied and Environmental Microbiology* 66, 1126-1132.
- Pancost, R.D., Bouloubassi, I., Aloisi, G., Sinninghe Damsté, J.S., and the Medinaut shipboard scientific party, 2001a. Three series of non-isoprenoidal dialkyl glycerol diethers in cold-seeps carbonate crusts. *Organic Geochemistry* 32, 695-707.
- Pancost R.D., E.C. Hopmans, J.S. Sinninghe Damsté and the Medinaut shipboard scientific party. 2001b. Archaeal lipids in Mediterranean cold-seeps: molecular proxies for anaerobic methane oxidation. *Geochimica et Cosmochimica Acta* 65, 1611-1627.

## References

---

- Paull, C.K., and Neumann, A.C., 1987. Continental margin brine seeps: their geological consequences. *Geology* 15, 545–548.
- Paull, C.K., Neumann, A.C., 1987. Continental margin brine seeps: their geological consequences. *Geology* 15, 545–548.
- Paull, C.K., Chanton, J.P., Neumann, A.C., Coston, J.A., Martens, C.S., Showers, W., 1992. Indicators of methane-derived carbonates and chemosynthetic organic carbon deposits: examples from the Florida Escarpment. *Palaios* 7, 361–375.
- Paull, C.K., Lorenson, T.D., Borowowski, W.S., Ussler, W., Olsen, K., Rodriguez, N.M., Wehner, H., 1999. Isotopic composition of CH<sub>4</sub>, CO<sub>2</sub> species, and sedimentary organic matter within ODP Leg 164 sample from the Blake Ridge: Gas source implications. *Proc. Ocean Drill. Program, Sci. Results* 164, 67-78.
- Peckmann, J., Thiel, V., Michaelis, W., Clari, P., Gaillard, C., Martire, L., Reitner, J., 1999a. Cold seep deposits of Beauvoisin (Oxfordian; southeastern France) and Marmorito (Miocene; northern Italy): microbially induced authigenic carbonates. *International Journal of Earth Sciences* 88, 60-75.
- Peckmann, J., Walliser, O.H., Reigel, W., Reitner, J., 1999b. Signatures of hydrocarbon venting in a middle Devonian carbonate mound (Hollard Mound) at the Hamar Laghdad (AntiAtlas, Morocco). *Facies* 40, 281-296.
- Peckmann, J., Reimer, A., Luth, U., Luth, C., Hansen, B.T., Heinicke, C., Hoefs, J., Reitner, J., 2001. Methane-derived carbonates and authigenic pyrite from the northwestern Black Sea. *Marine Geology* 177, 129-150.
- Peckmann, J., Goedert, J.L., Thiel, V., Michaelis, W., Reitner, J., 2002. A comprehensive approach to the study of methane-seep deposits from the Lincoln Creek Formation, western Washington State, USA. *Sedimentology* 49, 855-873.
- Peckmann, J., Goedert, J.L., Heinrichs, T., Hoefs, J., Reitner, J., 2003. The Late Eocene 'Wiskey Creek' methane-seep deposit (western Washington State): Part II. Petrology, stable isotopes, and biogeochemistry. *Facies* 48, 241-254.
- Peckmann, J., Thiel, V., 2004. Carbon cycling at ancient methane-seeps. *Chemical Geology* 205, 443-467.
- Pepper, A.S., Corvi, P.J., 1995. Simple kinetic model of petroleum formation. Part I: oil and gas generation from kerogen. *Marine Geology* 12, 291-319.
- Peters, K.E., Walters, C.C. Moldovan, J.M., 2005. *The Biomarker Guide*. 2nd Edition. Cambridge University Press, UK.
- Phelps, C.D., Kerkhof, L.J., Young, L.Y., 1998. Molecular characterization of a sulfate-reducing consortium which mineralizes benzene. *FEMS Microbial Ecology* 27, 269-279.
- Pimenov, N., Savvichev, A., Rusanov, I., Lein, A., Egorov, A., Gebruk, A., Moskalev, L., Vogt, P., 1999. Microbial processes of carbon cycle as the base of food chain of Haakon Mosby mud volcano benthic community. *Geomarine Letters* 19, 89-96.
- Pinheiro, L.M., Ivanov, M. K., Sautkin, A., Akhmanov, G., Magalhães, V. H., Volkonskaya, A., Monteiro, J. H., Somoza, L., Gardner, J., Hamouni, N., Cunha, M. R., 2003. Mud volcanism in the Gulf of Cadiz: results from the TTR-10 cruise. *Marine Geology* 195, 131-151.
- Popov, S.V., Stolyarov, A.S., 1997. Paleogeography and anoxic environments of Oligocene-Early Miocene Eastern Paratethys. *Israel Journal of Earth Sciences* 45, 161–167.
- Prasolov, E.M., Lohov, K.I., Belenkaya, I.J., Ivanov, M.K., Soloviev, V.A., Blinova, V.N., Mazurenko, L.L., 2002. Isotopic composition of carbon and oxygen from carbonate chimneys from the fluid discharge areas (the Gulf of Cadiz, NE Atlantic). Abstract. Conference devoted to the memory of Prof. P.N.Kropotkin: geodynamic, geofluids and petroleum. Moscow, 226-228.

## References

---

- Premoli Silva, I., Erba, E., Spezzaferri, S., Cita, M.B., 1996. Age variation in the source of the diapiric mud breccia along and across the axis of the Mediterranean Ridge accretionary complex. *Marine Geology* 132, 175-202.
- Prinzhofer, A., Pernaton, E., 1997. Isotopically light methane in natural gases: bacterial imprint or segregative migration? *Chemical Geology* 142, 193-200.
- Prinzhofer, A., Battani, A., 2003. Gas isotope tracing: an important tool for hydrocarbon exploration. *Revue de l'IFP, Special Publication for B. Tissot's Jubilee, June 2003. Oil and Gas Science and Technology. Rev. IFP*, 58, 2, 299-311.
- Rakhmanov, R.R., 1987. Gryazeviye vulkani I ikh znachenije v prognozirovanii neftegazonosnosti nedr. Moscow, Nedra (In Russian).
- Reeburgh, W.S. 1976. Methane consumption in Cariaco Trench waters and sediments. *Earth and Planetary Science Letters* 28, 337-344.
- Reeburgh, W. S., Ward, B. B., Whalen, S. C., Sandbeck, K. A., Kilpatrick, K. A., Kerkhof, L.J., 1991. Black Sea methane geochemistry. *Deep-Sea Res.* 38, Supplement 2, S1189-1210.
- Reitner, J., Peckmann, J., Reimer, A., Schumann, G., Thiel, V., 2005. Methane-derived carbonate build-ups and associated microbial communities at cold seeps on the lower Crimean shelf (Black Sea0. *Facies* 51, 71-84.
- Rice, D.D., Claypool, G.E., 1981. Generation, accumulation and resource potential of biogenic gas. *AAPG Bulletin* 65, 5-21.
- Richers, D.M., Jones, V.T., 1986. The 1983 Landsat soil-gas geochemical survey of Patrick Draw area, Wyoming. *AAPG Bulletin* 70, 869-887.
- Ritger, S., Carson, B., Suess, E., 1987. Methane-derived authigenic carbonates formed by subduction-induced pore-water expulsion along the Oregon/Washington margin. *Geological Society of America Bulletin* 98, 147-156.
- Roberts, H.H., Aharon, P., 1994. Hydrocarbon-derived carbonate buildups of the northern Gulf of Mexico continental slope: a review of submersible investigations. *Geo-Marine Letters* 14, 135-148.
- Robson, J. N., Rowland, S. J., 1986. Identification of novel widely distributed sedimentary acyclic sesterterpenoids. *Nature* 324, 561-563.
- Rohmer, M., Bouvier-Nave, P., Ourisson, G., 1984. Distribution of hopanoid triterpenes in prokaryotes. *Journal of General Microbiology* 130, 1137-1150.
- Rohmer, M., Bissert, P., Neunlist, S., 1992. The hopanoids, prokaryotic triterpenoids and precursors of ubiquitous molecular fossils, in: Moldowan, J.M., Albrecht, M., Philp, R.P. (Eds.), *Biological markers in sediments and petroleum*. Prentice Hall, London, pp. 1-17.
- Rowland, S. J., Robson, J. N., 1990. The widespread occurrence of highly branched acyclic C<sub>20</sub>, C<sub>25</sub> and C<sub>30</sub> hydrocarbons in recent sediments and biota - a review. *Marine Environmental Research* 30, 191-216.
- Sackett, W.M., 1978. Carbon and hydrogen isotope effects during the thermocatalytic production of hydrocarbons in laboratory simulation experiments. *Geochimica et Cosmochimica Acta* 42, 571-580.
- Sandstrom, M. W., Meredith, D., Kaplan, Isaac R., 1983. Hydrocarbon geochemistry in surface sediments of the Alaskan outer continental shelf; Part 2, Distribution of hydrocarbon gases. *AAPG Bulletin* 67, 2047-2052.
- Sassen, R., H. Roberts, P. Aharon, J. Larkin, E.W. Chinn and R. Carney. 1993. Chemosynthetic bacterial mats at cold hydrocarbon seeps, Gulf of Mexico continental slope. *Organic Geochemistry* 20, 77-89.
- Sassen R., Roberts, H.H., Carney, R., Milkov, A.V., DeFreitas, D.A., Lanoil, B., Zhang, C., 2004. Free hydrocarbon gas, gas hydrate, and authigenic minerals in chemosynthetic communities of

## References

---

- the northern Gulf of Mexico continental slope: relation to microbial processes. *Chemical Geology* 205, 195-217.
- Schäfer, H., Muyzer, G., 2001. Denaturing gradient gel electrophoresis in marine microbial ecology. *In* *Methods in Microbiology, Marine Microbiology* 30, J.H. Paul (ed.), Academic Press, pp. 425-468.
- Schlegel, H.G., 1985. *Allgemeine microbiologie*. Georg Thieme Verlag Stuttgart.
- Schoell, M., 1983. Genetic characterization of natural gases. *AAPG Bulletin* 67, 2225-2238.
- Schoell, M., McCaffrey, M.A., Fago, F.J., Moldovan, J.M., 1992. Carbon isotopic compositions of 28,30-bisnorhopanes and other biological markers in a Monterey crude oil. *Geochimica et Cosmochimica Acta* 56, 1391-1399.
- Schoell, M., Schouten, S., Sinninghe Damsté, J.S., de Leeuw, J.W., Summons, R.E., 1994. A molecular organic carbon isotope record of Miocene climate changes. *Science* 263, 1122-1125
- Schonheit, P., Kristjansson, J. K., Thauer, R. K., 1982. Kinetic mechanism for the ability of sulfate reducers to outcompete methanogens for acetate. *Arch. Microbiol.* 132, 285-288.
- Schouten, S., Van der Maarel, M.J.E.C., Huber, R., Sinninghe Damsté, J.S., 1997a. 2,6,10,15,19-Pentamethylcosenes in *Methanolobus bombayensis*, a marine methanogenic archaeon, and in *Methanosarcina mazei*. *Organic Geochemistry* 26, 409-414.
- Schouten, S., Schoell, M., Rijpstra, W.I.C., Sinninghe Damsté, J.S., 1997b. A molecular stable carbon isotope study of organic matter in immature Miocene Monterey sediments, Pismo basin. *Geochimica et Cosmochimica Acta* 61, 2065-2082.
- Schouten, S., Hoefs, M.J.L., Koopmans, M.P., Bosch, H-J., Sinninghe Damsté, J.S., 1998. Structural characterization, occurrence and fate of archaeal ether-bound acyclic and cyclic biphytanes and corresponding diols in sediments. *Organic Geochemistry* 29, 1305-1319.
- Schouten, S., Hopmans, E.C., Pancost, R.D, Sinninghe Damsté, J.S., 2000. Widespread occurrence of structurally diverse tetraether membrane lipids: evidence for the ubiquitous presence of low-temperature relatives of hyperthermophiles. *Proceedings of the National Academy of Sciences* 97, 14421-14426.
- Schouten, S., S.G. Wakeham and J.S. Sinninghe Damsté. 2001a. Evidence for anaerobic methane oxidation by archaea in euxinic waters of the Black Sea. *Organic Geochemistry* 32, 1277-1281.
- Schouten, S., E.C. Hopmans and R.D. Pancost. 2001b. Widespread occurrence of structurally diverse tetraether membrane lipids. *Proc. Nat. Acad. Sci.* 97, 14421-14426.
- Schouten, S., Hopmans, E.C., Schefuß, E., Sinninghe Damsté, J.S., 2002. Distributional variations in marine crenarchaeotal membrane lipids: a new tool for reconstructing ancient sea water temperatures. *Earth and Planetary Science Letters* 204, 265-274.
- Schouten, S., Wakeham, S.G., Hopmans, E.C., Sinninghe Damsté, J.S., 2003. Biogeochemical evidence that thermophilic Archaea mediate the anaerobic oxidation of methane. *Applied and Environmental Microbiology* 69, 1680-1686.
- Schouten, S., Hopmans, E.C., Sinninghe Damsté, J.S., 2004. The effect of maturity and depositional redox conditions on archaeal tetraether lipid palaeothermometry. *Organic Geochemistry* 35, 567-571.
- Schubert, C.J., Coolen, M.J.L., Neretin, L.N., Schippers, A., Abbas, B., Durisch-Kaiser, E., Wehrli, B., Hopmans, E.C., Sinninghe Damsté, J.S., Wakeham, S., Kuypers, M., 2006. Aerobic and anaerobic methanotrophs in the Black Sea water column. *Environmental Microbiology* 8, p.1844.
- Seifert, W.K., Moldovan, J.M., 1978a. Applications of steranes, terpanes and monoaromatics to the maturation, migration and source of crude oils. *Geochimica et Cosmochimica Acta* 42, 77-95.

## References

---

- Seifert, W.K., Moldovan, J.M., 1978b. First proof of a C<sub>28</sub>-pentacyclic triterpane in petroleum. *Nature* 271, 436–437.
- Sellanes, J., Quiroga, E., Gallardo, V.A., 2004. First direct evidence of methane seepage and associated chemosynthetic communities in the bathyal zone of Chile. *J Mar Biol. Ass. UK* 84, 1065-1066.
- Sharma, T., Clayton, R.N., 1965. Measurement of 18O/16O ratios of total oxygen in carbonates. *Geochimica et Cosmochimica Acta* 29, 1347– 1353.
- Shlikov, V.G., Kharitonov, V.D., 2001. On method of quantitative X-ray analysis of mineral composition of the rocks. *Geocology, Engineering, Geology, Hydrogeology. Geocryology* 2, 129– 140.
- Shnyukov, E.F., Starostenko, V.I., Rusakov, O.M., Kobolev, V.P., Maslakov, N.A., 2005. Gas volcanism in the Black Sea. Abstract. International workshop on methane in sediments and water column of the Black Sea: formation, transport, pathways and the role within the carbon cycle. Sevastopol, Ukraine, pp. 50-51.
- Sibson, R.H., Scott, J., 1998. Stress/fault controls on the containment and release of overpressured fluids: examples from gold-quartz vein systems in Juneau, Alaska, Victoria, Australia, and Otago, New Zealand. *Ore Geology Reviews* 13, 293-306.
- Sibuet, M., Juniper, S., Pautot, G., 1988. Cold-seep benthic communities in the Japan subduction zones: geological control of community development. *Journal of Marine Research* 46, 333-348.
- Sibuet, M. and K. Olu. 1998. Biogeography, biodiversity and fluid dependence of deep-sea cold-seeps communities at active and passive margins. *Deep-Sea Research* 45: 517-567.
- Silverman, S.R., 1971. Influence of petroleum origin and transformation on its distribution and redistribution in sedimentary rocks. 8<sup>th</sup> World Petroleum Congress Proceedings 2, 47-54.
- Simoneit, B.R.T., 1977. Organic matter in eolian dusts over the Atlantic Ocean. *Marine Chemistry* 5, 443-464.
- Sinninghe Damsté, J.S., Schouten S., Van Vliet, N.H., Huber, R., Geenevasen, J.A.J., 1997. A polyunsaturated irregular acyclic C<sub>25</sub> isoprenoid in a methanogenic archaeon. *Tetrahedron Letters* 38, 6881-6884.
- Sinninghe Damsté, J.S., Rijpstra, I.C., Schouten, S., Peletier, H., van der Maarel, M.J.E.C., Gieskes, W.W.C., 1999. A C<sub>25</sub> highly branched isoprenoid alkene and C<sub>25</sub> and C<sub>27</sub> n-polyenes in the marine diatom *Rhizosolenia setigera*. *OrganicGeochemistry* 30, 95-100.
- Sinninghe Damsté, J.S., Schouten, S., Hopmans, E.C., van Duin, A.C.T., Geenevasen, J.A.J., 2002a. Crenarchaeol: the characteristic core glycerol dibiphytanyl glycerol tetraether membrane lipid of cosmopolitan pelagic crenarchaeota. *Journal of Lipid Research* 43, 1641–1651.
- Sinninghe Damsté, J.S., Rijpstra, W.I.C., Hopmans, E.C., Prahl, F.G., Wakeham, S.G., Schouten, S., 2002b. Distribution of membrane lipids of planktonic Crenarchaeota in the Arabian Sea. *Applied and Environmental Microbiology* 68, 2997–3002.
- Sinninghe Damsté, J.S., Muyzer, G., Abbas, B., Rampen, S.W., Massé, G., Allard, W.G., Belt, S.T., Robert, J.-M., Rowland, S.J., Moldovan, J.M., Barbanti, S.M., Fago, F.J., Denisevich, P., Dahl, J., Trindade, L.A. F., Schouten, S., 2004a. The Rise of the Rhizosolenid Diatoms. *Science* 23, 304, 584-587.
- Sinninghe Damsté, J.S., Rijpstra, W.I.C., Schouten, S., Fuerst, J.A., Jetten, M.S.M., Strous, M., 2004b. The occurrence of hopanoids in planctomycetes: implications for the sedimentary biomarker record. *Organic Geochemistry* 35, 561-566.
- Soloviev, V., Ginsburg, G., 1997. Water segregation in the course of gas hydrate formation and accumulation in submarine gas-seepage fields. *Marine Geology* 137, 59-68.
- Somoza, L., Maestro, A., Lowrie, A., 1999. Allochthonous blocks as hydrocarbon traps in the Gulf of Cadiz. *Offshore Technology Conference OTC 10889*, 571-577.

## References

---

- Somoza, L., Battista, B.M., Gardner, J.M., Lowrie, A., 2001. Gulf of Cadiz (western Spain): characterized by a complex petroleum system. Abstract. 21<sup>st</sup> Annual GCSSEPM Foundation Bob F. Perkins Research Conference. Petroleum systems of deep-water basins: global and Gulf of Mexico experience, December 2-5, 2001.
- Somoza, L., Gardner, J.M., Diaz-del-Rio, V., Vazquez, T., Pinheiro, L., Hernández-Molina, F. J. and TASYO/ANASTASYA shipboard scientific parties, 2002. Numerous methane gas related seafloor structures identified in the Gulf of Cádiz. EOS Transactions, American Geophysical Union 83, 541-547.
- Somoza, L., Díaz-del-Río, V., León, R., Ivanov, M., Fernández-Puga, M. C., Gardner, J. M., Hernández-Molina, F. J., Pinheiro, L. M., Rodero, J., Lobato, A., Maestro, A., Vázquez, J.T., Medialdea, T., Fernández-Salas, L.M., 2003. Seabed morphology and hydrocarbon seepage in the Gulf of Cádiz mud volcano area: Acoustic imagery, multibeam and ultra-high resolution seismic data. *Marine Geology* 195, 153-176.
- Somoza, L., Díaz-del-Río, V., León, R., Ivanov, M., Fernández-Puga, M. C., Gardner, J. M., Hernández-Molina, F. J., Pinheiro, L. M., Rodero, J., Lobato, A., Maestro, A., Vázquez, J.T., Medialdea, T., Fernández-Salas, L.M., 2003. Seabed morphology and hydrocarbon seepage in the Gulf of Cádiz mud volcano area: Acoustic imagery, multibeam and ultra-high resolution seismic data. *Marine Geology* 195, 153-176.
- Sprott, G.D., Ekiel, I., Dicaire, C., 1990. Novel, acid-labile, hydroxydiether lipid cores in methanogenic bacteria. *Journal of Biological Chemistry* 265, 13735-13740.
- Sprott, G.D., Dicaire, C.J., Choquet, C.G., Patel, G.B., Ekiel, I., 1993. Hydroxydiether lipid structures in *Methanosarcina* spp. and *Methanococcus voltae*. *Applied and Environmental Microbiology* 59, 912-914.
- Srivastava, S.P., Schouten, H., Roest, W.R., Klitgord, K.D., Kovacs, L.C., Verhoef, J., Macnab, R., 1990. Iberian plate kinematics: a jumping plate boundary between Eurasia and Africa. *Nature* 344, 756-759.
- Stadnitskaia, A. 1997. Distribution and composition of hydrocarbon gas in the seabed sediments of the Sorokin Trough (Southeastern part of the Crimean margin). In *Gas and Fluids in Marine Sediments: Gas Hydrates, Mud Volcanoes, Tectonics, Sedimentology and Geochemistry in Mediterranean and Black Seas*. Fifth Post-cruise Meeting of the Training-through-Research Programme and International Congress. IOC/UNESCO Workshop Report No 129. Amsterdam, The Netherlands, 10 p.
- Stadnitskaya, A., Belenkaya, I., 1998. Gas hydrates in the seabed sediments on the Northeastern part of the Black Sea. Abstract. XXIII General Assembly of the European Geophysical Society. Nice, France, p. 299.
- Stadnitskaia, A., Baas, M., Ivanov, M.K., Van Weering, T.C.E., Sinninghe Damsté, J.S., 2003. Novel archaeal macrocyclic diether core membrane lipids in a methane-derived carbonate crust from a mud volcano in the Sorokin Trough, NE Black Sea. *Archaea* 1, 165-173.
- Stadnitskaia, A., Muyzer, T. G., Abbas, B., Coolen, M.J.L., Hopmans, E.C., Baas, M., van Weering, T.C.E., Ivanov, M.K., Poludetkina, E., Sinninghe Damsté, J.S., 2005. Biomarker and 16S rDNA evidence for anaerobic oxidation of methane and related carbonate precipitation in deep-sea mud volcanoes of the Sorokin Trough, Black Sea. *Marine Geology* 217, 67-96.
- Stadnitskaia, A., Ivanov, M.K., Blinova, V., Kreulen, R., van Weering, T.C.E., 2006a. Molecular and carbon isotopic variability of hydrocarbon gases from mud volcanoes in the Gulf of Cadiz, NE Atlantic. *Marine and Petroleum Geology* 23, 281-296.
- Stadnitskaia, A., Blinova, V., Ivanov, M.K., Baas, M., Hopmans, E. C., van Weering, T.C.E., Sinninghe Damsté, J.S., 2006b. Lipid biomarkers in sediments of mud volcanoes from the

## References

---

- Sorokin Trough, NE Black Sea: probable source strata for the erupted material. *Organic Geochemistry*, in press.
- Stahl, W.J., 1977. Carbon and nitrogen isotopes in hydrocarbon research and exploration. *Chemical Geology* 20, 121-149.
- Stahl, W.J., 1979. Carbon isotopes in petroleum geochemistry. In: Jäger, E., Hunziker, J.C., (Eds.). *Lectures in isotope geology*. Springer-Verlag, 274-282.
- Stahl, W.J., Faber, E., Carey, B.D., Kirksey, D.L., 1981. Near-surface evidence of migration of natural gas from deep reservoirs and source rocks. *AAPG Bulletin* 65, 1543-1550.
- Stahl, D.A., Amann, R., 1991. Development and application of nucleic acid probes. In: Stackebrandt, E., Goodfellow, M. (Eds.), *Nucleic Acid Techniques in Bacterial Systematics*, John Wiley & Sons Ltd., Chichester, England, pp. 205–248.
- Stakes, D.S., Orange, D., Paduan, J.B., Salamy, K.A., Maher, N., 1999. Cold-seeps and authigenic carbonate formation in Monterey Bay, California. *Marine Geology* 159, 93-109.
- Suess, E., Whiticar, M.J., 1989. Methane-derived CO<sub>2</sub> in pore fluids expelled from the Oregon subduction zone. *Paleogeography, Paleoclimatology, Paleoecology* 71, 119–136.
- Suess, E., Bohrmann, G., von Huene, R., Linke, P., Wallmann, K., Lammers, S., Sahling, H., Winckler, G., Lutz, R.A., Orange, D., 1998. Fluid venting in the Aleutian subduction zone. *J. Geophys. Res.* 103(B2), 2597-2614.
- Summons, R.E., Jahnke, L.L., Roksandic, Z., 1994. Carbon isotopic fractionation in lipids from methanotrophic bacteria: relevance for interpretation of the geochemical record of biomarkers. *Geochimica et Cosmochimica Acta* 58, 2853-2863.
- Summons, R.E., Jahnke, L.L., Hope, J.M., Logan, G.A., 1999. 2-Methylhopanoids as biomarkers for cyanobacterial oxygenic photosynthesis. *Nature* 400, 554-557.
- Taira, A., Hill, I., Firth, J., Berner, U., Brückmann, W., Byrne, T., Chabernaud, T., Fisher, A., Foucher, J.-P., Gamo, T., Gieskes, J., Hyndman, R., Karig, D., Kastner, M., Kato, Y., Lallement, S., Lu, R., Maltman, A., Moore, G., Moran, K., Olafsson, G., Owens, W., Pickering, K., Siena, F., Taylor, E., Underwood, M., Wilkinson, C., Yamano, M., and Zhang, J., 1992. Sediment deformation and hydrogeology of the Nankai accretionary prism: synthesis of shipboard results of ODP Leg 131. *Earth Planet. Sci. Lett.*, 109, 431–450.
- ten Haven, H.L., Rohmer, M., Rullkötter, J., Bissert, P., 1989. Tetrahymanol, the most likely precursor of gammacerane, occurs ubiquitously in marine sediments. *Geochimica et Cosmochimica Acta* 53, 3073–3079.
- Terrinha, P., Pinheiro, L.M., Henriët, J.-P., Matias, L., Ivanov, M.K., Monteiro, J.H., Akhmetzhanov, A., Volkonskaya, A., Cunha, T., Shaskin, P., Rovere, M., 2003. Tsunamigenic-seismogenic structures, neotectonics, sedimentary processes and slope instability on the southwest Portuguese Margin. *Marine Geology* 195, 55-73.
- Teske, A., Hinrichs, K.-U., Edgcomb, V., De Vera Gomez, A., Kysela, D., Sylva, S.P., Sogin, M.L., Jannasch, H.W., 2002. Microbial diversity of hydrothermal sediments in the Guaymas basin: evidence for anaerobic methanotrophic communities. *Applied and Environmental Microbiology* 68, 1994-2007.
- Thiel, V., Peckmann, J., Seifert, R., Wehrung, P., Reitner, J., Michaelis, W., 1999. Highly isotopically depleted isoprenoids: molecular markers for ancient methane venting. *Geochimica et Cosmochimica Acta* 63, 3959-3966.
- Thiel, V., J. Peckman, H.H. Richnow, U. Luth, J. Reitner and W. Michaelis. 2001. Molecular signals for anaerobic methane oxidation in Black Sea seep carbonates and microbial mat. *Marine Chemistry* 73, 97-112.
- Thiel, V., Blumenberg, M., Pape, T., Seifert, R., Michaelis, W., 2003. Unexpected occurrence of hopanoids at gas seeps in the Black Sea. *Organic Geochemistry* 34, 81-87.

## References

- Thompson, G.A. Jr., Nozawa, Y., 1972. Lipids of protozoa: phospholipids and neutral lipids. *Annual Review of Microbiology* 26, 249-278.
- Thomsen, T.R., Finster, K., Ramsing, N.B., 2001. Biogeochemical and molecular signatures of anaerobic methane oxidation in a marine sediment. *Applied Environmental Microbiology* 67, 1646-1656.
- Tissot, B.P. and Welte, D.H., 1984. *Petroleum Formation and Occurrence*. 2<sup>nd</sup> edition, Springer-Verlag, Berlin, Germany.
- Tornabene, T.G., Langworthy, T.A., Holzer, G., Oro, J., 1979. Squalanes, phytanes and other isoprenoids as major neutral lipids of methanogenic and thermoacidophilic "archaeobacteria". *Journal of Molecular Evolution* 13, 73-83.
- Treude, T., 2003. Anaerobic oxidation of methane in marine sediments. PhD thesis, Bremen University, Bremen, Germany.
- Tugolesov, D.A., Gorshkov, A.S., Meysner, L.B., Soloviov, V.V., Khakhalev, E.M., Akilova, Y.V., Akentieva, G.P., Gabidulina, T.I., Kolomeytseva, S.A., Kochneva, T.Y., Pereturina, I.G., Plashihina, I.N., 1985. Tectonics of the Mesozoic sediments of the Black Sea basin. 215 pp. Nedra, Moscow (in Russian).
- Tyson, R.V., 1995. *Sedimentary organic matter: organic facies and palynofacies*. Chapman & Hall, London.
- Ulmishek, G.F., Harrison, W., 1981. Petroleum geology and resource assessment of the Middle Caspian basin, USSR, with special emphasis on the Uzen field: Argonne National Laboratory Report ANL/ES-116, 146 p.
- Ulmishek, G. F. 2001. Petroleum geology and resources of the middle Caspian Basin, Former Soviet Union, Supersedes Open-File Report 99-0050-B; B 2201-A., 38 pp.
- Valentine, D.L., Reeburgh, W.S., 2000. New perspectives on anaerobic methane oxidation. *Environmental Microbiology* 2, 477-484.
- van Duin, A.C.T., Sinninghe Damsté, J.S., Koopmans, M.P., van de Graaf, B., de Leeuw, J.M., 1997. A kinetic calculation method of homohopane maturation: applications in the reconstruction of burial histories of sedimentary basins. *Geochimica et Cosmochimica Acta* 61, 2409-2429.
- Van Lith, I., Warthmann, R., Vasconcelos, C., Mckenzie, J.A., 2003. Sulphate-reducing bacteria induce low-temperature Ca-dolomite and high Mg-calcite formation. *Geobiology* 1, 71.
- Van Rensbergen, P., Depreiter, D., Pannemans, B., Henriot, J.-P., 2005. Seafloor expression of sediment extrusion and intrusion at the El Arraiche mud volcano field, Gulf of Cadiz. *J. Geophys. Res.* 110, No.F2,F02010.
- Versteegh, G.J.M., Bosch, H.-J., de Leeuw, J.W., 1997. Potential palaeoenvironmental information of C<sub>24</sub> to C<sub>36</sub> mid-chain diols, keto-ols and mid-chain hydroxy fatty acids; a critical review. *Organic Geochemistry* 27, 1-13.
- Vetriani, C., Jannasch, H.W., MacGregor, B.J., Stahl, D.A., Reysenbach, A.-L., 1999. Population structure and phylogenetic characterization of marine benthic archaea in deep-sea sediments. *Applied and Environment Microbiology* 65, 4375-4384.
- Vogt, P.R., Gardner, J., Crane, K., 1999. The Norwegian-Barents-Svalbard (NBS) continental margin: introducing a natural laboratory of mass wasting, hydrates, and ascent of sediment, pore water, and methane. *Geomarine Letters* 19, 2-21.
- Volgin, A.V., Woodside, J.M., 1996. Sidescan sonar images of mud volcanoes from the Mediterranean Ridge; possible causes of variations in backscatter intensity. *Marine Geology*, 132, 39-53.
- Volkman, J.K., Barrett, S.M., Dunstan, G.A., Jeffrey, S.W., 1992. C<sub>30</sub>-C<sub>32</sub> alkyl diols and unsaturated alcohols in microalgae of the class Eustigmatophyceae. *Organic Geochemistry* 18, 131-138.
- Volkman, J.K., Barrett, S.M., Dunstan, G.A., 1994. C<sub>25</sub> and C<sub>30</sub> highly branched isoprenoid alkenes in



## References

---

- laboratory cultures of two marine diatoms. *Organic Geochemistry* 21, 407-414.
- Volkman, J.K., Barrett, S.M., Blackburn, S.I., Mansour, M.P., Sikes, E.L., Gelin, F., 1998. Microalgal biomarkers: A review of recent research developments. *Organic Geochemistry* 29, 1163–1179.
- Volkman, J.K., Barrett, S.M., Blackburn, S.I., 1999. Eustigmatophyte microalgae are potential sources of C<sub>29</sub> sterols, C<sub>22</sub>–C<sub>28</sub> *n*-alcohols and C<sub>28</sub>–C<sub>32</sub> *n*-alkyl diols in freshwater environments. *Organic Geochemistry* 30, 307–318.
- Von Rad, U., Rösch, H., Berner, U., Geyh, M., Marchig, V., Schulz, H., 1996. Authigenic carbonates derived from oxidized methane vented from Makran accretionary prism off Pakistan. *Marine Geology* 136, 55-77.
- Voskoboynikov, N.I. and Gur'ev, A.V., 1832. Geologicheskoe opisanie poluoostrova Tamani, prinadlezhashey k zemle voyska Chernomorskogo. *Gorniy Zhurnal*, 1 (in Russian).
- Wakeham, S.G., 1990. Algal and bacterial hydrocarbons in particulate organic matter and interfacial sediments of the Cariaco Trench. *Geochimica et Cosmochimica Acta* 54, 1325-1336.
- Wakeham, S.G., Peterson, M.L., Hedges, J.I., Lee, C., 2002. Lipid biomarker fluxes in the Arabian Sea, with comparison to the equatorial Pacific Ocean. *Deep-Sea Research II* 49, 2265–2301.
- Wakeham, S.G., Lewis, C.M., Hopmans, E.C., Schouten, S., Sinninghe Damsté, J.S., 2003. Archaea mediate anaerobic oxidation of methane in deep euxinic waters of the Black Sea. *Geochimica et Cosmochimica Acta* 67, 1359-1374.
- Wallmann, K., Linke, P., Suess, E., Bohrmann, G., Sahling, H., Schlüter, M., Dähmann, A., Lammers, S., Greinert, J., von Mirbach, N., 1997. Quantifying fluid flow, solute mixing, and biogeochemical turnover at cold vents of the eastern Aleutian subduction zone. *Geochim. Cosmochim. Acta* 61, 5209–5219.
- Walter, L.M., 1986. Relative efficiency of carbonate dissolution and precipitation during diagenesis: a progress report on the role of solution chemistry. In Gautier, D.L. (Ed.), *Roles of Organic Matter in Sediment Diagenesis*. Spec. Publ.-Soc. Econ. Paleontol. Mineral. 38, 1-11.
- Weijers, J.W.H., Schouten, S., Hopmans, E.C., Geenevasen, J.A.J., David, O.R.P., Coleman, J.M., Pancost, R.D., Sinninghe Damsté, J.S., 2006. Membrane lipids of mesophilic anaerobic bacteria thriving in peats have typical archaeal traits. *Environmental Microbiology* 8, 648–657.
- Werne, J.P., Baas, M., Sinninghe Damsté, J.S., 2002. Molecular isotopic tracing of carbon flow and trophic relationships in a methane-supported benthic microbial community. *Limnology and Oceanography* 47, 1694-1701.
- White, R.S., 1982. Deformation of the Makran accretionary sediment prism in the Gulf of Oman (north-west Indian Ocean). In: Leggett JK (ed) *Trench-forearc geology: sedimentation and tectonics on modern and ancient active margins*. Geological Society, London, 351-372.
- Whiticar, M.J., Suess, E., Wehner, H., 1985. Thermogenic hydrocarbons in surface sediments of the Bransfield Strait, Antarctic Peninsula. *Nature* 314, 87-90.
- Whiticar, M.J., Faber, E., Schoell, M., 1986. Biogenic methane formation in marine and freshwater environments: CO<sub>2</sub> reduction vs. acetate fermentation-isotope evidence. *Geochem. Cosmochim. Acta* 50, 693-709.
- Whiticar, M. J., 1994. Correlation of natural gases with their sources. In: L. B. Magoon, W. G. Dow (Eds.). *The Petroleum System, From Source to Trap*, AAPG, 261-283.
- Wood, G.W. 1980. Complex lipids. In *Biogeochemical Application of Mass Spectrometry*. Eds. G.R. Waller and O.C. Dermer. A Wiley-Interscience Publication, John Wiley and Sons, Canada, pp 173-209.
- Woodside, J.M., Ivanov, M.K., Limonov, A.F. (Eds.), 1997. Neotectonics and fluid flow through seafloor sediments in the Eastern Mediterranean and Black Seas: Part II. Black Sea. Preliminary results of geological and geophysical investigations during the ANAXPROBE/TTR-6 cruise of

## References

---

- R/V Gelendzhik, July–August 1996. Intergovernmental Oceanographic Commission Technical Series 48, pp. 225.
- Woodside, J.M., Ivanov, M.K., Limonov, A.F. and shipboard scientists of the ANAXIPROBE expeditions, 1998. In: Henriot, J.-P. and Mienert, J. (Eds). Gas hydrates. Relevance to world margin stability and climatic change. Geological Society, London, Special Publications, 137, 177-193.
- Wuchter, C., Schouten, S., Boschker, H.T., Sinninghe Damste, J.S., 2003. Bicarbonate uptake by marine Crenarchaeota. *FEMS Microbiol Lett* . 219, 203–207.
- Zehnder, A.J.B., 1988. *Biology of anaerobic microorganisms*. Wiley, New York.
- Zehnder, A.J.B., Brock, T.D., 1979. Methane formation and methane oxidation by methanogenic bacteria. *Journal of Bacteriology* 137, 420-432.
- Zhang, C.L., Li, Y., Wall, J.D., Larsen, L., Sassen, R., Huang, Y., Wang, Y., Peacock, A., White, D.C., Horita, J., Cole, D.R., 2002. Lipid and carbon isotopic evidence of methane-oxidizing and sulfate-reducing bacteria in association with gas hydrates from the Gulf of Mexico. *Geology* 30, 239-242.
- Zitter, T., 2004. *Mud volcanism and fluid emissions in Eastern Mediterranean neotectonic zones*. Thesis, Free University of Amsterdam, the Netherlands, ISBN 90-9017859-7.
- Zorn, M. E., Lalonde, S.V., Gingras, M.K., Pemberton, S.G., Konhauser, K.O., 2006. Microscale oxygen distribution in various invertebrate burrow walls. *Geobiology* 4, 137.



## Acknowledgements

---

Most of the data provided in this thesis came from the scientific Training-through-Research (TTR) cruises organised by UNESCO-MSU Centre for Marine Geology and Geophysics at Moscow State University, Geological Faculty. These cruises gave me an outstanding experience, advance training in marine sciences, unique sampling collection used for this study, unforgettable time at sea, and a lot of friends with whom I shared my work and companionship afterwards.

I would like to express my gratitude to Prof. Dr. Michail K. Ivanov (Moscow State University, Geological Faculty, Department of Fuel Minerals), Director of the UNESCO-MSU Centre for Geology and Geophysics and founder of the TTR Programme, for my education and development in the marine research field, for his guidance, help, training, and sharing of his knowledge in marine science for more than ten years.

My greatest thanks must go to Prof. Dr. Tjeerd C.E. van Weering. Since the very beginning of my stay in the Netherlands, he gave me a very first insight into the Dutch culture, traditions, history, and beauty of this country, in particular the province North Holland. Besides scientific input in this thesis, valuable scientific advice and continuous support, his warmth and admirable immense optimism always helped me to overcome difficulties I have met. I am also grateful to Lineke van Weering for her constant hospitality and unforgettable Christmas time I had with her family.

My special sincere thank to Prof. Dr. Ir. Jaap S. Sinninghe Damsté, without whom this study would not have been possible. I am grateful, that he generated an extra interest in biogeochemistry in me, and, particularly, for his commitment to guide me during my doctoral study. His constructive criticism, systematic explanations and training, continuous support and insightful scientific discussions have not only enabled the achievement of this work, but have also played one of the major roles in content, discussion and presentation of this thesis. Besides, my special thanks for the time he has spent reading and correcting numerous drafts of my papers, followed by enduring explanations of “The art of writing a scientific article”.

I would like to extend my gratitude to my colleagues from the Department of Marine Biogeochemistry and Toxicology at Royal NIOZ, for the pleasant working environment, for being open and patient to my endless questions in the lab. I have really enjoyed working with all of you! My special thanks to Marianne Baas for general support, excellent work together at sea, for being very helpful during my lab experiments, and for sharing difficult times with me. I want to thank Michiel Kienhuis for technical and analytical assistance, for his friendly explanations about working peculiarities of scientific equipment I used during my study. It was not always diplomatic from my side, but very educational from yours. Michiel, I deeply appreciate your help with printing this thesis while I was away in a cruise.

## Acknowledgements

---

Henk de Haas, NIOZs' "sea-wolf", whom I know the longest. Thank you for your help with organization of my stay in the Netherlands and with the whole paperwork I had to go through. Besides, your scientific comments and just pleasant morning chats with green tea often "made my day".

I sincerely would like to address special thanks to my former teachers in organic geochemistry at the Departments of Fuel Minerals at Moscow State University, Dr. E.V. Soboleva, Prof. A.N.Guseva, Prof. Dr. O.K.Bazhenova and also to Dr. A.V.Egorov from the Institute of Oceanology (Russian Academy of Science), who rouse my interest in geochemistry of hydrocarbon gases.

I am grateful to all colleagues and friends from UNESCO-MSU Centre for Marine Geology and Geophysics, with whom I started my career as a student. Especially, I would like to thank Elena Kozlova, Andrey Akhmetzhanov, Pavel Shashkin, Valentina Blinova, Anna Volkonskaya, Anatoly Limonov, and all students and staff, who helped me during this study. I am particularly grateful to Grigory Akhmanov, who interested me in mud volcanoes and, in fact, saved my life, when I fell into one of them, during that unforgettable field-trip to mud volcanoes of the Kerch peninsular in 1995. I considered it as baptism-of-a-mud-volcano-business and still try hard to be in.

Varvara Polyanskaya, you are a person I would like to mention here in particular. Besides our whole-life-amity, you gave me a feeling of having The Friend close by even when thousands kilometres lie in between. I sincerely thank you for cherishing our solid and inestimable friendship

I have a heartfelt gratitude to Sergey Shtern, for your being my long-an-unfailing friend. I guess you are, indeed, the man who knows all about me, and still likes me. Thank you for your support and help every time I need it.

Importantly, I thank Katia Ivanova, who became my close friend in the Netherlands. Thank you for your support, kindness, openness, for the ability to listen, and for essential career advises.

I also thank Alexey E. Suzyumov, Svetlana Galagan, Dmitry Zezin, Marina Kulieva, Joana Cardoso, Ben Abbas, and many others for their support and friendship.

I am thankful to Sergey, Evgenya, and Vladimir Bouriak for their care, excellent times and sincere affection during my study.

My greatest debt of gratitude is owed to my boyfriend Leon M. Wuis and all his family who have given me ineffable support and understanding throughout the last three years.

Finally, the ones who always have been and always will be with me are Vera and Irina Stadnitskaia. There are no words to convey my deep love and gratitude for everything you did for me.

## Curriculum Vitae

---

Alina Nikolaievna Stadnitskaia was born at the 18<sup>th</sup> of July in 1974 in Moscow, USSR. After finishing polytechnic high school, she started to study Petroleum Geology in 1992 at the Lomonosov Moscow State University in Moscow, Russia. She received her Bachelor of Arts degree in Petroleum Geology and Geochemistry in 1997, and the Master of Science degree in Geology in 2000. In October 2000, she arrived to the Royal NIOZ for a probation period of one year due to receiving a fellowship of the President of the Russian Federation. In 2002, she received a grant from the Huygens Programme of the Netherlands Organization for International Cooperation in Higher Education (Nuffic) and continued her stay at the Royal NIOZ. From September 2003 she started her PhD project at the Royal NIOZ. From December 2003 until present, she was employed by the Royal NIOZ as a postdoctoral scientist within the ESF-funded project entitled “An integrated of seepage through the seabed of the Nile deep sea fan (2003-2006)” – MEDIFLUX. From March 2007 she will start her second postdoctoral research in the Royal NIOZ.















